Thiazolidinedione Treatment in Models of Insulin Resistance

Thesis submitted in accordance with the requirements of the University of Liverpool for the degree of Doctor of Philosophy

by

Lucy Cecilia Pickavance

April 2001

Declaration

I declare that the data submitted in this thesis are the result of my own work, with the exception of those presented in Chapter 3 (sections 3.2.5 and 3.3) on apoptosis in the rat pancreas. For these results I am indebted to Dr. John Foster of the Department of Pathology, Central Toxicology Laboratory, Astra-Zeneca, Macclesfield, Cheshire. I also gratefully acknowledge the help I received from many people in the Diabetes & Endocrinology Research Group, Department of Medicine at the University of Liverpool, particularly Dr. Peter Widdowson, whose assistance on much of the work presented in Chapter 3 was invaluable.

Signature... Lucy Pickavance ..... **Date**..... 19/07/01

Lucy Pickavance

Acknowledgements

Thanks must go primarily to Dr. John Wilding for his enthusiastic supervision and constant encouragement over the last three years to complete my degree. I am also grateful to Prof. Gareth Williams, who, along with John, has provided me with continuous employment on interesting projects. I also wish to acknowledge members of the Diabetes and Endocrinology Research Group, University of Liverpool, past and present: Chen Bing, Xue Cai, Lynda Capper, Roslyn Cassidy, Peter Collins, Simon Dryden, Helen Frankish, Joanne Harrold, David Hopkins, Peter King, Ebrahim Naderali, Sharon Smith and Qiong Wang. They have been very generous with their time, particularly in helping with tissue processing and in giving advice on laboratory techniques. In particular, I must also thank Dr. Peter Widdowson for his energetic assistance and demonstration of new methodology. Mr. Norman Usher has also shown unwavering support in various administrative, safety and technical matters.

All of the work presented in this thesis was supported financially by grants from Mitsubishi Chemical Corporation, Yokohama, Japan (Chapter 3), Novo Nordisk, Maløv, Denmark (Chapter 4), and SmithKline Beecham Pharmaceuticals (SKB), Essex, U.K. (Chapters 5, 6 and 7). I am therefore grateful to them all for supplying bulk materials and would like to thank Drs. H. Tanaka, S. Ishii, Robin Buckingham and Thomas Leonard for guidance on manuscript preparation. I also thank Robin for being a great source of knowledge and taking an interest on both a professional and personal level. I thank John Clapham, Sabrina Carter, Brian Bond and Gary Moore, also of SKB, for very timely results on TaqMan® analysis of tissues used in Chapter 6.2 and kind permission to refer to these as yet unpublished observations. I also appreciate the careful advice from Prof. Karsten Wassermann and Dr. Christian Brand on experimental organization. Similarly, Dr. Richard Vernon, of the Hannah Research Institute in Ayr, Scotland, has been a most knowledgeable collaborator, and the hospitality he and Christine Vernon have shown has been very much appreciated.

I am very grateful to the staff of the Biomedical Services Unit (BSU) at the University of Liverpool for being so accommodating and for their consciencious care of the animals throughout all studies presented here. Special thanks must go to Miss Juliet McAdams, Miss Joanne Sanders, Miss Catherine Edwards and Mr. Anthony Purvis for their meticulous help in carrying out studies of complex design. The BSU staff have been very supportive, too, in maintaining an unstintingly cheerful attitude over the years, including Dave Bohl, Barry Cotterill, Linda Horan, Andy Houghton, Maureen Kearns, Rhys Sweeney, Leigh Thompson, Anne Ward and John Waters. I also thank Miss Karen Owens and Mrs. Pamela Vincent of SKB for their technical assistance on the tissue processing required for the study presented in Chapter 5.

Finally, I am most grateful to Helen Frankish, Suzanne Hagan, Jo Wilson and Lynn Markert (of Ottawa, Canada) for their kind friendship and much-needed social diversion and for helping to keep things in perspective. Needless to say, my most heartfelt thanks go to my father and late mother for their love and support and the countless ways in which they have helped me.

ABSTRACT

Thiazolidinediones (TZDs) are a class of anti-diabetic drugs which improve insulin sensitivity in states of insulin resistance and diabetes. Their mechanism of action is only partly understood, but possibilities include substrate competition, alteration of genes involved in insulin signalling, and indirect modulation of insulin signalling by alteration of expression of cytokines such as leptin and tumour necrosis factor-alpha (TNFα). The primary target for TZDs is peroxisome proliferator activated receptor-gamma (PPARγ), a nuclear receptor thought to be important in the regulation of lipid metabolism. The fibrate class of lipid-lowering drugs act via PPARα, a receptor related to PPARγ. Adverse effects of TZD drugs include hyperphagia and weight gain, occurring possibly via changes in circulating free fatty acid (FFA) and leptin concentrations. At high doses, they can also cause fluid retention, which may lead to cardiac hypertrophy.

These studies were designed to investigate the effectiveness of a range of compounds in this therapeutic class and the mechanisms by which they might lead to the potentially important side effect of weight gain. Their effects were examined in (i) the obese Zucker Diabetic Fatty (ZDF) rat, a genetic model of type 2 diabetes, and (ii) the diet-induced obese (DIO) rat, a non-genetic model which can develop insulin resistance through consumption of a highly palatable diet (HPD). *In vivo* insulin sensitivity and secretory capacity were evaluated using glucose clamp techniques. Circulating mediators and key hypothalamic signals of weight gain were also evaluated by radioimmuno- and colorimetric assay and by Northern hybridisation.

Chronic treatment of young ZDF rats with the TZD, MCC-555, attenuated the development of overt diabetes by improving insulin sensitivity. Underlying pancreatic dysfunction was also normalised, as shown by reduced nitric oxide synthase activity and apoptosis. Both lean ZDF rats and polygenic Wistar rats became obese, hyperphagic and insulin-resistant on the HPD. Various PPARγ agonists (including non-TZDs) administered to the DIO ZDF rats at equipotent doses improved their metabolic profile and insulin resistance equally with an α/γ mixture, and better than an α agonist alone. The TZD rosiglitazone (RSG) was found to be more potent than pio- and troglitazone in DIO Wistars, reducing fasting plasma

glucose, insulin, FFA and triglyceride concentrations dose-dependently and at a threshold dose several-fold lower than that inducing haemodilution. The insulin-sensitising action of a high dose of RSG was also enhanced by preventing accompanying hyperphagia by pair-feeding to the intake of untreated DIO rats, although this was independent of a fall in FFAs. Pair-feeding also prevented RSG-related weight gain in lean controls, but not DIO rats, suggesting suppressed DIO thermogenic capacity, although uncoupling protein (UCP)-1 expression in brown fat and UCP-3 expression in skeletal muscle were unchanged. Nor did the mechanism of weight gain appear to be governed by hypothalamic mediators of appetite, neuropeptide Y or orexin, as their expression remained unchanged. The fall in FFAs was closely correlated with weight gain, suggesting that this could be an important hyperphagic signal in these animals. Other undiscovered mechanisms may also play a role, as FFA-lowering by α agonists does not improve insulin resistance or cause weight gain.

In conclusion, TZDs are effective in rat models of diabetes and insulin resistance. Intervention with these agents in the early stages of the disease may be beneficial by improving insulin sensitivity and maintaining ß-cell function. RSG, in particular, can be used at a dose which clearly separates efficacy from haemodilution. The improvements in metabolic status evoked by TZD treatment in DIO rats are greater if weight gain is prevented, suggesting that these drugs would be even more effective if weight gain was avoided. Weight gain appears to be closely related to the fall in FFAs which itself appears to underpin the therapeutic benefits of this class of drugs.

TABLE OF CONTENTS *page*

List of abbreviations

ADP:	adenosine-5'-diphosphate
AGRP:	agouti-related peptide
AMP:	adenosine-5'-monophosphate
ANOVA:	analysis of variance
AP:	alkaline phosphatase
ARC:	arcuate nucleus
ATP:	adenosine-5'-triphosphate
AUC:	area under the curve
BAT:	brown adipose tissue
BB:	BioBreeding rat
BF:	bezafibrate
BMI:	body mass index
CCK:	cholecystokinin
CMC:	carboxymethyl cellulose
CNS:	central nervous system
cpm:	counts per minute
CRF:	corticotropin releasing factor
CT:	computed tomography
d:	day
DAG:	diacylglycerol
DIG:	digoxigenin
DIO:	dietary obese or diet-induced obesity
DMH:	dorsomedial hypothalamic nucleus
DMPC:	dimethyl pyrocarbonate
DR:	dorsal raphe nuclei
DRF:	DRF 2593
FA:	fatty acid
FACoA:	fatty acyl coenzyme A
FAD:	flavin adenine dinucleotide
FFA:	free fatty acid
G-6-P:	glucose-6-phosphate

GAD:	glutamic acid decarboxylase
GI:	gastrointestinal
GLP-1:	glucagon-like peptide-1
GLP-2:	glucagon-like peptide-2
GSIS:	glucose-stimulated insulin secretion
HDL:	high density lipoprotein
HGP:	hepatic glucose production
HLA:	human leucocyte antigen
HOMA:	homeostasis model assessment
HPD:	highly palatable diet
5-HT:	5-hydroxytryptamine (serotonin)
ICV:	intracerebroventricular
IGT:	impaired glucose tolerance
IL-1β:	interleukin-1-beta
i.m.:	intramuscular
iNOS:	inducible nitric oxide synthase
i.p.:	intraperitoneal
i.v.:	intravenous
KO:	knock out
LDL:	low density lipoprotein
LHA:	lateral hypothalamic area
LPL:	lipoprotein lipase
MC1-R:	melanocortin-1 receptor
MC4:	melanocortin-4
MC4-R:	melanocortin-4 receptor
MCH:	melanin-concentrating hormone
MHC:	major histocompatibility complex
α-MSH:	α-melanocyte-stimulating hormone
NADH:	nicotinamide-adenine dinucleotide (reduced)
NADP:	nicotinamide-adenine dinucleotide phosphate
NADPH:	nicotinamide-adenine dinucleotide phosphate (reduced)
NIDDM:	non-insulin-dependent diabetes mellitus

NNC:	NNC 61-0029
NO:	nitric oxide
NOS:	nitric oxide synthase
NPY:	neuropeptide Y
NSB:	non-specific binding
NTS:	nucleus of the solitary tract
O.D.:	optical density
OGTT:	oral glucose tolerance test
PB:	phosphate buffer
PBS:	phosphate buffered saline
PCD:	programmed cell death
PDE 3B:	phosphodiesterase 3B
PDH:	pyruvate dehydrogenase
PEPCK:	phosphoenolpyruvate carboxykinase
PF:	paraformaldehyde
PFA:	perifornical (hypothalamic) area
PI-3K:	phosphatidylinositol-3 kinase
PIO:	pioglitazone
PKC:	protein kinase C
PPARα:	peroxisome proliferator-activated receptor-alpha
PPARγ:	peroxisome proliferator-activated receptor-gamma
PPRE:	peroxisome proliferator response element
PVN:	paraventricular nucleus
RIA:	radioimmunoassay
rpm:	revolutions per minute
RSG:	rosiglitazone
RT:	room temperature
RXR:	retinoid X receptor
SA:	specific activity
SEM:	standard error of the mean
SNS:	sympathetic nervous system
S-S:	steady-state

STZ: streptozotocin

t: time

TG: triglyceride

TNFα: tumour necrosis factor-alpha

TRO: troglitazone

TUNEL: terminal deoxynucleotidyl transferase (TdT)-mediated dUTP nick end-labelling

TZD: thiazolidinedione

UCP: uncoupling protein

VLDL: very low density lipoprotein

VMH: ventromedial hypothalamic nucleus

WAT: white adipose tissue

WBU: whole-body glucose uptake

WHR: waist-hip ratio

ZDF: Zucker Diabetic Fatty (rat)

List of figures *page*

List of tables *page*

Publications to support this work

Abstracts

Pickavance L, Buckingham R, Wilding J (1999) Insulin-sensitising action of rosiglitazone is enhanced by food restriction. *Diabetologia* **42**, suppl. 1: 674, A181

Pickavance L, Tadayyon M, Widdowson P, Buckingham R, Wilding J (1998) Therapeutic index for rosiglitazone in dietary obese rats and effects on body weight and plasma leptin. *British Diabetic Association Meeting*, Harrogate

Pickavance L, Widdowson PS, Buckingham RE, Wilding JPH (1998) Rosiglitazone therapeutic index: separation of glucose lowering and haemodilution. *Diabetologia* **41**, suppl. 1: 924, A239

Pickavance LC, Widdowson PS, Foster JR, Ishii S, Tanaka H, Williams G (1999) The thiazolidinedione, MCC-555, prevents nitric oxide synthase induction in the pancreas of the ZDF rat. *Br J Pharmacol* **128**: 116P

Pickavance L, Widdowson PS, Ishii S, Tanaka H, Williams G (1998) MCC-555 treatment to young ZDF rats attenuates the development of overt diabetes. *Br J Pharmacol* **124**: 138P

Full papers

Pickavance LC, Buckingham, RE, Wilding, JPH (2001) Insulin-sensitising action of rosiglitazone is enhanced by preventing hyperphagia. *Diabetes Obes Metab* **3**: 171-80

Pickavance L, Tadayyon M, Widdowson PS, Buckingham RE, Wilding JPH (1999) Therapeutic index for rosiglitazone in dietary obese rats: separation of efficacy and haemodilution. *Br J Pharmacol* **128**: 1570-76

Pickavance L, Widdowson PS, Ishii S, Tanaka H, Williams G (1998) The development of overt diabetes in young Zucker Diabetic Fatty (ZDF) rats and the effects of chronic MCC-555 treatment. *Br J Pharmacol* **125**: 767-70

CHAPTER 1

General Introduction

1.1. Fuel homeostasis

An organism's ability to maintain a stable internal environment is crucial to survival and health. Such stability can only be achieved through the operation of carefully co-ordinated physiological processes. These complex mechanisms include those which maintain energy and fuel homeostasis. This regulation of body energy content derived from food requires the integration of carbohydrate, protein and fat metabolism in the body's lean tissues and fat storage depots, and involves interconversions of these organic molecules, particularly by cells of the liver [Vander *et al.*, 1985].

1.1.1. Glucose and lipid metabolism

(i) The absorptive state

After a meal, the body is in the absorptive state, in which ingested nutrients enter the blood from the gastrointestinal (GI) tract. Glucose provides the major energy source, and most of the amino acids, fat and carbohydrate not oxidised for energy are transformed into adipose tissue and, to a lesser extent, glycogen.

Hence, fat can either be absorbed from the diet or synthesised *de novo* from glucose. Glucose is an important precursor of fat because it provides both the glycerol and fatty acid (FA) components of triglycerides (TGs), the storage form of lipid. Most ingested fat is absorbed into the lymph as chylomicrons, containing mainly TGs. These TGs are processed by releasing their FAs in adipose tissue where they combine with glycerol provided by glucose to form TGs once again.

Most absorbed amino acids enter muscle and liver cells as a supply for protein synthesis and to be stored as protein. Also in the liver, they may be converted to FAs, thereby contributing to hepatic fat synthesis, but mostly they are used here for gluconeogenesis.

Food ingestion induces a rapid surge of insulin secretion from the pancreatic β-cells in the islets of Langerhans in response to a range of signals. Firstly, absorbed nutrients, principally glucose, have insulin secretagogue actions, but amino acids are also active in this way, for example, after a high-protein meal. This, in turn, stimulates cellular uptake of these amino acids. Glucose first enters the β-cells via the GLUT-2 glucose transporter. Once inside the β-cell, glucose is metabolised by glucokinase to glucose-6-phosphate (G-6-P), generating adenosine triphosphate (ATP). This closes ATP-sensitive K^+ channels, causing membrane depolarisation which triggers Ca^{2+} influx, resulting in exocytosis of insulin secretory granules. Secondly, prandial insulin release is also stimulated by humoral signals: These are the incretins, hormones secreted by the gut into the circulation after eating, such as gastric inhibitory peptide (GIP) and glucagon-like peptide-1 (GLP-1), a gut-derived product of the preproglucagon gene [see below, 1.3.3 (ii) (3)]. These provide an anticipatory component to glucose regulation such that insulin secretion rises earlier than if plasma glucose were the only controller. Thirdly, autonomic nervous system signals, including vagal innervation of the islet, also stimulate insulin release at this time.

From the islet capillaries via a tributary of the portal vein, insulin is then delivered directly to the liver, where it exerts many of its metabolic effects. These effects include conversion of glucose to glycogen (glycogenesis) in liver and muscle, the formation of TG in fat (lipogenesis), stimulation of protein synthesis in many

tissues, and the inhibition of the opposing catabolic processes of glycogenolysis, lipolysis and proteolysis. Basal insulin levels are sufficient for inhibiting lipolysis and restraining glucose output by the liver by inhibiting glycogenolysis and gluconeogenesis, but much higher post-prandial levels of insulin are required to stimulate the uptake of glucose into muscle and fat by activating glucose transporter proteins in these tissues [Vander *et al.*, 1985; Wilding & Williams, 1997; Fig. 1.1].

(ii) The post-absorptive state

In contrast, during the post-absorptive state, the GI tract is empty and energy is supplied from the body's endogenous stores. Initially, these are mainly glycogen stores, but in the longer term oxidation of fat predominates. The events of the post-absorptive state primarily concern maintaining the blood glucose concentration when glucose is no longer being absorbed from the gut. Direct and indirect sources of glucose during this period include the glycogen stores in the liver and muscle, muscle protein and adipose tissue TGs. The breakdown of the latter liberates FAs into the blood and is essential during the transition from the absorptive to postabsorptive states to provide energy for virtually all organs while glucose is spared for use by the brain. The major effectors of this shift from feasting to fasting are the pancreatic hormones insulin, glucagon and somatostatin, adrenaline from the adrenal medulla, the liver, adipose tissue and muscle, as well as the sympathetic nerves to adipose tissue and liver [Vander *et al.*, 1985].

1.1.2. The Randle cycle

Thus, as well as glucose, fat is an important energy substrate for muscle. An increase in fat supply, when body weight rises as a result of increased adiposity,

means that muscle uses more fat and less glucose. This response by the body to changing proportions of fuel substrates is known as the Randle cycle [Randle *et al.*, 1963], and this shift toward fat as a preferred fuel used by muscle results in a decrease in insulin-stimulated glucose uptake and utilisation. This is known as insulin resistance. An individual's equilibrium between stored fat and circulating free fatty acids (FFAs) determines the amount of adipose tissue needed to increase fat utilisation by muscle [for review, see *Type II Diabetes*, 1996].

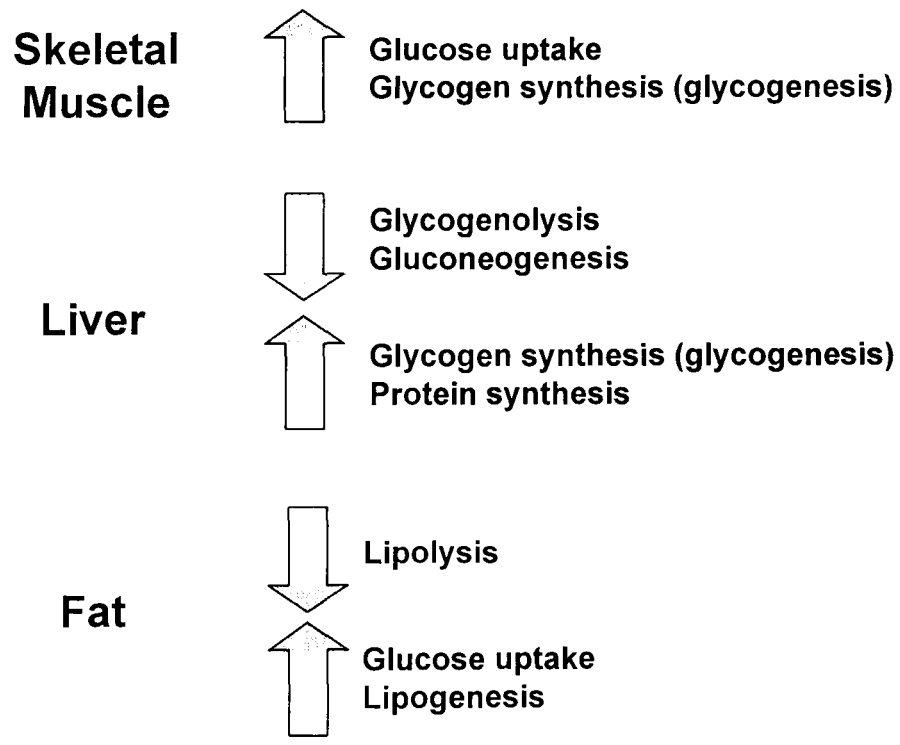

Figure 1.1. Summary of the effects of insulin during the absorptive state. Insulin secretion from the pancreatic β-cells is stimulated after a meal by glucose and amino acids absorbed from the gut, by incretin hormones secreted by the gut and by autonomic innervation of the islets. Its effects are primarily anabolic, to convert glucose and fat to their storage forms, as well as to promote protein synthesis, while inhibiting the opposing catabolic processes involving glycogen, lipid and protein breakdown.

1.2. *Diabetes mellitus*

1.2.1. *Type 1 diabetes*

Type 1 diabetes is also referred to as insulin-dependent diabetes mellitus (IDDM) because it identifies patients who cannot survive without insulin treatment. The commonest cause of the disease is autoimmune destruction of the β-cells. Insulin deficiency is so profound that ketoacidosis, the biochemical hallmark of the disease, will develop without insulin replacement. The ketone bodies, namely acetone, acetoacetate and 3-hydroxybutyrate, are important fuels when carbohydrate is in short supply or cannot be used efficiently. The increases in these substrates are fuelled by lipolysis and the mobilisation of body fat when the body cannot metabolise glucose. The culmination of this β-cell destruction also includes hyperglycaemia with excessive urination and thirst [for review, see Bowen Jones & Gill, 1997a and Kruszynska, 1997].

β-cell deterioration is thought to arise from the interaction of environmental factors, such as exposure to foreign antigens (e.g., through viral infection or ingestion of the protein in cow's milk), with an inherited susceptibility which does not depend on a single gene but is determined by several genes at different loci. The most important locus appears to reside in the human leucocyte antigen (HLA) major histocompatibility complex (MHC) class II region on the short arm of chromosome 6 [for review, see Bowen Jones & Gill, 1997a]. Viruses or other agents could induce β-cells to express HLA antigens and 'expose' autoantigens (viral antigens which could be expressed on β-cells, or a normal β-cell antigen which could mimic viral antigens). The autoantigen, when co-expressed with certain HLA antigens not normally expressed, has a configuration favourable to activating T-helper lymphocytes and triggers autoimmune damage. The enzyme glutamic acid

decarboxylase (GAD) and insulin itself may be the crucial β-cell autoantigens that react with T-cells and autoantibodies in the circulation [Yoon *et al.*, 2000].

Type 1 diabetes can also present after viral infections which may target and selectively attack β-cells, altering their activity or antigenicity [Wilding & Williams, 1997]. For example, it has been suggested that viral infection may directly mediate the initial β-cell destruction by the direct interaction of double-stranded RNA and interferon-γ (IFN-γ) with β-cells, stimulating inducible nitric oxide synthase (iNOS) expression and inhibiting insulin secretion through the production of nitric oxide (NO) [Heitmeier *et al.*, 1999].

1.2.2. Type 2 diabetes

Type 2 diabetes, also known as non-insulin-dependent diabetes mellitus (NIDDM), is a disease characterised primarily by hyperglycaemia due to defects in insulin action and secretion from the β-cells. The relative, but not complete, insulin deficiency results in abnormalities in carbohydrate, fat and protein metabolism. These give rise to the symptoms of the overt disease, including excessive thirst and urination, but also indirectly lead to dyslipidaemia and hypertension [Williams, 1994] and, if left untreated, will ultimately cause micro- and macrovascular and neuropathic complications.

Patients are often obese, and this is a major factor in the development of increased hepatic glucose production (HGP) and muscle insulin resistance. Adipose tissue is also resistant to the regulatory effects of insulin in type 2 diabetes, contributing to increased FFA and TG levels in the circulation. The central, or truncal, obesity displayed by many patients results in excess FFAs in the portal circulation, and, thus, the liver, giving these patients a characteristic dyslipidaemic

profile, including raised very low density lipoprotein (VLDL) and lowered high density lipoprotein (HDL) levels. Raised concentrations of circulating cholesterol contribute to increased coronary artery risk, and the inverse relationship between HDL concentration and the risk of cardiovascular disease is well established. Insulin resistance is also associated with reduced lipoprotein lipase (LPL) activity, LPL being the enzyme responsible for splitting these lipoproteins into glycerol and FAs and partitioning lipid fuels between storage and oxidation. This, in turn, leads to a decrease in VLDL clearance.

The liver is also the site of gluconeogenesis which is a major source of hyperglycaemia in type 2 diabetes. Muscle glucose oxidation is reduced by competition from FFA oxidation, as already mentioned. Pancreatic β-cells produce less insulin, another defect characteristic of the pathology of the disease, and the FFAs inhibit insulin binding. These factors all compound the hyperglycaemia, which, in itself, may be toxic to β-cells ('glucotoxicity'), and further exacerbates the cycle by impairing insulin release and glucose transport. The deposition of amyloid, a substance composed mainly of islet amyloid polypeptide (IAPP), is associated with atrophy of the β-cells in type 2 diabetes, but whether it actively inhibits insulin secretion or is merely a marker of β-cell failure is unknown. It is unlikely that there is a single biochemical abnormality responsible for type 2 diabetes. The disease is heterogeneous; insulin resistance and pancreatic insufficiency are present in most patients, but one or the other may predominate in different patients and at different stages of the disease [for review, see *Dyslipidaemia*, 1997 and *Type II Diabetes*, 1996].

1.3. The importance of insulin resistance

1.3.1. Overview: the causes of insulin resistance and type 2 diabetes

(i) Obesity

Although the pathogenesis of type 2 diabetes is not fully understood, it is certain that both genetic and environmental factors are involved. Obesity is the most important environmental factor in the development of type 2 diabetes, although it is important to note that obesity itself may be genetically determined. As such, obesity is the most important modifiable risk factor for the disease, to the point where even moderate weight loss, although it cannot reverse pancreatic dysfunction, can prevent or delay the onset of the disease and will alleviate much of the metabolic disturbance and prevent complications once the disease has developed [for review, see Gavin *et al.*, 1998 and *Type II Diabetes*, 1996].

Obesity is the result of energy intake grossly exceeding energy expenditure over a prolonged period of time. Energy intake can be measured assuming the macronutrient energy composition of the diet is known. Energy expenditure can be measured in the laboratory using indirect calorimetry by measuring the ratio of CO_2 produced and O_2 consumed. The clinical definition of obesity is based on the body mass index (BMI), which is calculated as weight in kilograms divided by the square of the person's height in metres (kg/m^2). Clinical obesity is defined as a BMI > 30 kg/m^2, and an elevated BMI is associated with increased risk of the development of type 2 diabetes (Fig. 1.2) in both sexes, as well as with development of pre-diabetic conditions, such as impaired glucose tolerance (IGT) and insulin resistance. There is no one ideal body weight, but a band of healthy weights, defined as a BMI ranging from 18.5-25 kg/m^2, within which the risks of ill health and premature mortality are

considered to be minimal [for review, see Jebb, 1999a,b and *Type II Diabetes*, 1996].

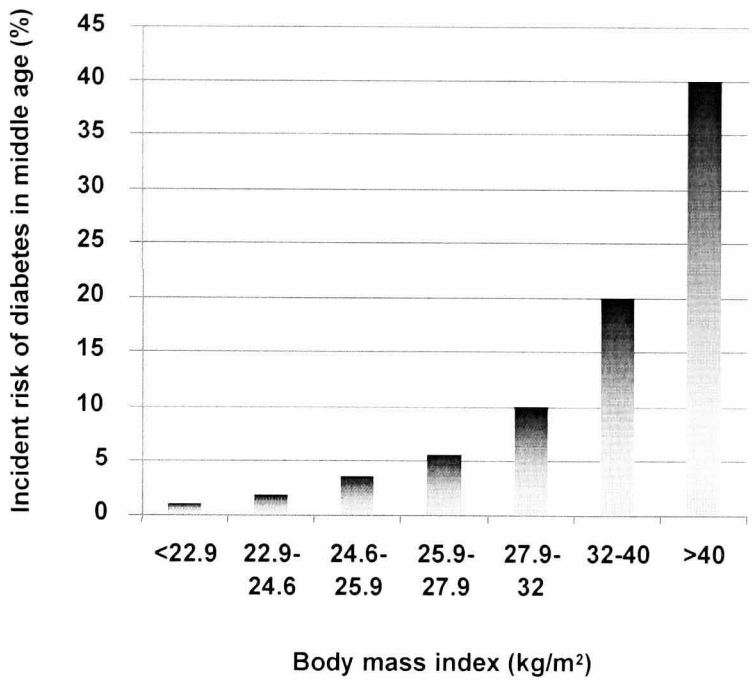

Figure 1.2. Relative risk of developing type 2 diabetes with increasing weight in middle-aged men. Adapted from Jebb S (1999) *The Weight of the Nation*; p. 8.

(a) Central obesity

Fat distribution is an important element in determining the risk of developing type 2 diabetes. Central obesity, also referred to as abdominal, visceral, upper-body or truncal obesity, puts people at greater risk for the disease than lower-body obesity. For this reason, although a high BMI is a good indicator of total body fat mass, it underestimates the power of the link between adiposity and type 2 diabetes. Hence, indicators of central obesity have been sought to provide a positive correlation with the disease development [Carey *et al.*, 1997; Ohlson *et al.*, 1985]. These include waist-hip ratio (WHR; Fig. 1.3) and waist circumference. The 'gold standard', however, for detecting excessive visceral fat deposition is computed tomographic (CT) scanning.

Central distribution of fat is associated with many pathogenetic factors that contribute to the disruption of normal glucose homeostasis. As mentioned above, these include high plasma FFAs, increased HGP and peripheral insulin resistance. Insulin resistance is probably fundamental to the link between obesity and diabetes, as it is specifically correlated, along with hyperinsulinaemia, with the amount of visceral adipose tissue. These two abnormalities presage the development of type 2 diabetes, and can accompany the pre-diabetic state of IGT [for review, see Gavin *et al.*, 1998 and *Type II Diabetes*, 1996].

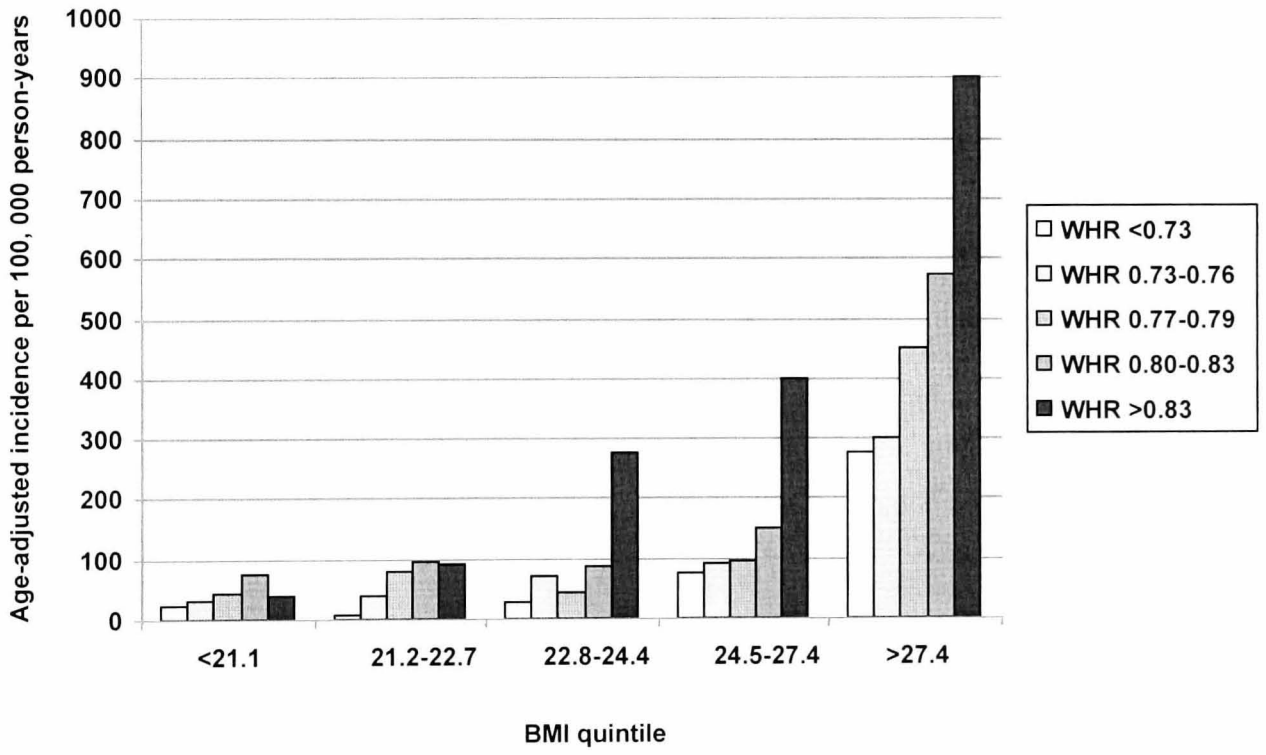

Figure 1.3. Age-adjusted incidence rates of type 2 diabetes per 100,000 person-years, cross-classified according to quintile of BMI and WHR. The shade in the bars identifies the WHR quintiles according to the key in each plot. Adapted from Carey *et al.* (1997) *Am J Epidemiol* **145**: 614-619

(ii) Progression from IGT to overt diabetes

The insulin secretory response which occurs after an acute secretagogue challenge (such as an intravenous or oral glucose bolus) can be resolved into an immediate first phase surge lasting a few minutes, followed by a slowly rising second phase which declines when the stimulus ends [Wilding & Williams, 1997]. Deviation from this

normal pattern is an indication of how far the diabetes has progressed in an individual.

When the blood glucose concentration is normal (70-100 mg/dL, or 4-6 mM), the insulin level in plasma is very low; the strongest stimulus for insulin secretion is an increase in the blood glucose level. The test of the strength of this response after drinking a solution containing 75 g of glucose is known as the oral glucose tolerance test [OGTT; Keen & Barnes, 1997], and it is described more fully in General Methods [2.2.3 (i)]. IGT is defined as plasma glucose levels during the OGTT that are intermediate between normal and diabetic values (2-hour value 7.0-11.1 mM; Fig. 2.2).

In the early stages of type 2 diabetes, insulin-stimulated glucose uptake in insulin-sensitive tissues, including adipose tissue, and particularly skeletal muscle, becomes impaired. This leads to the development of IGT, a state which may prevail for many years [DeFronzo, 1988], as the reduction in insulin sensitivity is compensated for by an increase in insulin secretion, thus preventing the development of marked hyperglycaemia. Not all individuals with IGT go on to develop diabetes [for review, see Gavin *et al.*, 1998], but of those that do, the ß-cells become 'exhausted', for reasons that are not fully understood, resulting in a fall in insulin secretion to normal or subnormal levels. In the presence of insulin resistance, this allows glucose levels to rise into the range of the uncontrolled hyperglycaemia observed in overt diabetes [Harris, 1996; Polonsky *et al.*, 1996; Fig. 1.4]. At this stage, HGP is increased [for review, see Gavin *et al.*, 1998].

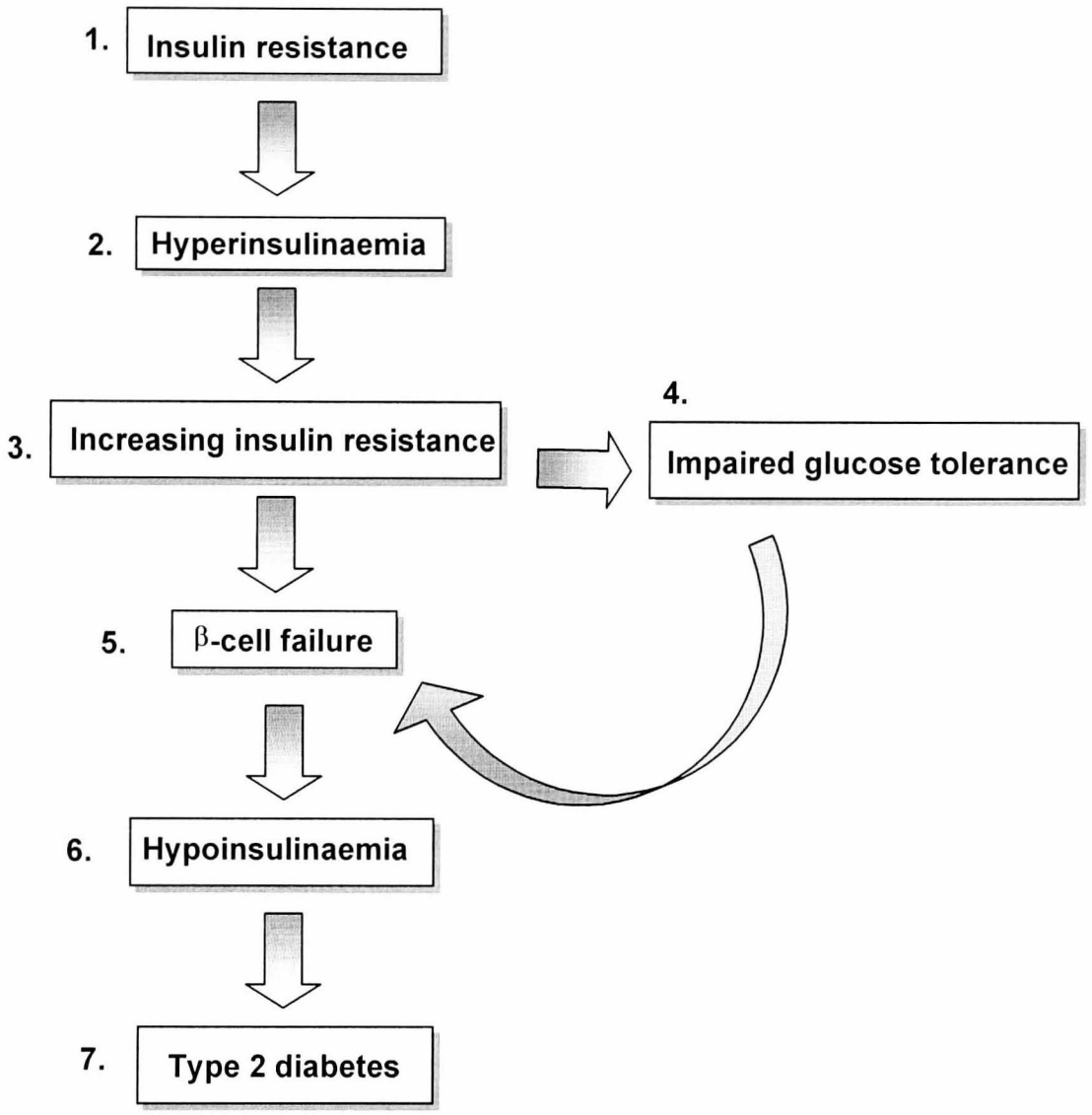

Figure 1.4. Relationship between IGT and insulin resistance in the pathogenesis of type 2 diabetes. Insulin resistance (i.e., resistance to insulin-stimulated glucose uptake, which may result from a genetic defect in glycogenesis in skeletal muscle) (1) leads to both slightly elevated blood glucose and insulin levels (2), even in non-obese individuals with normal glucose tolerance. The degree to which glucose tolerance deteriorates seems to be a function of the ability of the β-cell to compensate for the defect in insulin action. In the presence of raised plasma FFA concentrations in obese individuals and possibly a genetic defect in the β-cell, there may be a failure of the β-cell to secrete sufficient quantities of insulin in response to glucose, leading to further increases in fasting levels of plasma glucose and, hence, exacerbated insulin resistance (3); therefore, there is a further decline in glucose uptake and increased post-prandial plasma glucose (4). Insulin resistance also involves resistance to insulin suppression of elevated circulating FFAs, resulting in increased HGP in the diabetic individual and further exacerbating fasting hyperglycaemia. This, in itself, can impair β-cell function through glucose toxicity (5) and eventually lead to failure of β-cell compensation (6) and type 2 diabetes (7). Adapted from Reaven GM (1988) *Diabetes* **37**: 1595-1607 and Beck-Nielsen H & Groop LC (1994) *J Clin Invest* **94**: 1714-1721

(a) Mechanisms of progression from IGT to diabetes

(1) Genetic defects in the β-cell

Known genetic causes of β-cell dysfunction in type 2 diabetes account for only a few percent of all cases of the disease and are thought to disrupt three general aspects of β-cell function, namely glucose signalling, insulin secretion and insulin synthesis. The only mutations identified so far are in the following: the glucokinase gene (encoding the enzyme responsible for converting glucose, once it has been transported into the β-cell, into G-6-P); mitochondrial DNA; hepatocyte nuclear factor-1 alpha (HNF-1α), a transcription factor thought to regulate expression of insulin genes and development of type 2 diabetes [Lee *et al.,* 1998]; prohormone convertase 2 (a proinsulin processing enzyme); and the insulin gene itself.

Other possible sites and mechanisms of β-cell dysfunction are in the genes encoding GLUT-2, in the K^+-channel protein in the β-cell membrane, and in the deposition of IAPP [for review, see Matthews & Clark, 1997]. Study of animal models with genetic mutations in the leptin gene or its receptor have suggested that it may be the failure of leptin, a hormone produced by white fat in direct proportion to fat mass and which regulates food intake [for review, see Widdowson & Wilding, 1999], to inhibit insulin secretion from the β-cells that explains, in part, the development of hyperinsulinaemia and progression to type 2 diabetes in these models [Kieffer *et al.*, 1997]. This mechanism is less likely to be relevant in most human type 2 diabetes, where leptin and its receptor are normal. The inadequacy of compensatory β-cell mass expansion in response to insulin resistance appears to result from an increased rate of cell death by apoptosis, rather than a reduced proliferation or neogenesis [Pick *et al.*, 1998].

Finally, the underexpression of the insulin gene and impaired glucose-stimulated insulin secretion (GSIS) may be mediated by down-regulation of uncoupling protein-2 (UCP-2), a mitochondrial protein responsible for regulating energy balance in the pancreas, as well as in a variety of other tissues [see below, 1.3.3 (iii)]. This leads to a chronically decreased ATP:ADP ratio, which, in turn, inhibits the ATP-sensitive K^+ channels, part of the machinery required to oxidise long-chain FAs and dissipate energy thereby produced [Wang *et al.*, 1999]. Mutations in β-cell mitochondrial DNA, which encodes some of the polypeptides of the respiratory chain enzyme complexes, have been shown to lead to altered mitochondrial metabolism in diabetes characterised by impaired insulin secretion [Wollheim, 2000].

(2) The lipotoxicity theory

There is evidence to suggest that increased tissue levels of fatty acyl coenzyme A (FACoA), the precursor in the biosynthesis of lipids, causes the ß-cell abnormalities of type 2 diabetes. In uncomplicated obesity, there is a relative increase in plasma FFA levels and presumably in tissue levels of FACoA. This hyperlipidaemia may be a consequence of the expanded adipocyte mass and/or of insensitivity of adipocytes to the antilipolytic action of insulin. The presumed increase in tissue FFA levels throughout the body interferes with normal glucose metabolism. In tissues targeted by insulin, such as muscle, this interference is known as insulin resistance. These increased FFA levels in islets stimulate insulin secretion and induce β-cell proliferation and expansion of low-affinity glucose metabolism, increasing basal insulin secretion. At this stage, insulin resistance and insulin hypersecretion are

perfectly matched and glucose tolerance is normal, since FFA-induced changes in tissues are proportional to FFA levels.

In obesity that leads to diabetes, FFAs rise to still higher levels and tissues are 'marbleised', as FACoAs are increasingly esterified to TGs. In muscle, this intensifies insulin resistance, while islets are incapable of further increases in insulin secretion to match the insulin resistance. The FFA overload interferes with glucose metabolism and impairs the capacity of the β-cells to respond to post-prandial hyperglycaemia. Hyperinsulinaemia, at this point, no longer matches the increase in insulin resistance, and type 2 diabetes begins [Unger, 1995].

Although the exact mechanism of ß-cell impairment and eventual failure is unknown, there are suggestions that it may involve an apoptotic mechanism triggered by the induction of NOS and the overproduction of NO, which is cytotoxic to certain cell types, including ß-cells [Shimabukuro *et al.,* 1997b; Unger, 1997].

1.3.2. Epidemiology and the medical cost of obesity and diabetes

Type 2 diabetes mellitus is a common disease affecting more than 2% of overall populations in developed countries, and 10% of those over 70 years of age. It is a major cause of morbidity and mortality, shortening life expectancy by up to 8 years, and it is a major drain on health care resources. Estimates by the World Health Organization (WHO) suggest that its prevalence is likely to nearly double to 210 million people worldwide by the year 2010, largely as a result of the increase in obesity that is already occurring. Obesity is one of the fastest growing health epidemics in developed and developing countries, and its prevalence has increased over the last few decades to such an extent that it is now perceived by some health professionals to be an epidemic. In fact, if current trends continue, more than a

quarter of British adults will be obese within the next ten years. Indeed, body weight and weight change are emerging as the most important predictors of the likelihood of developing the disease, with the risk of developing type 2 diabetes being raised by up to 10-fold in people who are only mildly overweight.

To understand the epidemiology of obesity and diabetes, we must study the relationships of various factors determining the frequency and distribution of these conditions in the human community. Although, next to smoking, obesity is the most preventable cause of ill health in Britain, it is associated with increased risk of premature death and is estimated to account for 6-8% of direct health care budgets in developed countries, which translates into about £3.5 billion per year in the U.K. More than just a social or cosmetic issue, obesity is a risk factor for chronic diseases which are the principal causes of death in the U.K., including heart disease, stroke and some cancers. It is also responsible for conditions which reduce quality of life. These can be metabolic, including hypertension, respiratory disorders, infertility and diabetes; mechanical, such as arthritis, lower back pain and sleep difficulties; and psychiatric, namely depression. Its rapid rise in the U.K. (Fig. 1.5) parallels that in the U.S.A., with a time lag of about 15 years, indicating that it is not a self-limiting problem. There has also been a pronounced shift in the population distribution towards greater body weights, whilst the proportion of people of relatively low weights remains largely unchanged.

Individual behaviours are critically important in determining the long-term risk of obesity. Not only does overeating associated with a high-fat diet and sedentary lifestyle contribute to the population-wide increase in this disease, but subjects notoriously under-report the true extent of their dietary intake [for review, see Jebb, 1999a,b and Prentice, 1998].

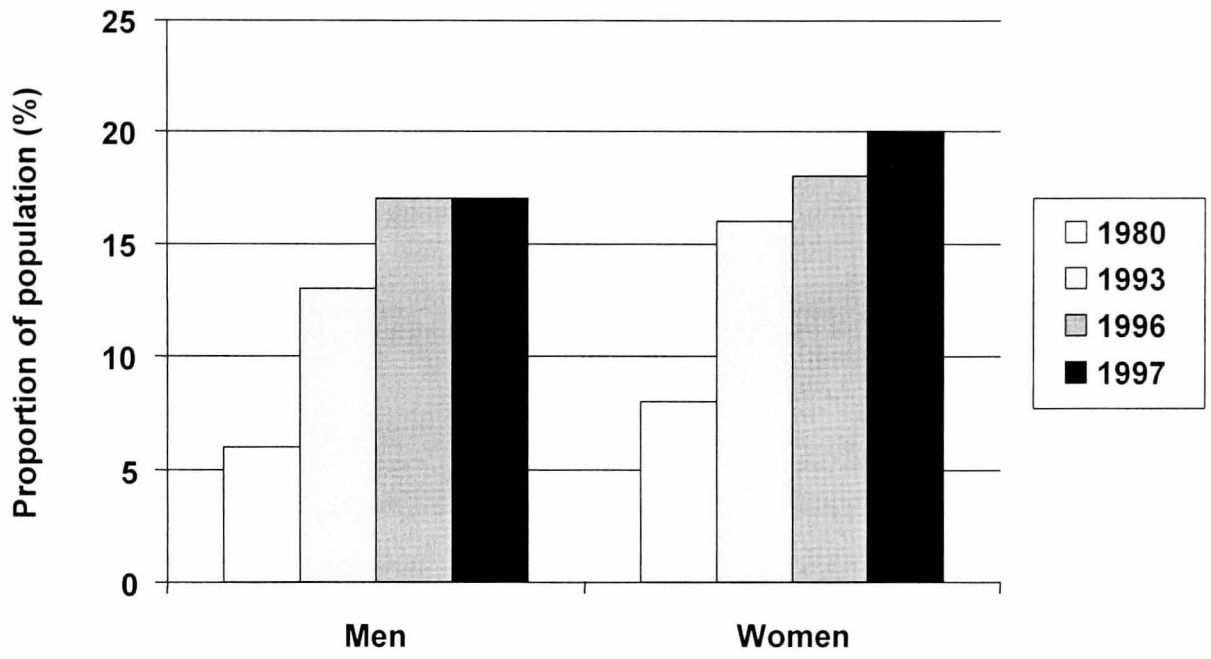

Figure 1.5. Prevalence of clinical obesity in the U.K. Adapted from Jebb S (1999) *The Weight of the Nation*; p.5.

1.3.3. Molecular influences on obesity and diabetes

Profound obesity can result from defects in a few major genes at single loci. These govern the production of key signalling molecules involved in a regulatory system of hypothalamic neuronal circuits controlling food intake and having relatively large effects on fat mass. Identification of these has required the recruitment of morbidly obese families and the establishment of their DNA profiles. The rarity of such defects in humans has encouraged the study of various mutations in animal (mostly rodent) models of obesity and type 2 diabetes, discussed in later sections [1.5.1 and 2.1.2 (i)], which have allowed for much insight to be gained in this field through more practical means.

(i) Peripheral adiposity signals

The signalling pathways controlling food intake are regulated in turn by hormones released from peripheral tissues in response to food ingestion. These signal the brain in a feedback loop to match energy intake to energy output, thus controlling energy stores both acutely and in the long term. These include the classic adipogenic hormone, insulin, and the more newly discovered members of the cytokine family, leptin and tumour necrosis factor-alpha (TNFα).

(a) Leptin

Leptin is an adipocyte hormone that regulates the size of the adipose tissue mass. The *OB* (obese) gene which encodes leptin was cloned in 1994 [Zhang *et al.*, 1994], and its discovery was soon followed by the cloning of the *DB* (diabetes) gene, which encodes its receptor [Chua *et al.,* 1996]. Leptin binds to receptors which exist in different forms, and which reside in its major site of action, the hypothalamus. Intrahypothalamic injection of leptin lowers body weight by decreasing food intake and increasing thermogenesis [Vaisse *et al.,* 1996], the dissipation of excess food energy as heat.

Families have been found to have monogenic forms of obesity resulting from a mutation in the leptin receptor gene, validating the role of leptin in regulating body weight in humans. These patients have been identified with a homozygous mutation which results in a truncated leptin receptor lacking both transmembrane and intracellular domains. A mutation in the gene encoding leptin itself has also been observed in some patients, such that a dysfunctional hormone enters the circulation, even though the receptor is intact. However, studies of susceptibility genes suggest that the *ob* and *db* loci do not play a major role in more common forms of obesity,

but, nevertheless, their influence in the polygenic background of obesity cannot be excluded. Many obese animals and humans have high circulating levels of leptin and may be leptin-resistant. How this arises is undergoing active research [for review, see Clément, 1999, Jebb, 1999a and Tremblay *et al.,* 1999].

(b) Insulin

Like leptin, insulin is a long-term regulator of body weight [Wilding *et al.,* 1997] and circulates at levels proportional to body fat content, entering the central nervous system (CNS) in proportion to its plasma concentration. Its receptors are also expressed by brain neurons involved in energy intake, and its administration directly into the brain reduces food intake, whereas its deficiency has the opposite effect. There is increased insulin secretion as obesity progresses and this is hypothesised to increase insulin delivery to the brain, where it helps to limit further weight gain.

In contrast to leptin, however, obesity is not induced by insulin deficiency, even if food is consumed in large amounts, because insulin promotes both fat storage and leptin synthesis by fat cells; for example, in uncontrolled diabetes, the disease is characterised by insulin deficiency, food intake is increased markedly, but levels of body adiposity and plasma leptin remain low. Because of this, diabetic hyperphagia could potentially result from reduced CNS signalling by low levels of insulin or leptin or both. However, replenishing leptin to non-diabetic levels in animal models of type 1 diabetes prevents hyperphagia, suggesting that leptin has the more critical role in energy homeostasis [for review, see Schwartz *et al.,* 2000].

(c) Tumour necrosis factor-alpha

Tumour necrosis factor-alpha (TNFα) is another cytokine secreted by white adipose tissue (WAT). It induces insulin resistance by down-regulating the signal transduction of the insulin receptor by inhibiting its tyrosine kinase activity and by decreasing the expression of GLUT-4 glucose transporters in muscle and fat. It also reduces LPL activity in WAT and stimulates hepatic lipolysis, thereby counteracting metabolic effects of insulin [for review, see Halle *et al.,* 1998]. Its receptors are overexpressed in the adipose tissue of genetic models of obesity, with or without accompanying diabetes [Hotamisligil *et al.,* 1993] and in that of humans. Indeed, weight reduction which results in improved insulin sensitivity is associated with decreased TNFα mRNA expression [Hotamisligil *et al.,* 1995], and its plasma levels are dependent on the amount of visceral (intra-abdominal) fat, especially known to be associated with insulin resistance [Bertin *et al.,* 2000]. Leptin treatment decreases TNFα expression by 40% in young rats; therefore, leptin regulates TNFα expression in adipose tissues [Qian *et al.,* 1998]. TNFα may also play a role in control of adipocyte number and adipocyte mass, as it induces apoptosis in culture adipocytes; perhaps beyond a critical point, this mechanism is not able to deal with increased fat mass, and obesity then develops [for review, see Nisoli & Carruba, 2000].

Abrogation of TNFα action in TNFα-knockout (KO) mice completely prevents insulin resistance resulting from diet-induced obesity [see below, 1.5.1 (ii) (a)] and the leptin mutation. This occurs through the lowering of circulating levels of FFAs and amelioration of the obesity-related reduction in insulin receptor signalling in muscle and fat. Higher GLUT-4 protein levels are also observed in the muscle tissue of this model [Uysal *et al.,* 1997], further supporting a role for this molecule in insulin resistance.

In contrast to fat, skeletal muscle does not become insulin resistant in response to short-term exposure to TNFα [Nolte *et al.,* 1998]. Both acute and chronic treatment with TNFα upregulates glucose uptake activity in human muscle. Therefore, in conditions of TNFα excess, it may serve as a compensatory mechanism in the insulin resistance of type 2 diabetes [Ciaraldi *et al.,* 1998]. Its effects in muscle suggest that it may also play a role in energy expenditure; for example, TNFα administration also results in increased UCP-2 and UCP-3 mRNA in rat skeletal muscle, suggesting, therefore, a possible mechanism for cytokine-induced thermogenesis [Busquets *et al.,* 1998].

(d) Resistin

Resistin is a newly discovered unique signalling molecule secreted by adipocytes which appears to link obesity with type 2 diabetes. Its circulating levels are increased in rodent models of obesity, in which administration of an anti-resistin antibody improves blood glucose concentration and insulin action. Moreover, treatment of normal mice with recombinant resistin impairs glucose tolerance and insulin action. Insulin-stimulated glucose uptake by adipocytes is enhanced by neutralisation of resistin and is reduced by resistin treatment [Steppan *et al.,* 2001]. A summary of the effects of these peripheral obesity signals in the development of type 2 diabetes is presented in Fig. 1.6.

(ii) Central neuropeptide mediators of adiposity signals

Several hypothalamic neuronal circuits, distinguished by the neuropeptide signalling molecules they contain, have been discovered, indicating the sheer complexity of the food intake process. Some of these candidate mediators of leptin and insulin are

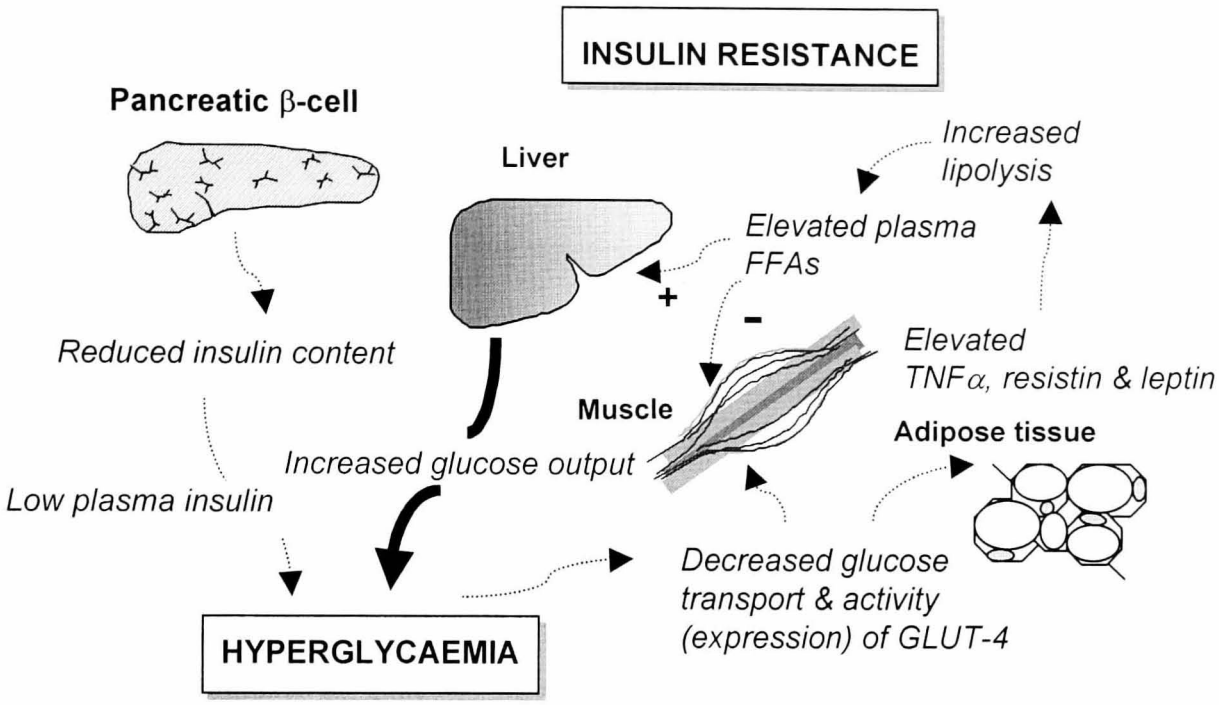

Figure 1.6. Influence of peripheral adiposity signals on type 2 diabetes. As introduced in Fig. 1.4, the interaction of insulin resistance and relative insulin deficiency result in IGT and type 2 diabetes, although which is the primary defect is debatable. Insulin-stimulated glucose uptake and, therefore, utilisation in liver, skeletal muscle and fat is impaired and coupled to impaired suppression of HGP. Fat cells in the insulin resistance of type 2 diabetes are larger than in normal subjects, producing increased amounts of FFAs and the two cytokines, TNFα and leptin, all of which lead to insulin resistance in the liver and skeletal muscle. This results in a need for increased peripheral insulin, which is generated by the β-cells of the pancreas. FFAs inhibit glucose uptake into skeletal muscle (-) and enhance HGP from the liver (+), raising blood glucose concentrations to above normal levels. Until recently, it appeared that FFAs would provide the link between obesity and diabetes, but the fact that adipocytes secrete numerous peptides has led to speculation regarding other possible molecular mechanistic links. TNFα and leptin are both overexpressed in adipocytes of obese people. Whereas TNFα can cause insulin resistance through effects on insulin-mediated cellular signalling pathways, it is not yet clear how alterations in leptin might affect insulin resistance. In contrast to rodents in which leptin deficiency leads to obesity, leptin levels in most obese people are higher than normal. Resistin, therefore, may provide the adipocyte-derived key mediator of insulin resistance. Although it suppresses insulin's ability to stimulate glucose uptake into adipocytes, it is not known whether it also acts on important physiological targets such as muscle and liver. Adapted from Turner NC & Clapham JC (1998) *Prog Drug Res* **51**: 33-94, Flier JS (2000) *Nature* **409**: 292-293 and Kahn CR *et al.* (2000) *J Clin Invest* **106**: 1305-1307.

orexigenic, meaning that they stimulate food intake, and prominent among these is neuropeptide Y (NPY) [for review, see Schwartz *et al.*, 2000].

(a) Orexigenic signals

(1) Neuropeptide Y

Neuropeptide Y (NPY) is also an anabolic peptide involved in the promotion of positive energy balance from its major site of synthesis in neurons of the arcuate nucleus (ARC) at the base of the hypothalamus. These project throughout the hypothalamus, notably to the paraventricular nucleus (PVN) and perifornical area (PFA), where NPY is released from synaptic terminals.

Experimental manipulations with NPY show that it stimulates food intake. NPY increases food intake through its interaction with a unique NPY receptor, Y5, pharmacologically distinct from other known NPY receptors and expressed largely in the hypothalamic structures associated with feeding. NPY profoundly inhibits thermogenesis, as well as increasing pancreatic insulin secretion via the vagus nerve, to the point of hyperinsulinaemia, shifting the animal toward obesity, through excessive energy intake and storage of excess calories as fat through lipogenic actions of insulin. The corollary of this, that hypothalamic NPY neurons are activated and NPY synthesis in the ARC enhanced in conditions of negative energy balance, suggest that its role is to restore body energy stores; e.g., NPY concentrations are elevated during starvation, food restriction and type 1 diabetes. Indeed, the hyperphagic response to type 1 diabetes is accompanied by increased hypothalamic NPY synthesis and release. Thus, as depletion of fat stores and reduced leptin/insulin signalling to the brain increases NPY expression and secretion in the

hypothalamus, it stands to reason that leptin also inhibits ARC NPY gene expression [for review, see Schwartz *et al.,* 2000; Wilding *et al.,* 1997].

NPY-KO mice that are also homozygous for the leptin mutation (*ob/ob*) show reduced hyperphagia and obesity, indicating that the full response to leptin deficiency requires NPY signalling. That mice lacking NPY, but otherwise genetically normal, have intact feeding responses, raises questions about the need for NPY when leptin and insulin levels are normal. Congenital absence of such a major neuropeptide may elicit compensatory responses by other anabolic effector signalling molecules, masking consequences of NPY deficiency. Examples of these are the following: Melanin-concentrating hormone (MCH) is another orexigenic peptide, which, along with NPY, is located in the lateral hypothalamic and perifornical areas (LHA and PFA). Its synthesis is also elevated by energy restriction and leptin deficiency, and MCH-KO mice have reduced food intake and are excessively lean [for review, see Schwartz *et al.,* 2000]. Galanin is another peptide found at high concentrations, as are its receptors, in the PVN. It also stimulates feeding and reduces energy expenditure, although both are short-lived responses, and, unlike with NPY, chronic administration of galanin does not induce obesity [for review, see Williams & Wilding, 1997]. In studies of adrenalectomised rats, weight gain is prevented and the effects of NPY are attenuated, suggesting that under normal circumstances, glucocorticoids may be important as permissive agents for NPY [Wilding *et al.,* 1997].

(2) Orexin

The two forms of the orexin peptide, A and B, are also considered candidate anabolic effector signalling molecules. Like NPY, they are down-regulated by adiposity

signals [for review, see Schwartz *et al.*, 2000]. Orexigenic neurons are implicated in feeding behaviour, as they are distributed in the LHA and are innervated by leptin-responsive cells residing in the ARC. They receive terminal appositions from neurons expressing NPY, as well as agouti-related peptide (AGRP) and alpha-melanocyte stimulating hormone (α-MSH), an anabolic and catabolic peptide, respectively, described below. In turn, orexin neurons themselves send fibres to neurons expressing NPY, AGRP and pro-opiomelanocortin (POMC) mRNA [from which α-MSH is derived, as described below; see 1.3.3 (ii) (b) (1)].

When administered by the intracerebroventricular (ICV) route, orexin-A stimulates food consumption. Application of various tools give support to the physiological role of this peptide, namely an antagonist at one of its receptors (OX_1) and antibodies raised against OX_1 and orexin-A itself. These all inhibit feeding. Orexin mRNA is also up-regulated by fasting, suggesting its expression is regulated by an animal's nutritional status.

Although orexin is weaker than other stimulants of food intake, chiefly NPY and AGRP, its supplementary role as a mediator of appetite should not be underestimated. It appears to play an important role particularly in situations in which the demand for food is high, as enhanced hypothalamic or gut expression of orexin mRNA occurs during fasting or hypoglycaemia. Although orexins play no part in mediating the obesity of animals that have a defective leptin system, it does appear that reduced orexin synthesis may play a role in the hypophagic response to leptin [for review, see Arch, 2000].

(b) Anorexigenic signals

Opposing the effects of central orexigenic signals are a wide range of neuropeptides that suppress food intake, and, hence, are termed anorexigenic.

(1) Melanocortins

The melanocortin system is remarkably complex and important to energy homeostasis. Like all catabolic systems, it suppresses food intake and promotes negative energy balance, and the neuronal synthesis of its component peptides increases in response to increased adiposity signalling in the brain [for review, see Schwartz *et al.,* 2000]. In addition to the peptides themselves, derived from the N-terminal region of POMC, their antagonists and receptors have also been strongly implicated in body weight regulation.

There are two ligands which act on the melanocortin 4 receptor (MC4-R), and their actions oppose each other. They are α-MSH, derived from POMC and a high-affinity agonist of MC4-R, and AGRP, expressed in neurons distinct from those producing POMC, and antagonising the activation of MC4-R by α-MSH. Neurons expressing both are located in the ARC. Accordingly, transgenic mice overexpressing AGRP are hyperphagic and obese, and leptin links the melanocortin system and regulation of food intake by modulating the expression of both POMC and AGRP in the ARC. Decreased leptin levels, as seen in the *ob/ob* mouse or the fasting state, reduce POMC expression and dramatically increase AGRP expression in this nucleus. Since both POMC and AGRP neurons project to the MC4-R-expressing PVN, this leads to inactivation of the receptor and an increase in food intake [for review, see Vaisse, 1999]. Families have been found to have monogenic

forms of obesity resulting from mutations in the MC4-R gene, validating the role of MC4 in human obesity [for review, see Clément, 1999].

(2) Corticotropin releasing factor

Corticotropin releasing factor (CRF), or hormone (CRH), is a peptide expressed in the PVN, from which it regulates adrenocorticotropic hormone (ACTH) secretion. It is suggested that it has an opposing influence on NPY, as its injection into the PVN causes weight loss by reducing appetite and stimulating thermogenesis. Furthermore, CRF mRNA expression is decreased in conditions of energy deficit such as type 1 diabetes. Indeed, there is evidence of synaptic connections between CRF and NPY neurons in the PVN [Wilding *et al.,* 1997]. This balance between mutually antagonistic NPY and CRF may regulate energy homeostasis. In fasting and type 1 diabetes, CRF mRNA levels fall, while NPY mRNA rises, and there is evidence that CRF neurons are underactive in the hypothalamus of the fatty Zucker rat [for review, see Williams & Wilding, 1997], an animal model of insulin resistance described in a later section [1.5.1 (a)].

(3) Glucagon-like peptide-1 and -2

Glucagon-like peptide-1 and -2 (GLP-1 and -2) are both products of the pre-proglucagon gene expressed in both gut and CNS. GLP-1 reduces food intake when injected ICV, and its receptors are found in appetite-regulating areas of the CNS, such as the PVN. Although it is released into the circulation after a meal, it does not alter feeding when peripherally administered [Wilding *et al.,* 1997; for review, see Williams & Wilding, 1997], suggesting that it is synthesised in the CNS in response to other peripheral signals.

Recently, GLP-2 has been found to be expressed in the nucleus of the solitary tract (NTS) in the brainstem and released onto target neurons in the dorsomedial hypothalamic nucleus (DMH), another area regulating food intake. GLP-2 behaves like GLP-1 by inhibiting food intake [Tang-Christensen *et al.,* 2000].

(4) Serotonin

The serotonin (or 5-hydroxytryptamine, 5-HT) system is also comprised of cell bodies in the brainstem that project widely throughout the brain, but its inhibitory actions on food intake are localised to the PVN and the ventromedial hypothalamic nucleus (VMH). This system is the primary target of several centrally acting drugs developed for obesity treatment such as sibutramine, a monoamine re-uptake inhibitor which elevates the synaptic concentration of 5-HT.

Leptin increases 5-HT turnover, raising the possibility that some of leptin's weight-reducing effects are mediated through enhanced 5-HT signalling [for review, see Schwartz *et al.,* 2000; Wilding *et al.,* 1997]. Following intrahypothalamic injections, 5-HT inhibits food intake, and these actions may be mediated partly through the NPY pathway, as suggested by predicted alterations in hypothalamic NPY expression and neuronal activity after 5-HT pharmacological manipulation.

In particular, it is the 5-HT_{2C} receptor subtype which is implicated in the process of food intake suppression, as food intake and body weight are increased in the 5-HT_{2C}-KO model. Therefore, maintenance of normal energy homeostasis seems to require intact serotonin signalling; however, obesity in this model is modest, especially when compared to the phenotype of mice lacking MC4 or leptin receptors. On the other hand, leptin-induced anorexia is intact in this model, indicating that

leptin's ability to reduce food intake does not require signalling at this receptor subtype [for review, see Schwartz *et al.,* 2000].

(iii) Uncoupling proteins

One of the ways in which energy is expended is through the production of heat (thermogenesis), and abnormalities in this process result in obesity. Energy dissipation is regulated at the molecular level in mitochondria, the organelles which convert food to carbon dioxide, water and ATP. Uncoupling proteins (UCPs) are a family of proteins located on the inner membranes of mitochondria and are distinguished by their expression in different tissues. It appears likely that they all have heat-producing activity and act by dissipating the mitochondrial proton gradient produced by the respiratory chain [for review, see Boss *et al.,* 1998 and Lowell & Spiegelman, 2000].

(a) Cold-induced adaptive thermogenesis

UCP-1 is a mitochondrial inner membrane protein that uncouples proton entry from ATP synthesis, especially in the presence of FFAs. This results in energy being released in the form of heat instead of ATP, a process known as adaptive thermogenesis, and it is influenced by environmental temperature and diet. When this adaptation is perturbed and energy intake exceeds energy expenditure, obesity results. UCP-1 is uniquely found in brown adipose tissue (BAT), which is heavily innervated by sympathetic nerves and is responsible for much of thermogenesis during cold exposure in rodents. Stimulation of β-adrenergic receptors expressed on brown adipocytes by cold exposure or pharmacological agents has both acute and

chronic effects on UCP-1, including increased activity and protein levels as well as hypertrophy of BAT.

(b) Diet-induced adaptive thermogenesis

Diet-induced thermogenesis (DIT) evolved primarily as a mechanism that 'wastes' energy by converting excess food energy directly to heat. This allows animals to eat large quantities of poor-quality diets in order to obtain a sufficient intake of essential nutrients without being burdened by the deposition of excess, non-essential energy as fat. This improves the nutritional quality of the diet, such that the rate of DIT is elevated only when the diet is unbalanced, either above or below requirements, and is minimal when the diet is nutritionally adequate.

Therefore, one role of DIT in energy balance regulation is of resistance to obesity, but this is secondary to its role as a mechanism to ensure an adequate supply of essential nutrients. This protective adaptation against obesity induced by overfeeding is influenced by genetic background. Abnormal responses to diet arising because of this background could contribute to the development of obesity. Thus, when people consume a well-balanced diet, it may be hard to detect high levels of DIT, and, on top of this, there is great inter-individual variation in energy efficiency, such that some gain weight easily and some do not. Once again, we see that there is both a genetic and environmental basis for susceptibility to obesity [for review, see Stock, 1999 and Lowell & Spiegelman, 2000].

Evidence for BAT being important in DIT in rodents is strong, as they have discrete deposits of this tissue. Perhaps surprisingly, however, DIT continues to be manifested by mice without BAT. Ablation of BAT is carried out using a transgene which causes diptheria toxin to be expressed with UCP-1 (UCP-DTA mice). These

mice develop obesity and insulin resistance [for review, see Bailey & Flatt, 1997], whereas UCP-1-KO mice with intact BAT do not, suggesting the existence of alternative thermogenic effectors in BAT. In fact, two homologues of UCP-1 have been identified, UCP-2 and UCP-3. UCP-2 is expressed in most tissues, whereas UCP-3 is predominantly found in BAT and skeletal muscle. The fact that adult humans, in contrast to rodents, do not have BAT depots but do have skeletal muscle making up to 40% of total body weight, which is endowed with significant mitochondrial capacity, has encouraged recent investigations into this tissue as a contributing site of adaptive thermogenesis.

As all UCPs are found in BAT and all have proton transport activity, it has been suggested that they could all contribute to adaptive thermogenesis, but some observations argue against this: For example, although UCP-1-KO mice are predictably cold-sensitive, they are not obese. This shows that UCP-1 is either not essential for body weight control, or that its absence can be compensated for by other proton-dissipating pathways. Indeed, in this model, UCP-2 mRNA expression is elevated in BAT. Therefore, functional BAT with UCP-2 may be sufficient to prevent obesity [for review, see Boss *et al.,* 1998]. Also, the expressions of both UCPs –2 and –3 paradoxically increase with starvation, a state known to be associated with a decrease in energy expenditure. Thus, whether UCP-2 and –3 have a protective role against obesity is an area of active investigation at present [for review, see Lowell & Spiegelman, 2000].

(iv) Satiety signals

The amount of food consumed during individual meals, or the frequency of meals, or both, must be regulated if energy homeostasis is to be achieved. The major

determinant of meal size is satiety, a biological state induced by neurohumoral stimuli generated during food ingestion that leads to meal termination. It is proposed that afferent input related to satiety from the liver, GI tract and humoral signals are transmitted through the vagus and sympathetic fibres to the NTS where they are integrated with descending hypothalamic input from pathways involved in energy homeostasis.

Cholecystokinin (CCK), synthesised within the gut wall and released into the portal cirulation, particularly in response to the presence of FAs within the gut, has long been suggested as one of these humoral signals. There is evidence supporting its role in controlling meal size and meal termination in animals and humans. It decreases food intake when injected peripherally or centrally, and blockade of its receptors, found in both the GI tract and CNS, increases food intake by delaying the onset of satiety in rats. CCK also stimulates receptors on the vagus nerve, which sends signals to the brain stem (probably the area postrema), and, thus, to other appetite-regulating areas such as the PVN, where CCK acts as a neurotransmitter [Wilding *et al.*, 1997].

The pancreatic peptide, bombesin, has also been proposed as a satiety factor. At physiological concentrations, it reduces satiety in humans and rodents, and its action can be blocked by disconnection of the sympathetic nerve supply to the gut combined with vagotomy. Furthermore, food intake is increased when a bombesin antagonist is administered [Wilding *et al.*, 1997].

In addition to exerting control over feeding behaviour from various brain loci, orexins and their receptors may also play a role in regulating satiety peripherally. They are present in the enteric nervous system, and the endocrine cells of the gut and

pancreas. Orexin-A, in particular, stimulates gut motility, insulin secretion and, when given centrally, gastric acid secretion [for review, see Arch, 2000].

1.3.4. Environmental factors influencing obesity and diabetes

It used to be highly likely that a seriously obese person would have a genetic susceptibility to this condition, perhaps resulting from a major gene defect or cluster of minor gene variants. However, gene defects cannot account for the epidemic increases in obesity, because gene pools have remained essentially constant. Monogenic disorders (single gene mutations), such as those present in some small animals, that would explain profound obesity in humans, are very rare. It appears more likely that body weight is under the control of a multitude of genes; i.e., that obesity is a polymorphic genetic disorder (Fig. 1.7). Yet the presence of genetic variation *per se* is not sufficient to explain the clinical expression of the disorder, and probably requires interaction with other factors, including environmental ones. Although the limitations of an unfavourable genetic background may explain why some obese people remain overweight even while maintaining a healthy lifestyle, genuine genetic susceptibilities are being obscured by the sheer volume of lifestyle-driven obesities.

Lifestyle changes have involved a sharp decline in energy requirements due to reduced physical activity in both leisure pursuits and jobs. Although this implies that adherence to a healthy diet and levels of activity should bring about weight loss in obese people, the observation is that it rarely results in weight loss to match that of lean controls. At least four reasons may account for this observation: (1) unknown genetic factors, (2) weight cycling, which permanently affects the regulation of energy balance such that obese people can never comfortably recover the body

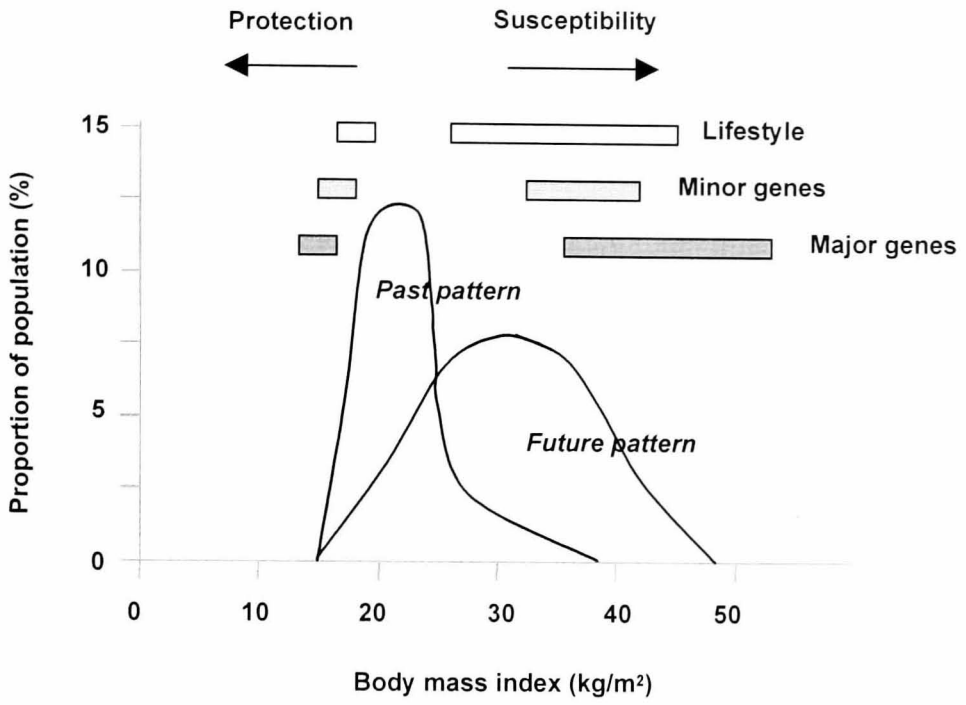

Figure 1.7. A schematic illustration of the changing role of genetic and lifestyle influences on obesity. Adapted from Prentice A (1998) *Obesity matters* **1**: 17-20.

weight level of the pre-obese state, (3) stress and (4) pollution. Stressful life conditions may give rise particularly to depression, the mechanistic side of which involves increased circulating levels of stress hormones (corticosteroids), which promote food intake and decrease thermogenesis, both favouring a positive energy balance. The additional burden imposed on adipose tissue by a polluted environment comes through the use of organochlorine compounds, used as pesticides and fire retardants. Extremely stable and lipophilic, they are absorbed from food and accumulate in the fat compartment over an organism's lifetime. Thus, fat gain may be a protective adaptation, attenuating vulnerability to stress and allowing for storage of pollutants which are otherwise carcinogenic if released in the plasma. However, it may be misleading to think of this as a *cause* of obesity.

Thus, the concept of genetic susceptibility has lost value and attention has turned to those people who seem genetically resistant to weight gain [for review, see

Clément, 1999; Jebb, 1999a; Prentice, 1998 and Tremblay *et al.,* 1999]. This concept has been studied in detail in dietary obese rodent models by Levin and colleagues, and is discussed below [1.5.1 (ii) (a) (2)].

(i) The influence of affluence and the 'Western' lifestyle

In addition to the profound increase in sedentary lifestyles since WWII, another specific behavioural risk factor for weight gain has emerged: This is the consumption of a diet containing a high proportion of fat and low proportion of carbohydrate. It has been suggested that availability of high-energy, high-density fatty foods, the composition of which is manipulated by the food industry, circumvents normal appetite control mechanisms. Because fat has more than twice as many calories as carbohydrate (9 *vs* 4 kcal/g), a high-fat/low-carbohydrate food is more energy-dense than a high-carbohydrate/low-fat food of the same weight. Thus, foods rich in fat promote 'passive over-consumption' because they are low in bulk and, therefore, are unable to satisfy the desire for food, and because they are often highly palatable. People do not necessarily eat more of this type of food in terms of volume, but they do eat more calories. Further exacerbating this situation, the energy costs of digesting and storing fat are smaller than for any other macronutrient. Not only is dietary fat converted to body fat with minimal wastage of energy, but the body has an innate preference to burn carbohydrate rather than fat, such that increases in carbohydrate intake cause an increase in carbohydrate oxidation, but increases in fat intake fail to elicit a compensatory increase in fat oxidation [for review, see Jebb, 1999a].

Obesity is associated with increasing affluence in transitional countries or societies, and this is gradually replaced with an inverse association between obesity

and social class and level of education [for review, see Jebb, 1999a and Tremblay *et al.,* 1999]. Type 2 diabetes itself affects at least 2% of Western populations. Its prevalence is low (less than 1%) in many developing societies (e.g., rural Papua New Guinea) and very high (40-50%) in certain groups which have undergone rapid Westernisation; for example, the Pima Indians of Arizona and certain Pacific Islanders. In the early 20th century before they were forced to abandon their traditional farming lifestyle, diabetes was rare amongst the Pima Indians. Longitudinal studies of this population have shed light on the heritability of different defects in the disease. They previously survived in the Arizona desert despite periodic droughts. In the last century, diversion of their water supply resulted in famine; agriculture in the desert was abandoned and their diet altered from naturally grown foods to commercially grown produce. Levels of physical activity also declined. With these lifestyle changes, the prevalence of obesity and type 2 diabetes has risen to be the highest known in the world. Presently, over 75% of adults are obese, and 45% have type 2 diabetes. Thus, the Pima Indians exemplify the 'thrifty gene' hypothesis, a theory which accounts for genetic predisposition to obesity and type 2 diabetes [for review, see Bowen Jones & Gill, 1997b and Jung, 1997] by suggesting that certain people are able to rigidly guard a set body weight in the face of a limited nutritional supply.

1.4. Energy homeostasis

1.4.1. Definition of energy balance

Although obesity is a multi-factorial condition, weight gain will only occur when energy intake exceeds energy expenditure; i.e., maintenance of a healthy body weight requires a balance between the calories actually needed by the body and those

consumed as food and drink. Thus, the body obeys a fundamental law of thermodynamics. In practice, energy imbalance is usually reached quite insidiously, with significant weight gain occurring over many years, reflecting an average caloric imbalance of only 1-2% each day [for review, see Jebb, 1999a].

1.4.2. Hervey's theory

In 1969, Hervey proposed a theory of energy balance regulation, the 'lipostatic hypothesis', in which the amount of fat in the body would be measured as the store of energy in the body. Any difference between energy intake and output would alter this store by a corresponding amount. This store would have some internal quantity which would reflect the current state of energy balance and monitor it, showing a response to sudden disturbances. The level of the store would also integrate all past changes over an indefinite period and include a 'sensing' side, or means by which this information could be transmitted to the hypothalamus.

Hervey first proposed that a steroid could fulfil the criteria of a suitable hormonal feedback signal which might act as the internal quantity: Steroids are soluble in plasma, persisting in the body for a long time, and their concentration in plasma varies inversely to their concentration in fat. When steroids are given experimentally, the hypothalamus responds by causing the animal to increase its food intake [Hervey, 1969].

Cabanac and Richard (1996) then refined Hervey's set-point hypothesis of body weight to propose that long-term stability of body weight is dependent on the concentration of glucocorticoids in the blood. Because these are soluble in lipids, it follows that low fat stores will increase their circulating concentrations, and high fat stores will lower them. The set point of body weight could also be adjusted by

intracerebral CRF [see 1.3.3 (ii) (b) (2)]. However, since then, leptin has been discovered as an alternative circulating signal of lipid mass.

1.4.3. Evolutionary importance of energy balance

Genes involved in body weight act through the control of food intake rather than energy expenditure, such that the body has evolved to conserve energy in times of shortage. Although energy-efficient individuals, such as the Pima Indians, in an environment where food was scarce would once have survived because of adequate fat stores, they are no longer at an advantage in a modern world where the problem is more one of over-nutrition [for review, see Jebb, 1999a]. The adaptive value of decreasing energy expenditure when food intake is limited is obvious. However, this response is counter-productive during dieting, contributing importantly to the poor long-term efficacy of this treatment for obesity [for review, see Lowell & Spiegelman, 2000].

1.5. Animal models of energy imbalance

1.5.1. Rodent models of positive energy balance: obesity, insulin resistance and type 2 diabetes

Much of our knowledge of conditions of energy imbalance and how these perturb adiposity signalling systems is provided by animal models. Models of type 2 diabetes in particular are widely used in the preclinical evaluation of new anti-diabetic drugs. Syndromes of glucose intolerance and type 2 diabetes can occur spontaneously or be induced experimentally, including transgenically, in various species, including rodents, rabbits and monkeys, but no single syndrome faithfully mimics human type 2 diabetes. However, all animal models of type 2 diabetes have in common disturbed

ß-cell function, notably manifested as defects in insulin secretion and in the ß-cell itself, many of which appear to be caused by the glucose toxicity of hyperglycaemia. In almost all of these syndromes, insulin resistance is the important aetiological factor, developing initially in skeletal muscle and liver, while fat remains relatively insulin-sensitive, such that TG deposition is favoured under the influence of high insulin levels, and becoming resistant later. Peripheral insulin receptor numbers are reduced probably in response to hyperinsulinaemia, but defects in post-receptor signalling, possibly contributed to by increased expression of TNFα in WAT, are probably more important in determining insulin resistance [for review, see Bailey & Flatt, 1997].

(i) Monogenic models

(a) The Zucker and Zucker Diabetic Fatty rats

The Zucker and Zucker Diabetic Fatty (ZDF) rat are related and carry the same defect in the long form of the leptin receptor (Gln^{269} to Pro^{269}), a mutation referred to as *fa*, but expressed on different genetic backgrounds. Both exhibit hyperphagia and IGT from a young age, but only the ZDF progresses to overt diabetes. Thus, the Zucker is the main genetic model of a spontaneous IGT syndrome and insulin resistance, and the ZDF is considered a better model of human type 2 diabetes because it also develops progressive β-cell failure, and their appropriateness as such is discussed in greater detail in General Methods [2.1.2 (i) (a), (b)]. Both of these rats also show ß-cell hyperplasia and become obese through reduced stimulation of BAT thermogenesis, hyperphagia and hyperinsulinaemia early in the syndrome. This is then followed by insulin resistance and glucose intolerance. In Zucker rats, it has been shown that hypothalamic and neuroendocrine abnormalities are also present,

with increased corticosterone secretion and increased activity of NPY neurons. ZDF rats show the biochemical changes thought to be responsible for the ß-cell damage culminating in frank diabetes [Clark & Palmer, 1982; Peterson, 1994] and go on to develop micro- and macrovascular complications similar to those in human diabetes [for review, see Bailey & Flatt, 1997].

(b) The ob/ob *and* db/db *mouse*

These models have provided the key to the discovery and characterisation of leptin and its mechanism of action. The traits displayed by both types of mouse, including very early onset obesity, have resulted, like those of the Zucker and ZDF rats, from autosomal recessive single gene mutations. In the *ob/ob* mouse, the *ob* gene encoding leptin, on mouse chromosome 6, is mutated such that abnormal leptin is produced. This causes hyperphagia, reduced energy expenditure and obesity. On the other hand, the *db/db* mouse produces normal leptin, and circulating levels are greatly increased. The *db* gene, on chromosome 4, carries a mutation in the leptin receptor, different from the one occurring in the *fa/fa* rat. Also in contrast to the fatty Zucker rat, the *db/db* mouse may progress to overt hyperglycaemia and diabetes [for review, see Bailey & Flatt, 1997].

Mutations of the leptin and leptin receptor genes have been identified in humans presenting with extreme and very early onset obesity syndromes. The *ob/ob* and *db/db* mice are syntenic with these rare syndromes, but are less than ideal matches for common human obesity syndromes, which are characterised by maturity-onset obesity without any associated endocrine defects other than those linked to insulin resistance.

(1) Aetiology of spontaneous rodent syndromes of IGT and type 2 diabetes

The hormonal and hypothalamic disturbances present in rodent models of IGT and type 2 diabetes may hinge on their overexpression of leptin and high circulating leptin levels. Since leptin normally enters the hypothalamus to inhibit NPY neurons, it follows that loss of the leptin signal through mutations in the *ob* gene allows overactivity of NPY neurons, leading to hyperphagia and obesity. Increased fat mass induces insulin resistance by increasing insulin and perhaps TNFα secretion. Indeed, immunoneutralisation studies in the fatty Zucker rat suggest that its insulin resistance is largely attributable to increased secretion of TNFα. The chronic hyperinsulinaemia of these models may also contribute to insulin resistance by down-regulating insulin receptors, and their increased corticosterone secretion may also exacerbate this condition. Overall, the secretory drive on the ß-cells would be increased, eventually leading to their failure [for review, see Bailey & Flatt, 1997].

(c) The agouti *mouse*

The *agouti* mouse shows a maturity-onset obesity syndrome characterised by hyperphagia, increased adiposity, hyperglycaemia and hyperinsulinaemia. Intense scrutiny of the molecular pathway leading to this phenotype has led to the implication of melanocortins and their receptors in the regulation of body weight. The gene encoding the *agouti* protein was cloned and found to be overexpressed in this mouse. This protein acts as an antagonist at the melanocyte-expressed α-MSH receptor, or melanocortin-1 receptor (MC1-R), involved in the regulation of coat colour, explaining why this model also has a pigmentation defect and presents with a yellow coat. Since the *agouti* alleles causing obesity are associated with gene re-arrangements resulting in ectopic expression of the protein, it was suggested that the obesity was due to an interaction of *agouti* with another melanocortin receptor.

Hence, four other melanocortin receptors homologous to MC1-R have been described. Of these, MC4-R is the only one for which the *agouti* protein acts as a specific antagonist. Its expression is restricted to the brain, where it is found in regions involved in food intake regulation, as described above [see 1.3.3 (ii) (b) (1)]. ICV injection of an MC4-R antagonist induces increased food intake in normal mice, while that of an agonist strongly inhibits food intake in fasted animals. Targeted disruption of MC4-R leads to obesity in mice, implicating this receptor in energy homeostasis regulation. Thus, neurons expressing MC4-R exert a tonic inhibition on feeding behaviour, and development of the *agouti* obesity syndrome is caused by chronic antagonism of MC4-R signalling by the *agouti* protein.

Although they involve different modes of transmission, both dominant and recessive defects in the melanocortin pathway and mutations of the components therein give rise to early-onset forms of obesity in humans. These individuals display obesity because of a recessive defect in the POMC gene resulting in the absence of α-MSH agonist activity on MC4-R, or a frameshift mutation in the MC4-R gene, which, affecting certain transmembrane domains of the receptor, abolishes its function. In contrast to the human form, however, the *agouti* mouse has a maturity-onset obesity syndrome, as mentioned above. Nevertheless, its other phenotypic and metabolic characteristics are all in common with human obesity and insulin resistance [for review, see Vaisse, 1999].

(d) The MC4-R knockout mouse

Mice lacking both alleles of MC4-R (-/-), although normal in coat colour, duplicate the metabolic defects of the *agouti* mouse. Unlike the *ob/ob* and *db/db* mice, they have a maturity-onset obesity without any associated endocrine defects other than

those linked to insulin resistance, and so present an obesity syndrome mimicking common human obesity. Interestingly, alteration in only one allele is sufficient to lead to obesity, as seen in heterozygous KO mice that have a body weight intermediate between that of wild-type (+/+) and homozygous (-/-) mutants.

(e) The mahogany *mouse*

The mahogany (*mg*) locus was first identified as a recessive suppressor of *agouti*, blocking not only the ability of *agouti* to induce a yellow coat colour when expressed in the skin, but also the obesity, hyperinsulinaemia, hyperleptinaemia and hyperglycaemia resulting from ectopic expression of *agouti* in the brain. Remarkably, however, *agouti* mice also homozygous for *mg* remain hyperphagic. Furthermore, *mg/mg* alone stimulates feeding and increases basal metabolic rate, implying pathways of action of *mg* gene products independent of those involving suppression of *agouti* and AGRP [Dinulescu *et al.,* 1998]. Furthermore, the *mg* receptor has recently been implicated in potential therapeutic intervention in common human obesity because it is involved in the suppression of diet-induced obesity and is down-regulated in the VMH of *mg/mg* mice. This is particularly interesting because other neuropeptides and receptors involved in body weight regulation, including MC4-R, are expressed here [Nagle *et al.,* 1999].

(ii) Polygenic models

Fifty-five trait loci have been reported for polygenic models of obesity in animals, distributed on 20 chromosomes. In humans, however, the situation is more complex, with associations having been made between many candidate genes, including those encoding leptin and its receptor, MC4-R, BMI and body fat content [for review, see

Ricquier, 1998]. Common human obesity and its associated insulin resistance may turn out to be the consequence of an interaction between different rare mutations in multiple genes (with variable penetrance and expressivity) and the environment.

Feeding animals from a polygenic background with diets high in saturated fats or sucrose is one way in which models of human obesity, insulin resistance and diabetes can be experimentally induced. Consumption of these diets increases insulin concentrations, enhances adipose tissue deposition, reduces insulin sensitivity and impairs glucose tolerance, even if total energy intake is not increased. Progression to overt diabetes appears to require genetic susceptibility, however, as with desert-adapted rodents. As has been postulated for the Pima Indians, their normally high metabolic efficiency of these rodents may be due to the natural selection of 'thrifty' genes which ensure their survival in their usual habitat of food scarcity [for review, see Bailey & Flatt, 1997].

(a) Diet-induced obesity

Since the majority of human obesity is associated with a Western lifestyle, including ready availability of highly palatable food, the dietary obese (DIO) rodent is a relevant animal model, and this relevance is discussed further in General Methods [see 2.1.2 (ii)]. Dietary obesity can be induced in rats by exposure to diets of various compositions, usually with a high fat content, and which bring about varying degrees of obesity.

As well as being hyperinsulinaemic, rats fed high-fat or highly palatable diets develop insulin resistance and hyperleptinaemia [Chang *et al.*, 1990; Harrold *et al.*, 2000a; Kraegen *et al.*, 1991; Pickavance *et al.*, 1999b, 2001; Storlien *et al.*, 1986], similar to obese humans [for review, see Kopelman, 2000]. They also show initial

enhancement of sympathetic activity which later returns to normal or becomes depressed [Levin *et al.,* 1983], similar to the response of the sympathetic nervous system (SNS) to energy changes in humans [for review, see *The Sympathetic Nervous System*, 1998].

(1) The 'cafeteria' diet

Studies conducted over the last two decades using a 'cafeteria' diet, in which experimental animals are offered a choice of palatable human food items, have been very valuable in contributing to our understanding of DIT and energy balance regulation. Overall, these studies have provided evidence that it is the hyperphagia associated with this type of feeding, rather than the altered dietary composition, which is the primary stimulus to DIT, which then varies inversely with the degree of adiposity obtained [Rothwell & Stock, 1988]. More recently, however, it has been suggested that obesity in DIO models may result from leptin resistance [Halaas *et al.,* 1997], as well as reduced thermogenic capacity.

(2) Obesity-prone vs *obesity-resistant rats*

Although a link between dietary fat and obesity has been firmly established in humans, a genetic propensity toward weight gain appears to be a prerequisite for obesity. The same is true of animals; for example, the Osborne-Mendel rat has an increased susceptibility to obesity. It has a preference for dietary fat to which an enhanced sensitivity to opioid stimulation may contribute [Lin *et al.,* 1996; Ookuma *et al.,* 1998]. However, even polygenic populations of rats can often be divided into those prone to weight gain and those resistant to it.

Changes in sympathetic function occur in all rats fed a high-calorie diet, despite only about half becoming obese [Levin *et al.,* 1983]. On high-calorie, high-fat diets, both obesity-resistant and obesity-prone rats show increased sympathetic activity in BAT, but only the obesity-prone show reduced activity in heart and pancreas. The obesity-prone have higher plasma insulin levels and continue to eat more than the obesity-resistant when switched back to a chow diet [Levin *et al.,* 1987]. Obesity-prone and -resistant rats chronically fed a high-fat diet show the same FFA, TG and glucose levels, suggesting that early increases (at 1 week) in body and fat weight in obesity-prone rats are due to a greater suppression of LPL in muscle and lesser suppression of LPL favouring fat storage [Pagliassotti *et al.,* 1994]. Indeed, dietary obesity is prevented in transgenic mice overexpressing skeletal muscle LPL [Jensen *et al.,* 1997].

Selective breeding for dietary obesity and resistance in Sprague-Dawley rats has shown that these traits (a bimodal pattern of weight gain) appear to be due to a polygenic pattern of inheritance, as there are two genetically distinct populations of animals within the Sprague-Dawley strain [Levin *et al.,* 1997]. These differing body weight set-points are also vigorously defended against subsequent changes in diet composition [Levin & Keesey, 1998].

(3) The high-fat diet

High-fat feeding causes widespread insulin resistance in peripheral tissues of rats, especially in skeletal muscle [Kraegen *et al.,* 1986], even when it does not cause a major increase in body weight or basal hyperinsulinaemia. Moreover, metabolic changes induced by high-fat feeding persist even after weight loss accompanying a

change in diet and can also precede body weight change [Harrold *et al.,* 2000b; Levin *et al.,* 1987].

A possible mechanism of insulin resistance in the WAT of rats fed high-fat/low carbohydrate diets is depletion of intracellular glucose transport systems [Hissin *et al.,* 1982]. The insulin resistance does not involve defects in insulin receptor function, however, and is more likely to be induced by post-receptor defects in skeletal muscle [Ozel *et al.,* 1996]. In support of this, Lin *et al.* [1998] found that the insulin receptor tyrosine kinase inhibitor gene is differentially expressed in rats that differ in susceptibility to developing obesity.

Hypothalamic concentrations of NPY and NPY mRNA have been found to be lower in some high-fat-fed rats, suggesting that NPY acts in a counter-regulatory mechanism for limiting overconsumption of food [Beck *et al.,* 1994; Giraudo *et al.,* 1994], but results in this area are inconsistent. For instance, exposure to a highly palatable diet (HPD), with a moderately raised fat composition, does not effect ARC NPY mRNA levels, unless fed at 60% of *ad lib* intake, suggesting that NPY in the ARC responds to energy deficits rather than to hyperphagic stimuli related to palatability [Kim *et al.,* 1998]. However, this may be due to the differences between the two types of diet, as high-fat diets are not necessarily palatable. Yet rats fed a high-energy diet overexpress ARC NPY mRNA and fail initially to regulate it to subsequent food restriction [Levin & Dunn-Meynell, 1997]. In addition, Wang *et al.* [1998] have found that regardless of whether the diet is high-carbohydrate or high-fat, it is high body fat that is associated with higher NPY in the ARC.

DIO mice develop peripheral but not central resistance to leptin [Van Heek *et al.,* 1997]. Consistent with this is the upregulation of blood-brain barrier leptin receptor gene products in rats fed a high-fat diet [Boado *et al.,* 1998]. The leptin

response to dietary fat in mice that are high-fat-fed for 1 month is dependent on whether or not they are obesity- and diabetes-prone. Leptin levels rise more gradually in prone animals and to a level two-fold lower than that in obesity- and diabetes-resistant animals, along with significant increases in adiposity, hyperglycaemia and hyperinsulinaemia; therefore, leptin may be an important predictor of the development of subsequent dietary obesity [Surwit *et al.,* 1997]. This was also found by Harrold *et al.* [2000b] with rats placed on an HPD: Rats with relatively high plasma leptin levels after 1 week of consumption showed subsequently lower food intake and weight gain after 8 weeks on the diet. It is thought that an early leptin response may 'program' subsequent feeding behaviour and weight gain by regulating neurons that project selectively to the VMH. However, it has been suggested that the mechanism by which a high-fat diet causes insulin resistance may be quite different from that associated with obesity and overeating due to an abnormality in the leptin system, as in fatty Zucker rats. In these animals, the activity of hepatic phosphatidylinositol-3 kinase (PI-3K), responsible for translocation of GLUT-4 in response to insulin, is severely impaired, whereas high-fat-fed rats that have become insulin resistant show increased PI-3K activation in the liver [Anai *et al.,* 1999].

(4) The highly palatable diet

The DIO rat model fed the HPD is characterised by hyperphagia, increased thermogenesis, hyperleptinemia and mild insulin resistance [McCormack *et al.,* 1989; Widdowson *et al.,* 1997; Wilding *et al.,* 1992b]. Studies with this diet have shed more light on what may be mediating DIO centrally. Obesity develops as a result of hyperphagia because of the diet's palatability rather than a high-fat content

[McCormack *et al.,* 1989]. Work with the HPD has clarified that it is the degree of food intake which is the critical factor in determining susceptibility in dietary obesity, since, in an unselected population of Wistar rats, other factors, such as body temperature and UCP-2 and -3 expression, are unrelated to the severity of the obesity [Harrold *et al.,* 2000a].

As discussed above, the importance of NPY in dietary obesity is uncertain; NPY mRNA levels do not change in the DIO model fed the HPD [Wilding *et al.,* 1992a], and weight loss produced pharmacologically in this model is not mediated by changes in hypothalamic NPY [Wilding *et al.,* 1992b]. Up-regulation of NPY 'Y5' feeding receptors in HPD-fed DIO rats [Widdowson *et al.,* 1997] suggest reduced regional release of NPY, and yet increased NPY levels in hypothalamic nuclei have been found by Wilding *et al.* [1992a] in this model. ICV injection of the NPY antagonist, 1229U91, also fails to inhibit the hyperphagia of DIO rats on this diet [Widdowson *et al.,* 1999].

The inconclusive results obtained with NPY have encouraged a search for an alternative hypothalamic pathway which could explain dietary obesity. There is down-regulation of MC4-Rs in HPD-fed DIO rats, which may indicate increased α-MSH secretion in an attempt to limit overeating. This model therefore provides further evidence that the MC4-R is a physiological inhibitor of feeding [Harrold *et al.,* 1999a]. Because AGRP concentrations increase in DIO rat hypothalami, but α-MSH levels do not differ from controls, it has subsequently been suggested that MC4-R activity is not regulated by changes in hypothalamic agonist (α-MSH), but by antagonist (AGRP) availability [Harrold *et al.,* 1999b].

In contrast to the apparent central leptin sensitivity in DIO rats and mice fed high-fat diets, rats fed the HPD show an impaired hypophagic response to exogenous

leptin, suggesting reduced receptor sensitivity, or, in keeping with previous findings, near total occupation of receptors by endogenous leptin molecules, levels of which are raised in plasma [Widdowson *et al.,* 1997].

1.5.2. Models of negative energy balance: type 1 diabetes

Type 1 diabetes can be induced in animals by the administration of various chemicals, notably alloxan and a single high dose of streptozotocin (STZ). Multiple low doses of STZ can produce type 2 diabetes-like syndromes as well [for review, see Bailey & Flatt, 1997]. Diabetic syndromes analagous to human type 1 diabetes can also develop spontaneously in certain rodent strains and other species. These may involve damage to the β-cell at several sites, including the glucose transport proteins in the cell membrane, glucokinase and DNA. The best rodent models of this are the BioBreeding (BB) rat and non-obese diabetic (NOD) mouse. The BB rat has a genetic predispostion to diabetes, and defects in islet immunity are involved in its pathogenesis, including the presence of antibodies against GAD and other β-cell antigens, as in human type 1 diabetes. Also like humans with this disease, these rats are hypoinsulinaemic, hyperglycaemic and ketotic, and the diabetes is fatal unless insulin is given. Pathogenesis is similar in the NOD mouse [for review, see Bone & Gwilliam, 1997].

1.6. Treatment of type 2 diabetes

The treatment of type 2 diabetes hinges on diet and lifestyle measures, backed up by oral anti-diabetic agents and insulin. Diet is the cornerstone of the treatment, especially incorporating a restriction of fat intake [Williams, 1994]. If dietary compliance fails, anti-diabetic agents are used which lower blood glucose

concentrations by delaying intestinal glucose absorption, increasing insulin concentrations or mimicking insulin action, or by metabolic effects that enhance glucose utilisation or reduce glucose production [for review, see Bailey *et al.,* 1997].

1.6.1. Sulphonylureas

(i) Mechanism of action

Sulphonylureas such as glibenclamide, chlorpropamide and tolbutamide and their derivatives (e.g., glimepiride), as well as benzoic acid derivatives, stimulate insulin secretion by interacting with specific receptors on the β-cell surface that act to close ATP-sensitive K^+ channels in the membrane; the resulting depolarisation allows Ca^{2+} to enter the β-cell, which triggers the release of insulin-containing secretory granules. Sulphonylureas enhance certain insulin actions, including glucose transport and the shutting off of HGP. They improve insulin sensitivity and secretion by alleviating 'glucose toxicity'.

(ii) Side effects

The absorption of sulphonylureas is impaired by hyperglycaemia. Although most are cleared rapidly and metabolised to, and excreted as, inactive products, glibenclamide accumulates within β-cells. Its metabolites retain hypoglycaemic activity, while chlorpropamide is cleared slowly and excreted unchanged. Both of these agents, therefore, cause prolonged hypoglycaemia, which can be fatal, and neither can be used if renal function is at all impaired. Also, many drugs interact with sulphonylureas.

Weight gain, undesirable in already obese patients, may also occur, due to the anabolic effects of increased insulin levels. Thus, those patients with type 2 diabetes

who do not respond adequately to diet alone, but do not require insulin and are not obese, are usually treated with sulphonylureas.

1.6.2. Biguanides

(i) Mechanism of action

Biguanides, such as metformin and phenformin, on the other hand, lower blood glucose mainly by inhibiting HGP. In the gut wall, glucose is thought to be diverted through anaerobic glycolysis to form lactate which can then undergo gluconeogenesis in the liver to produce glucose, which may explain why these drugs do not cause hypoglycaemia. They are not insulin secretagogues, like the sulphonylureas, but may enhance insulin sensitivity at post-receptor levels and stimulate insulin-mediated glucose disposal [Williams, 1994].

(ii) Side effects

Those who are overweight and therefore not ideal candidates for sulphonylurea treatment are often given metformin instead. It is less likely to cause weight gain, probably because this type of drug does not stimulate insulin secretion. However, its side effects include gastrointestinal symptoms which may reduce appetite (and therefore cause weight loss, sometimes to the point of anorexia), but also make patients reluctant to take the drug. Lactic acidosis is rare but often fatal.

In conclusion, sulphonylureas and biguanides have similar glucose-lowering effects after diet has failed, but individual responses are variable and unpredictable. Combination therapy is often given if monotherapy fails, as the different mechanisms of action of these drugs should synergise. If treatment targets are not then achieved, insulin is added or substituted [for review, see Bailey *et al.*, 1997; Williams, 1994].

1.6.3. Other treatments for type 2 diabetes

Other inhibitors of carbohydrate digestion and absorption include dietary fibre supplements such as guar gum and pectins. These have modest glucose-lowering effects due to interference with intestinal glucose absorption and reduced plasma insulin concentrations after meals. As with biguanides, inhibitors of intestinal α-glucosidases (e.g., acarbose, miglitol) can decrease the rate of starch hydrolysis in the gut lumen and, therefore, also lower blood glucose concentrations by delaying glucose absorption. Similarly, they can also have limited compliance because of gastrointestinal side effects.

Other potentiators of insulin secretion include GLP-1, which reduces post-prandial glucose concentrations when injected subcutaneously. Experimental glucose-lowering drugs have also been devised. These include insulin-mimetic drugs, such as the vanadium salts, which may act by inhibiting the dephosphorylation and inactivation of the insulin receptor, insulin administered orally or intranasally, and glucagon antagonists.

(i) Modifiers of lipid metabolism

These are inhibitors of FA production and metabolism, which may enhance glucose utilisation through the Randle cycle. They include antilipolytic agents, such as nicotinic acid and its analogue acipimox. These acutely improve glucose tolerance in type 2 diabetic patients by inhibiting TG breakdown and causing a fall in circulating FFAs, but tend to be short-acting. Other agents that lower lipid concentrations include the fibric acid (fibrate) derivatives, discussed in a later section [1.6.5 (iii) (b)]. Agents that inhibit FA oxidation redress the imbalance between the reduced glucose utilisation and increased gluconeogenesis of diabetes; these include

inhibitors of the enzyme carnitine palmitoyl-transferase 1 (CPT-1), the rate-limiting enzyme for the transfer of long-chain fatty FACoA derivatives into the mitochondria of the liver. Examples of these are etomoxir and methylpalmoxirate, which lower blood glucose as well as TG concentrations, but the latter may impair metabolism in cardiac muscle.

(ii) β-3-adrenoceptor agonists

The endogenous ligands of the β-3-adrenergic receptors are the catecholamines, which induce lipolysis in WAT and stimulate thermogenesis in BAT. Treatment of rodent models of obesity and type 2 diabetes with β-3-adrenoceptor agonists decreases food intake, while stimulating energy expenditure, mobilising body fat and improving glycaemic control. Although these agents can cause weight loss in patients, clinical use of the current generation of compounds is limited by their sympathomimetic side effects (i.e., tachycardia and sweating) and their partial selectivity for the β-3-adrenoceptor.

(iii) Anti-obesity drugs

D-fenfluramine has been extensively studied as a centrally acting anti-obesity drug. It effectively reduces food intake, and it has the added benefit of improving insulin sensitivity even in the absence of weight loss. However, a sizeable proportion of patients do not respond to it, and it has been withdrawn from use because of cardiovascular toxicity. Sibutramine is another centrally acting serotonin and noradrenaline re-uptake inhibitor that has been recently licensed. It is hoped that in the near future highly specific and potent appetite-suppressing drugs, such as

antagonists at the NPY 'feeding' receptor and agonists at the hypothalamic leptin receptor will also be developed [for review, see Bailey *et al.,* 1997].

1.6.4. The need for new anti-diabetic agents

The pharmacology and various side effects of the agents described above reveal that these drugs can be problematic. As highlighted by the recent findings of the United Kingdom Prospective Diabetes Study (UKPDS), treatment of type 2 diabetes is difficult and remains unsatisfactory. This study showed that, despite maximal treatment with diet, oral hypoglycaemic drugs and insulin, glucose tolerance continues to deteriorate during the course of the disease (UKPDS Group, 1998). Thus, although this study confirms the long-held view that good control of blood glucose can prevent complications of diabetes, such control is impossible to achieve in many patients with currently available treatments. There is, therefore, a pressing need to develop new agents to treat this disease. An ideal drug might be expected to prevent the transition from the pre-diabetic state of IGT to overt type 2 diabetes, improve insulin resistance, correct the underlying lipid disturbance and preserve β-cell function. The presumed central role of both peripheral and hepatic insulin resistance in the pathogenesis of type 2 diabetes suggests that potentiation of insulin action might be a more direct pharmacological approach to treatment and invites the development of agents such as the thiazolidinediones [Bailey *et al.,* 1997].

1.6.5. Thiazolidinediones

(i) Definition and history

The thiazolidinediones (TZDs) represent a novel class of oral anti-hyperglycaemic compounds that improve insulin sensitivity in subjects with insulin-resistant states,

including type 2 diabetes and IGT, but have little or no insulin secretagogue activity [Barman Balfour *et al.,* 1999; Day, 1999; Henry, 1997; Kaneko, 1997; Saltiel & Olefsky, 1996]. They lower HGP and insulin concentrations, and stimulate peripheral glucose uptake in animals and humans (Fig. 1.8A). They may also improve dyslipidaemia and hypertension [for review, see Bailey *et al.,* 1997].

A major breakthrough in the effort to synthesise drugs which potentiate insulin action was made in 1982 with the discovery of ciglitazone (Fig. 1.9; Table 1.1), pre-dating the discovery of the nuclear receptors (PPARγ) for which these drugs are synthetic ligands [described below; see 1.6.5 (ii)]. Ciglitazone reduced insulin resistance in obese diabetic animals. However, it was later abandoned because its side effect profile rendered it unacceptable for long-term human studies. All of the subsequently developed related compounds contain a substituted TZD structure (Fig. 1.9), with modifications selected to improve their pharmacological efficacy. However, it is not known whether increased potency results from changes in bioavailibility, metabolism or mechanistic efficacy. The anti-diabetic properties of one such compound, troglitazone, were reported in 1983 [Saltiel & Horikoshi, 1995; Whitcomb & Saltiel, 1995]. Additional TZD compounds based on the pharmacological profile of ciglitazone were later synthesised and tested, and have progressed to late-stage clinical development and licensing for human use. These include englitazone, darglitazone, pioglitazone and rosiglitazone [Henry, 1997; Kaneko, 1997; Nolan *et al.,* 1994; Saltiel & Horikoshi, 1995; Saltiel & Olefsky, 1996; Whitcomb & Saltiel, 1995; Fig. 1.9; Table 1.1]. These compounds vary considerably in potency, but all show qualitatively similar metabolic activity [Bailey *et al.,* 1997].

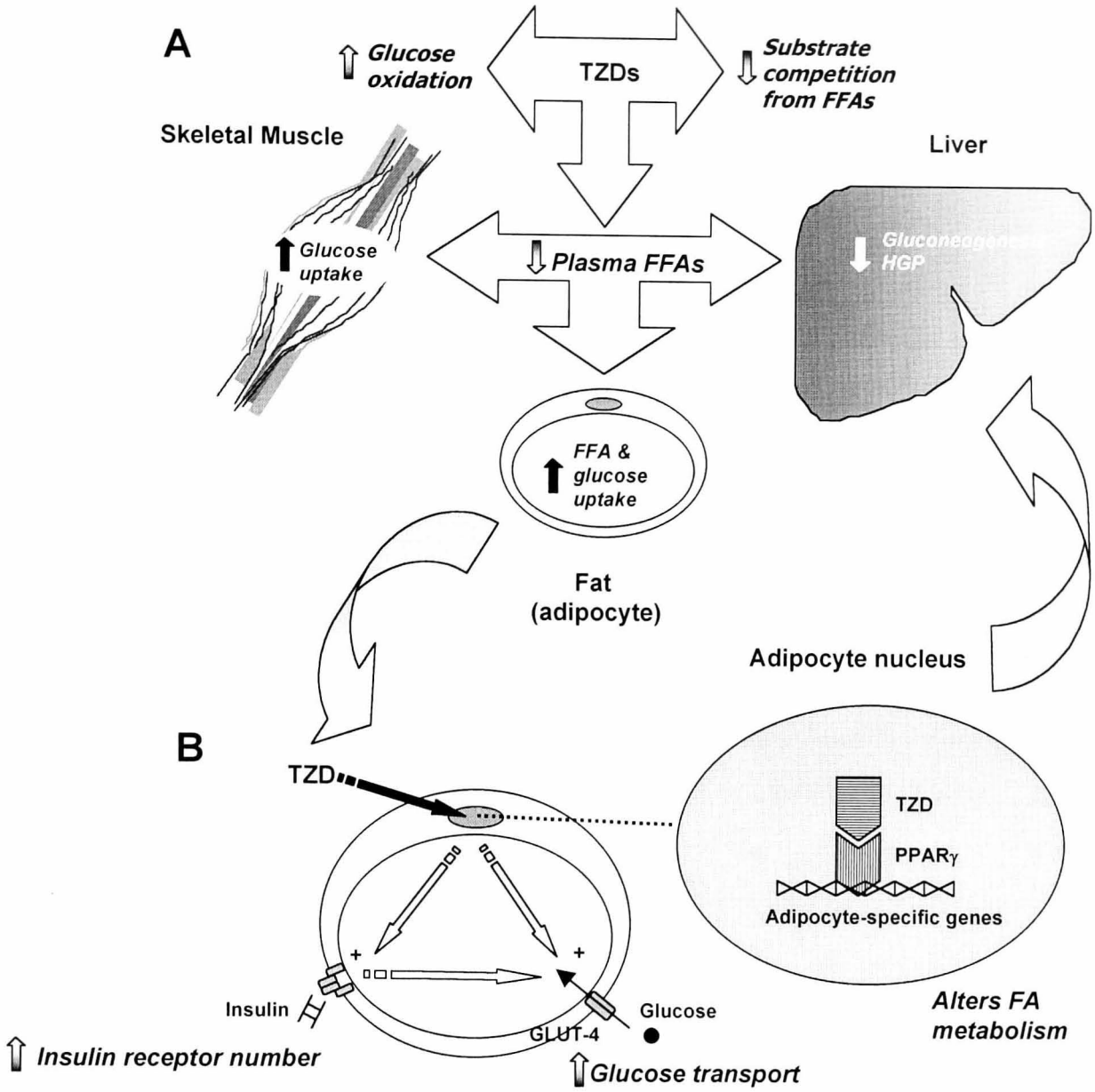

Figure 1.8. Mode of action of TZDs. (A) TZDs lower levels of circulating FFAs that contribute to insulin resistance. Glucose, therefore, becomes the preferred fuel substrate, and its uptake is enhanced in peripheral tissues, primarily skeletal muscle, in which up to 80% of glucose disposal occurs, and which is the major site of insulin resistance in type 2 diabetes [Kahn *et al.*, 2000]. (B) TZDs are synthetic ligands at PPARγ in the nucleus of the adipocyte where they exert a number of effects: They stimulate transcription of genes which (1) encourage retention of TGs, thereby discouraging lipolysis and release of FFAs into the circulation. As introduced in Fig. 1.6, the elevated FFA concentrations in type 2 diabetes stimulate HGP and gluconeogenesis, contributing to hyperglycaemia. Their circulating levels are lowered by TZDs, thereby normalising these two processes. Excess FFAs are taken up into adipocytes where they are esterified to TGs (see A). (2) The enhanced glucose uptake referred to in (A) occurs as a result of TZD-induced increase in GLUT-4 gene expression and, therefore, glucose transport, and in insulin receptor number.

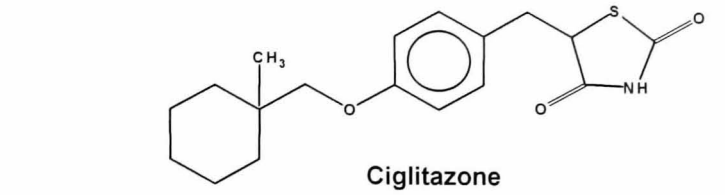

Ciglitazone

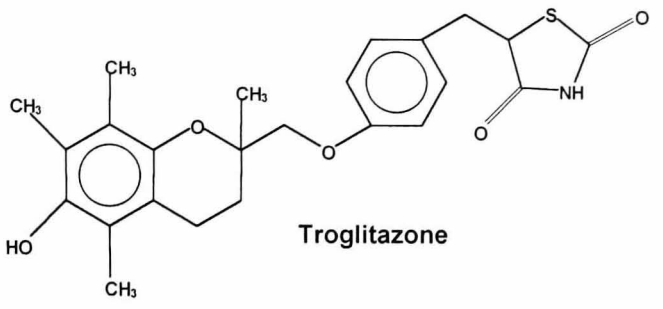

Troglitazone

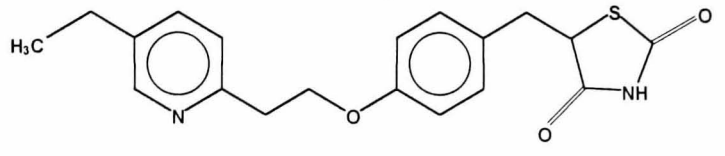

Pioglitazone

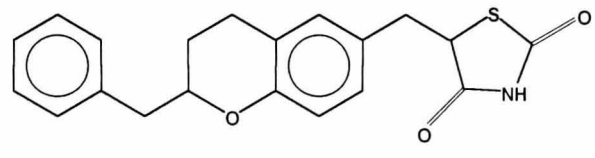

Englitazone

Rosiglitazone

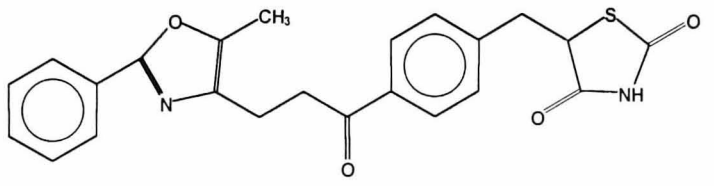

Darglitazone

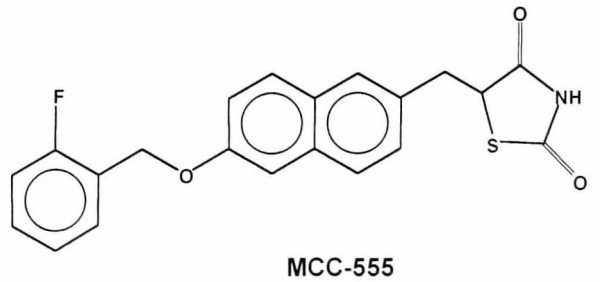

MCC-555

Figure 1.9. Structures of TZDs.

Table 1.1. Some TZDs that have been under clinical investigation.

Agent	Commercial Name	Reference number	Company	Year of first main publication
Ciglitazone		ADD-3878	Takeda, Japan	1982
Troglitazone	Rezulin®	CS-045	Sankyo, Japan	1988
Pioglitazone	Actos®	ADD-4833	Takeda, Japan	1990
Englitazone		CP-68722	Pfizer, U.S.A.	1990
Rosiglitazone	Avandia®	BRL 49653	SmithKline Beecham, U.K.	1994
Darglitazone		CP 86 325	Pfizer, U.S.A.	1995
		MCC-555	Mitsubishi, Japan	1996

Troglitazone, the first TZD licensed for clinical use in humans, was designed to combine the insulin-sensitising activity of the TZD class with a potent lipid peroxide-lowering activity. Lipid peroxides have been suggested as one of the major causative factors of atherosclerosis and are frequently elevated in diabetic subjects [Whitcomb & Saltiel, 1995]. Troglitazone attenuates overt diabetic symptoms, including severe hyperglycaemia, in young ZDF rats [Sreenan *et al.,* 1996], presumably through its ability to reduce TG accumulation in the islets of these animals [Lehmann *et al.,* 1995].

Rosiglitazone is the most potent of the TZDs and is now licensed for use in humans in both the U.S.A. and Europe. Attenuation of overt diabetic symptoms, including severe hyperglycaemia, in young ZDF rats has also been reported following treatment with this drug [Smith *et al.,* 1997].

Whereas the above-mentioned TZDs are full PPARγ-agonists, MCC-555 [Ishii *et al.,* 1996; Upton *et al.,* 1997] is a novel TZD with appreciable anti-diabetic properties despite only weak capacities to bind to PPARγ, making a notable

exception to the rule that PPARγ binding correlates with clinical efficacy. This TZD can function either as a full or partial agonist or an antagonist depending on cell type and the sequence recognition site. This property can be explained by unique cofactor recruitment by this compound and indicates that it may be possible to produce other tissue and promoter-specific PPARγ modulators [Auwerx, 1999].

(ii) The TZD mechanism of action and distribution of PPARs

As mentioned briefly above, TZDs are selective agonists at the gamma isoform of the nuclear transcription factor, peroxisome proliferator-activated receptor (PPARγ) [Adams *et al.*, 1997; Berger *et al.*, 1996; Forman *et al.*, 1995; Lambe & Tugwood, 1996; Lehmann *et al.*, 1995; Shao *et al.*, 1998; Willson *et al.*, 1996; Young *et al.*, 1998]. This receptor is highly expressed in adipose tissue of both animals and man and to a lesser degree in several other mammalian tissues and cells [Braissant *et al.*, 1996; Elbrecht *et al.*, 1996; Mukherjee *et al.*, 1997; Vidal-Puig *et al.*, 1997]. TZDs mimic eicosanoid prostaglandin J2, a proposed endogenous agonist, which also promotes adipocyte differentiation [Forman *et al.,* 1997; Kliewer *et al.,* 1995]; other proposed natural ligands include linoleic acid and other circulating FAs, although these bind the receptor with relatively low affinity [Kliewer *et al.,* 1997]. Their effect is to induce differentiation of pre-adipocytes in brown and white adipose tissue [Schoonjans *et al.,* 1996] through stimulation of numerous genes which act to favour the retention of TGs, thus lowering circulating FFA concentrations (Fig. 1.8B). However, until recently, there has been no direct evidence to conclusively implicate PPARγ in the control of mammalian glucose homeostasis, insulin sensitivity and blood pressure. Study of severely insulin resistant subjects with normal BMI has led to the discovery that dominant negative (loss of function) mutations in human

PPARγ are indeed associated with severe insulin resistance, diabetes mellitus and hypertension [Barroso *et al.,* 1999].

PPARγ is only one member of a nuclear hormone receptor superfamily which modulates transcription of target genes. This modulation occurs via formation of heterodimeric transcription factor complexes with the retinoid X receptor (RXR), another nuclear hormone receptor [Kastner *et al.,* 1995; Fig. 1.10]. Presently, three PPAR (α, β, also known as δ, and γ) and three RXR (α, β, and γ) genes have been identified in mammals [Amri *et al.,* 1995; Issman and Green, 1990; Greene *et al.,* 1995; Gottlicher *et al.,* 1992; Kliewer *et al.,* 1994; Mukherjee *et al.,* 1994; Schmidt *et al.,* 1992; Xing *et al.,* 1995; Zhu *et al.,* 1993]. The PPAR isoforms each modulate different combinations of target genes, and there is evidence that all combinations of PPAR-RXR heterodimers are active at peroxisome proliferator response elements (PPREs) [Kliewer *et al.*, 1994; see Fig. 1.10]; accordingly, nine possible arrays of target genes can be differentially modulated by different PPAR-RXR combinations. Furthermore, PPARγ exists in two isoforms, γ_1 and γ_2, which further widens the range of possible effects [Elbrecht *et al.,* 1996].

The PPAR and RXR isoforms exhibit distinct tissue distributions; for example, PPARα is the most abundant in hepatocytes, with lower levels in the heart and kidney, whilst PPARγ is expressed predominantly in adipocytes, but has recently been discovered in all cell types of human pancreatic islets [Dubois *et al.,* 2000]. PPARβ is present in varying abundance in most tissues [Braissant *et al.,* 1996]. All PPAR and RXR isoforms are also expressed in the developing and neonatal rat CNS, as well as in many adult brain cell types [Cullingford *et al.,* 1998].

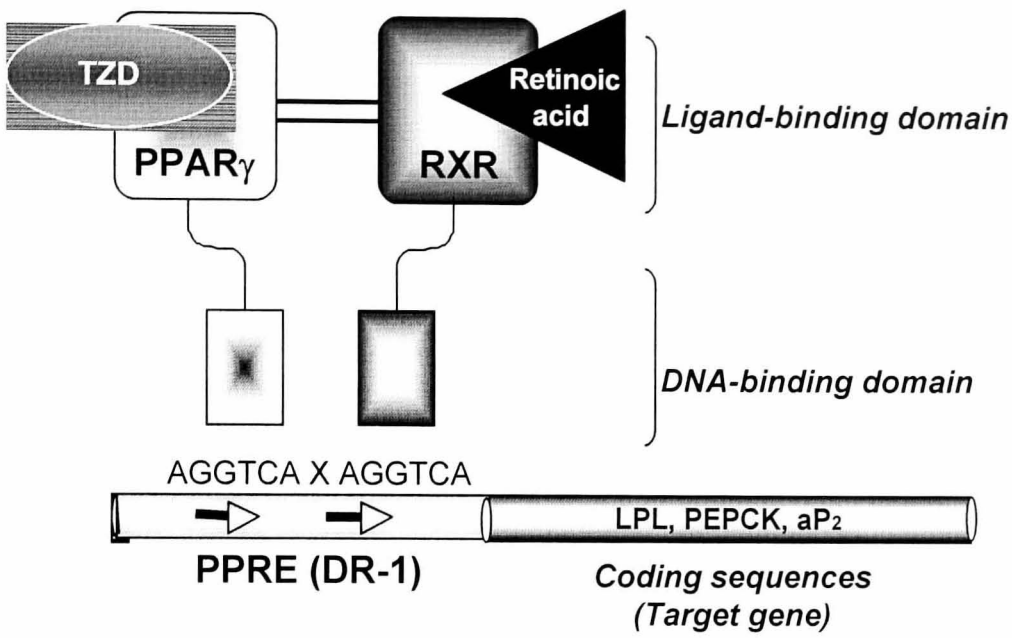

Figure 1.10. PPARγ activation by TZDs alters expression of specific genes. PPARs regulate gene expression by forming heterodimers with RXRs. This produces an active transcription complex that binds to specific peroxisome proliferator response elements (PPREs) in the promoter regions of target genes. These genes include those encoding lipoprotein lipase (LPL), which splits lipoproteins into glycerol and FAs, phosphoenolpyruvate carboxykinase (PEPCK), the rate-limiting enzyme of gluconeogenesis, and aP_2, the adipocyte marker protein which indicates differentiation of stem cells into adipocytes. PPREs contain one or more copies of the DNA sequence AGGTCA arranged as a direct repeat spaced by one nucleotide (hence, termed DR-1). PPAR γ and PPARα recognize distinct PPREs. When the ligand, such as a TZD, binds, it induces a conformational change that causes dissociation of co-repressors, which otherwise prevent transcriptional activation by sequestration of the heterodimer from the promoter. Adapted from Murphy GJ & Holder JC (2000) *TiPS* **21**: 469-474.

(a) TZDs and insulin-signalling pathways

Pioglitazone has been shown to potentiate insulin action at post-receptor sites by ameliorating high glucose-induced desensitisation of insulin receptor kinase *in vivo* [Maegawa *et al.*, 1993]. Troglitazone prevents TNFα-induced insulin resistance, which occurs through interference with insulin receptor signal transduction [see 1.3.3 (i) (c)] and pioglitazone used in combination with metformin reverses it [Miles *et al.*, 1997; Solomon *et al.*, 1997]. Pioglitazone also normalises overexpression of TNFα mRNA and its receptors in mice with obesity-linked diabetes [Hofmann *et al.*, 1994].

TZDs also enhance expression of glucose transporters in pre-adipocytes *in vitro* by increasing their mRNA transcript stability and protein levels, thereby establishing the cells in an active state for glucose uptake [Ciaralidi *et al.,* 1995; Sandouk *et al.,* 1993].

(b) TZDs and skeletal muscle metabolism

Troglitazone acutely stimulates glucose metabolism in normal rat muscle *in vitro*, stimulating glucose uptake and decreasing muscle glycogen content in the presence of insulin [Fürnsinn *et al.,* 1997; Okuno *et al.,* 1997]. It also reduces the increased skeletal muscle glycogen and TG stores in ZDF rats, increasing the turnover of both in this tissue. Troglitazone treatment of ZDF and Zucker rats also normalises abnormally low pyruvate dehydrogenase (PDH) activity, an enzyme involved in glucose oxidation, and decreased glucose incorporation into TG. These changes may underlie the improvements in intracellular substrate utilisation and energy stores which lead to the decreased serum TG and glucose and improved insulin sensitivity also observed in these animals [Oshida *et al.,* 1999; Sreenan *et al.,* 1999]. In the isolated soleus muscle of Wistar fatty rats, improvements in insulin-stimulated glycogen synthesis and glycolysis are seen with pioglitazone treatment, and, similarly, in glucose uptake in obese Zucker rats treated with englitazone [Whitcomb & Saltiel, 1995].

(c) TZDs and liver metabolism

In vitro studies have shown that pioglitazone stimulates glycolysis and inhibits gluconeogenesis in rat liver, independently of insulin [Nishimura *et al.,* 1997]. This decreased HGP in the absence of insulin also occurs with troglitazone treatment of

rat hepatocytes through alterations of gluconeogenic/glycolytic enzymes [Raman *et al.,* 1998], showing that both of these TZDs have 'insulinomimetic' effects.

(iii) Metabolic effects of TZDs

TZDs reduce hyperglycaemia in animal models of type 2 diabetes, without stimulating insulin secretion. They are not effective in severely insulin-deficient models, however, implying that their mode of action requires the presence of insulin. Moreover, they only improve insulin sensitivity in conditions of insulin resistance, and have little action in animals with normal insulin sensitivity. Their blood glucose-lowering effect is typically accompanied by a decrease in plasma insulin concentrations, and they do not normally tend to produce overt hypoglycaemia. In animals with type 2 diabetes-like syndromes, TZDs increase insulin-stimulated glucose disposal and also inhibit glucose production. They increase glycogenesis and glycolysis in muscle, stimulate glucose oxidation and lipogenesis in adipose tissue, and reduce gluconeogenesis in liver [for review, see Bailey *et al.,* 1997].

(a) PPARγ activation

Activation of PPARγ by TZDs in adipose tissue causes an increase in the expression of certain adipogenic genes [Glorian *et al.*, 1998; Harris & Kletzien, 1994; Lefebvre *et al.*, 1997; Martin *et al.*, 1997; Pearson *et al.*, 1996; Rieusset *et al.*, 1999] that may contribute to differentiation of pre-adipocytes to mature adipocytes [Adams *et al.*, 1997; Lehmann *et al.*, 1995]. It also induces apoptosis in fully differentiated adipocytes and results in increased gene transcription and the *de novo* synthesis of proteins involved in glucose and lipid metabolism, all suggesting a continuous role in re-modelling of adipose tissue [Auwerx, 1999; Gimble *et al.*, 1996; Ibrahimi *et al.*,

1994; Martin *et al.*, 1997; Lefebvre *et al.*, 1997; Paulik & Lenhard, 1997; Pearson *et al.*, 1996; Tai *et al.*, 1996]. However, the anti-diabetic actions of TZDs, as such, are independent of their effects on adipose tissues [Burant *et al.*, 1997].

In isolated cellular and tissue systems, animal models and clinical studies, relative potency at PPARγ is correlated with potency in reducing insulin resistance and improving glycaemic control [Adams *et al.*, 1997; Berger *et al.*, 1996; Henry, 1997; Kaneko, 1997; Kawamori *et al.*, 1997a; Kawamori *et al.*, 1997b; Patel *et al.*, 1997; Patel *et al.*, 1998; Wasada *et al.*, 1996; Willson *et al.*, 1996; Young *et al.*, 1998]. There is a significant delay after the start of treatment before there is an improvement in insulin sensitivity; one possible explanation for this is that activation of PPARγ induces its own expression [Spiegelman, 1998]. One way in which TZDs are thought to improve insulin resistance is through inhibition of adipocyte expression of the cytokine, TNFα, and TNFα-induced lipolysis [Hofmann *et al.*, 1994; Souza *et al.*, 1998]. TNFα exerts its anti-adipogenic action in part by the down-regulation of the expression of adipogenic factors such as CCAAT/enhancer binding protein alpha (C/EBPα), a transcription factor thought to have an interplay with the PPARγ/RXR heterodimer in adipogenesis, and PPARγ itself [Auwerx, 1999]. TZD-induced improvement in sensitivity of fat and liver to the effects of insulin may arise from direct effects on genes involved in insulin signalling, such as c-Cbl-associated protein (CAP), where c-Cbl is a proto-oncogene involved in tyrosine kinase-mediated signal transduction [Ribon *et al.*, 1998].

An additional adipose tissue-based action of TZDs is the improvement of the anti-lipolytic action of insulin via restoration of phosphodiesterase (PDE) 3B gene expression [Tang *et al.*, 1999]. PDE 3B is the key enzyme in the mediation of this process. However, whether this action is via PPARγ activation is unknown. The net

result of these actions of TZDs is the reduction of the supply of FFAs to the circulation. In turn, the fall in plasma FFAs reduces substrate competition between glucose and FFAs for uptake into skeletal muscle [Randle *et al.,* 1963], and it also reduces intramuscular TG and diacylglycerol (DAG) content [Oakes *et al.,* 1994, 1997]. TZDs also reduce protein kinase C (PKC) activation and translocation from cytosolic to particulate fractions in red skeletal muscle, reducing in turn the inhibitory effects of PKC on insulin signalling and thereby improving muscle insulin sensitivity [Schmitz-Pfeiffer *et al.,* 1997]. These effects are believed to underpin the improved muscle insulin sensitivity seen with TZD treatment. Although PPARγ seems to have its primary effects on adipose tissue, it is not clear how PPARγ agonists improve insulin sensitivity in muscle. Muscle is responsible for most of the glucose uptake, yet only trace amounts of PPARγ are present in normal human muscle. These minute amounts may be sufficient to account for the improvement in insulin sensitivity seen after treatment with TZDs, or may be induced by treatment leading to a direct PPARγ-mediated response in muscle to TZDs. Alternatively, there may be an indirect insulin-sensitising response in muscle generated by adipocyte-derived lipid or protein signals, such as TNFα, leptin and FAs. Certainly, TZDs reduce TNFα expression, leptin and resistin production in WAT, possibly contributing to improved insulin sensitivity and insulin-stimulated glucose disposal, in this tissue. TZD treatment selectively induces expression of adipogenic enzymes in adipose tissue, but not in muscle tissue, which might 'trap' FAs in adipose tissue, reducing their systemic availability and uptake into muscle [Auwerx, 1999; Steppan *et al.,* 2001].

In contrast, very little is known about regulation by PPARγ of genes directly involved in glucose homeostasis. Some TZDs can increase expression of the GLUT-

4 glucose transporters in adipose tissue, and restore the ability of insulin to suppress the expression in the liver of PEPCK, the rate-limiting enzyme of gluconeogenesis. TZDs have also been suggested to stimulate the tyrosine kinase activity of the insulin receptor, and they also promote the activity of insulin-inducible transcription factors, but the mechanism of these actions is not completely understood. It is important to stress that adipose-independent mechanisms may also contribute to insulin-sensitising effects of TZDs, since these compounds retain their activity in transgenic mice totally lacking adipose tissue [Auwerx, 1999; for review, see Bailey *et al.*, 1997]. Fig. 1.11 summarises these insulin-sensitising properties of TZDs.

In addition to affecting adipocyte metabolism, PPARγ activation could favour adipocyte-sustaining responses consisting of decreased concentrations of the two main adipocyte-derived signalling factors, leptin and TNFα; therefore, PPARγ has been proposed as a master gene controlling a co-ordinated 'thrifty' response leading to efficient energy storage. More recently, this nuclear receptor emerged from a role limited to metabolism in diabetes and obesity to a significant one involved in general transcriptional control of numerous cellular processes, perhaps most notably implicated in carcinogenesis.

The paradoxical anti-diabetic effect of PPARγ agonists, when they induce adipogenesis, which is associated with insulin resistance, is explained by the fact that adipose tissue is a requirement for whole body glucose homeostasis in response to insulin. Indeed, subjects with lipoatrophy and transgenic animals which lack adipose tissue are extremely insulin-resistant, indicating that storage of energy reserves in adipocytes favours insulin sensitivity, with the adipogenic activity of PPARγ contributing to the insulin sensitisation of TZDs [Auwerx, 1999].

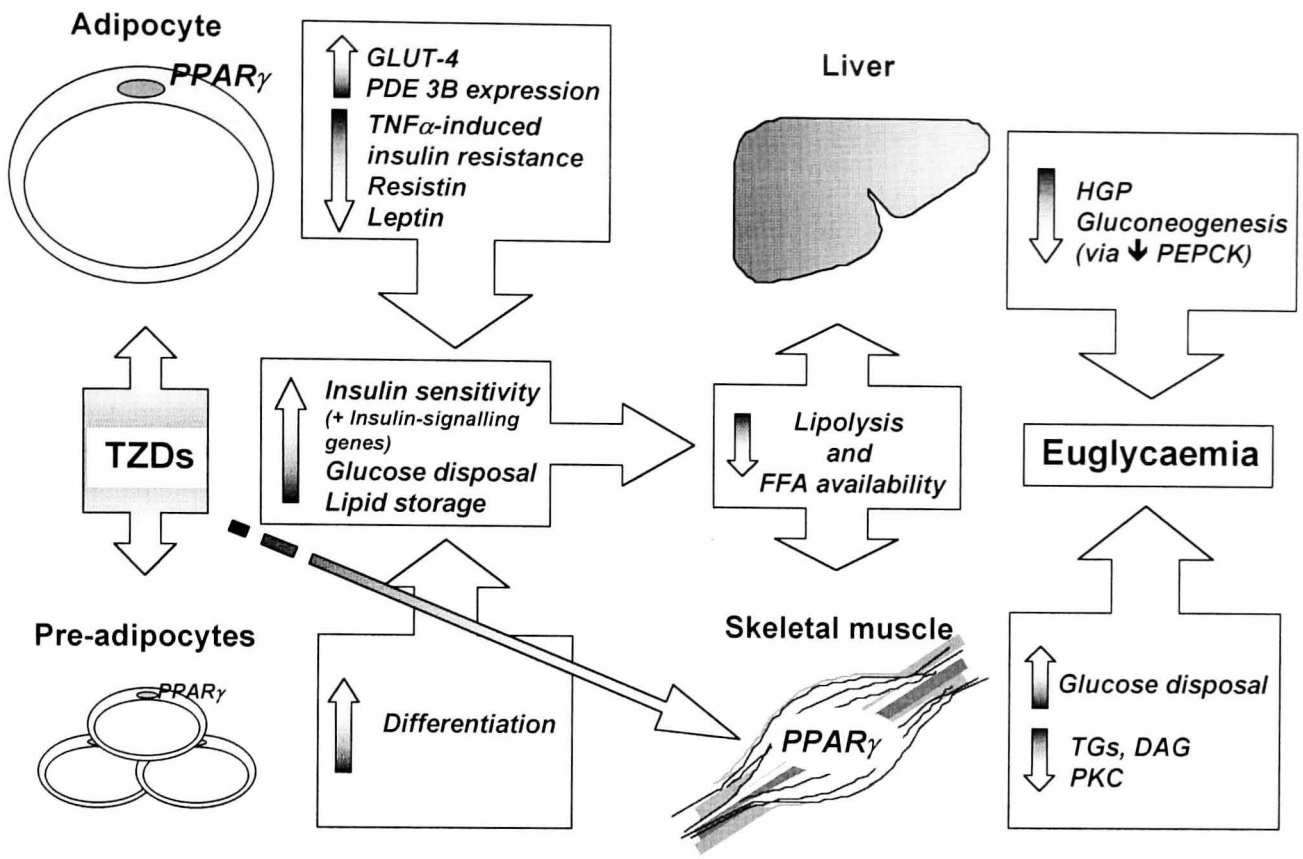

Figure 1.11. Activation of PPARγ enhances insulin action and reduces hyperglycaemia. See 1.6.5 (iii) (a) for discussion.

(b) PPARα activation

PPARα is the nuclear receptor target for the fibrate group of lipid-lowering drugs. These drugs improve non-insulin mediated glucose uptake by reducing circulating TG concentrations. In turn, this leads to reduced lipolysis and an increase in glucose oxidation in non-insulin-sensitive tissues. Fibrates are also thought to alter lipoprotein patterns, reducing concentrations of atherogenic particles such as small dense LDL cholesterol. Although TZDs and fibrates act via different receptors in different tissues (fibrates exerting their effects primarily via the liver), they both have lipid-lowering effects; whereas TZDs induce LPL mRNA levels and activity primarily in adipose tissue, fibrates selectively induce LPL mRNA levels and activity

in the liver and decrease apolipoprotein (apo) C-III mRNA levels and protein production, both key components of plasma TG metabolism [Staels *et al.,* 1997]. Hepatic PPARα is involved in the transduction of eicosanoid and long-chain FA signalling on peroxisomal, mitochondrial and microsomal FA catabolism through expression of target genes [Schoonjans *et al.,* 1996]. Experiments with PPARα-deficient male and female mice implicate oestrogen signalling pathways in the role this nuclear receptor plays in cardiac and hepatic lipid metabolism and glucose homeostasis [Djouadi *et al.,* 1998].

Treatment with one fibrate in particular, bezafibrate, has shed light on a putative role for Randle's cycle in the pathogenesis of lipoatrophic diabetes, a rare clinical syndrome characterised by lipoatrophy and severe insulin resistance. This fibrate improves glucose tolerance in these patients after progressively lowering TG and FFA levels, suggesting that the pathogenesis may be more related to abnormal lipid regulation than glucose metabolism [Panz *et al.,* 1997]. In comparisons with statins, a class of hypolipidaemic drugs which inhibit cholesterol synthesis [for review, see Betteridge, 1997], fibrates appear to be more effective overall in patients with type 2 diabetes [Jeck *et al.,* 1997].

Recent evidence has emerged which suggests that PPARα expression may also be important in the pancreatic islets. Expression of PPARα is reduced in ZDF rats, but this abnormality can be corrected by *in vitro* introduction of a normal leptin receptor [Zhou *et al.,* 1998]. Thus, normal PPARα expression in the islets is dependent on the presence of an intact leptin receptor, and abnormal expression is associated with TG accumulation in the islets, a feature associated with eventual β-cell failure. The significance of TG accumulation and PPARα activation in other

models of diabetes with an intact leptin receptor is not known, nor is it known whether PPARα activation can improve islet function *in vivo*.

(c) Combined PPAR agonists

The distinct tissue-specific transcriptional regulation of genes involved in lipid metabolism by fibrates and TZDs has encouraged research into compounds with effects on both liver and adipose tissue in order to enhance the therapeutic efficacy in restoring insulin resistance in type 2 diabetes to normal. This has uncovered some novel oral anti-diabetic agents with activity toward both PPARα and γ, such as KRP-297 and JTT-501, thus widening the tissue-specific activity and pharmacological properties of both types of agonist [Auwerx, 1999]. JTT-501 is a derivative of the isoxazolidinediones, insulin-sensitising agents structurally distinct from the TZDs, but which also improve insulin sensitivity in both genetic (ZDF) and non-genetic (high-fat-fed) insulin-resistant rodent models [Shibata *et al.,* 1998], and which have a superior TG-lowering activity than some TZDs [Shibata *et al.,* 1999]. Recently, ligands able to bind and activate both PPARγ and δ have also been reported, although little is known about their mode of action [Auwerx, 1999]. KRP-297 is more effective than rosiglitazone in inhibiting enhanced lipogenesis and TG accumulation in the liver of Zucker fatty rats [Murakami *et al.,* 1998].

(iv) Regulation of UCP expression by PPARs

Another candidate gene that may contribute to human obesity is a variant in the promoter of the UCP-1 gene, again illustrating the polygenic nature of human obesity, where susceptibility alleles of numerous genes could increase the probability of developing obesity. This enhancer element has putative binding sites for PPARγ,

essential for its function. Thus, TZDs could represent key components of the BAT thermogenic response, and, indeed, administration of TZDs can promote BAT cell differentiation and hypertrophy.

PPARs may also regulate transcriptional control of UCP-2 and -3. Treatment with TZDs and fibrates have shown this. Given that FAs are the natural ligands for these receptors, PPARs may account for nutritional regulation of UCP-2 and -3, as they are shown to be regulated by various nutritional changes such as food restriction and a high-fat diet, in a tissue-selective manner [for review, see Lowell & Spiegelman, 2000]. Specifically, rodents on a high-fat diet show increased levels of UCP-1 and UCP-3 mRNA in BAT, but unchanged levels of UCP-3 mRNA in skeletal muscle. UCP-2 expression under these conditions is unchanged in muscle and BAT, but increased in WAT.

The increase in UCP-3 gene expression during severe but not moderate food restriction could be mediated by FFAs, the circulating levels of which rise during fasting but not during moderate food restriction. As FFAs are ligands for PPARγ, this receptor may mediate the effects of FFAs on UCP-3 expression in muscle. UCP-2 mRNA expression is enhanced by PPARγ agonists in pancreatic islets, WAT and BAT; thus, it is hypothesised that a high level of UCP-2 could decrease insulin secretion and might, by decreasing cellular ATP levels, blunt GSIS. Secondly, increased levels of FFAs in islet cells may enhance UCP-2 expression and impair insulin secretion. This effect may be mediated by PPARγ, as troglitazone has been shown to increase UCP-2 mRNA levels in islets [for review, see Boss *et al.,* 1998].

(v) Problems with TZD treatment

Despite having proved to be a significant advance in the treatment of the insulin resistance of type 2 diabetes, TZDs fall short of being the ideal treatment for this condition for a number of reasons. The efficacy of all the existing TZDs is similar, with a net reduction in fasting glucose of around 2-3 mM and reductions in the haemoglobin species which carries glucose, HbA_{1c}, of about 1%; this is similar to the improvements seen with other oral hypoglycaemic agents, such as sulphonylureas and metformin. Although this is beneficial, it only results in normalisation of glycaemia in a minority of patients, and additional treatment is often necessary [Bethge *et al.,* 1998; Johnson *et al.,* 1998].

(a) Side effects of TZDs

(1) Haemodynamic effects

Haemodilution has been noted as one side effect of TZD therapy. The mechanism of this effect is currently unclear, although inhibition of L-type Ca^{2+} channels is one possibility [Asano *et al.,* 1999; Nakamura *et al.,* 1998]. A potential outcome of prolonged haemodilution, if caused by significant plasma volume expansion, is cardiac hypertrophy, and this is cited as a side effect of TZDs in animals [e.g., Ghazzi *et al.,* 1997] without explanation of the mechanism. Nonetheless, cardiac hypertrophy has not been observed in patients taking troglitazone, even after 96 weeks of follow-up [Driscoll *et al.,* 1997; Ghazzi *et al.,* 1997], suggesting that the degree of haemodilution seen in humans is unlikely to be clinically significant, except in some patients with pre-existing cardiac failure, where plasma volume expansion may predispose them to decompensation.

(2) Hepatic toxicity

A second side effect of TZD administration is more extreme; i.e., hepatic toxicity. It is a potentially lethal but rare complication of troglitazone therapy in humans [Shibuya *et al.*, 1998; Watkins & Whitcomb, 1998], due to troglitazone's different structure from other TZDs and, therefore, its different hepatic metabolism [Kawai *et al.,* 1997; Whitcomb & Saltiel, 1995]. This has led to its withdrawal from clincal use worldwide, but, at present, there is no evidence that this is a class effect of TZDs. Although the evidence to date suggests this is unrelated to the pharmacological mode of action of the drug [Shibuya *et al.,* 1998], doubt is likely to remain until other compounds are proven to be safe in long-term use.

(3) Effects on energy balance

Other side effects observed in animal models, and to a lesser extent in humans, include increased food consumption and weight gain [de Souza *et al.*, 1995; De Vos *et al.*, 1996; Wang *et al.*, 1997; Zhang *et al.*, 1996]. One study with troglitazone in 20 patients with poorly controlled type 2 diabetes reported complaints of increased hunger in two-thirds of the study participants [Shimizu *et al.*, 1998]. This effect is possibly related to a fall in plasma leptin concentrations, due, in turn, to direct suppression of leptin synthesis by TZDs [De Vos *et al.*, 1996], and resulting in a reduced inhibitory feedback signal to the organism to stop eating.

Weight gain has been noted as a further side effect of troglitazone treatment in man [see Gorson, 1999] and has been demonstrated in both human [Patel *et al.*, 1999; Shimizu *et al.*, 1998] and animal studies after treatment with several other TZDs as well [Arakawa *et al.*, 1998; de Souza *et al.*, 1995; Hirshman *et al.*, 1995; Ikeda *et al.*, 1990; Inoue *et al.*, 1995; Pickavance *et al.*, 1998a, 1999a,b, 2000;

Yoshioka *et al.*, 1993; Zhang *et al.*, 1996], although it is not a side effect unique to TZD therapy; weight gain is also a common accompaniment to other therapies in type 2 diabetes, particularly sulphonylureas and insulin [UKPDS Group, 1998]. Whilst a proportion of the weight gain with TZD treatment is almost certainly due to a small expansion in plasma volume [Dogterom *et al.*, 1999], increased fat mass appears to be the major component. This may be related partly to the increased energy intake [Shimizu *et al.*, 1998; Wang *et al.*, 1997] and partly to PPARγ activation itself and resultant adipogenesis [Gimble *et al.*, 1996; Ibrahimi *et al.*, 1994; Lefebvre *et al.*, 1997; Martin *et al.*, 1997; Paulik & Lenhard, 1997; Pearson *et al.*, 1996; Tai *et al.*, 1996]. This fat seems to be compartmentalised, being located at subcutaneous sites [Adams *et al.*, 1997; Kawai *et al.*, 1999] rather than in the abdominal cavity where it might add to cardiovascular risk [Kaplan, 1989]; indeed, there is evidence of fat re-distribution away from visceral sites in patients taking troglitazone [Kawai *et al.*, 1999; Kelly *et al.*, 1999]. Other putative components of the weight gain mechanism include reduced urinary glucose excretion, antilipolytic actions [Oakes *et al.*, 1994, 1997; Souza *et al.*, 1998] and changes to energy expenditure [Oakes *et al.*, 1997].

1.7. Hypotheses and aims

The studies presented in this thesis were designed to investigate the effectiveness of a range of compounds in the TZD and related classes and the mechanisms by which they might lead to the potentially important side effect of weight gain. It was hoped that improvements could be shown at two levels, the metabolic (improved insulin sensitivity) and the cellular (β-cell preservation), because any future treatment for type 2 diabetes would ideally target both the underlying insulin resistance, and

provide some protection against continuing β-cell damage. The particular agents used in these studies were tested because they were still in pre-clinical development and further information was required to complete this.

In the first part of the thesis, the effects of treatment with TZDs and TZD-like compounds are examined in the ZDF rat. It was thought that MCC-555 treatment of juvenile ZDF rats would help to extend the results of previous studies in which adult Zucker and ZDF rats showed improved insulin sensitivity with this agent. Treatment was begun at the 'pre-diabetic' stage, the stage at which there is the potential to develop the disease, but at which it is not known if the animal will progress to overt diabetes. Attenuation of progression to frank diabetes was tested for and support for any improved metabolism was expected to be reflected by β-cell changes (Chapter 3). The potential advantages of new drugs with PPARγ- and PPARα/γ-binding capabilities were compared in lean ZDF rats made obese on a highly palatable diet to determine whether or not the exogenous stimulus of the diet might reveal a genetic susceptibility to diabetes in the lean ZDF rat (Chapter 4).

The second part of the thesis continues to focus on comparison of the dose-response relationships for the disparate actions of various better-established TZDs. In Chapters 5 and 7, rosi-, pio- and troglitazone treatment in the non-mutant Wistar DIO rat model was investigated, allowing comparison of each of these compounds in terms of their capacity to separate potentially therapeutic effects (improvement in insulin sensitivity, glycaemia and lipid profile) from adverse effects (hyperphagia, weight gain, cardiac hypertrophy and haemodilution).

In Chapters 6.1 and 6.2, the effects of one TZD, rosiglitazone, on energy balance were examined in more depth to find out if hyperphagia and weight gain compromise the efficacy of TZDs, and, if so, if the prevention of hyperphagia and

weight gain enhances the insulin-sensitising efficacy of this drug. Exploratory analysis of some of the potential contributions of central and peripheral mediators of energy homeostasis to TZD-related hyperphagia, body weight gain and insulin sensitivity were also carried out.

CHAPTER 2

General Methods

2.1. Animals and treatment

2.1.1. The need for animal experimentation

Animal experimentation in the United Kingdom is strictly governed by Home Office regulations which have been devised to ensure that animals are treated humanely. Thus, throughout all studies presented here, codes of conduct and treatment outlined in the Animal Scientific Procedures Act (1986) were followed. This publication sets out to make clear the definitions of a 'protected animal' and regulated scientific and experimental procedures which may be applied to such an animal. It also serves to outline the conditions under which these protected animals are to be killed and the humane methods by which this is to be done. It also states that before work can commence, both personal and project licences approved by the Home Office must be acquired. Experimental procedures allowed under these licences were tailored to the specific requirements of the studies described here.

One of the goals of the Home Office is to encourage researchers to reduce the number of animals used in their experiments, and to try to find other means by which to address their scientific hypotheses. The studies presented here were designed to strike a balance between this mandate and the number of rats required to give a sufficient statistical power to the results. This would then give confidence in the findings such that repetition of studies, and, hence, use of even more animals would be unnecessary.

As described in the following sections, the use of rodents was necessary to provide appropriate models of type 2 diabetes and to enable results to be provided at

the *in vivo* level. Without this, interpretations could not have been made with regard to whole metabolic systems. It is the usual step in pharmacological development that animal testing be performed before clinical trials begin in humans, and that it complements human work by providing mechanistic and other data regarding therapeutic and adverse effects; all of the studies included here provided useful information in this respect.

2.1.2. Rationale for selection of species and breeding suppliers

(i) Genetic models of type 2 diabetes

Several animal models of type 2 diabetes have been characterised and are widely used in the preclinical evaluation of new anti-diabetic drugs. The genetic models of type 2 diabetes and impaired glucose tolerance (IGT) involve mostly single gene defects of leptin production or signalling. In the case of the former, the model used is the *ob/ob* mouse, and in the case of the latter, the *db/db* mouse and the Zucker and Zucker Diabetic Fatty (ZDF) rats are used.

(a) The Zucker rat

The original obesity trait in this rat, identified by the Zuckers [Zucker & Zucker, 1961], arises from an insensitivity to leptin. This insensitivity is in turn due to a single mutation (Gln^{269} to Pro^{269}) at the locus coding for the long form of the leptin receptor, *fa*. The genetic designation of this rat is, therefore, *fa/fa*. The hyperphagia which develops as a result of this inability to monitor fat stores eventually causes obesity, insulin resistance, hyperinsulinaemia and glucose intolerance, as is found in the human form of type 2 diabetes. However, unlike humans with type 2 diabetes, these rats are only mildly hyperglycaemic and do not show frank diabetes associated

with their obese condition [Zucker & Zucker, 1962]. As such, the Zucker rat is not the optimal model of type 2 diabetes.

(b) The ZDF rat

(1) The origin of the ZDF rat

The ZDF strain was discovered and the colony begun by Richard Peterson at the Indiana University School of Medicine [Peterson, 1994; Fig. 2.1]. Like the Zucker, this rat is leptin insensitive, but in addition to the traits expressed in the Zucker rat, it develops progressive β-cell failure and is, thus, considered a better model of human type 2 diabetes. The diabetes is, therefore, the manifestation of an autosomal recessive trait (*fa/fa*), and it is spontaneously expressed on a Zucker background. Lean littermates are either heterozygous (+/*fa*) or homozygous (+/+). The lean ZDF rats used in Chapter 4 were genotyped (Novo Nordisk, Maløv, Denmark) and all found to be heterozygous (+/*fa*), reducing potential variability in this experiment.

Although the related Zucker strain has been maintained in numerous locations around the world, the ZDF rats used here were imported from Genetic Models Inc. [(GMI), Indianapolis, IN, U.S.A.], the only supply of such animals in the Western hemisphere. They are, hence, given the genetic designation, ZDF/Gmi-*fa*.

The current inbred ZDF/Gmi-*fa* colony at GMI owes its origin to a non-inbred colony which included some obese rats which went on to develop overt diabetes [Clark & Palmer, 1983]. This characteristic could not be perpetuated, however, when the rats were maintained in the non-inbred condition. More recently, a characteristic diabetic trait has been demonstrable after a few generations of inbreeding and caesarian derivation [Peterson, 1994]. This model is now inbred at this point >30 generations. It has shown diabetic characteristics, including severe

hyperglycaemia, which are more consistent with those of human type 2 diabetes than are those of any other established rat models.

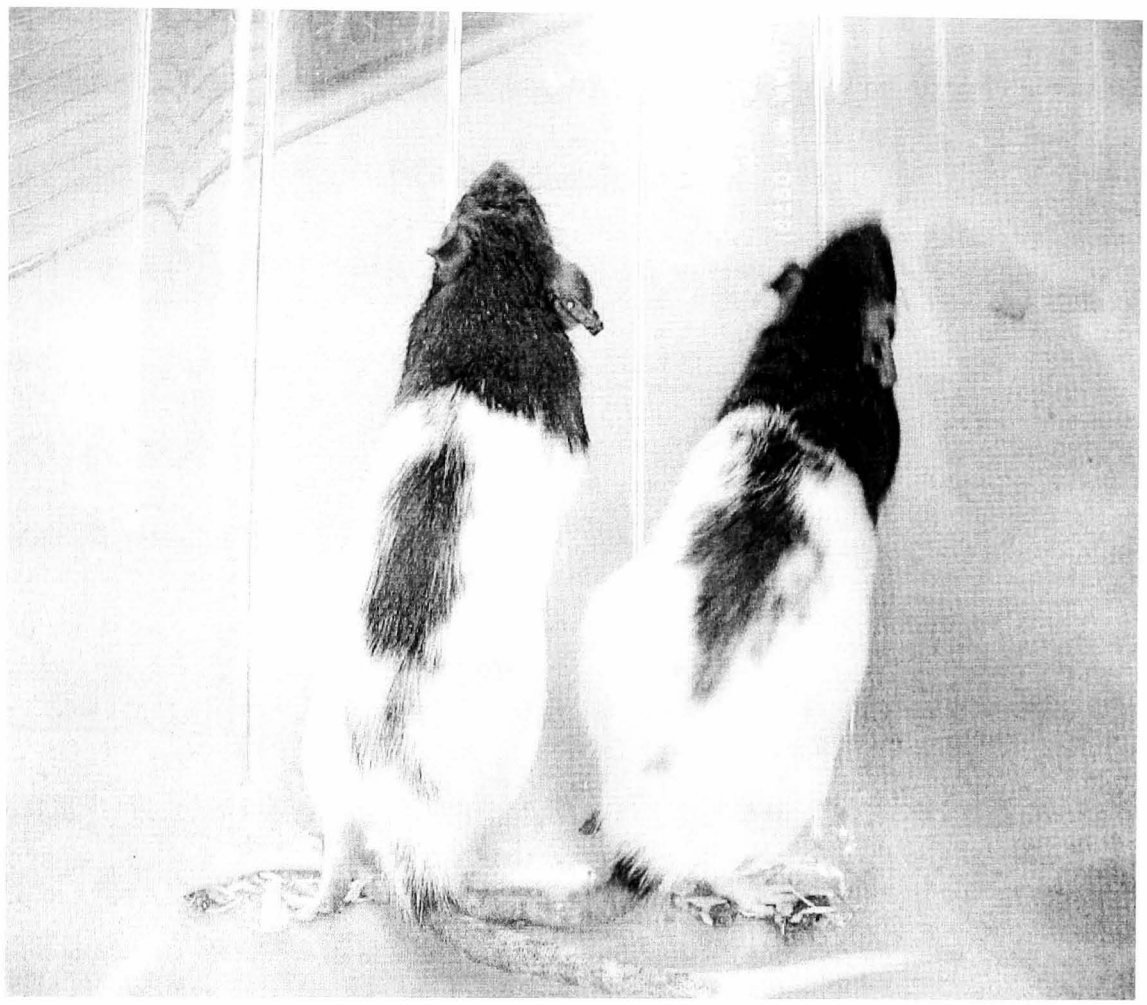

Figure 2.1. Lean (left) and obese (right) ZDF littermates at 10 weeks of age. Photograph courtesy of Genetic Models, Inc., Indianapolis, IN (2001).

(2) Metabolic defects in the ZDF rat

Hyperglycaemia is initially manifested at about 7 weeks of age, and all obese male rats are fully diabetic by 12 weeks of age, with a circulating glucose concentration of >28 mM in the fed state. Male ZDF rats were selected for study because they develop overt diabetes, whereas females do not [Peterson, 1994], unless fed a diabetogenic diet high in lipids and sugar (GMI-supplied). Glycaemia increases slightly for several weeks thereafter. Between 7 and 10 weeks of age, circulating insulin concentrations are also high, but, by about 16 weeks of age, these have dropped below those of lean

controls. This is because the pancreatic β-cells have ceased to respond to the glucose stimulus [Orci *et al.,* 1990; Unger *et al.,* 1991], a change associated with the disappearance of GLUT-2 glucose transporters on the β-cells [Ohneda *et al.,* 1994]. The model has also been shown to have reduced numbers of GLUT-4 receptors in skeletal muscle in long-term diabetes [Friedman *et al.,* 1991].

Plasma TG and cholesterol concentrations are also higher than those of lean rats and can be induced to reach very high levels by feeding rats a diet high in saturated fat and sucrose. In fact, when fed such a diet, containing no cholesterol, cholesterol and TG concentrations can reach 44 and 110 mM, respectively, as compared to ~1 and 2 mM in controls (Chapter 4). ZDF rats also develop other pathogenic features characteristic of type 2 diabetes. These include nephropathy, neuropathy and moderate hypertension [Kawaguchi *et al.,* 1999; Peterson, 1994].

(3) The cause of diabetes in the ZDF rat

The mechanisms of adipogenic diabetes in ZDF rats involve an increased, ultimately cytotoxic, fat content in the islets. This accumulation can be partly attributed to the hyperphagia resulting from the mutation in the leptin receptor. The importance of an intracellular, more so than a plasma, build-up of FFAs in insulin resistance forms the basis of the lipotoxicity theory, which has been explained in the Introduction [1.3.1 (ii) (a) (2)].

Chronic TG overload in β-cells occurs after intracellular esterification of long-chain FAs. This upregulates expression of the inducible form of nitric oxide synthase (iNOS), the enzyme catalysing the formation of nitric oxide (NO) from arginine. Cytotoxic levels of NO are then generated and impair the function of the β-cells, reducing their ability to secrete insulin to compensate for insulin resistance.

which then results in hyperglycaemia. The β-cells then undergo apoptosis, as has been shown by significant rises in DNA-laddering, an index of apoptosis, in isolated islets from diabetic ZDF rats. These effects can be almost completely blocked and diabetes prevented by iNOS inhibitors, such as nicotinamide or aminoguanidine, and by measures that lower intracellular TG independently of the leptin receptor; e.g., dietary restriction and anti-lipolytic drugs such as TZDs [Shimabukuro *et al.,* 1998c; Unger, 1997].

(4) The potential of the lean ZDF counterpart as a model of diet-induced obesity and insulin resistance

Lean ZDF rats, of either the homo- or heterozygous genotype, are thought to be genetically equal to fatty rats, except for the obesity trait. Although there are currently no hard data available which demonstrate phenotypic differences from other lean control rats such as Wistars, lean ZDF rats are typically used as controls for obese ZDF rats. Aside from this, the lean ZDF rat that has become obese through the consumption of high-calorie food may prove to be a useful model of human type 2 diabetes. This dietary obese (DIO) rodent model is described below and in the General Introduction [1.5.1 (ii) (a)], but, in short, as its metabolic symptoms, including insulin resistance, arise from the consumption of a very palatable, energy-dense, lipogenic diet, it can be argued that it more closely resembles human insulin resistance than do the genetic rodent models.

(5) Continuation of previous ZDF work

The use of the ZDF rat in Chapter 3 was carried out in order to expand on the work of colleagues Upton *et al.* [1998]. They had discovered that the TZD, MCC-555,

improved insulin sensitivity in the mature ZDF rat with established diabetes, but it remained to be seen if this drug could, in addition, delay the onset of the disease if administered to younger, pre-diabetic animals.

As described above, experimental (fatty) rats were of the genotype *fa/fa* (-/-), and lean rats (+/+ or +/-) served as non-diabetic controls. Studies began with rats in the pre-diabetic state, at 6-7 weeks of age (200-240 g) and continued until they had become fully diabetic (10 weeks of age) and sometimes longer (up to 21 weeks of age in the case of lean rats fed the palatable diet; see Chapter 4).

(ii) The diet-induced model of obesity and insulin resistance

Generally, mutant rodent strains show severe insulin resistance and β-cell failure, features which are not usually typical of human type 2 diabetes. This has led to the search for a model more representative of the human form of the disease; i.e., one which has IGT and mild insulin resistance resulting from the obesity acquired from the intake of a high-energy, palatable diet.

Rats have a variable response to an obesity-inducing diet, in that no two randomly selected populations will gain weight to exactly the same extent or within exactly the same time period; e.g., a population of Wistars, purchased from outside suppliers, was found to show a significant separation from controls after 7 weeks on a highly palatable diet (+4%; $p<0.05$; see Chapter 5 and Pickavance *et al.,* 1999b). Another, obtained from the in-house colony at the Biomedical Services Unit (BSU), University of Liverpool, was 6% heavier ($p<0.01$) after only 4 weeks on the highly palatable diet (HPD), compared with their chow-fed controls (Chapter 5). This polygenic response is similar to that of human populations.

In addition, moderate insulin resistance may develop in this model, either with or without mild hyperglycaemia, and, therefore, it is more typical of early type 2 diabetes in humans. There is extensive literature to show that rats fed high-fat or highly palatable diets become progressively more obese than chow-fed littermates, and develop insulin resistance and hyperleptinaemia [Chang *et al.,* 1990; Harrold *et al.,* 2000a; Kraegen *et al.,* 1991; Pickavance *et al.,* 1999b, 2000; Storlien *et al.,* 1986; Chapters 4-7], similar to obese humans [for review, see Kopelman, 2000]. They do not develop overt diabetes, but the absence of a genetic defect in the production of leptin or its receptor, and the development of obesity on a polygenic background, make this an attractive model.

For these reasons, in studies of dietary obesity, non-mutagenic outbred Wistar rats fed an HPD were used. Males were selected with a starting weight ranging between 175-250 g (Chapters 5 & 6) and were obtained from Charles River U.K. Ltd. (Margate, U.K.). Females age-matched to males had starting weights between 170-180 g (Chapter 7). They were purchased from A. Tuck & Son (Essex, U.K.) rather than Charles River for reasons of cost, numbers required and speed of delivery. By convention, males were used for earlier studies. Females were required for later comparative studies of TZDs because it had been found by other researchers that one of the TZDs to be compared, troglitazone, has greater bioavailability in female than male rats. This is reflected in greater plasma concentrations of troglitazone in females and lower concentrations of a metabolite produced by sulfonation of the drug, this latter activity occurring at higher levels in males [Kawai *et al.,* 1997].

(a) Induction of dietary obesity

Rats were fed the HPD for 7-10 weeks to induce mild obesity. Obesity was defined as excess fat, later proved by significant increases in fat pad mass above control (chow-fed) levels. The palatable diet consisted of 33% powdered chow (ground using a Crypto Peerless K55 catering blender, Birmingham, U.K.), 33% condensed milk (Nestlé U.K. Ltd., York, U.K.) and 7% sucrose (Tate & Lyle, London, U.K.) by weight, with the remainder being added tap water. This provided 65% of energy as carbohydrate, 19% as protein and 16% as fat [Wilding *et al.,* 1992b]. Age-matched controls were fed pelleted chow [CRM (P), Biosure, Cambridge, U.K.], which consisted of 60% of energy as carbohydrate, 30% as protein and 10% as fat. From these statistics, it is clear that the proportion of fat in the HPD is not much greater than that in normal chow; i.e., only 6% higher. It is presumed that it is the palatable texture of the diet, as well as its composition, which induces hyperphagia in rats. The diet was made up in 8-to-15-kg batches, mixed by hand, and either stored at 4°C or frozen for prolonged storage.

2.1.3. Monitoring the progress of diabetes and insulin resistance

To monitor disease progression in ZDF rats and any drug-induced metabolic changes therein, blood glucose and insulin concentrations were measured at regular intervals, once or twice weekly. Daily water intake was also determined as an indication of the progression of the polydipsia symptom of the disease. Similarly, daily food intake was measured as an indication of the development of hyperphagia.

(i) Repeated blood sampling for measurement of circulating hormones and metabolites

Blood was obtained for diagnostic assay by extraction from the tail. This was performed once a week during periods of oral drug administration [see 2.1.7], and throughout terminal glycaemic clamping procedures [see 2.2.3 (iii)]. During drug administration periods, rats were first lightly anaesthetised with an intramuscular (i.m.) injection of Hypnorm™ (fentanyl/fluanisone; 0.4 ml/kg; Janssen Pharmaceutical Ltd., Oxford, U.K.). Fentanyl is an analgesic, and fluanisone is a neuroleptic (antipsychotic agent). A reduced dose meant that time spent unconscious and potentially interfering with food intake, being measured daily at this stage of experiments, was as short as possible.

The extreme tip of the rat's tail was then cut off, avoiding the terminal vertebrae. This method is known as tail scarification, and it allows for repeated sampling from the same rats in studies following the progression of metabolic changes, such as the development of diabetes. It enabled quantities of blood (~250 µl), yielding plasma in sufficient volume for assay, to be quickly and painlessly removed from the rat. A scab would form at the tail tip overnight and was simply snipped off for the next sampling a few days later.

At the end of each week of drug treatment, concentrations of insulin and FFAs in the blood were determined by first collecting the tail blood in microfuge tubes set on ice and centrifuging the same day at 14,000 revolutions per minute (rpm) for 5 minutes (min) (Eppendorf 5415C centrifuge, Eppendorf, Germany). Plasma was then stored at –40°C for the later measurement of insulin concentrations by radioimmunoassy (RIA) kit and FFAs by colorimetric kit [see below for descriptions of these assays: 2.2.1 (i) (c) and (ii) (b)]. This procedure also allowed blood glucose

concentrations to be measured immediately at the time of the tail snip with an electrochemical meter and blood glucose electrodes [Precision Q.I.D.™ Sensor and Precision Plus electrodes, Medisense®, Abingdon, Oxon, U.K.].

2.1.4. Anaesthesia and analgesia

The small body size of the rat makes intravenous (i.v.) injection difficult, and drugs are usually administered by intraperitoneal (i.p.) or i.m. routes. If these routes are used, it is not possible to administer the drug gradually, and the anaesthetic must be given as a single, calculated dose. Because of the wide variation in drug response between different strains of rat, between male and female animals and between individuals, it is best to use a drug or drug combination providing a wide margin of safety.

The anaesthetic combination of choice for rats is fentanyl/fluanisone (Hypnorm™), together with diazepam (Valium®, Roche, Welwyn Garden City, Herts., U.K.; both 0.8 ml/kg, i.m.), or midazolam. Diazepam is a benzodiazepine, one of a widely used group of drugs with powerful tranquilising action on the CNS. It also acts as a skeletal muscle relaxant [Hopkins, 1985] and is long-acting. Benzodiazepines, however, have no analgesic action [British National Formulary (BNF), 1994], hence the combination of diazepam with Hypnorm™. The effects of this combination last approximately 20-40 min. The longer periods of anaesthesia required for eu- and hyperglycaemic clamping (Chapters 3-5) were achieved by administration of additional doses of Hypnorm™ (~0.1 ml/kg i.m. every 30-40 min) [Flecknell, 1986; University's Accreditation Scheme Training Group, 1995]. In Chapter 5, this mixture was given as a 1:1:2 i.p. injection of Diazemuls®, Hypnorm™

and water (3.3 ml/kg). Diazemuls® (Dumex Ltd., Tring, Herts., U.K.) is an emulsion preparation of the oil-based diazepam, but less irritant, and with less erratic absorption from the site of injection.

However, in Chapter 3, rats undergoing hyperinsulinaemic-euglycaemic clamps were anaesthetised instead with i.p. injections of pentobarbitone (30 mg/kg, i.p.; Sagatal®, Harlow, Essex, U.K). Sagatal® (6% sodium pentobarbitone w/v; Rhône Mérieux Ltd., Essex, U.K.) was used because it is a sedative and general anaesthetic for small animals and sedation was easily maintained by administration of further incremental doses (Sagatal® package insert, 1994). By the time subsequent clamping experiments were undertaken, it was discovered that the diazepam/Hypnorm™ combination and route of delivery were preferable to the use of Sagatal® because they caused the animals to become fully anaesthetised more quickly.

2.1.5. Housing and maintenance

All rats were housed singly in solid-bottomed cages during periods of drug treatment, to allow for individual measurements of food and water intake. They were maintained at 22 ± 2 °C on a 12-hour light-dark cycle (lights on at 07.00), except for those administered troglitazone (Chapter 7). As this drug is better absorbed with food, and rats consume the majority of their food at night [Sidlo *et al.*, 1995; Tachi *et al.*, 1981], the drug was administered just before the dark period. Therefore, for the sake of convenience, these rats were maintained on a reverse phase schedule (lights on 03.00-15.00).

All rats had free access to tap water throughout each experiment. In addition, except for those fed on the HPD (Chapters 4-7) and those used in pair-feeding

paradigms (Chapter 6), all rats had free access to standard pelleted rodent chow. The HPD was dispensed in stainless steel troughs (115 x 75 x 47 mm) placed within the cages. These troughs were made to order (Arrowmight, Biosciences, Hereford, U.K.) in such a way that they were stable and only very rarely tipped over when the rats fed from them. The HPD was replaced with a fresh helping daily. All control rats were housed on sawdust. Cages housing rats on the HPD were lined with absorbent paper (Beta-Sorb, Beta Medical and Scientific, Datesand Ltd., Sale, U.K.), as past observations had shown that the rats tended to toy with the diet, mixing it with the sawdust.

Body weight and food intake were measured daily throughout dosing periods to monitor drug-induced changes in both. Rats were placed one at a time in a small bowl or tub, the weight of which had been previously tared on the balance, and, over a 4-second time period, readings were averaged by a weighing box attached to the balance and designed to compensate for the animal's movement (Precisa Precision 2200C, Milton Keynes, Bucks., U.K.).

ZDF rats were imported under the regulations of the Ministry of Agriculture, Fisheries and Food (MAFF) in the U.K. to a designated quarantine unit in the BSU, where they remained for the duration of the studies and within which all procedures were performed.

2.1.6. Drug sources

MCC-555 (Chapter 3) was obtained from Mitsubishi Chemical Corporation, Yokahama, Japan. Other PPARγ agonists tested in ZDF rats (Chapter 4) were supplied by Novo Nordisk, Maløv, Denmark. The PPARα agonist used in this study, bezafibrate, came from a commercial source (Sigma Chemical Company, Poole,

Dorset, U.K.). It was selected because there was evidence in the literature that it was an effective lipid-lowering compound, significantly reducing plasma TGs by 51% at a daily dose of 30 mg/kg after only 14 days' administration [Kazumi *et al.*, 1990]. All TZDs used in dose-response studies of the DIO model (rosi-, pio- and troglitazone; Chapters 5-7) were supplied by SmithKline Beecham Pharmaceuticals, Harlow, Essex, U.K.

2.1.7. Drug administration

Drugs were dissolved in vehicle [0.5-1% sodium carboxymethyl cellulose (CMC; Sigma Chemical Company, Poole, Dorset, U.K.)], which itself was administered orally to control animals at 1 (Chapters 4-7) or 5 ml/kg/d (Chapter 3). Drugs were also administered orally every day for periods ranging from 2-4 weeks. A metal feeding cannula [gauge: 18; length: 50 mm; tip: 2.25 mm diameter (Interfocus Ltd., Haverhill, Suffolk, U.K.)] fixed to a 1-ml syringe (B-D® Plastipak®, Becton Dickinson, Madrid, Spain) was used for all drugs except for the highest concentration of troglitazone (1000 mg/kg; Chapter 7). Due to the thickness of this suspension, a cannula with a wider bore (guage: 16; tip: 3 mm diameter) fixed to a 2.5 ml syringe was required for ease of administration. Also, whereas all other dosages were given in a single bolus, the latter was administered in two separate halves, separated by a period of 20-60 min, because the viscosity made it difficult for the rats to swallow except in a small volume. Control animals in this study received placebo (excipient mix from crushed troglitazone tablets) at a dose of 10 mg/kg dissolved in 1% CMC, as a suspension of this concentration was easily administered. All drugs and troglitazone placebo formed suspensions which required agitation by inversion of the vials in which they were stored before administration to each individual rat.

Suspensions were prepared on an approximately weekly basis and stored at 4°C when not in use.

2.1.8. Termination

With the exception of those ZDF rats described in Chapter 3, which were terminated in the fed state, rats were terminated after a 4- (Chapters 5-7) or 12-h fast (Chapter 4) to reduce variability in plasma concentrations of hormones and metabolites. Rats that underwent glycaemic clamping (Chapters 3-5) did not recover from anaesthesia and were killed by cardiac exsanguination while still anaesthetised. In all other studies, rats were killed by inhalation of a saturated atmosphere of CO_2 in a small enclosed chamber followed by cardiac exsanguination.

2.2. Acquisition of metabolic data and tissue mass

2.2.1. Terminal plasma concentrations of hormones and metabolites

(i) Radioimmunoassays

The advantages of the RIA are severalfold: It is a very sensitive method, often capable of detecting very low concentrations [as little as a few femtomoles (fmol)] of hormone or peptide, beyond the capabilities of most other assay types. Because of its sensitivity, it allows for the assay of small volumes, useful when samples are precious. The RIA can also be extremely specific, especially when the antibody binding site is specific to a 3-4 amino acid region (the antigenic determinant) particular to the molecule of interest. The RIA system also lends itself readily to the simultaneous estimation of large numbers of samples, especially as gamma counting is now automated. Although other technologies, such as the enzyme-linked immunosorbent assay (ELISA), provide a potential alternative, they do not improve

on antibody avidity or assay error, the two critical parameters determining assay detection limit. The RIA provides scope to increase working accuracy, precision and sensitivity [Bloom & Long, 1982].

(a) Principle of the RIA

The concentrations yielded by an RIA depend on the competition between a radioactively labelled and unlabelled peptide or hormone for the specific binding site of an antibody. The amounts of antibody and labelled peptide are fixed, the only variable being the unlabelled peptide concentration. The higher the concentration of unlabelled peptide, the less radioactively labelled peptide will bind to the antibody. The bound peptide is then separated from the free peptide, and the amount of labelled peptide bound to the antibody can be determined by counting the radioactivity. Known quantities of pure peptide are used to construct a standard curve to which quantities of unknown samples are compared. Enough standards must be included to cover the full range of expected unknown values. The amount of antibody in the assay is such that it binds about 50% of the label added in the absence of unlabelled peptide. This point is midway between the non-specific binding (NSB) of the label and the maximal binding by excess antibody, giving the steepest slope of the standard curve and optimal precision in counting.

(b) RIA requirements

The requirements of a good RIA are precision or reproducibility, ability to measure small amounts of peptide (sensitivity) and specificity, such that the antibody shows as little cross-reaction with other peptides as possible. A sensitive assay will have a steep standard curve slope and only small errors between replicates; i.e., precision.

This allows small differences between unknown concentrations to be measured with confidence. In the case of RIAs using radioactive iodine (^{125}I), such as the insulin and leptin RIAs used in the studies described here, the addition of one radioactive iodine atom to each peptide molecule is the practical maximum. The peptides labelled in this way, therefore, have a high specific activity, and the amount of each which can be added to an assay tube can be reduced to ~1 fmol without requiring a compensatory long counting time. Sensitivity also depends on length of incubation time and temperature; thus, the sensitivity of an assay increases with longer incubations and reduced temperature [Bloom & Long, 1982].

(c) Insulin and leptin RIAs

In the studies described here, when rats were terminated, blood was removed transcardially, placed in lithium-heparin-coated tubes and plasma separated by centrifugation at 2,500 rpm for 20 min at 4°C and stored at –40°C until assayed. Insulin and leptin concentrations were determined using commercially available RIA kits (Pharmacia/Upjohn Diagnostics U.K., Lewes, Sussex, U.K. and Linco Research, Biogenesis, Poole, Dorset, U.K., respectively). The antibodies in these two RIAs were raised against human insulin and mouse leptin, respectively. Standards and tracers were prepared with human insulin or mouse leptin. These two peptides are highly homologous to their rat counterparts, and, therefore, the kits were considered appropriate for measurement of these peptide concentrations in rat plasma.

Both RIA procedures were based on the double antibody principle: Insulin or leptin in the plasma sample competes with a fixed amount of ^{125}I-labelled insulin or leptin for the binding sites on the specific antibodies. Bound and free insulin or leptin are separated by addition of a second antibody immunoadsorbent suspension

followed by centrifugation and decanting. The radioactivity in the pellet is then measured and is inversely proportional to the quantity of insulin or leptin in the sample. The insulin RIA was sensitive, with a detection limit of <2 μU/ml (<12 pM) and had high precision, with intra- and inter-assay coefficients of variation (CVs) of approximately 6% [Pharmacia Insulin RIA 100 package insert, 1998]. The limit of sensitivity of the leptin assay was also high, 0.2 ng/ml, and sample results greater than 20 ng/ml were diluted and assayed again, multiplying the result by the dilution factor. Intra- and inter-assay CVs ranged between 5-11% and 3-15%, respectively [Linco mouse leptin RIA kit package insert, 1997].

All radioactive counts per minute (cpm) were obtained using a gamma counter (COBRA™ Auto-Gamma®, Canberra Packard International S.A., Zurich, Switzerland) with a counting efficiency of ~80%. The counter's RiaSmart™ software package subtracted the NSB from each count (except total counts), prior to final data reduction to either μU/ml (insulin) or ng/ml (leptin). Samples were run in duplicate in most cases, except where collected blood volumes were too small (i.e., from tail snips performed during drug treatment periods or clamping procedures). Counts from each pair of tubes (duplicate samples) were also averaged by the counter software.

(ii) Enzymatic assays

The enzymatic assay is a useful method for the quantitative determination of the concentration of a particular biological compound within a solution, often plasma or serum. It exploits the fact that the compound of interest will be converted, dependent on the presence of a certain enzyme or enzymes, into another compound, through a series of reactions. This commonly produces a chromophore, such that the

concentration of the compound of interest is directly related to the depth of colour in the solution and is thereby quantitated at a particular wavelength using a spectrophotometer (Lightwave UV/Vis Diode-Array Spectrophotometer, WPA, Cambridge, U.K.).

Such assays are of obvious diagnostic value, and many have been conveniently streamlined by pharmaceutical companies to provide all of the required components of the enzymatic pathway in a single kit. This speeds up routine laboratory analyses significantly. The plasma samples assayed in this way were obtained as described above [2.2.1 (i) (c)].

(a) Principle of the glucose assay

The test kit for glucose (non-colorimetric; Roche Diagnostics; Milton Keynes, Bucks., U.K.) is based on the following principle: D-glucose is phosphorylated to D-glucose-6-phosphate (G-6-P) in the presence of the enzyme hexokinase (HK) and adenosine-5'-triphosphate (ATP), with the simultaneous formation of adenosine-5'-diphosphate (ADP):

$$\textbf{D-glucose + ATP} \xrightarrow{HK} \textbf{G-6-P + ADP}$$

In the presence of the enzyme glucose-6-phosphate dehydrogenase (G6P-DH), G-6-P is oxidised by nicotinamide-adenine dinucleotide phosphate (NADP) to D-gluconate-6-phosphate with the formation of reduced nicotinamide-adenine dinucleotide phosphate (NADPH):

$$\textbf{G-6-P + NADP}^{+} \xrightarrow{G6P\text{-}DH} \textbf{D-gluconate-6-phoshpate + NADPH + H}^{+}$$

The amount of NADPH formed in this reaction is stoichiometric to the amount of D-glucose. The increase in NADPH is measured by means of its light absorbance at 340 nm in the UV range.

(1) Protocol for determination of glucose concentration in plasma

First, plasma samples had to be de-proteinised. This involved mixing 1 ml of 3% perchloric acid with 100 µl of plasma in a 1.5-ml Eppendorf tube and centrifuging for 5 min at 5000 rpm. Then, 1 ml of a solution containing NADP and ATP was added to an empty 3-ml plastic cuvette (the 'blank') as well as to cuvettes containing 100-µl volumes of the de-proteinised plasma solution. The volumes were made up to 3 ml by adding 2 ml of distilled water to all cuvettes. The final concentrations of NADP and ATP were 0.8 mg/ml and 1.9 mg/ml, respectively. The solutions were mixed and the first set of absorbances (A_1) read at 340 nm at room temperature (RT) after about 3 min, referencing against the blank. Next, 20 µl of a suspension containing HK and G6P-DH (final concentrations 1.94 U/ml and 0.97 U/ml, respectively) were added to each cuvette and the solutions mixed. After allowing the reaction to proceed for 15 min (the endpoint of the reaction), the second set of absorbances were read (A_2) at 340 nm. These absorbances were then applied to the general equation for calculating concentrations (**c**):

$$\mathbf{c} = \frac{\mathbf{V}}{\mathbf{v} \times \mathbf{d} \times \varepsilon} \times \Delta\mathbf{A},$$

where

V = final volume (ml)

v = sample volume (ml)

d = light path (cm)

ε = absorption coefficient of the dyestuff at the wavelength; in this case, ε=extinction coefficient of NADPH at 340 nm = 6.3

ΔA = the absorbance difference $(\mathbf{A_2 - A_1})$

This reduces to the formula

$$\mathbf{52.49 \times \Delta A}$$

to yield the concentration of glucose in plasma in mM units [D-glucose package insert, Roche Diagnostics, 2000].

(b) Principle of the FFA assay

The test kit for determination of FFA concentration in plasma came from the same commercial source as that for glucose and is based on the following principles: FFAs are, in the presence of the enzyme acyl-CoA synthetase (acyl CS), converted by ATP and coenzyme A (CoA) into acyl-coenzyme A (acyl-CoA), resulting in adenosine-5'-monophosphate (AMP) and pyrophosphate. Acyl CoA reacts with oxygen (O_2) in the presence of acyl-CoA oxidase (ACOD) to form 2,3-enoyl-coenzyme A (enoyl-CoA).

The resulting hydrogen peroxide (H_2O_2) converts 2, 4, 6-tribromo-3-hydroxy-benzoic acid (TBHB) and 4-aminoantipyrine (4-AAP) to a red dye in the presence of peroxidase (POD). The dye is measured in the visible range at 546 nm.

$$\mathbf{FFAs + CoA + ATP} \xrightarrow{\textit{Acyl CS}} \mathbf{acyl\text{-}CoA + AMP + pyrophosphate}$$

$$\mathbf{Acyl\text{-}CoA + O_2} \xrightarrow{\textit{ACOD}} \mathbf{enoyl\text{-}CoA + H_2O_2}$$

$$\mathbf{H_2O_2 + 4\text{-}AAP + TBHB} \xrightarrow{\textit{POD}} \mathbf{red\ dye + 2\ H_2O + HBr}$$

(1) Protocol for determination of FFA concentration in plasma

One ml of a solution containing ATP, CoA, acyl CS, POD and 4-AAP and TBHB was added to an empty 1-ml plastic cuvette (the 'blank') as well as to cuvettes containing 50-µl volumes of plasma. The volume of the blank was made up with 50 µl of distilled water. The solutions were mixed and allowed to sit for 10 min at RT. Fifty µl of a solution containing N-ethyl-maleinimide was then added to all cuvettes for the removal of an existing surplus of CoA before the oxidation of the activated FFAs by ACOD. The solutions were then mixed and the first set of absorbances (A_1) read at 546 nm measured against water. The reaction was started by adding 50 µl of a solution containing ACOD to all cuvettes. The solutions were mixed again and the end of the reaction reached at RT after 15 min. The second set of absorbances (A_2) were then read, again at 546 nm. The absorbance differences ($A_2 - A_1$) were calculated for both blank and unknown (plasma) samples and applied to the formula

$$\Delta A = \Delta A_s - \Delta A_b,$$

where ΔA_s and ΔA_b are the absorbance differences of each unknown sample and the blank, respectively. These values were then applied to the formula

$$\mathbf{1.192 \times \Delta A}$$

derived from the general formula for calculating the concentration outlined above [see 2.2.1 (ii) (a) (1)], and where

ε = absorption coefficient of the red dye at 546 nm = 19.3,

to yield the concentration of FFAs in plasma in mM units [free fatty acids, half-micro test package insert, Roche Diagnostics, 2000].

(c) Principle of the triglyceride assay

The assay system for determination of triglyceride (TG) concentration in plasma (Sigma-Aldrich Co., Ltd., Poole, Dorset, U.K.) involved a series of reactions as follows:

TGs are enzymatically hydrolysed by lipoprotein lipase (LPL) to FFAs and glycerol:

$$\mathbf{TGs + H_2O} \xrightarrow{LPL} \mathbf{glycerol + FFAs}$$

The glycerol is phosphorylated by ATP with glycerol kinase (GK) to produce glycerol-3-phosphate and ADP:

$$\mathbf{Glycerol + ATP} \xrightarrow{GK} \mathbf{glycerol\text{-}3\text{-}phosphate + ADP}$$

Glycerol-3-phosphate is oxidised to dihydroxyacetone phosphate (DAP) by glycerol phosphate oxidase (GPO) producing hydrogen peroxide (H_2O_2):

$$\mathbf{Glycerol\text{-}3\text{-}phosphate + O_2} \xrightarrow{GPO} \mathbf{DAP + H_2O_2}$$

In a colour reaction catalysed by peroxidase (POD), the H_2O_2 reacts with 4-aminoantipyrine (4-AAP) and 3,5 dichloro-2-hydroxybenzene sulfonate (3,5 DHBS) to produce a red-coloured dye. The absorbance of this dye is proportional to the concentration of TGs present in the sample:

$$\mathbf{H_2O_2 + 4\text{-}AAP + 3,5\ DHBS} \xrightarrow{POD} \mathbf{Quinoneimine\ dye + 2H_2O}$$

(1) Protocol for determination of TG concentration in plasma

Only a single reagent was required for this test, and its active ingredients included ATP, 4-AAP, 3,5 DHBS, POD, GK, GPO and LPL. One ml was added to 1-ml

plastic cuvettes containing 10-µl volumes of plasma samples and distilled water, in the case of the blank. The final concentrations of the above ingredients were 2.5 mM, 0.8 mM, 1 mM, 5.4 U/ml, 0.56 U/ml, 6 U/ml and 31 U/ml, respectively. As calibration was also required for this test, one cuvette contained 10 µl of an aqueous solution of glycerol standard (250 mg/dL stock concentration; 0.025 mg/ml final concentration; Sigma-Aldrich Co., Ltd., Poole, Dorset, U.K.) and 1 ml of the reagent. The solutions were mixed, and after a reaction time of 15 min at RT, absorbances were read at 520 nm, referencing against the blank. These values were then applied to the formula

$$\textbf{[TG, mM]} = \frac{\textbf{absorbance of unknown}}{\textbf{absorbance of calibrator}} \textbf{ x calibrator value x 0.0113},$$

where

calibrator value = 250 mg/dL, and

0.0113 = unit conversion from mg/dL to mM

to give plasma concentrations of TG [Infinity™ Triglycerides Reagent package insert, Sigma Diagnostics®, 2000].

(d) Principles of the total and HDL cholesterol assays

The assay system for determination of cholesterol concentration in plasma (Sigma-Aldrich Co., Ltd., Poole, Dorset, U.K.) involved a series of reactions as follows:

Cholesterol esters are enzymatically hydrolysed by cholesterol esterase (CE) to cholesterol and FFAs:

$$\textbf{Cholesterol esters} \xrightarrow{CE} \textbf{cholesterol + FFAs}$$

Free cholesterol is then oxidised by cholesterol oxidase (CO) to cholest-4-en-3-one and hydrogen peroxide:

$$\textbf{Cholesterol} + \mathbf{O_2} \xrightarrow{CO} \textbf{cholest-4-en-3-one} + \mathbf{H_2O_2}$$

The hydrogen peroxide combines with hydroxybenzoic acid (HBA) and 4-aminoantipyrine (4-AAP) in the presence of peroxidase (POD) to form a chromophore (quinoneimine dye) which may be quantitated at 500 nm:

$$\mathbf{2H_2O_2 + HBA + 4\text{-}AAP} \xrightarrow{POD} \textbf{quinoneimine dye} + \mathbf{4H_2O}$$

(1) Protocol for determination of total and HDL cholesterol concentrations in plasma

Only a single reagent was required for this test, and its active ingredients were CO, CE, POD, 4-AAP and HBA. One ml was added to 1-ml plastic cuvettes containing 10-µl volumes of plasma samples and distilled water, in the case of the blank. The final concentrations of the above ingredients were 0.1 U/ml, 1.25 U/ml, 0.8 U/ml, 0.25 mM and 10 mM, respectively. As calibration was also required for this test, one cuvette contained 10 µl of an aqueous cholesterol solution (200 mg/dL stock concentration; 0.02 mg/ml final concentration; Sigma-Aldrich Co., Ltd., Poole, Dorset, U.K.) and 1 ml of the reagent. The solutions were mixed, and after a reaction time of 15 min at RT, absorbances were read at 500 nm, referencing against the blank. These values were then applied to the formula

$$\textbf{[cholesterol, mM]} = \frac{\textbf{absorbance of unknown}}{\textbf{absorbance of calibrator}} \textbf{ x calibrator value x 0.0259},$$

where

calibrator value = 200 mg/dL, and

0.0259 = unit conversion from mg/dL to mM

to give plasma concentrations of total cholesterol [Infinity™ Cholesterol Reagent package insert, Sigma Diagnostics®, 2000].

The active ingredients in the reagent used to isolate the HDL fraction of the plasma samples were dextran sulfate and magnesium ions. These precipitate LDLs, VLDLs and most IDLs, leaving the HDL fraction in solution. Thus, 25 µl of reagent was added to 250 µl of plasma in microcentrifuge tubes, vortexed to mix, and allowed to stand at RT for 5 min. The tubes were then vortexed again and centrifuged for 5 min at 14, 000 rpm. The assay was performed exactly as described above using the total cholesterol reagent, except with 10-µl samples of the HDL-containing supernatant in the place of plasma samples and the calibrator reduced to one quarter of the stock concentration (50 mg/dL).

2.2.2. Assessment of side effects of TZD treatment

(i) Fat pad mass

The masses of a couple or more fat pads can be taken as an accepted index of body composition in rodents when expressed as a percentage of whole body weight, or representation of body fat as a whole when expressed as absolute weights and have been used as such by various researchers [Clapham *et al.*, 2000; Upton *et al.*, 1998; Widdowson *et al.*, 1997].

To determine the effects of the different drug treatments on fat stores in different depots, various fat pads were dissected free and weighed at termination. White adipose tissue (WAT) pads included perirenal, gonadal and subcutaneous. The male gonadal fat pad was the epididymal (Chapters 3-6) and the female pad the

parametrial (Chapter 7). The subcutaneous fat pad was dissected from the abdomen immediately below the sternum (Chapter 4) to be used as a more reliable measure of real body fat content changes [see General Introduction, 1.6.5 (v) (a) (3)]. Interscapular brown adipose tissue (BAT) was also dissected and weighed (Chapter 4). Weights were then expressed as a percentage of total body weight to give a measure of body fat content.

(ii) Heart mass and packed cell volume

At termination, hearts were excised, blotted and weighed as an assessment of cardiac hypertrophy. As an index of haemodilution, packed red cell volume (PCV) was measured by drawing up samples of blood into microhaematocrit capillary tubes [Scientific Laboratory Supplies (SLS) Ltd., Nottingham, U.K.], plugging one end with Cristaseal® (Hawksley, Sussex, U.K.), separating plasma by centrifugation (3 min, 3000 rpm; Mikro 20 haematocrit centrifuge, Andreas Hettich GmBH & Co., Tuttlingen, Germany) and reading PCV as a percentage off a microhaematocrit standard reader (SLS, as above).

2.2.3. Measurement of insulin sensitivity

β-cell sensitivity to glucose and body tissue sensitivity to insulin are the two primary physiological variables which must be assessed in order to understand the mechanism of disorders of glucose homeostasis, such as type 2 diabetes [DeFronzo *et al.*, 1979].

(i) The oral glucose tolerance test and other indices

Early attempts to assess these variables made use of the oral glucose tolerance test (OGTT). This test involves the ingestion of a bolus of glucose (e.g., 75 g) by the

subject, after which the changes in blood glucose and plasma insulin concentrations are monitored over several hours. As a result of gastrointestinal absorption, blood glucose concentration rises, and plasma insulin concentrations increase in association with this, with a slight time lag in normal subjects [Vander *et al.,* 1985]. The duration of this lag and the degree to which insulin is secreted in response to the glucose stimulus, reflected in the absolute insulin concentration, indicate how tolerant the subject is to glucose. Obese subjects show exaggerated glucose and insulin responses to the oral glucose challenge [for review, see Kopelman, 2000]. Sometimes pre-diabetic subjects who have IGT show an increased time-lag and lower insulin concentration compared to normal subjects. In other cases, subjects with IGT are insulin-resistant, and so show paradoxically higher insulin concentrations. They usually tend to show a delayed first phase and exaggerated second phase insulin response. The insulin response is lost later when these subjects become diabetic [see 1.3.1 (ii) and Fig. 2.2]. However, concentration curves obtained from individuals, as opposed to whole populations, tend to be erratic. This has led to the use of various insulin-glucose concentration ratios as indices of β-cell response and tissue sensitivity to insulin. The problem with these computations is that they incorporate some unsound assumptions. For example, the [glucose]/[insulin] ratio, used as an index of tissue sensitivity to insulin, assumes that in the feedback loop between glucose and insulin, one varies while the other remains constant, such that the rises and falls in response to each other are sequential, when, in fact, they are simultaneous [DeFronzo *et al.,* 1979]. This has led to a search for other models that can be used to assess insulin sensitivity.

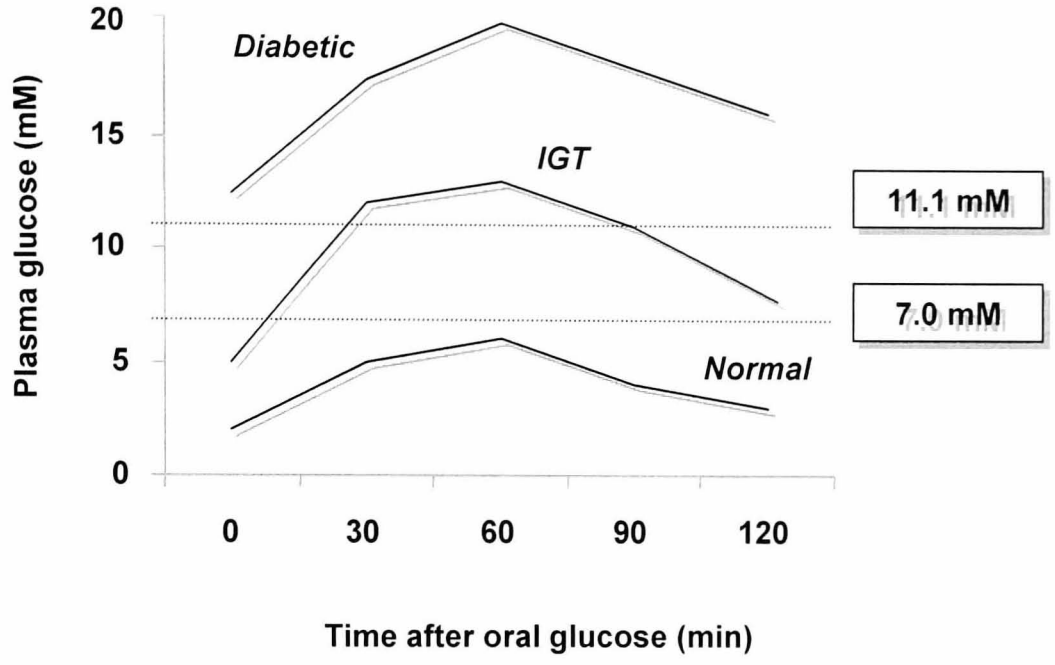

Figure 2.2. Outcome of the OGTT, showing schematic profiles for overt diabetes, IGT and normality. A 'casual' (random) concentration that exceeds 11.1 mM or a fasting value of $\geq$ 7.0 mM establishes the diagnosis. Adapted from Keen H & Barnes DJ (1997) In Pickup J & Williams G (eds) *Textbook of Diabetes;* p. 2.4.

(ii) Homeostasis Model Assessment (HOMA)

This model incorporates measures of fasting plasma concentrations of glucose and insulin. Thus, terminal concentrations of glucose and insulin, obtained as described above [2.2.1(i) (c) and (ii) (a)], were used to calculate an index of insulin resistance as

$$\frac{[\text{insulin}] \times [\text{glucose}]}{22.5}$$

where insulin concentration is expressed in units of μU/ml and glucose in mM. Note that, as is the convention in many publications, plasma insulin concentration is given in pmol/l (pM) units throughout this thesis, using the conversion factor of 6.0; i.e., μU/ml x 6 = pM. Exceptions to this are when insulin concentration units are

incorporated into HOMA, as described above, or when expressing the units of insulin secretory response during the hyperglycaemic clamp; i.e., μU/ml/min (see Chapter 4).

The accuracy of the HOMA estimate has been validated against independent measures of insulin resistance using euglycaemic clamps, and these correlate highly [Bonora *et al.,* 2000; Emoto *et al.,* 1999; Matthews *et al.,* 1985]. This correlation accords with the hypothesis that basal glucose and insulin interactions are largely determined by a simple feedback loop. Homeostatic concentrations of insulin and glucose arise from varying degrees of β-cell deficiency and insulin resistance. The model assumes that normal subjects have 100% β-cell function and an insulin resistance of 1 and predicts plasma glucose and insulin values for a series of different β-cell functions and insulin resistance values. Insulin resistance for any individual may be estimated, therefore, by entering fasting observations of plasma glucose and insulin on the grid generated by the computer model [Matthews *et al.,* 1985].

(iii) The glucose clamp technique

The glucose clamp was developed to put the plasma glucose concentration under the investigator's control, mimicking the type of control obtained with excised pancreata perfused at fixed glycaemic and insulinaemic levels and, thus, breaking the simple glucose-insulin feedback loop [DeFronzo *et al.,* 1979]. There are two glucose clamp techniques, the hyperglycaemic and hyperinsulinaemic-euglycaemic, and both were developed by Reubin Andres and colleagues (Andres *et al.,* 1966). Put simply, the hyperglycaemic clamp quantifies β-cell sensitivity to glucose, and the hyperinsulinaemic-euglycaemic clamp quantifies body tissue sensitivity to insulin.

(a) The hyperinsulinaemic-euglycaemic clamp

The hyperinsulinaemic-euglycaemic clamp technique, along with the OGTT, is one of the most commonly used ways of assessing peripheral tissue sensitivity to insulin; i.e., peripheral glucose metabolism (mostly that of the muscle mass). It is considered the 'gold standard' measurement of this parameter. Its advantage over the OGTT is that a steady-state (S-S) glucose level is achieved, and this can be maintained at any level of hyperinsulinaemia [Elahi, 1996]. In this technique, the plasma insulin concentration is acutely raised and maintained by a priming and continuous infusion of insulin. The artificially increased plasma insulin levels will, of course, differ in lean and obese or control and diabetic individuals [Terrettaz & Jeanrenaud, 1983]. The plasma glucose concentration is held constant at basal (euglycaemic) levels by a variable glucose infusion using the negative feedback principle. The profile of glucose administration is a quantitative measure of the time course of insulin action. Under the S-S condition of euglycaemia, the glucose infusion rate equals glucose uptake by all the tissues in the body and is therefore a measure of tissue sensitivity to exogenous insulin [DeFronzo *et al.,* 1979; Fig. 2.3].

As euglycaemia prevails, hepatic glucose production (HGP) is not shut off [Terrettaz & Jeanrenaud, 1983], as it would be if hypoglycaemia were allowed to prevail in response to the hyperinsulinaemia. Intracellular glucose levels are increased in relation to plasma levels, and can be measured in lean/non-diabetic as well as obese/diabetic rats/humans by the following methods and principles. The effect of insulin on HGP and glucose utilisation or metabolism by the body; i.e., whole body glucose uptake (WBU), can be determined by isotopic glucose turnover before (basal) and during (clamp) insulin treatment.

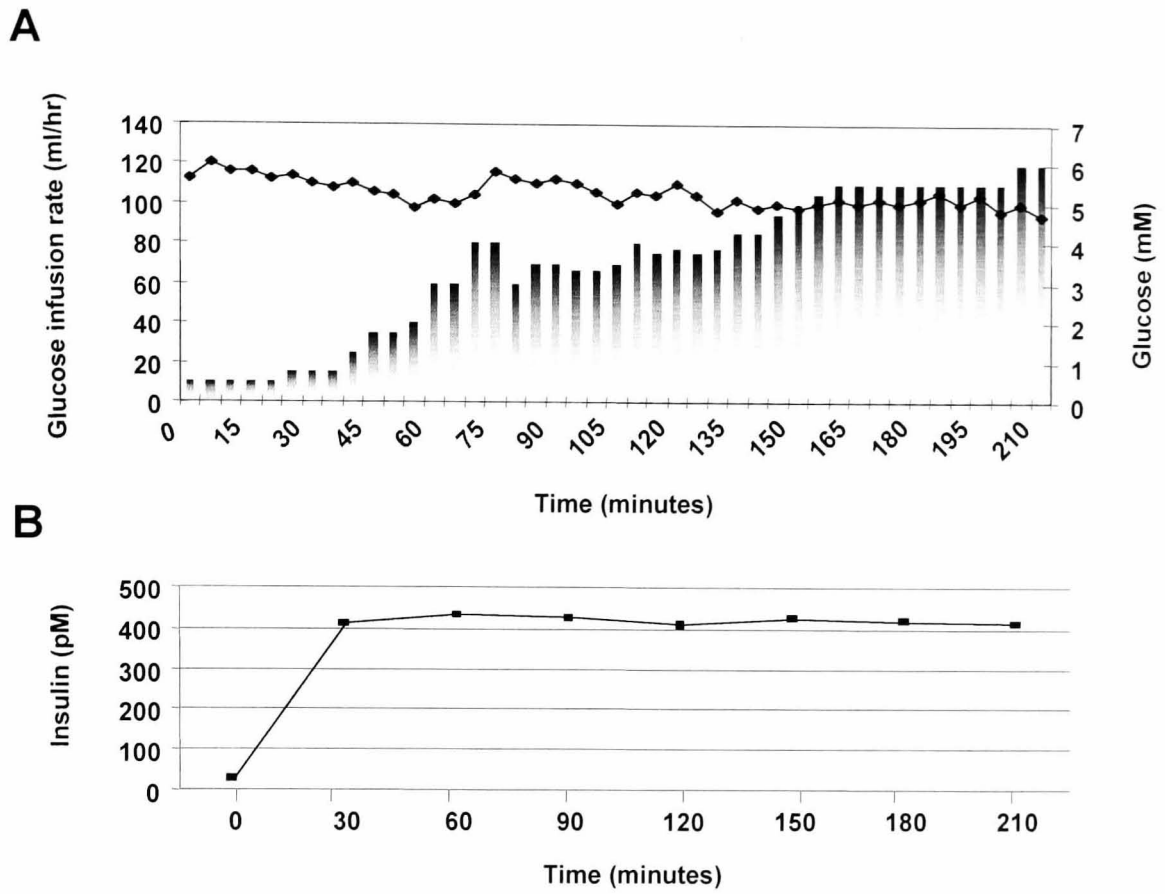

Figure 2.3. Principle of the euglycaemic clamp. Panel A shows that blood glucose concentration is measured frequently after hyperinsulinaemia is established through continuous intravenous insulin infusion (panel B). Hypoglycaemia is avoided through continuous intravenous infusion of glucose which is adjusted so as to maintain the blood glucose level at a constant normal value (e.g., 5.5 mM). The rate of glucose administration over this time-course reflects the subject's insulin sensitivity.

(1) The basal phase and measurement of HGP

In the experiments described in Chapters 3 and 5, after the drug treatment period, rats were deeply anaesthetised, as described above [see 2.1.4], and cannulated in the right jugular vein with polythene tubing (0.4 mm I.D., 0.80 mm O.D.; Portex®, Hythe, Kent, U.K.) flushed with heparinised saline (10U/ml; Multiparin, Holder CP Pharmaceuticals Ltd., Wrexham, U.K.). A 1-ml sample of blood was withdrawn (t=0) with a 1-ml syringe attached to the cannula and plasma separated either immediately by centrifugation or stored on ice for later (same-day) centrifugation and determination of pre-clamp insulin concentration by RIA [see 2.2.1 (i) (c)]. Prior to

the clamping procedure, a priming 4-μCi i.p. injection of 6-[^{3}H]glucose (38.0 Ci/mmol; Amersham International, Little Chalfont, Bucks., U.K.) was given to rats which were then infused continously for 30 min with the same solution (0.2 μCi/min), at which point another sample of blood was withdrawn (t=30). All infusions, including this initial one, were carried out in two rats simultaneously using 10-ml syringes mounted on precision pumps (Pump 22, Harvard Apparatus, Massachusetts, U.S.A.; CMA/100 Microinjection Pump, Biotech Instruments Ltd., Beds., U.K.). This was an equilibration period required to approach the complete mixing of the injected glucose with the whole of the body glucose pool. The glucose pool is assumed to be contained in a compartment of the plasma and tissue fluids [Steele, 1959], and a stable S-S blood glucose specific radioactivity, needed for the later calculation of basal glucose turnover, is reached by the end of this period [Upton *et al.*, 1998].

The determination of HGP relies on the metabolism of 3- or 6-[^{3}H]glucose by tissues because ^{3}H in these positions of the glucose molecule are lost to water in the glycolytic pathway and cannot be re-incorporated into glucose. 3- or 6-[^{3}H]glucose are, therefore, considered to be irreversible tracers. This is as opposed to ^{3}H in the 2-position which is lost in the liver during futile cycling between glucose, G-6-P and fructose-6-phosphate, before the first committed step of glycolysis, a process which can be increased in poorly controlled diabetes, falsely raising HGP values.

In both the basal and hyperinsulinaemic clamp states, the rate of glucose appearance in the blood compartment, R_a, is equal to the rate of glucose disappearance from plasma, R_d. Glucose appears in the systemic circulation through HGP (and a small amount of production in the kidney) and, under clamp conditions,

glucose infusion. Glucose disappears via peripheral uptake into tissues (primarily muscle, but adipose tissue as well). R_a is equal to R_d in the post-absorptive state, and both can be calculated by the isotope dilution method [Kruszynska, 1997; Terrettaz & Jeanrenaud, 1983; Fig. 2.4]:

$$\textbf{Glucose } R_a \textbf{ (mol/min)} = R_d = \frac{\textbf{rate of tracer infusion (dpm/min)}}{\textbf{Glucose SA (dpm/mol)}},$$

where **dpm** = disintegrations per minute = radioactive counts per minute (cpm) x scintillation counter efficiency, and **SA** = specific activity of blood glucose at equilibrium.

The S-S plasma glucose SA is determined by the relative rates of entry of ^{3}H-labelled and 'cold' (unlabelled) glucose, both being handled similarly by peripheral tissues. During the clamp, R_a represents the sum of the rates of HGP and exogenous glucose infusion, whereas R_d equals the rate of WBU. The rate of HGP can thus be obtained by subtracting the amount of exogenous glucose infused per unit of time from the isotopically determined R_a:

$$\textbf{Rate of HGP (mol/min)} = R_a \textbf{ - glucose infusion rate}$$

(2) The clamp phase

After the basal period, hyperinsulinaemia was achieved by infusing a mixture of human soluble insulin (Humulin-S®, Eli Lilly and Company, Basingstoke, Hants., U.K.) in isotonic saline containing 1% (w/v) bovine serum albumin (Sigma Chemical Company, Poole, Dorset, U.K.) and 6-[^{3}H]glucose at a constant flow rate of 20 µl/min (14 mU/min in obese and 2 mU/min in lean animals and 0.2 µCi/min, respectively) into the right jugular vein for 1 h. After 1 min, 5% glucose solution in

isotonic saline was co-infused at an initial rate of 1 mg/min and then at variable rates to maintain euglycaemia (approximately 4.2 mM in lean and 20 mM in diabetic ZDF rats). These rates were recorded and pre- determined based on electrochemical readings of blood glucose concentration obtained every 5 min from tail-vein blood samples, as described above [see 2.1.3 (i)]. A final (t=90) 2-ml sample of blood was obtained at cardiac exsanguination [see 2.2.1 (i) (c)] for later assay of post-clamp insulin concentrations.

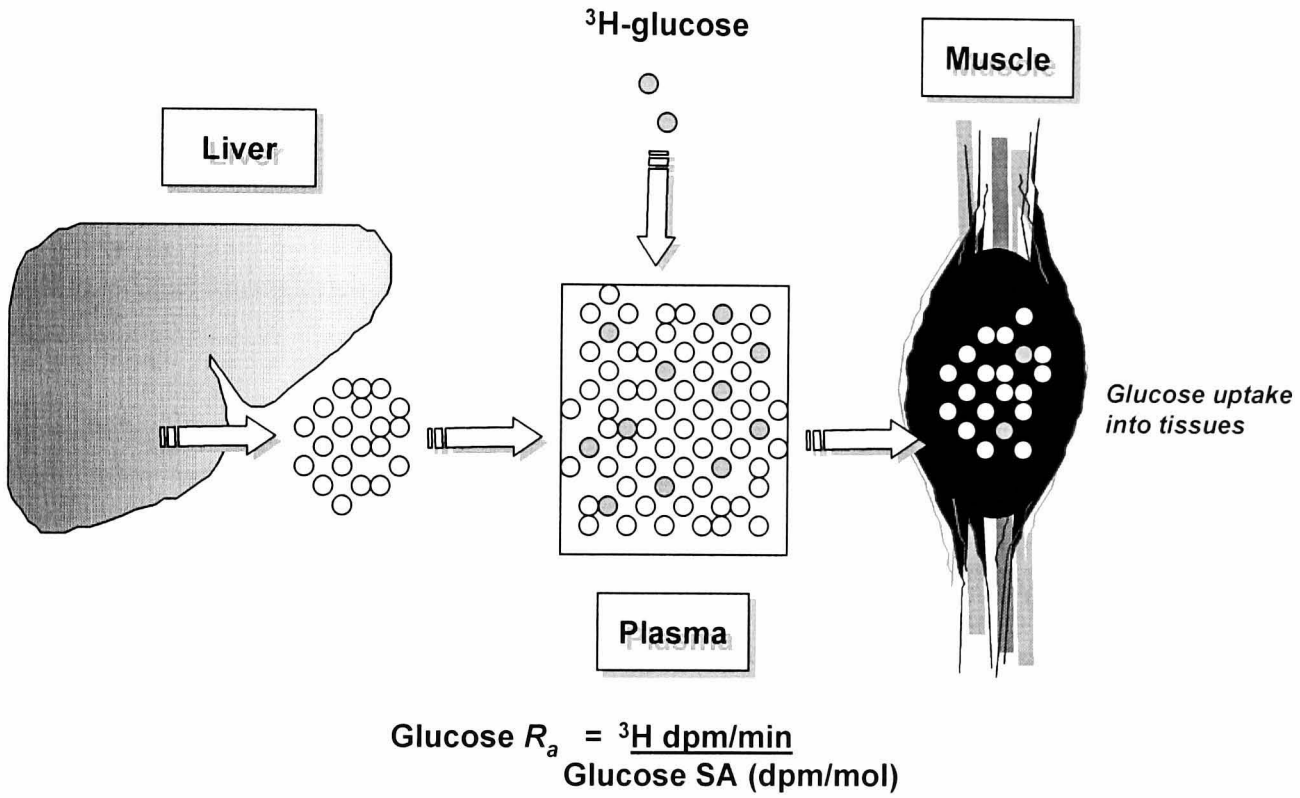

Figure 2.4. Isotope dilution method for estimating rates of glucose appearance (R_a) and disappearance (R_d) from plasma into body tissues (primarily muscle), using ^{3}H-glucose. The glucose pool is labelled by a primed constant infusion of tracer. After equilibrium (30 min in the case of the rat), steady-state (S-S) plasma glucose specific activity (SA) is determined. In the post-absorptive state, glucose R_a=R_d, and the S-S plasma glucose SA is determined by the relative rates of entry of ^{3}H- and 'cold' glucose arising primarily from the liver. Adapted from Kruszynska Y (1997) In Pickup J & Williams G (eds) *Textbook of Diabetes*; p. 29.3.

Basal and clamp blood glucose SA was determined by first de-proteinising 50-µl plasma samples with 25 µl each of 83 mM $ZnSO_4$ and 87 mM $Ba(OH)_2$, centrifuging at 14, 000 rpm for 1 min. Fifty µl of the supernatant was evaporated to

dryness at 70°C to remove tritiated water and reconstituted in 100 µl of water. Radioactivity was measured by scintillation spectrometry using 3 ml of scintillation cocktail (Cocktail T, BDH, Poole, Dorset, U.K.) and an LKB counter (counting efficiency = 45%).

Insulin sensitivity was also assessed by comparing plasma insulin concentrations before and at the end of clamping, as well as final glucose infusion rates (mg/min) between treated and control groups.

(b) The hyperglycaemic clamp

The hyperglycaemic clamp can be used to supplement the information obtained with the euglycaemic clamp, by providing a measure of β-cell sensitivity to glucose. The β-cells of human subjects or animals within the same experiment are stimulated with the same glucose concentration, thus enabling assessment of β-cell response to identical plasma glucose levels. Comparison of insulin secretory responses to stable hyperglycaemic stimuli can be made in glucose-tolerant and –intolerant states [Elahi, 1996], for example, in lean, diabetic or DIO rats (Chapter 4).

In this technique, the plasma glucose concentration is acutely raised above basal levels by a priming infusion of glucose. The desired hyperglycaemic plateau is subsequently maintained by adjustment of a variable glucose infusion, based on the negative feedback principle. Because the plasma glucose concentration is held constant, the glucose infusion rate is an index of glucose metabolism. Under these conditions of constant hyperglycaemia, the plasma insulin response is biphasic, with an early burst of insulin release during the first few minutes followed by a gradually progressive increase in plasma insulin concentration [DeFronzo *et al.*, 1979].

(1) Infusion of solutions

The hyperglycaemic clamp technique was used to assess insulin secretion in response to glucose in lean ZDF rats made dietary-obese and their lean ZDF controls in Chapter 4. After anaesthetising and cannulating rats, as for hyperinsulinaemic-euglycaemic clamps, just prior to glucose infusion a sample of blood was taken for later measurement of pre-clamp insulin, glucose and FFA concentrations [see 2.2.1 (i) (c) and (ii) (a), (b)]. In humans, a priming concentration of 125 mg/dL (~7 mM) above basal levels is sufficient to bring about the early insulin response after only 6 min [DeFronzo *et al.,* 1979]. In an attempt to induce a similar response in rats used here, a priming infusion of 20% unlabelled D-glucose in water (w/v) was begun at 100 mg/kg/min, which was gradually reduced to 70, 57, 46 and 35 mg/kg/min every two minutes for the first 11 minutes of infusion, based on the method of Vettor *et al.* (1998). The infusion rate was then adjusted according to blood glucose measurements taken every 10 minutes [as described in 2.1.3 (i)] during a further 70-min maintenance period to clamp the glucose concentration at a hyperglycaemic level of 22 mM. Thus, samples of tail-vein blood (~200 µl) were collected at 1, 3, 5, 7, 9 and 11 min and then at 10-min intervals between 20 min and 90 min for later measurement of plasma insulin levels released endogenously as a consequence of the imposed hyperglycaemic clamp. As with hyperinsulinaemic-euglycaemic clamps, two rats were infused simultaneously.

(2) Calculation of insulin secretion

β-cell response was calculated as the degree of insulin secretion in response to the glucose stimulation of the clamp. After plasma samples collected throughout the

clamp had been assayed for insulin concentration, these values (μU/ml) were plotted against time (min) and the area under the curve (AUC) calculated for the first (early; t=0-11 min) and second (late; t=20-90 min) phase insulin secretory responses, similar to that described previously by Giaccari *et al.* [1995]. Pre-clamp estimates of insulin sensitivity were made by calculating HOMA values using the pre-clamp, fasting plasma glucose and insulin concentrations, as described above [2.2.3 (ii)].

2.2.4. mRNA analysis

(i) The Northern blot

(a) Advantages of this technique

The Northern blot is so-named because it is patterned after the Southern blot. The latter technique, named after its originator, Edward Southern, is used to map restriction sites around a particular sequence of DNA that is of interest. This is realised by determining which restriction fragments hybridise to a specific labelled probe sequence. The Northern blot, on the other hand, is used to detect the presence of specific mRNA molecules. The RNA molecules in a sample are denatured by mixing them with an agent, such as formaldehyde, to prevent hydrogen bonds between base pairs and ensure that the RNA is in unfolded, linear form. The total RNA from the tissue sample is then separated according to size by gel electrophoresis; as in a Southern blot, the distributions of the RNA fragments in the gel is preserved as they are denatured and transferred by blotting to a solid substrate with a charged surface (a nitrocellulose filter) to which the extended denatured RNA will adhere. The filter is then exposed to a specific labelled nucleic acid sequence (the DNA probe). The blotted mRNA fragments that are complementary to the probe hybridise with them, and their location on the filter can be revealed by

autoradiography or other visualisation methods. The Northern blot indicates the amount as well as the presence and size of a specific mRNA in a sample and the technique is widely used to compare the amounts of a specific mRNA in samples under different conditions [Darnell *et al.,* 1990].

(b) RNA extraction

A rapid procedure for isolating total RNA was reported by Chomczynski & Sacchi (1987). The method, which could be completed in 4 h, provided a pure preparation of undegraded RNA in high yield. It was particularly useful for processing large numbers of samples and for isolation of RNA from minute quantities of cells or tissue samples. It involved the use of guanidine thiocyanate and phenol, two products which have since been conveniently combined in commercially available mono-phase solutions, such as Tri-Reagent™ (Sigma, Poole, Dorset, U.K.), such that the total extraction time is much reduced. This reagent simultaneously isolates RNA, DNA and protein in a single-step liquid phase separation. It first dissolves them on homogenisation and then, after adding chloroform and centrifuging, separates the mixture into 3 phases: an aqueous phase containing the RNA, the interphase containing DNA, and an organic phase containing proteins. The RNA is then further isolated by separating it from the other phases by pipetting it into a fresh tube. This procedure is effective for isolating RNA molecules of all types from 0.1-15 kb in length, a range covering all of the mRNAs of interest in the experiments presented here [see below, 2.2.4 (i) (f)]. It yields intact RNA with little or no contaminating DNA and protein [Tri-Reagent™ technical bulletin, 1998], a fact which was confirmed by my colleagues and I by the fact that we obtained higher optical density (O.D.) ratios of RNA solutions measured at 260/280 nm [see description below, 2.2.4

(i) (d)] than we generally obtained using the multi-step guanidine thiocyanate-phenol extraction procedure.

To investigate the potential roles of leptin and thermogenic mechanisms causing weight gain, epididymal fat and gastrocnemius muscle were dissected free, weighed, and snap-frozen in liquid nitrogen and stored at -80°C for later analysis of *OB* and UCP-3 mRNA levels, respectively (Chapter 6.1). Gastrocnemius muscle was the selected skeletal muscle because of its ease of removal and because it has already been shown to have changes in UCP-3 mRNA regulation induced by exercise [Tsuboyama-Kasaoka *et al.,* 1998]. Hypothalami were also removed *en bloc* from dissected brains, as described previously [Williams *et al.*, 1988], for the later measurement of NPY or orexin mRNA concentrations (Chapter 6.1 & 6.2, respectively).

(c) Sample preparation

All mRNAs were detected by Northern blotting according to the method of Trayhurn & Duncan [1994]. Total RNA samples were prepared according to a modified version of the Tri-Reagent™ protocol (Sigma, St. Louis, MO, U.S.A., 1998). All reagents were of a suitably pure grade for molecular biological work, and all solutions prepared with purified water treated with dimethyl pyrocarbonate (DMPC; Sigma, Poole, Dorset, U.K.), to a final concentration of 0.1%, in order to destroy endogenous RNAses [Sambrook *et al.,* 1989]. Tissue samples of 50-100 mg were removed from –80°C storage and placed in 5-ml polypropylene round-bottomed tubes (Sarstedt, Leicester, U.K.) containing 1 ml of Tri Reagent™, such that the volume of the tissue did not exceed 10% of the Tri- Reagent™ volume. These tubes were selected for their close fit around the homogeniser and their larger capacity

which prevented spillage of the homogenate over the edges at high homogenisation speeds. Tissues were homogenised for ~30 s each at 24, 000 rpm using a Polytron homogeniser (Ultra Turrax T25, Janke & Kunkel, IKA®-Labortechnik, Stauffen, Germany). Homogenates were then transferred to 2-ml Eppendorf microcentrifuge tubes with screw-tops.

To remove excess fat and insoluble material such as extracellular membranes, polysaccharides and high molecular weight DNA, the homogenate was then centrifuged for 15 min at 14, 000 rpm at 4°C in a microcentrifuge (Eppendorf 5417 C/R, Hamburg, Germany). If fatty material was present, especially in preparations of white or brown fat, it appeared as a colourless layer on the surface of the aqueous supernatant containing RNA and protein and was pipetted off. The supernatant was then transferred to a fresh tube and allowed to stand at RT for 5 min to ensure complete dissociation of nucleoprotein complexes. To separate the RNA from DNA and proteins, 0.2 ml of chloroform (+99% isoamyl alcohol-free; Sigma, Poole, Dorset, UK) were added to each tube. Tube lids were screwed on tightly, and each tube shaken vigorously by hand for 1 min, vortexed, and then allowed to stand for 15 min at RT. This mixture was then centrifuged at 14, 000 rpm for 15 min at 4°C. This separated the mixture into 3 phases: an organic pellet, containing protein, a DNA-containing interphase, and an RNA-containing supernatant. To precipitate the RNA, this supernatant was transferred to a fresh tube and 0.5 ml of isopropanol (Sigma, Poole, Dorset, U.K.) added. The mixture was vortexed and allowed to stand for 15 min at RT, before being centrifuged at 14, 000 rpm for 15 min at 4°C. The RNA precipitate formed a white pellet at the bottom of the tube. The supernatant was removed and the RNA pellet washed by adding 1 ml of 75% ethanol, vortexing, and centrifuging at 7, 500 rpm for 5 min at 4°C. This step was repeated, and the ethanol

then removed and pellets allowed to air dry for 5-10 min. To dissolve the pellets, 20 µl of DMPC-treated water were placed in each tube and the tubes then placed in a water bath at 65°C for 15 min. Samples were then stored at -80 °C until measurement of RNA content.

(d) Measurement of RNA purity

The final preparations of RNA were meant to be free of DNA and proteins. To determine purity, the optical densities of 2 µl of sample in 1 ml of DMPC-treated water were measured on a spectrophotometer [see 2.2.1 (ii)] at wavelengths of 260 and 280 nm. Purity was indicated by a 260/280 ratio ≥1.7. Readings were taken against a reference sample of DMPC-treated water.

(e) Pre-hybridisation

Pre-hybridisation was performed by inserting membranes into temperature-resistant glass roller bottles containing 20 ml of DIG Easy Hyb® (Roche Diagnostics, Milton Keynes, Bucks., U.K.) pre-warmed to 42°C. This hybridisation solution is ready-made, DNAse- and RNAse-free, and especially designed for use with nucleic acid blots that are to be probed with digoxigenin (DIG)-labelled probes [see below, 2.2.4 (i) (g)]. This volume is recommended for every 100 cm^2 of membrane. The transfer surface of the membrane faced the lumen of the bottle for optimal exposure to the buffer and was continuously rotated in a hybridisation oven (Hybaid, Middlesex, U.K.) for at least 1 h at 42°C. The appropriate hybridisation temperature is calculated by approximating probe length and guanine/cytosine (GC) content, adding 4°C for each G or C and 2°C for each T (thymine) or A (adenine). Hybridisations are recommended to be performed 10°C below this calculated temperature [*The DIG*

System User's Guide, 1995]. All hybridisations were of the DNA:RNA type, and, in general, 50°C is the recommended hybridisation temperature for this type. The actual temperature was adjusted to 42°C because of the GC content and homology of the probe to the target [DIG Easy Hyb package insert, 1999].

(f) Hybridisation

The pre-hybridisation solution was poured off and immediately replaced with a fresh 20 ml of solution. This was also pre-warmed to 42°C and contained appropriate volumes of probes. Hybridisation was continued overnight at 42°C with a 33-mer (*OB*), 30-mer (NPY and UCP-3) or ~400-mer (orexin) oligonucleotide (25 ng/ml; all from Eurogentec, OXON, U.K.) end-labelled with DIG.

(g) The DIG system: Non-radioactive labelling and detection of nucleic acids

Radioactivity has traditionally been used for labelling and detection in nucleic acid analysis, as it has been unequivocally accepted as giving the highest level of sensitivity in detection of single-copy genes or rare mRNAs. However, there are drawbacks to the use of isotope labels for visualisation, including short half-lives, health and environmental hazards, and the inconvenience of adhering to complex safety regulations regarding handling, storage and disposal. The DIG system has thus provided an alternative method which avoids these drawbacks while remaining sensitive and convenient. In addition, because DIG is a steroid hapten which occurs exclusively in *Digitalis* plants, it avoids the endogenous background problems of other haptens, such as biotin [Boehringer Mannheim catalogue, 1997].

(1) Visualisation

Membranes were incubated at RT for 30 min with anti-DIG antibody conjugated to alkaline phosphatase (anti-DIG-AP; Boehringer Mannheim, Germany) at a final concentration of 1/10, 000 in neutral pH buffer containing 100 mM maleic acid, 150 mM NaCl, 0.3% Tween® 20 and 1% 'blocking reagent' to lower background. This antibody is prepared in a stable solution for the detection of DIG-labelled compounds in various immunodetection procedures. The antibody was raised in sheep after immunisation with DIG, then purified, and the specific IgG isolated. Fab fragments were conjugated with AP [Anti-Digoxigenin-AP, Fab fragments package insert, 1999].

Membranes were then washed in 0.25 mM CDP-star® chemiluminescence substrate (Tropix, Massachusetts, USA) and exposed to Hyperfilm-ECL® (Amersham, Little Chalfont, Bucks, UK). The densities of bands corresponding to *OB* (4.1 kb), NPY (0.5 kb), UCP-3 (2.5 and 2.8 kb) and orexin (0.7 kb) mRNAs were measured using scanning densitometry (AIS, Imaging Research Inc., St. Catherines, Ontario, Canada). For standardisation, blots were stripped and re-probed for 18S rRNA with a 31-mer DIG-labelled antisense oligonucleotide at 10 pg/ml [Trayhurn *et al.*, 1995]. Amounts of mRNA are expressed as optical density (O.D.) units, relative to those of 18S rRNA.

2.3. Assessment of β-cell dysfunction

In Chapter 3, pancreata from ZDF rats were dissected at termination and divided into two portions. Half of each organ was snap-frozen in liquid nitrogen and stored at

-80°C for later measurement of insulin content, nitrate/nitrite concentrations and NOS activity, all indicators of β-cell status, the cytotoxic role of the latter two having been mentioned in the General Introduction [see 1.3.1 (ii) (a) (2)]; the other half of the pancreas was fixed overnight in 4% paraformaldehyde in 10 mM phoshpate buffer (PB) for later assessment of degree of apoptosis. Pancreatic insulin content was also determined in lean ZDF rats placed on the HPD (Chapter 4).

2.3.1. Pancreatic insulin concentration

Although the insulin RIA kit described above [2.2.1 (i) (c)] was designed for the quantitative determination of insulin in serum [Pharmacia Insulin RIA 100 package insert, 1998], it was readily applied to measurement of insulin concentrations in tissue homogenate. This is a good index of islet dysfunction because it is based on the fundamental knowledge that the severity of diabetes is reflected in the capacity for synthesis of insulin by the β-cells.

Proteins were extracted from ~50-mg pieces of frozen pancreas by boiling in 0.5 ml of 0.1 M acetic acid for 5 minutes, cooling to RT and then sonicating for 30 s until well-homogenised. Protein was then pelletted by centrifugation at 14,000 rpm for 5 min. Two-hundred and fifty µl of the supernatant was then neutralised with 215 µl of 1 M NaOH, and insulin concentration then measured by RIA in the same way as for plasma concentration [see 2.2.1 (i) (c)]. The concentration of pancreatic insulin was then expressed per gram of tissue.

2.3.2. Pancreatic NO and NOS

NO is produced in trace quantities by various cell types, including the islet cells, acting as a second messenger molecule. It readily diffuses through cell membranes to

exert its biological effects, and its excess generation leads to the formation of peroxynitrite and other destructive entities. The transient nature of NO makes it unsuitable for most convenient detection methods. However, since most NO is oxidised to nitrate (NO_3^-) and nitrite (NO_2^-), the concentrations of these anions can be used as a quantitative measure of NO production. After the enzymatic conversion of nitrate to nitrite by nitrate reductase, total nitrite is detected spectrophotometrically as a coloured azo-dye product of the Greiss reagent [Green *et al.,* 1982; Haendeler *et al.,* 1999].

NO is synthesised from arginine by the action of NOS and the essential co-factor, nicotinamide adenine dinucleotide phosphate (NADPH). This reaction also generates citrulline, the measurement of which, therefore, can be used as an index of NOS activity [Bredt & Snyder, 1989; Lowenstein *et al.,* 1994].

(i) Nitrate/nitrite concentrations

Nitrate/nitrite concentrations were measured in ~50-mg blocks of fresh-frozen pancreatic tissue, as described previously [Widdowson *et al.,* 1996]. The pieces of pancreas were placed in 400 µl each of 50 mM potassium phosphate buffer, pH 7.4, at RT, and then disrupted by sonication for 10 s. One hundred µl of the homogenate were removed and proteins precipitated with 5% trichloroacetic (TCA) acid and pelleted by centrifugation at 14, 000 *g* for 10 min. The proteins were resuspended in 1 M NaOH and the protein concentrations measured using the Lowry method [Lowry *et al.,* 1951] such that results could be expressed per mg of protein.

The remaining homogenate was centrifuged at 14, 000 *g* and 100 µl of supernatant incubated for 1 h at 37°C with 20 µl of nitrate reductase (5000 mU/ml; Sigma, Dorset, U.K.) in 50 mM potassium phosphate buffer containing 5 mM flavin

adenine dinucleotide (FAD) and 1 mM NADH (Sigma, Dorset, U.K.). The nitrite concentrations were measured by spectrophotometry (Benchmark Microplate Reader, BIO-RAD, Japan) in a 96-well microplate by the addition of 100 µl each of supernatant and Greiss reagent (0.1% naphthylethylenediamine and 1% sulphanilimide in 5% phosphoric acid; Sigma, Dorset, U.K.). Nitrite reacts with this reagent to form a purple azo dye, the colour of which is developed in the warm bath (37°C). O.D. at 550 nm was measured and nitrite concentrations calculated by comparison of the O.D. of standard solutions. These ranged from 0-100 µM and were made by diluting stock sodium nitrate (100 µM) with water and adding 40 µl of the FAD/NADH solution to each tube.

The Lowry method of protein measurement is based on the principle that protein reacts with copper in an alkaline solution ($CuSO_4 \cdot 5H_2O$; Sigma, Dorset, U.K.) such that it is then able to reduce the Folin phenol (phosphomolybdic-phosphotungstic) reagent (BDH Laboratory Supplies, Poole, U.K.) to produce a colour the intensity of which is proportional to the concentration of protein in the solution. Its advantages over other protein assays were discovered when Lowry [1951] found that it was many times more sensitive, specific to intact proteins rather than amino acids, less liable to disturbance by turbidities, and simpler to use.

Standards were made from a stock solution of 1 mg/ml BSA in 0.1 M HCl and ranged from 0.2-1 µg/µl. Fifty µl of standard or sample were placed in cuvettes, followed by 50 µl of 0.1 M NaOH and 100 µl of 0.9% NaCl to make a total volume of 200 µl. One ml of a 50:1 solution of 189 mM sodium carbonate/100 mM sodium hydroxide : 20 mM $CuSO_4 \cdot 5H_2O$/1% sodium citrate was then added to each cuvette and the reaction allowed to proceed for 10 min. One hundred µl of Folin reagent

diluted 1:1 with water were then added and the reaction continued for 30 min. O.D.'s were then read on the spectrophotometer at 750 nm and μg/μl of protein calculated.

(ii) NOS activity

NOS activity was also determined in 50-mg pieces of frozen pancreas, as described previously [Widdowson *et al.,* 1996], by measuring the conversion of [^{3}H]-arginine to [^{3}H]-citrulline. Pieces of pancreas were homogenised in 500 μl of 20 mM Tris-HCl buffer containing 2 mM disodium EDTA, pH 7.4 at 4°C and centrifuged at 10, 000 *g* for 15 min. Twenty-five μl of the supernatant containing the NOS enzyme was added to 50 μl of 50 mM Tris-HCl buffer containing 3 mM $CaCl_2$, 2 mM NADPH (Sigma, Dorset, U.K.) and 0.5 μCi [^{3}H]-arginine (Sigma, Dorset, U.K.). Finally, either 25 μl of water or of 10 μM L-N^G-nitroarginine methyl ester (L-NAME; Sigma, Dorset, U.K.), a NOS inhibitor, was added to make a final volume of 100 μl and the mixture incubated at 0°C for 15 min and transferred to a water bath at 37°C for a further 15 min. The incubation was stopped by the addition of 2 ml of ice-cold 20 mM HEPES buffer containing 2 mM disodium EDTA, pH 5.5, and the total volume added to mini-columns containing Dowex AG-50WR-8 resin (Bio-Rad Laboratories, Herts., U.K.) which had been previously equilibrated with the 20 mM HEPES/2 mM EDTA buffer. Eluate containing [^{3}H]-citrulline was collected in scintillation vials and the radioactivity estimated by liquid scintillation. Protein concentrations were also measured, as described above [2.3.2 (i)].

2.3.3. Islet cell apoptosis

Apoptosis, a mechanism of cell suicide, is an intrinsic biological event that plays an essential role in development and homeostasis, as well as in several disease processes. Culling extra cells in a precise and systematic way is an important aspect of normal development. Hence, the other term for the process is programmed cell death (PCD). However, in several degenerative diseases, including diabetes, the cell death program goes awry such that the disease may result in, or be the result of, excessive apoptosis.

(i) Apoptosis detection

Apoptosis was originally defined in terms of morphological changes, such as reduction in cell volume, condensation of the nucleus and membrane blebbing. Cells undergoing apoptosis fragment into membrane-bound apoptotic bodies that are readily phagocytosed and digested by macrophages or other neighbouring cells without generating an inflammatory response. This is in contrast to necrosis, which results from gross insult to the cell, characterised by cell swelling, release of lysosomal enzymes, cellular disintegration and inflammation. Apoptosis occurs in multiple cell types and can be triggered by multiple extracellular stimuli. With the discovery of several cell death genes conserved across numerous species, the cell death pathways are currently under intensive study. Morphological changes are observed in the nucleus of apoptotic cells, and DNA fragments are generated through the action of endogenous endonucleases, including the caspase-dependent DNase, CAD [Enari *et al.*, 1998].

Apoptosis detection used to be inferred from gel electrophoresis of a pooled DNA extract, as PCD was shown to be associated with fragmented DNA, one of the

biochemical hallmarks of apoptosis. Later, methods were developed for the *in situ* visualisation of PCD at a single-cell level, while preserving tissue architecture. This continued to rely on the identification of apoptosis through DNA fragmentation, but the fragments were labelled at their 3'-OH ends with a biotinylated poly deoxynucleotide (dUTP). This was introduced by terminal deoxynucleotidyl transferase (TdT), and then stained using avidin-conjugated peroxidase, such that the reaction was specific to nuclei located at positions where PCD was expected [Gavrieli *et al.,* 1992]. Typically, the DNA of apoptotic cells is cleaved into a population of fragments, composed of multimers of 180-200 bp in length. There are now various commercially available *in situ* cell death detection systems which work by end-labelling the fragmented DNA of apoptotic cells, based on a modified version of the TUNEL (TdT-mediated dUTP nick end-labelling) assay described above.

Understanding the process of cell death associated with numerous disease states is essential for resolving the pathogenesis and identifying possible therapeutic approaches. In many diseases, it is not obvious whether cell death occurs by apoptosis or by some other cytolitic pathway. Verification of apoptosis used to require multiple lines of evidence, but analysis with the TUNEL system simplifies this process and can provide the first step toward understanding the mechanism of cell death in disease states, such as that of β-cell death in type 1 and type 2 diabetes [O'Brien *et al.,* 1998].

(ii) TUNEL-labelling protocol

As mentioned above, pancreatic tissue was immersion-fixed in ~15 ml of 4% paraformaldehyde (PF) in 100 mM phosphate buffer (PB) overnight (approx. 24 h) and paraffin wax-embedded. Ten-μm-thick sections were cut on a microtome

(Shandon AS325, Anglia Scientific Instruments Ltd., Cambridge, U.K.), mounted onto glass microscope slides (Superfrost Plus, BDH Laboratory Supplies, Merck Ltd., Poole, Dorset, U.K.), heated at 60°C and then immersed in three washes of xylene to de-wax. This was followed by rehydration through a graded series of ethanol and distilled water. Apoptotic cells in the islets were then identified using a cell death kit (Roche Diagnostics, Mannheim, Germany).

Tissue sections were pre-treated by incubating with proteinase K (20 μg/ml in 10 mM Tris-HCl, pH 7.4) for 15 min at RT and then rinsed twice in 10 mM PBS. Endogenous peroxidase was blocked by incubating with 3% H_2O_2 in methanol for 10 min at RT. Sections were then permeabilised by incubating in 0.1% Triton X-100® in 0.1% sodium citrate for 2 min at 4°C. Sections were rinsed again twice in PBS, the areas around them dried, and 50 μl of TUNEL reaction mixture placed on top. This had been prepared previously by making a 1:10 mixture of supplied solutions of terminal deoxynucleotidyl transferase (TdT) enzyme and nucleotide mixture in reaction buffer. Sections were covered with small squares of parafilm to avoid evaporative loss during incubation at 37°C for 60 min and were then rinsed 3 times in PBS. The area around each section was then dried and 50 μl of a ready-to-use horseradish peroxidase solution was then applied. Sections were protected with parafilm and incubated again at 37°C for 30 min. Slides were rinsed 3 times with PBS and 50 μl of a supplied diaminobenzidine (DAB) substrate solution added to each section. Following incubation for 10 min at RT, slides were again rinsed in PBS and mounted under coverslips for analysis with light microscopy.

The apoptotic index was derived by counting the number of apoptotic cells in six islets from each animal (4 animals/group), using an ocular reticle at the

microscope and expressing this as a ratio to the total number of cells within those islets.

2.4. Statistical analyses

Data are shown as mean ± standard error of the mean (SEM). All statistical analyses were performed using ARCUS Pro-Stat (version 3.23 © Iain E. Buchan, 1990, 1994), and all results were considered statistically significant at the $p<0.05$ level, or, in the case of analysis of variance (ANOVA; see below), at a level less than the critical p given for multiple comparisons.

2.4.1. Genetic (ZDF) studies

Three-way comparisons were made between ZDF untreated diabetic, MCC-555-treated diabetic and non-diabetic control rats (Chapter 3) to study the effect of both diabetes and drug treatment on various parameters. These were performed by 2-way ANOVA followed by *post hoc* Bonferroni modified *t*-tests. In Chapter 4, differences between DIO untreated (vehicle) ZDF and chow-fed (vehicle) control rats were compared using unpaired (2-sample) *t*-tests for all parameters, or Mann-Whitney test for non-normally distributed samples. Comparisons between DIO untreated and all groups of DIO drug-treated animals were made by 1-way ANOVA followed by Bonferroni *t*-tests for multiple comparisons.

2.4.2. Dietary obesity studies

In all experiments referred to below, differences between DIO untreated (vehicle) and chow-fed (vehicle) control rats were compared using unpaired *t*-tests or Mann-Whitney tests for all parameters.

(i) Dose-response studies

In Chapter 5, both DIO and chow-fed groups were administered a range of drug doses. Therefore, dose-response relationships were studied separately for DIO and chow-fed rats. In this and the other dose-response experiments (Chapter 7), the significance of dose was determined by 1-way ANOVA for each of the parameters. Comparisons of each dose to vehicle control were then made by Bonferroni *t*-tests.

Also in Chapter 5, correlation coefficients were calculated by simple linear regression to determine whether or not there were relationships between plasma leptin, FFA and insulin concentrations and body weight gain or calorie intake during the treatment period.

(ii) Pair-feeding studies

In Chapter 6.1, DIO and chow-fed control groups were both treated with a single drug dose and allowed to feed *ad lib* or were pair-fed to the level consumed by untreated control groups (i.e., 6 groups in total). In Chapter 6.2, only DIO rats were treated with a single therapeutic drug dose and compared with DIO rats that remained untreated and with chow-fed controls (i.e., 4 groups). In both of these chapters, comparisons between DIO (vehicle) and chow-fed (vehicle) control rats were performed with unpaired *t*-tests or Mann-Whitney tests, and multiple comparisons were made by 1-way ANOVA followed by Bonferroni *t*-tests.

CHAPTER 3

MCC-555 treatment attenuates the development of overt diabetes, preventing nitric oxide synthase induction and ß-cell apoptosis in the pancreas of the young Zucker Diabetic Fatty rat

3.1. Introduction

MCC-555 is a partial agonist at the peroxisome proliferator receptor-gamma (PPARγ), and, like other thiazolidinediones (TZDs), has been shown to improve insulin sensitivity in animals and humans [Ishii *et al.*, 1996; Upton *et al.*, 1997]. The structure of this compound is shown in Fig. 1.9 and its properties are described in the General Introduction [1.6.5 (i)], as is the progression from impaired glucose tolerance (IGT) to overt diabetes [1.3.1 (ii)]. In summary, this involves the gradual development of insulin resistance in peripheral tissues which is initially compensated for by increased pancreatic insulin secretion. Although this serves to prevent the development of severe hyperglycaemia in the early stages [DeFronzo, 1988], the pancreatic ß-cells ultimately fail, and insulin secretion falls to normal or subnormal levels, allowing glucose concentrations to rise into the range of frank diabetes [Harris, 1996; Polonsky *et al.*, 1996].

Clinical studies have suggested that early therapeutic intervention with the TZD, troglitazone, in humans with IGT can delay the onset or attenuate the development of overt diabetes [Nolan *et al.*, 1994]. It was of interest to discover whether or not the novel TZD, MCC-555, had the same property and determine if and how β-cell function was preserved, in addition to the expected improvement in insulin sensitivity. To achieve these aims, the effect of the drug was investigated in

an animal model of insulin resistance and type 2 diabetes, the Zucker Diabetic Fatty (ZDF) rat, while it was in the 'pre-diabetic' state. As described in the General Introduction [1.5.1 (i) (a)] and Methods [2.1.2 (i) (b) (1-3)], similar to the human condition, this mutant displays IGT at an early age, with moderate hyperglycaemia, insulin resistance and hyperinsulinaemia, and subsequently progresses to overt diabetes through a failure of ß-cell function [Clark & Palmer, 1982; Peterson, 1994]. Thus, in the experiment presented here, chronic MCC-555 treatment of young ZDF rats was undertaken in an attempt to arrest the progressive development of diabetes.

The second part of the experiment involved investigation of the potential mechanism(s) responsible for this attenuation and any metabolic improvements due to treatment with MCC-555. In the ZDF rat, ß-cell damage is thought to arise indirectly from a mutation in the leptin receptor. Insensitive to circulating leptin levels, these animals overeat and accumulate lipid in many tissues, principally adipose tissue, but also in muscle and in the ß-cells. The 'lipotoxicity' phenomenon [see 1.3.1 (ii) (a) (2)] is a mechanism by which ß-cell secretory function is impaired by chronically raised levels of free fatty acids (FFAs). This may then trigger an apoptotic mechanism by the induction of nitric oxide synthase (NOS) and the cytotoxic overproduction of nitric oxide (NO) [Unger, 1997]. The islets of ZDF rats have an increased capacity to esterify FFAs and a decreased capacity to oxidise them [Lee *et al.,* 1997], and it is thought that this somehow causes the greater induction of NOS expression by FFA, perhaps by increasing intracellular levels of FFA. Although the mechanism by which FFA or high triglyceride (TG) increases NOS expression and NO production in pancreatic islets is unknown, increased levels of diglyceride, or diacylglycerol (DAG), the precursor of triglyceride, and/or ceramide,

a molecule of two long-chain fatty acids (FAs) and initiator of the apoptotic cascade, are among the possibilities [Shimabukuro *et al.,* 1997b, 1998a].

Furthermore, the long-term hyperglycaemia of diabetes may have deleterious effects analagous to those of chronic hyperlipidaemia. This is the 'glucotoxicity' theory, whereby excessive levels of glucose compromise ß-cell function [for review, see Yki-Järvinen & Williams, 1997].

In the event that chronic MCC-555 treatment did attenuate the metabolic disturbances characteristic of type 2 diabetes in the ZDF rat, I set out to show that this attenuation involved the ability of this compound to protect against ß-cell dysfunction by modulating pancreatic NOS activity and accumulation of NO.

3.2. Methods

3.2.1. Animals and treatment

Figure 3.1 shows the design of this experiment. Six-week old male ZDF (fatty) 'pre-diabetic' (240 g) and non-diabetes prone ZDF (lean) control rats (200g) were divided into three groups (n=9/group). One group of 'pre-diabetic' rats received daily oral doses (by gavage) of MCC-555 (10 mg/kg) suspended in 0.5% sodium carboxymethycellulose (CMC) for 28 days, whilst the other 'pre-diabetic' rats were given vehicle alone (5 ml/kg/d). A group of non-diabetic rats also received daily oral doses of vehicle. Body weight and food and water intake were measured daily. Suppliers of animals and a description of their general maintenance are given in General Methods [2.1.2 (i) (b) (1) and 2.1.5]. Suppliers of drugs and chemicals are also given in this chapter [2.1.6-7].

3.2.2. Repeated blood sampling

Every 4 days, tail-vein blood glucose concentrations were measured (with rats in the fed state) with an electrochemical meter (Medisense®, Abingdon, Oxon, U.K.). At the end of each week, animals were lightly anaesthetised [see General Methods 2.1.3 (i) and 2.1.4 for anaesthetic protocols] and 200 µl of tail-vein blood collected and placed in cooled microfuge tubes. The blood was immediately centrifuged (14,000 rpm for 3 min) and 100 µl of plasma frozen for the later measurement of plasma insulin concentrations by RIA. Refer to General Methods [2.2.1 (i) (c)] for suppliers of analytic kits.

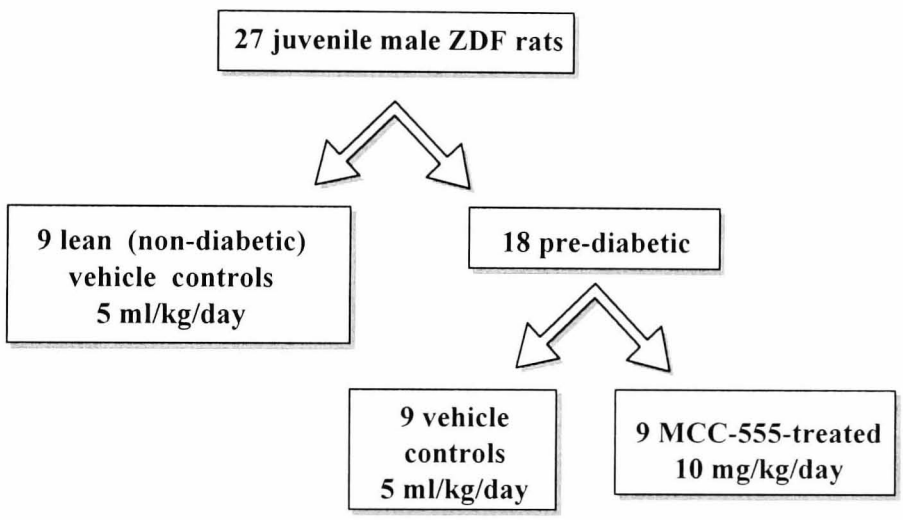

Figure 3.1. Experimental design for MCC-555 treatment of young ZDF rats. Weight gain and food and water intake were measured daily and the drug administered for 28 days. Animals underwent terminal euglycaemic-hyperinsulinaemic clamps in the fed state, blood was collected by cardiac puncture, and plasma concentrations of glucose and insulin measured. Epididymal and perirenal fat pad masses were determined at termination and pancreata collected for later measurement of insulin content, apoptotic index, NO concentration and NOS activity.

3.2.3. Euglycaemic clamp

After 28 days, rats were deeply anaesthetised and their insulin sensitivity measured using the hyperinsulinaemic-euglycaemic clamp technique. Human insulin was

infused at a constant flow rate of 14 mU/min in obese and 2 mU/min in lean ZDFs into the right jugular vein to produce hyperinsulinaemia. A 5% glucose solution was co-infused with the insulin at variable rates to maintain euglycaemia. All rats were also infused with 6-[^{3}H]glucose (0.2 mCi/min) prior to the clamping procedure, for the later measurement of whole-body glucose uptake (WBU) and hepatic glucose production (HGP), as described in General Methods [2.2.3 (iii) (a)].

At the end of the clamp, rats were killed by cardiac exsanguination and the perirenal and epididymal fat pads dissected free and weighed for assessment of drug efficacy. The pancreata were also dissected free and half of each snap-frozen in liquid nitrogen for later assays of NO and NOS. The other half was fixed in 4% paraformaldehyde for histological assessment of apoptosis.

3.2.4. Measurement of pancreatic insulin content, NO generation and NOS activity

Pieces of frozen pancreas (~50 mg) were placed in 0.5 ml of 0.1 M acetic acid, boiled for 5 min, sonicated and the protein pelleted by centrifugation (14, 000 rpm). After neutralisation of the supernatant with 1 M NaOH, the insulin concentration was measured by RIA. Nitrate/nitrite concentrations (an index of NO generation) and NOS activity were measured in 50-mg pieces of frozen pancreas. These parameters, as well as protein concentrations for standardisation were measured as previously described [2.3.2].

3.2.5. Quantification of apoptosis

Paraformaldehyde-fixed portions of pancreas were wax-embedded and 10-μm serial sections were taken. Cells with DNA damage (apoptotic) were visualised by a

modified TUNEL assay using a cell death kit [see 2.3.3 (ii)] followed by microscopic examination. The apoptotic index is expressed as a percent ratio of the number of apoptotic cells to the total number of cells in a minimum of six islets from the pancreata of each group of rats (n = 4/group).

3.2.6. Statistical analyses

Data are expressed as mean ± SEM. Differences between MCC-555-treated diabetic, untreated (vehicle) diabetic and untreated (vehicle) non-diabetic rats were analysed using 2-way ANOVA followed by Bonferroni modified t-tests. Results were considered statistically significant at the $p<0.05$ level.

3.3. Results

At the start of the experiment, 'pre-diabetic' ZDF rats had significantly greater body weight, daily food intake and plasma insulin concentrations than non-diabetic controls (all $p<0.0001$; Figs. 3.2 and 3.3C). 'pre-diabetic' ZDF rats also displayed moderate hyperglycaemia, as compared to non-diabetic rats ($p<0.05$; Fig. 3.3B). At the end of the second week of the study, plasma insulin concentrations in the untreated (vehicle) 'pre-diabetic' rats began to fall, as compared to the start of the study, becoming significantly lower by 32% and 52% at the end of weeks 3 and 4, respectively ($p<0.01$; Fig. 3.3C; Table 3.1). These animals also became severely hyperglycaemic and polydipsic by day 10, as compared to untreated (vehicle) non-diabetic rats ($p<0.0001$ and $p<0.01$, respectively; Fig. 3.3A,B; Table 3.1). As a result of the development of overt diabetic symptoms, the body weight gain in untreated (vehicle) 'pre-diabetic' rats was blunted by day 14, although the rats remained

significantly heavier than non-diabetic control rats throughout the study ($p<0.0001$; Fig. 3.2A).

In contrast to untreated (vehicle) 'pre-diabetic' rats, MCC-555-treated 'pre-diabetic' rats maintained initial plasma insulin concentrations throughout the study ($p<0.01$; Table 3.1). Concomitantly, the rise in hyperglycaemia and polydipsia in MCC-555-treated rats was attenuated, as compared to untreated (vehicle) 'pre-diabetic' rats (both $p<0.01$; Fig. 3.3A,B; Table 3.1). Consistent with plasma insulin data, insulin levels in the pancreata of untreated (vehicle) 'pre-diabetic' rats were lower than those in non-diabetic controls. In MCC-555-treated 'pre-diabetic' rats, they were greater than those in untreated (vehicle) 'pre-diabetic' rats, although they remained lower than those in non-diabetic controls (Table 3.1).

Table 3.1. Insulin and glucose concentrations in young ZDF rats after 28 days of treatment with MCC-555 or vehicle.

Group/Treatment	**Plasma insulin** (pM)	**Blood glucose** (mM)	**Pancreatic insulin** (pmol/g tissue)
Non-diabetic (vehicle)	85.8± 9.0	5.7±0.3	562±82
Diabetic (vehicle)	139.2± 12.6**	24.5±0.5**	205±30 **
Diabetic (MCC-555)	240.0 ± 54.0**†	19.7±2.2**†	339±36 **†

Significance of statistical differences *vs* non-diabetic controls: **$p<0.01$; *vs* untreated 'pre-diabetic' ZDF rats: †$p<0.05$. Data shown as mean±SEM.

MCC-555-treated rats continued to gain weight throughout the study, as did untreated non-diabetic rats, but MCC-555 did not alter daily food intake in 'pre-diabetic' rats, as compared to untreated 'pre-diabetic' controls ($p>0.05$; Fig. 3.2).

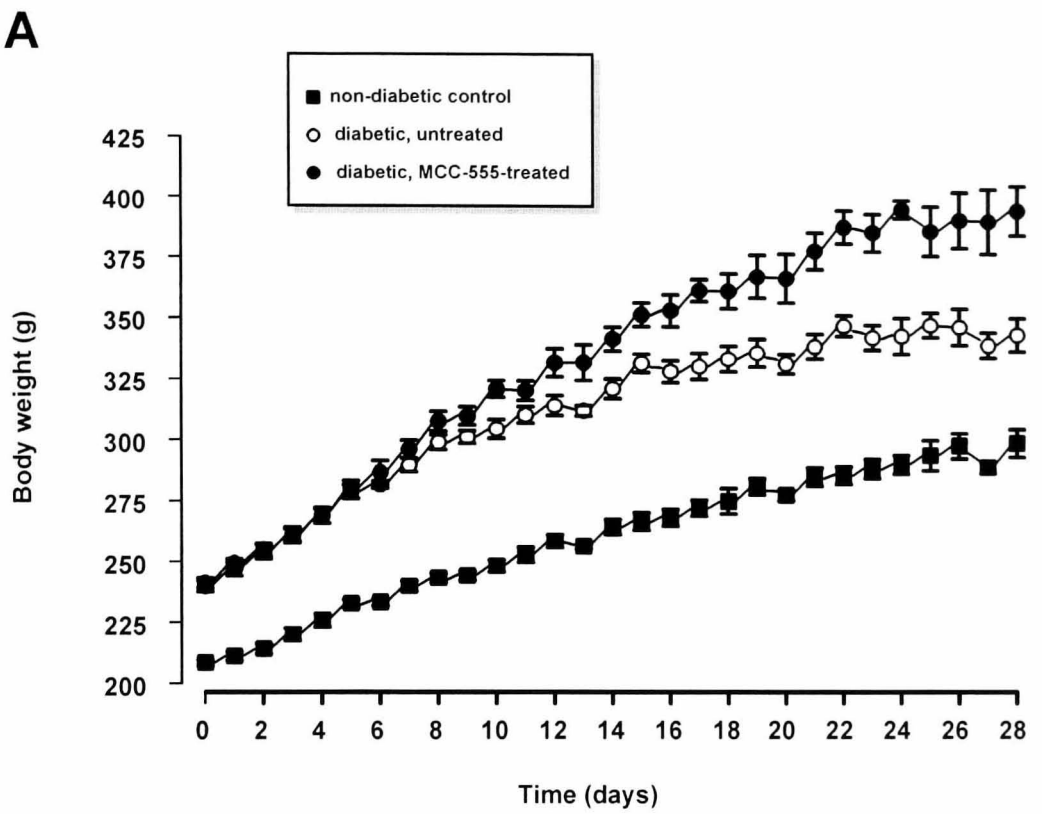

Figure 3.2. (A) Body weight and (B) daily food consumption in untreated diabetic ZDF rats, MCC-555-treated diabetic ZDF rats and non-diabetic controls over the 28-day experimental period. See text for complete description of statistical results.

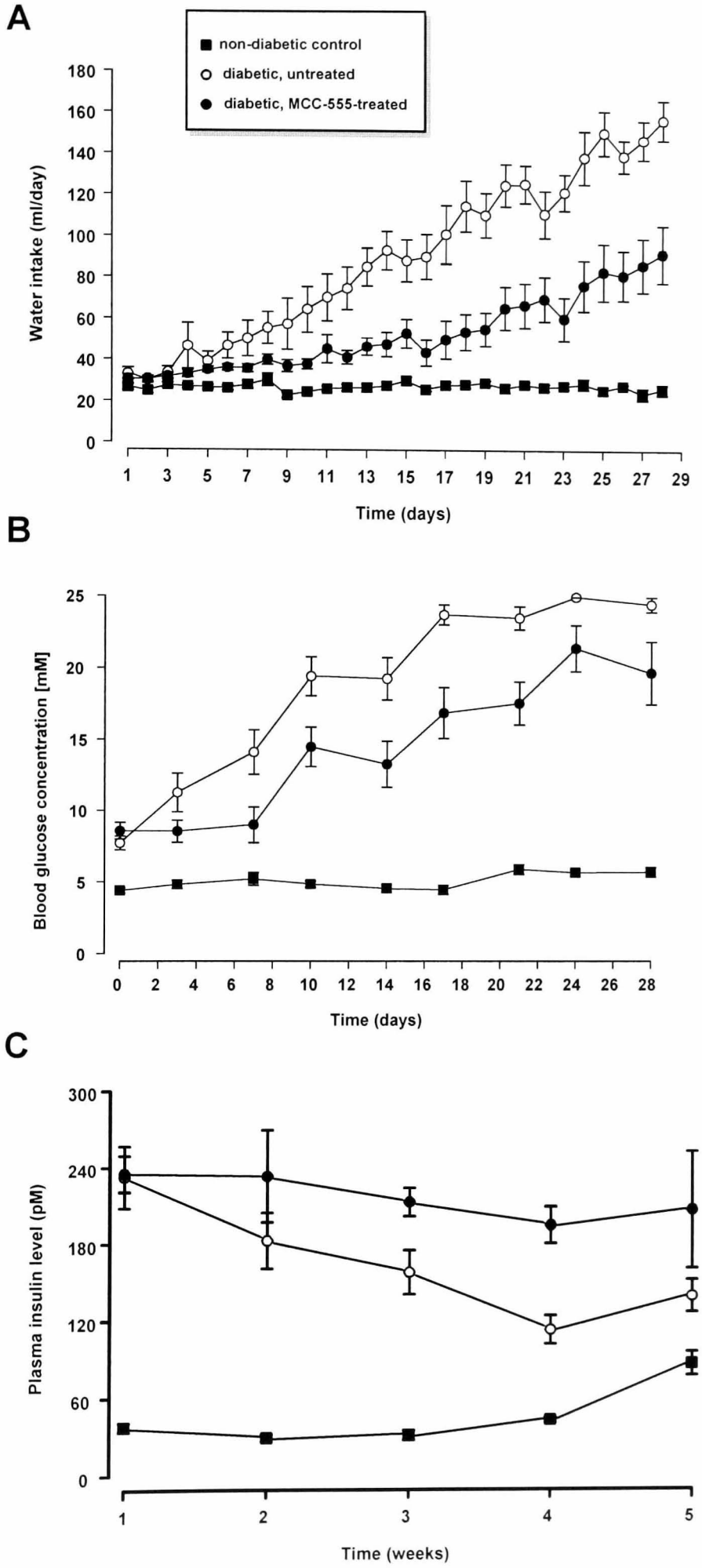

Figure 3.3. (A) Daily water intake, (B) blood glucose and (C) plasma insulin concentrations in untreated diabetic ZDF rats, MCC-555-treated diabetic ZDF rats and non-diabetic controls over the 28-day experimental period. See text for complete description of statistical results.

Gonadal fat pad mass was significantly greater in MCC-555-treated rats, as compared to untreated 'pre-diabetic' rats at the end of the study ($p<0.01$), whilst both gonadal and perirenal fat pad masses were significantly greater in both 'pre-diabetic' rat groups than in the non-diabetic rats ($p<0.01$; Fig. 3.4).

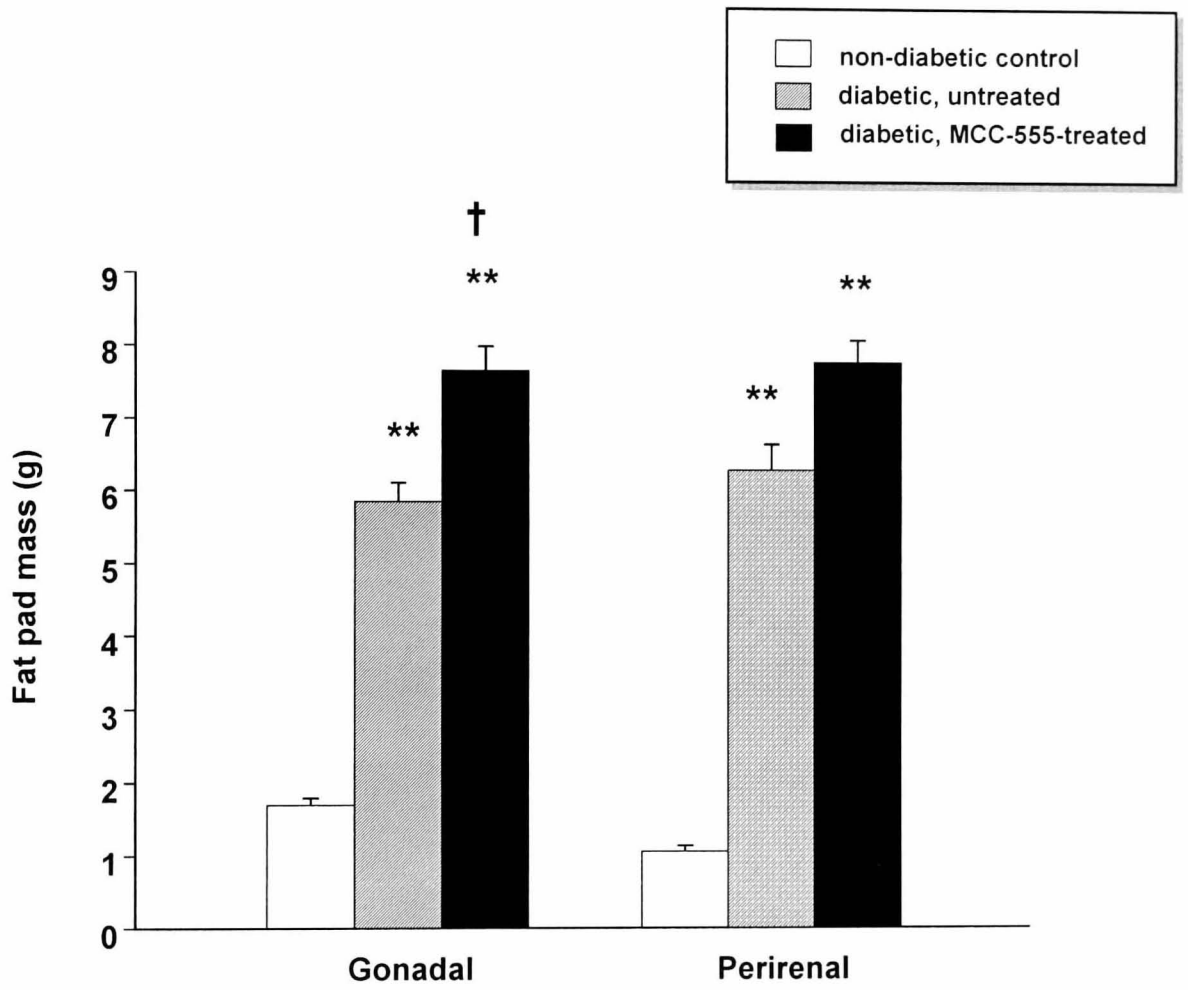

Figure 3.4. Gonadal and perirenal fat pad mass in untreated ZDF diabetic rats, MCC-555-treated diabetic ZDF rats, and non-diabetic controls. $^{**}p<0.01$ *vs* non-diabetic; $\dagger p<0.05$ *vs* untreated diabetic.

Steady-state (S-S) final glucose infusion rates during the hyperinsulinaemic-euglycaemic clamp were significantly greater in the MCC-555-treated than in the untreated 'pre-diabetic' rats ('pre-diabetic' = 0.06±0.03 mg/min; MCC-555-treated = 0.72±0.22 mg/min; $p<0.01$) demonstrating a significant (12-fold) improvement in insulin sensitivity in the treated group.

Basal HGP and WBU rates were significantly greater in 'pre-diabetic' ZDF rats, as compared to lean rats ($p<0.0001$). During the clamp, there was a significant suppression of HGP in both untreated lean and MCC-555-treated 'pre-diabetic' rats (both $p<0.01$). Although there was a concomitant increase in WBU under clamp conditions in treated 'pre-diabetic' ZDF rats, reaching 37% of the uptake in lean controls, this failed to reach significance ($p=0.07$). Under clamp conditions, HGP and WBU in untreated 'pre-diabetic' rats did not alter significantly from basal levels ($p>0.05$; Fig. 3.5).

Microscopic examination of islets also revealed several apoptotic cells (visualised as a positive TUNEL reaction) in many islets of untreated 'pre-diabetic' rats. In contrast, only one apoptotic cell could be found within only some islet sections taken from MCC-555-treated 'pre-diabetic' rats, similar to non-diabetic controls. Quantitation of TUNEL-positive cells showed that untreated diabetic rats had a greater apoptotic index than did non-diabetic controls, but this was reduced by MCC-555 treatment (Fig. 3.6).

There was a marked increase in NOS activity (+66%) in pancreata of untreated 'pre-diabetic' rats, compared to non-diabetic controls, which was normalised by MCC-555 treatment (Fig. 3.7A). Correspondingly, raised nitrate/nitrite concentrations in untreated diabetic rats (+124%) were also significantly reduced by MCC-555 treatment (-36%) to levels that were not significantly different from those of non-diabetic controls (Fig. 3.7B).

3.4. Discussion

These findings demonstrate that, in agreement with the literature [Clark & Palmer, 1982; Peterson, 1994], 'pre-diabetic' ZDF rats displaying hyperinsulinaemia and

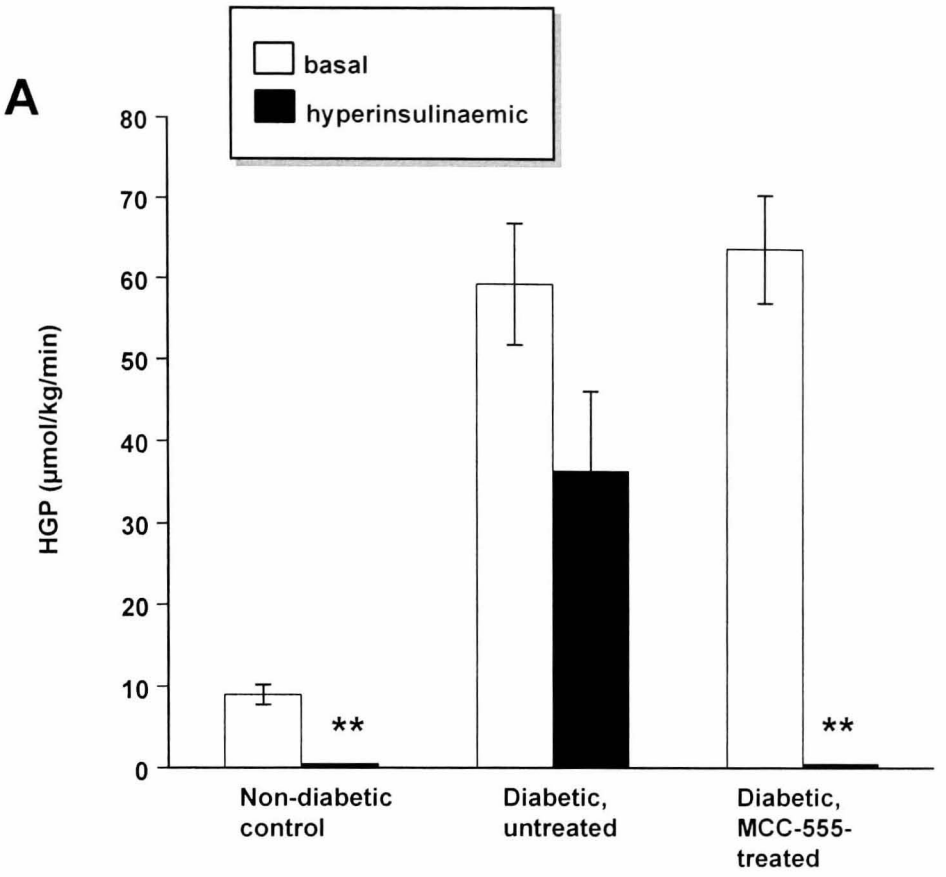

Figure 3.5. (A) HGP and (B) WBU in untreated diabetic ZDF rats, MCC-555-treated diabetic ZDF rats and non-diabetic controls under basal and hyperinsulinaemic conditions after 28-day treatment. $^{**}p<0.01$ *vs* basal HGP or WBU.

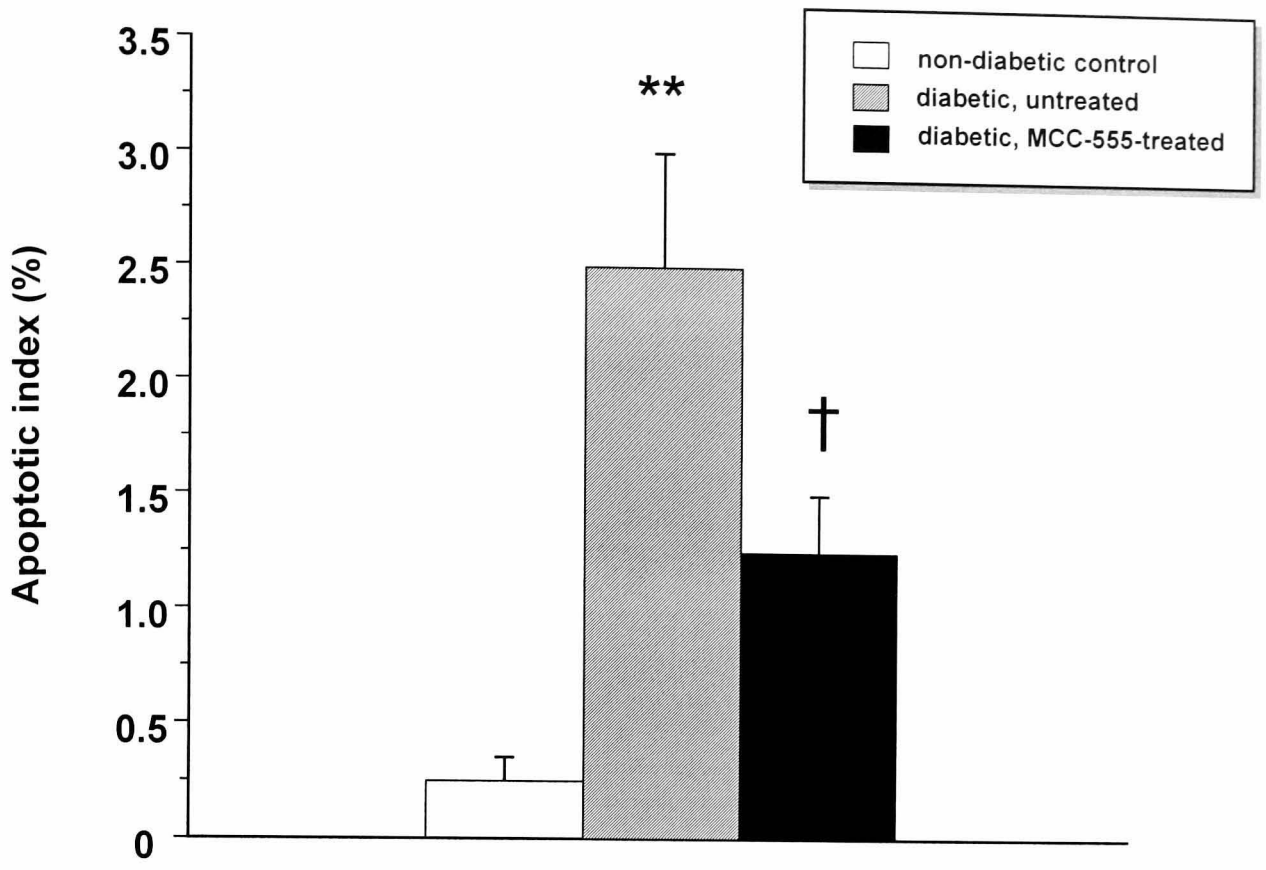

Figure 3.6. The apoptotic index measured in the pancreatic islets of untreated non-diabetic controls, untreated 'pre-diabetic' ZDF rats and MCC-555-treated 'pre-diabetic' ZDF rats. $^{**}p<0.01$ *vs* non-diabetic controls; $\dagger p<0.05$ *vs* untreated 'pre-diabetic' ZDF rats.

moderate hyperglycaemia progress to ß-cell failure and overt diabetes between 6 and 10 weeks of age. These rats also manifest overt diabetes with severe hyperglycaemia (>20 mM), polydipsia and attenuated body weight gain. As demonstrated previously in older diabetic ZDF rats [Upton *et al.,* 1997], they also show reduced insulin sensitivity, as compared to their non-diabetic counterparts.

MCC-555 treatment of the young 'pre-diabetic' rats, on the other hand, significantly improved insulin sensitivity, as shown by the hyperinsulinaemic-euglycaemic clamp technique. Improved metabolic status was evident in the return of insulin-sensitive inhibition of hepatic gluconeogenesis observed under clamp conditions in the drug-treated group, and was further suggested by the tendency toward increased glucose uptake into body tissues. This has also been shown

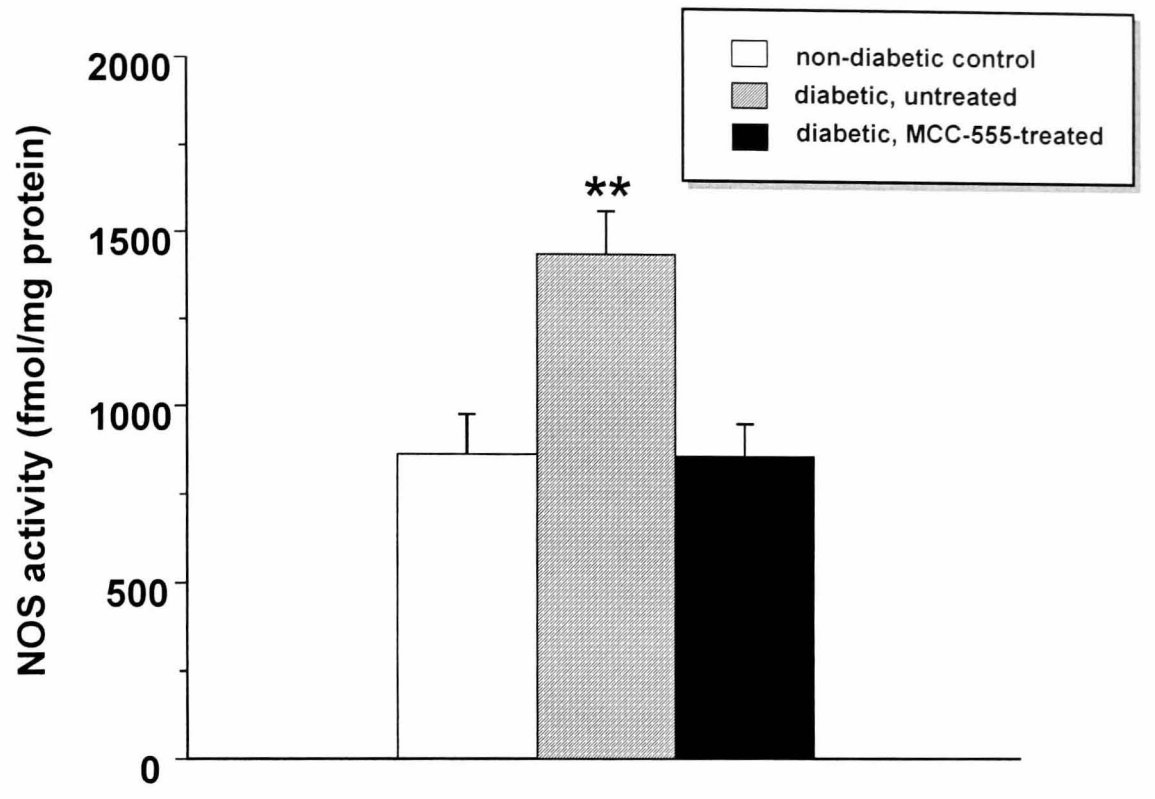

Figure 3.7. (A) Pancreatic NOS activity and (B) concentrations of nitrate/nitrite in untreated non-diabetic controls and untreated and MCC-555-treated 'pre-diabetic' ZDF rats. $^{**}p<0.01$ *vs* non-diabetic controls; $^{\dagger}p<0.05$ *vs* untreated 'pre-diabetic' ZDF rats.

previously in older diabetic ZDF rats [Upton *et al.,* 1997].

As a result of the sustained hyperinsulinaemia in the 'pre-diabetic' MCC-555-treated rats, coupled with a partial restoration in insulin sensitivity, the development of overt diabetes was significantly attenuated in these rats, as demonstrated by lower blood glucose concentrations, reduced thirst and continued increase in body weight gain and maintenance of body fat levels. One probable mechanism responsible for the maintenance of insulin levels is the alleviation of glucose toxicity; i.e., lowering glucose will non-specifically improve ß-cell function (which is impaired by high blood glucose) [see Yki-Järvinen & Williams, 1997]. Alleviation of lipotoxicity is also likely to maintain insulin levels. TZDs are known to reduce circulating FFA concentrations, which, when they reach excessive levels, accumulate in ß-cells leading ultimately to their death by apoptosis [Oakes *et al.,* 1994, 1997; Unger, 1997]. The significant increase in gonadal fat pad mass in MCC-555-treated ZDF rats, as compared to untreated diabetic ZDF rats, is probably a consequence of three processes: Firstly, the partial restoration in insulin sensitivity results in increased glucose entry into adipose tissue with subsequent conversion to TGs. Secondly, there is attenuation of the lipolysis resulting from catabolic metabolic processes associated with overt diabetes. Thirdly, as selective agonists at PPARγ [Forman *et al.,* 1995, Lehmann *et al.,* 1995], TZDs induce adipogenesis by regulating expression of adipocyte-specific genes [Harris & Kletzien, 1994].

Overall, these results suggest that MCC-555 treatment of ZDF rats may arrest the development of diabetes by preventing pancreatic β-cell failure and thereby maintaining a higher level of insulin secretion. The mechanism underlying this β-cell failure is still unknown; however, results stemming from closer examination of metabolic and histological changes in the pancreata of these rats provide indirect

evidence that intracellular lipid build-up sets in motion a chain of events leading to cell death by NO accumulation.

Certainly, β-cell apoptosis was almost completely prevented by MCC-555 treatment, demonstrating a cytoprotective effect of this drug, as was the induction of NOS and resultant increases in pancreatic nitrate/nitrite concentrations which occur during β-cell failure. These results suggest a link between NOS activation and β-cell damage. Indeed, numerous studies have demonstrated that NO can induce apoptosis in various cell types *in vitro* [Dawson *et al.,* 1991], and increased NOS activity has been implicated in cellular damage *in vitro* [Widdowson *et al.,* 1996]. This suggests that induction of NOS activity in β-cells may underlie the cellular damage leading to β-cell failure and ultimately to cell death through the apoptotic pathway [McDaniel *et al.,* 1996]. Moreover, this is the mechanism thought to operate in type 1 diabetes [Corbett *et al.,* 1993]. Nevertheless, it is important to emphasise that although an association between reduced levels of NO and β-cell preservation has been demonstrated, given the complexities of the apoptotic cascade, whether this is a causal relationship is unclear, and will require further study.

It is also important to note the possibility that the NOS activity, as measured in this experiment, may have come from sources other than the islets. Measurements were done on pieces of whole pancreas, rather than isolated islets, and, because islets comprise only about 2% of the pancreatic cell population of adult animals, the measurements made may have pertained mainly to pancreatic exocrine cells. The increase in TUNEL positivity may also have reflected DNA damage in endocrine islet cells other than β-cells; i.e., glucagon-, somatostatin- or pancreatic polypeptide-producing cells [Bishop & Polak, 1997].

We have yet to establish, however, the mechanism by which MCC-555 could be preventing this NOS induction. It could be that altered metabolism is involved, because β-cell failure in young (hyperphagic) ZDF rats can be prevented by dietary restriction [Ohneda *et al.,* 1995]. In particular, the accumulation of FFAs and their esterification to TG in pancreatic islets of these animals may mediate the upregulation of iNOS [Unger, 1997]. This may explain why MCC-555 is cytoprotective, for, as described above, TZDs are known to significantly reduce lipid concentrations in the blood, through activation of adipocyte PPARγ [Whitcomb & Saltiel, 1995; Wilson *et al.,* 1996]. Previous work with MCC-555 shows that it significantly depresses circulating levels of FFAs in both Zucker and ZDF rats [Upton *et al.,* 1998]. The sustained body weight and fat pad mass and improved insulin sensitivity of treated ZDF rats also suggest that FFAs are being removed from the circulation and glucose used as a preferred fuel via the Randle cycle [Randle *et al.,* 1963]. Thus, there is experimental evidence to support the theory that elevations in FFA concentrations in the pancreas of hyperphagic ZDF rats may lead to β-cell damage.

In addition, like another TZD, troglitazone, MCC-555 may restore β-cell function by exerting direct lipopenic effects: Troglitazone has been shown to lower islet fat content by increasing FA oxidation and reducing mRNA expression of key enzymes involved in FA esterification [Shimabukuro *et al.,* 1998b]. This action protects against the cytotoxic effect of interleukin-1β (IL-1β) implicated in the autoimmune destruction of β-cells in type 1 diabetes, by reducing NO production and enhancing β-cell viability in ZDF rats [Shimabukuro *et al.,* 1997a].

3.5. Conclusion

Chronic treatment of young ZDF rats with the TZD MCC-555 attenuates the symptoms of overt diabetes through a combination of partial restoration of insulin sensitivity and maintenance of ß-cell function, which, in turn, maintains elevated insulin secretion. It appears to do this by partially protecting pancreatic β-cells from apoptosis and cellular damage that may involve the induction of NOS and excess production of NO. Such attenuation has also been reported following treatment with two other TZDs, troglitazone [Sreenan *et al.,* 1996] and rosiglitazone [Smith *et al.,* 1997]. I suggest, therefore, that MCC-555 may eventually join troglitazone [Nolan *et al.,* 1994] in being of significant potential therapeutic value in humans with IGT, in preventing or attenuating the development of type 2 diabetes.

CHAPTER 4

Comparisons of PPAR agonists: *Effects on metabolic profile and insulin secretion in diet-induced obesity in the lean Zucker Diabetic Fatty rat*

4.1. Introduction

The results of the experiment described in Chapter 3 showed that chronic treatment with the thiazolidinedione (TZD), MCC-555, improves insulin sensitivity and preserves β-cell function in the obese Zucker Diabetic Fatty (ZDF) rat. The diabetic phenotype of the obese (-/- or *fa/fa*) ZDF rat arises from a leptin receptor defect, but because human type 2 diabetes does not arise from a single gene defect, the polygenic dietary obese (DIO) model may be more appropriate as a model of insulin resistance and perhaps early type 2 diabetes.

Lean ZDF rats are either heterozygous (+/*fa*) or homozygous (+/+) and, apart from the leptin receptor mutation, are genetically equivalent to obese ZDF rats. Although there are currently no data available that demonstrate phenotypic differences from other lean control rats, such as Wistars, lean ZDF rats are typically used as controls for obese ZDF rats.

The DIO ZDF rat may prove to be a useful model of human type 2 diabetes. Lean Wistar rats fed a highly palatable diet (HPD) develop hyperphagia, hyperleptinaemia, insulin resistance and hyperinsulinaemia [Harrold *et al.*, 2000a; Pickavance *et al.*, 1998a; 1999a,b; 2000; Widdowson *et al.*, 1997; Wilding *et al.*, 1992b], features shared by the obese ZDF rat, but purely because of its leptin

receptor defect. Interestingly, this is in contrast to the fatty Zucker rat, which has the same leptin mutation but a different strain background and does not go on to develop diabetes. It would seem, therefore, that there is an inherent tendency to develop β-cell dysfunction in the ZDF strain that is not present in the fatty Zucker rat.

Thus, the development of obesity in lean ZDF rats would occur without the confounding factor of this mutation, but with a genetic background that is conducive to the development of β-cell dysfunction in response to weight gain (as compared to other strains, such as the fatty Zucker rat), possibly as a result of triglyceride (TG) accumulation in the islets [Unger, 1997].

I have shown that MCC-555, a TZD partial ligand of PPARγ, is capable of attenuating β-cell failure [Chapter 3; Pickavance *et al.,* 1998c, 1999c]. In addition, Shimabukuro and colleagues [1998b] have shown that troglitazone, another ligand activator of PPARγ, ameliorates the abnormalities in fatty acid (FA) metabolism of ZDF islets. However, as the PPARα, β, δ and γ isoforms are all expressed in rat islets [Braissant *et al.,* 1996; Zhou *et al.,* 1998], it is possible that greater protection of β-cell function might arise by targeting more than one of them. Potential additional benefits of activating PPARα, as well as PPARγ, would result from lipid-lowering effects, and are outlined in the General Introduction [1.6.5 (iii) (b)]. In short, these would include improved non-insulin-mediated glucose uptake, increased glucose oxidation in non-insulin-sensitive tissues and reduced circulating cholesterol concentrations [Harmon *et al.,* 2000; Kazumi *et al.,* 1990; Matsui *et al.,* 1997]. In the obese ZDF rat, abnormal expression of PPARα in the islets is associated with the leptin receptor defect [Zhou *et al.,* 1998]. It is not known what effect PPARα activation would have on TG accumulation in the islets of a model with an intact leptin receptor. Fibrate treatment of the lean ZDF with induced dietary obesity could

reveal this, as well as helping to determine whether or not activation of PPARα can improve islet function *in vivo*.

TZDs bind to both PPARγ_1 and γ_2 isoforms [Elbrecht *et al.*, 1996], although no systematic comparative data across all TZDs have been collected. Thus, the γ agonists tested here bind to both γ_1 and γ_2 sites. These are pioglitazone (PIO), a TZD licensed for use in humans with type 2 diabetes, the properties of which are described elsewhere [see General Introduction, 1.6.5 (i)-(iii) (a)], and DRF 2593 (DRF), a non-TZD, still in the initial stages of development, and found by *in vitro* activation assay to be γ_2-preferring [Novo Nordisk, unpublished observations]. The mixed ($\alpha/\gamma_1, \gamma_2$) agonist, NNC 61-0029 (NNC), another non-TZD, is also currently under development. The α agonist chosen was bezafibrate (BF) because it appears to have been the fibrate most commonly tested in rodents [e.g., Cabrero *et al.*, 1999; Matsui *et al.*, 1997] and because its use in humans is also well-documented [e.g., Goa *et al.*, 1996].

Thus, the aim of this experiment was two-fold: It would address the question of whether or not the exogenous stimulus of the HPD might reveal a genetic susceptibility to diabetes in the lean ZDF rat. Observation of the effects of the different compounds on the development of insulin resistance would allow comparison of potentially therapeutic effects (improvement in insulin sensitivity, insulin secretory capacity, glycaemia and lipid profile) and adverse effects (hyperphagia, weight gain, cardiac hypertrophy and haemodilution).

4.2. Methods

4.2.1. Animals and treatment

Figure 4.1 shows the design of this experiment. Forty-eight 6-week-old male lean heterozygous (+/-) ZDF rats (148 ± 2 g) were housed in groups of four (genotyping was performed at Novo Nordisk, Maløv, Denmark). Forty of these were given HPD for a period of 10 weeks, and the remaining 8 continued to feed on normal pelletted chow [as described in General Methods, 2.1.2 (ii) (a)]. At the end of this run-in period, by which time significant obesity had developed in the HPD-fed rats, all rats were singly housed and daily oral drug administration begun for a period of 28 days. Each of the four drugs tested was suspended in 1% CMC vehicle and administered to a randomly assigned group of 8 DIO rats (PIO: 30 mg/kg; DRF: 3 mg/kg; NNC: 1.5 mg/kg; BF: 100 mg/kg). These drug concentrations were selected because they had shown therapeutic effectiveness in rodents in previous studies [PIO: Chapter 7; Kawamori *et al.,* 1998; DRF and NNC: unpublished observations; BF: Haubenwallner *et al.,* 1995] as well as equivalent potency in receptor binding assays [K. Wassermann, personal communication]. The remaining 8 DIO rats received vehicle (1 ml/kg), as did the 8 chow-fed controls. Body weight and food and water intake were measured daily. [Suppliers of animals and a description of their general maintenance are given in General Methods, 2.1.2 (i) (b) (1) & 2.1.5 and suppliers of drugs and chemicals in 2.1.6-7].

4.2.2. Repeated blood sampling

In order to follow the potential development of insulin resistance and β-cell dysfunction in this model, tail-vein blood was collected once weekly during the treatment period and blood glucose concentration measured immediately

electrochemically [see 2.1.3 (i)], and plasma insulin concentrations later by RIA [2.2.1 (i) (c)].

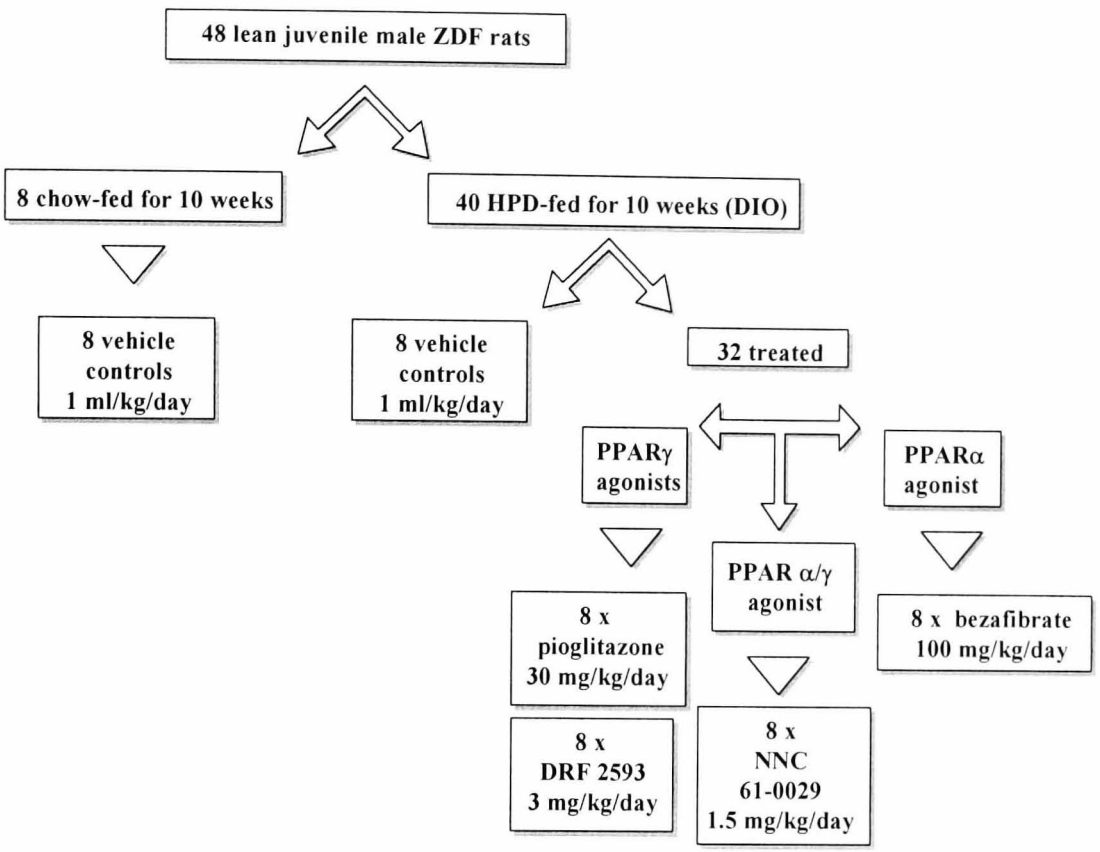

Figure 4.1. Experimental design for PPAR agonist treatment of lean ZDF rats with DIO. Weight gain and food and water intake were measured daily during treatment and drugs administered for 28 days. Animals were killed in the fasted state after undergoing hyperglycaemic clamps. Trunk blood was collected, and plasma concentrations of glucose, insulin, TGs, FFAs, leptin and cholesterol measured. Heart mass and PCV, as well as epididymal, perirenal, subcutaneous and brown fat pad masses were determined at termination.

4.2.3. Hyperglycaemic clamp

After the 28-day treatment period, and after a 12-h fast, all rats were deeply anaesthetised and their insulin secretory capacity measured using the hyperglycaemic clamp technique. This method is described in General Methods [2.2.3 (iii) (b)]. In summary, it involved catheterisation of the right jugular vein, followed by infusion of 20% percent glucose over a 90 min period. Tail-vein blood glucose concentration

was measured just prior to infusion (baseline), every 2 min during the first 11 min of the clamp and then every 10 min thereafter. The rate of glucose infusion was adjusted according to these readings in order to maintain hyperglycaemia at approximately 22 mM. Tail-vein blood samples were also taken at each of these time points for later measurement of plasma insulin by RIA during the early and late phases of insulin secretion.

4.2.4. Metabolic data and tissue mass

Pre-clamp (baseline) plasma concentrations of glucose, insulin and FFAs were measured in a blood sample withdrawn from the jugular vein just prior to glucose infusion. Insulin sensitivity was measured from this sample by HOMA, derived from the insulin and glucose concentrations [see General Methods, 2.2.3 (ii)]. Haemodilution was also determined at this stage by measuring the packed cell volume (PCV) of this sample.

At the end of the clamp, rats were terminated by cardiac exsanguination and their hearts excised and weighed to determine the degree of cardiac hypertrophy. Body fat content was determined by weighing dissected perirenal and epididymal white fat pads and the interscapular brown adipose tissue (BAT). Body fat distribution was determined by removing the subcutaneous fat pad from below the sternum, and expressing its mass relative to those of the perirenal and epididymal fat pads. To standardise the subcutaneous fat pad mass, it was expressed as a ratio with the perimeter of the overlying square of dissected abdominal muscle. The pancreas was also removed and snap-frozen in liquid nitrogen for later measurement of insulin content by RIA. Post-clamp plasma concentrations of glucose, FFAs, TGs, and total and HDL cholesterol were measured by diagnostic kits, and those of insulin and

leptin by RIA. Commercial sources of these assays are noted in General Methods [2.2.1 (i) (c), (ii)].

4.2.5. Statistical analyses

Data are expressed as mean ± SEM. Parameters were compared between DIO and chow-fed controls by unpaired *t*-tests or Mann-Whitney test. The drug effect on each of the parameters was measured by comparing values in each of the treated DIO groups with those in the DIO (vehicle) control group by 1-way ANOVA followed by Bonferroni modified *t*-tests (critical *p* for 4 comparisons = 0.0125). Effect of duration of treatment was measured by comparing values at each of the first 3 weeks of treatment (in the fed state) within each DIO group by 1-way ANOVA followed by Bonferroni *t*-tests (critical *p* for 2 comparisons = 0.025). Parameters were compared between the first (fed state) and last (fasted state) weeks of treatment (weeks 1 and 4) by paired *t*-tests. Pre- and post-clamp values for the same group were also compared by paired *t*-test. Differences were considered statistically significant at $p<0.05$. Insulin secretion (μU/ml/min) was calculated as area under the curve (AUC) of plasma insulin concentration (μU/ml) during the 90-min hyperglycaemic clamp [Fig.P® For Windows, BIOSOFT®, Cambridge, U.K.). Steady-state (S-S) glucose infusion rate was taken as the mean rate over the final 30 min of the clamp.

4.3. Results

4.3.1. Dietary obesity

Prior to the start of the experiment, the groups destined to remain on chow and to be given HPD were of similar body weight (152 ± 10 *vs* 148 ± 2 g, respectively; $p>0.05$). After being fed the HPD for 10 weeks prior to drug treatment, rats were

12% heavier than chow-fed rats (410 ± 4 *vs* 365 ± 32 g; $p<0.0001$) and remained so until the end of the study (426 ± 6 g *vs* 380 ± 8 g; $p<0.01$).

DIO (vehicle) control rats also had greater absolute subcutaneous, epididymal, perirenal and brown fat masses than chow-fed controls (+65%, 85, 101 and 52%, respectively; all $p<0.01$; Table 4.1), indicating significant obesity. Both

Table 4.1. Effects of 28-day administration of PPAR agonists on terminal absolute fat pad mass (g) in (+/-) DIO and chow-fed male ZDF rats in the fasted state.

Drug/Dose (mg/kg/d)	**Epididymal**	**Perirenal**	**Brown**	**SC**
Palatable diet-fed (DIO)				
vehicle	2.45±0.06	3.00±0.12	0.76±0.04	0.362±0.034
BF (100)	2.60±0.14	3.07±0.18	0.83±0.06	0.332±0.071
PIO (30)	3.68±0.22***	3.47±0.24	1.78±0.07***	0.375±0.078
DRF (3)	3.16±0.14**	3.72±0.10**	1.41±0.10***	0.482±0.074
NNC (1.5)	3.62±0.13***	4.02±0.25**	1.62±0.10***	0.476±0.103
***Chow-fed** (vehicle)*	1.32±0.06***	1.49±0.09***	0.50±0.05**	0.219±0.015**

Significance of statistical differences *vs* DIO (vehicle): **$p<0.01$; ***$p\leq0.0001$. Data are expressed as mean ± SEM. SC=subcutaneous.

epididymal and perirenal fat pads comprised a greater proportion of body mass in these rats than in their chow-fed counterparts (+40% and 79%, respectively; both $p<0.0001$). Similarly, a greater proportion of body weight in DIO controls could be attributed to the interscapular brown fat pad than in chow-fed controls (+38%; $p<0.05$). The subcutaneous-to-epididymal and –perirenal body fat distributions were no different between DIO and chow-fed controls, however ($p>0.05$; Table 4.2).

DIO control rats were hyperinsulinaemic (+92%; $p<0.01$) and more insulin-resistant than chow-fed controls (100% increase in HOMA; $p<0.05$; Table 4.3), but

Table 4.2. Effects of 28-day administration of PPAR agonists on relative fat pad mass relative to body weight in (+/-) DIO and chow-fed male ZDF rats in the fasted state.

Drug/Dose (mg/kg/d)	**Epididymal fat mass** (%)	**Perirenal fat mass** (%)	**Brown fat mass** (%)	**SC/muscle**	**SC/epididymal**	**SC/perirenal**
Palatable diet-fed (DIO)						
vehicle	0.58±0.02	0.70±0.03	0.18±0.01	0.032±0.003	0.147±0.013	0.121±0.011
BF (100)	0.59±0.03	0.69±0.04	0.19±0.02	0.029±0.007	0.128±0.026	0.108±0.022
PIO (30)	0.78±0.04***	0.74±0.04	0.38±0.01***	0.034±0.007	0.104±0.022	0.114±0.025
DRF (3)	0.69±0.02**	0.81±0.02	0.31±0.02***	0.042±0.007	0.154±0.022	0.132±0.021
NNC (1.5)	0.78±0.01***	0.86±0.02**	0.35±0.03***	0.042±0.009	0.135±0.029	0.125±0.027
Chow-fed *(vehicle)*	0.35±0.01***	0.39±0.02***	0.13±0.01*	0.020±0.001**	0.167±0.012	0.150±0.012

Significance of statistical differences *vs* DIO (vehicle): *$p<0.05$; **$p<0.01$; ***$p\leq0.0001$. Data are expressed as mean ± SEM. Fat pad mass expressed as % of terminal body weight. SC=subcutaneous.

Table 4.3. Effects of 28-day administration of PPAR agonists on plasma insulin and glucose concentrations, insulin sensitivity (HOMA) and pancreatic insulin content in (+/-) DIO and chow-fed male ZDF rats in the fasted state.

	Pre-clamp			Post-clamp	
Drug/Dose (mg/kg/d)	**Insulin** (pM)	**Glucose** (mM)	**HOMA**	**Insulin** (pM)	**Pancreatic insulin** (nmol/g)
Palatable diet-fed (DIO)					
vehicle	58.8±9.0	6.3±0.3	2.8±0.5	49.8±6.6	5.8±2.4
BF (100)	38.4±12.0	7.8±1.1	2.5±1.2	43.2±6.0	7.3±2.2†
PIO (30)	40.8±6.6	4.7±0.9	1.3±0.3	49.2±4.2	5.9±1.2†
DRF (3)	37.8±3.6	5.2±0.6	1.4±0.2	54.0±4.8‡	6.0±1.9†
NNC (1.5)	50.4±7.2††	5.4±1.1	2.0±0.4	60.0±5.4	4.6±1.0†
***Chow-fed** (vehicle)*	30.6±1.8**	6.4±0.5	1.4±0.1*	47.4±7.2‡	1.8±0.4*

Significance of statistical differences *vs* DIO (vehicle): *$p<0.05$; **$p<0.01$; *vs* chow-fed controls: $^{\dagger}p<0.05$; $^{\dagger\dagger}p<0.01$; *vs* corresponding pre-clamp values: $^{\ddagger}p<0.05$. Data are expressed as mean ± SEM.

remained normoglycaemic. They had 61% higher FFA and 90% higher TG concentrations in plasma, and more than two-fold higher plasma leptin concentrations than chow-fed controls (+112%; all $p<0.01$). Although total cholesterol concentration was 14% lower ($p<0.05$) in DIO controls, the HPD did not change HDL cholesterol concentration ($p>0.05$), nor did it change the total:HDL cholesterol ratio ($p>0.05$; Table 4.4).

4.3.2. Effects of PPAR agonists on metabolic parameters

The concentrations of plasma glucose and insulin were not significantly different between DIO controls or any of the drug-treated groups, although there was a trend for them to be lower with each of the PPARγ agonists (all $p>0.05$; Table 4.3).

Table 4.4. Effects of 28-day administration of PPAR agonists on plasma lipid concentration in (+/-) DIO and chow-fed male ZDF rats in the fasted state.

	Pre-clamp	**Post-clamp**					
Drug/Dose (mg/kg/d)	**FFA** (mM)	**FFA** (mM)	**TG** (mM)	**Leptin** (ng/ml)	**Total cholesterol** (mM)	**HDL cholesterol** (mM)	**Total:HDL ratio**
Palatable diet-fed (DIO)							
vehicle	2.07±0.09	1.97±0.10	1.90±0.15	6.8±0.7	1.72±0.07	1.38±0.12	1.28±0.08
BF (100)	1.43±0.15**	1.21±0.12***	1.09±0.14***	5.2±1.0	1.06±0.04***†††	0.88±0.06***†††	1.23±0.08
PIO (30)	0.86±0.08***	0.70±0.04***††	0.78±0.04***	7.4±0.6	2.16±0.13**	1.65±0.05	1.31±0.05
DRF (3)	1.00±0.10***	0.69±0.08***††	0.92±0.03***	6.1±0.4	2.21±0.06**	1.70±0.04**	1.30±0.05
NNC (1.5)	1.07±0.15***	0.90±0.07***	0.93±0.09***	7.2±0.6	2.02±0.11*	1.63±0.09	1.25±0.05
Chow-fed (vehicle)	1.07±0.10***	1.22±0.14**	1.00±0.11**	3.2±0.4**	2.00±0.07*	1.65±0.07	1.22±0.06

Significance of statistical differences *vs* DIO (vehicle): *$p<0.05$; **$p<0.01$; ***$p\leq0.0001$; *vs* chow-fed controls: $^{\dagger\dagger}p<0.01$; $^{\dagger\dagger\dagger}p\leq0.0001$. Data are expressed as mean ± SEM.

Importantly, however, BF, PIO and DRF normalised plasma insulin to chow-fed control levels ($p>0.05$ *vs* chow-fed vehicle; Table 4.3). The insulin resistance of DIO rats was improved by all drugs, and, in particular, PIO and DRF appeared to normalise insulin sensitivity, although this did not reach statistical significance (all $p>0.05$; Table 4.3).

Fasting plasma FFA concentrations in DIO rats were significantly reduced by all drugs (all $p<0.0001$). Plasma TG concentrations were also normalised by all drug treatments in DIO rats (all $p<0.0001$). None of the treatments, however, reduced the plasma leptin concentration in DIO rats (all $p>0.05$; Table 4.4).

Plasma total cholesterol concentrations rose in both PPARγ- (PIO, DRF) and the α/γ- (NNC) treated groups (+17-28%; all $p<0.05$) and fell, as expected, in response to BF (α agonist) treatment (-38%; $p<0.0001$) to levels below that of chow-fed controls (-47% *vs* chow-fed controls; $p<0.0001$). Effects of γ agonists on circulating HDL cholesterol were not as marked, the only significant change being a rise in response to DRF treatment (+23%; $p<0.01$). As with total cholesterol, HDL fell by 36% with BF treatment ($p<0.0001$), to 47% below normal (chow-fed control) concentrations ($p<0.0001$), but the total:HDL cholesterol ratio was unchanged from that of DIO controls ($p>0.05$). None of the γ agonist treatments had any effect on this ratio (all $p>0.05$; Table 4.4).

4.3.3. Haemodynamic factors

DIO control rats had increased heart weight in comparison to chow-fed controls; i.e., the HPD itself caused an increase in cardiac mass (+14%; $p<0.05$). There was also a trend toward an increase in heart weight with all treatments, in comparison to DIO controls, but none of these reached statistical significance ($p>0.05$). BF and PIO

were the only drugs that affected PCV. Although not significantly lower than that of DIO controls, these PCV values were 7% below normal (i.e., *vs* chow-fed controls; $p<0.01$ and $p<0.05$, respectively). Despite this, BF had no effect on cardiac mass ($p>0.05$; Fig. 4.2) .

4.3.4. Food and water intake and body weight

DIO vehicle controls were hyperphagic, consuming 10% more energy than chow-fed rats ($p<0.0001$), but all treatments enhanced food consumption further (+11-14% compared with DIO untreated controls, all $p<0.01$). As expected, because the HPD had a much higher water content than normal chow, the water intake of DIO controls was almost half that of chow-fed controls (-45%; $p<0.0001$; Table 4.5).

Weight gain paralleled the food intake pattern, as DIO controls gained 64% more weight than chow-fed controls over the course of vehicle administration ($p<0.05$), and all γ agonist treatments augmented weight gain in DIO rats (+100-117%; $p<0.0001$; Table 4.5), an effect which coincided with a 29-134% increase in all white fat masses but the subcutaneous (except PIO in the case of perirenal fat). The most pronounced increase occurred in brown fat (all $p<0.01$; Table 4.1).

The proportion of body weight in DIO rats attributable to epididymal fat was further increased by all γ agonists (+19%-34%; all $p<0.01$). That attributable to perirenal fat was enhanced (to a lesser extent) only by the mixed α/γ agonist, NNC (+23%; $p<0.01$). Treatment with the α agonist, BF, had no effect on these parameters or on the proportion of body mass made up by interscapular brown fat mass (all $p>0.05$), whereas all γ agonists further augmented this proportion, similar to their effect on white (epididymal) fat (+72-111%; all $p<0.0001$: Table 4.2).

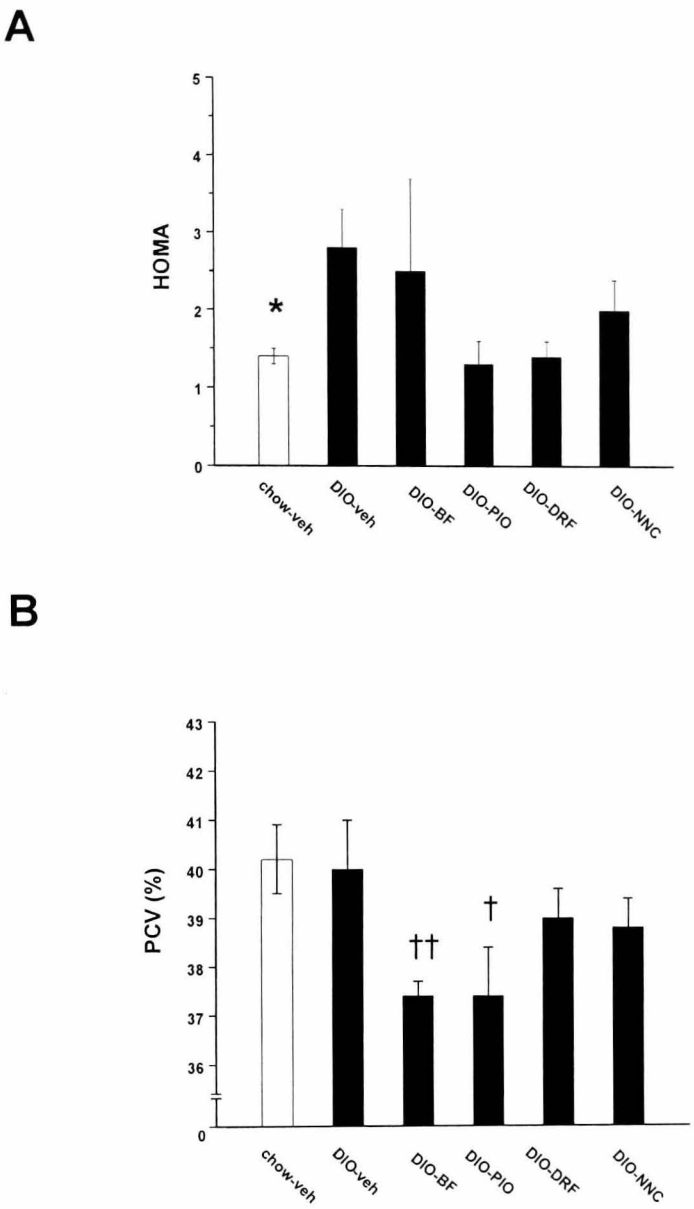

Figure 4.2. (A) Final HOMA values, (B) PCV and (C) cardiac mass in chow-fed, untreated (vehicle) controls (chow-veh) and DIO rats treated with PPAR agonists for 4 weeks (n=8/group). Significance of statistical differences *vs* DIO controls (DIO-veh): $^{*}p<0.05$; *vs* chow-fed controls: $^{\dagger}p<0.05$; $^{\dagger\dagger}p<0.01$.

Table 4.5. Effects of 28-day administration of PPAR agonists on cumulative energy intake, water intake and body weight gain in (+/-) DIO and chow-fed male ZDF rats in the fed state.

Drug/Dose (mg/kg/d)	**Energy intake** (kJ)	**Water intake** (ml)	**Body weight gain** (g)
Palatable diet-fed (DIO)			
vehicle	9760±80	363±11	23±3
BF (100)	10573±230**	410±13	22±2
PIO (30)	11171±163***	393±15	50±2***
DRF (3)	10818±152***	386±14	49±4***
NNC (1.5)	11146±232***	407±14	46±2***
***Chow-fed** (vehicle)*	8859±120***	656±15***	14±3*

Significance of statistical differences *vs* DIO (vehicle): *$p<0.05$; **$p<0.01$; ***$p\leq0.0001$. Data are expressed as mean ± SEM.

There were no changes in the ratios of subcutaneous-to-epididymal or -perirenal fat between DIO and chow-fed controls, nor with any of the treatments (all $p>0.05$). There was an increase in the subcutaneous fat mass-to-muscle ratio, but this did not reach significance ($p>0.05$; Table 4.2).

4.3.5. Progression of insulin resistance

Blood glucose concentrations remained the same throughout the treatment period and were not changed by any of the drugs at the doses used here (all $p>0.05$; Table 4.6). Nor were they changed by the 12-h fast prior to the clamp procedure. Circulating insulin concentrations were higher in DIO than chow-fed controls, in general, but high variation obscured any potentially significant relationships. Similarly, insulin

concentrations tended to be lower in treated animals, and dropped, as would be expected, after the 12-h fast, but not significantly in most cases (Table 4.7).

Generally, plasma FFA concentrations were higher throughout the treatment period in DIO than chow-fed controls ($p<0.05$; Table 4.8), and the reduction in these concentrations produced by all the drugs was maintained throughout (all $p<0.01$), except in the case of the α agonist, BF. After only two weeks of treatment, all γ agonists, on the other hand, had reduced FFA concentrations to below the levels of chow-fed controls (all $p<0.05$). As expected, circulating FFA concentrations rose

Table 4.6. Effects of PPAR agonist administration on weekly blood glucose concentration (mM) in (+/-) DIO and chow-fed male ZDF rats.

Drug/Dose (mg/kg/d)	**Week 1** (fed)	**Week 2** (fed)	**Week 3** (fed)	**Week 4** (pre-clamp; fasted)
Palatable diet-fed (DIO)				
vehicle	7.5±0.4	9.8±1.2	10.4±1.9	9.5±0.5
BF (100)	8.2±0.4	11.9±1.4	11.3±0.8	11.7±1.0
PIO (30)	7.0±0.2	8.2±0.8	8.4±0.8	8.2±0.6
DRF (3)	7.6±1.2	7.9±0.4	10.1±1.9	8.5±0.6
NNC (1.5)	8.5±1.5	8.5±0.8	10.2±1.3	9.1±1.0
***Chow-fed** (vehicle)*	7.7±0.8	7.6±0.7	7.4±0.6	9.0±0.8

No statistically significant differences between any groups. Data are expressed as mean ± SEM.

after the pre-clamp fast, although they remained significantly lower than those of the DIO controls (all $p<0.01$). FFA levels gradually increased over the treatment period, although not significantly, even in control chow-fed rats, probably as a result of their natural weight gain. DIO rats also showed this pattern, but it was arrested by drug treatment (Table 4.8).

4.3.6. Insulin secretion

There were no significant differences between the blood glucose concentrations attained in any group over the final 30 min of the clamp (all $p>0.05$). There were also no differences between the S-S glucose infusion rates required to maintain hyperglycaemia in each of the groups (all $p>0.05$), suggesting no difference in pancreatic secretory capacity for insulin. This was confirmed by no significant differences in total (90-min) glucose-stimulated insulin secretion (GSIS), although

Table 4.7. Effects of PPAR agonist administration on weekly plasma insulin concentration (pM) in (+/-) DIO and chow-fed male ZDF rats.

Drug/Dose (mg/kg/d)	**Week 1** (fed)	**Week 2** (fed)	**Week 3** (fed)	**Week 4** (pre-clamp; fasted)
Palatable diet-fed (DIO)				
vehicle	103.8±22.8	179.4±89.4	87.6±9.6	51.6±9.6
BF (100)	76.8±10.8	68.4±5.4	223.2±120.0	29.4±3.6
PIO (30)	66.0±11.4	61.2±6.0	73.2±16.8	37.2±8.4††
DRF (3)	54.0±3.6	135.0±49.8	76.8±13.2	34.2±4.2
NNC (1.5)	69.6±8.4	66.0±3.0	217.2±103.2	41.4±4.8
***Chow-fed** (vehicle)*	48.0±5.4	55.2±6.6**	68.4±10.2	25.8±1.8**†

Significance of statistical differences *vs* DIO (vehicle): **$p<0.01$; *vs* corresponding week 1: $^{\dagger}p<0.05$; $^{\dagger\dagger}p<0.01$. Data are expressed as mean ± SEM.

comparisons between DIO groups tended toward significance (1-way ANOVA, $p=0.09$). The DRF-treated group showed an impaired first phase insulin response ($p<0.01$) and reduced total insulin secretion, but this did not reach significance. The NNC-treated group also tended toward a reduced early insulin response in comparison to DIO controls, verging on significance (*post hoc* Bonferroni modified *t*-test $p=0.0126$, where critical $p=0.0125$). Late phase insulin responses were all

equivalent, with that of the chow-fed group appearing slightly exaggerated, although, again, this was not statistically significant (Table 4.9).

Table 4.8. Effects of PPAR agonist administration on weekly plasma FFA concentration (mM) in (+/-) DIO and chow-fed male ZDF rats.

Drug/Dose (mg/kg/d)	**Week 1** (fed)	**Week 2** (fed)	**Week 3** (fed)	**Week 4** (pre-clamp; fasted)
Palatable diet-fed (DIO)				
vehicle	1.21±0.11	1.62±0.28	1.74±0.21	2.07±0.09‡‡
BF (100)	0.85±0.04**	0.90±0.13**	1.30±0.14	1.43±0.15**‡
PIO (30)	0.40±0.12***	0.40±0.07***††	0.35±0.06***†††	0.86±0.08***‡
DRF (3)	0.38±0.04***††	0.57±0.10***††	0.54±0.10***†††	1.00±0.10***‡
NNC (1.5)	0.44±0.02***†††	0.68±0.10***†	0.68±0.23***†	1.07±0.15***‡
***Chow-fed** (vehicle)*	0.76±0.02*	1.04±0.12	1.21±0.08*‡‡	1.07±0.10***

Significance of statistical differences *vs* DIO (vehicle): *$p<0.05$; **$p<0.01$; ***$p\leq0.0001$; *vs* chow-fed controls: $^{†}p<0.05$; $^{††}p<0.01$; $^{†††}p<0.0001$; *vs* corresponding week 1: $^{‡}p<0.05$; $^{‡‡}p<0.01$. Data are expressed as mean ± SEM.

4.3.7. Pancreatic insulin content

Pancreatic insulin content was more than three-fold higher in DIO controls than chow-fed rats (+222%; $p<0.05$), but this was not altered by any of the drug treatments (all $p>0.05$; Table 4.3).

4.4. Discussion

The DIO model was successfully established in this experiment. Lean ZDF rats developed insulin resistance after 14 weeks on the HPD. Glucose concentrations remained unchanged, however, in DIO controls and in their treated counterparts, an

Table 4.9. Effects of PPAR agonist administration on insulin secretory capacity in (+/-) DIO and chow-fed male ZDF rats in the fasted state.

Drug/Dose (mg/kg/d)	**Early Insulin Response** (μU/ml/min)	**Late Insulin Response** (μU/ml/min)	**Total Insulin Response** (μU/ml/min)	**Steady-State Glucose Infusion Rate** (mg/kg/min)	**Steady-State Blood Glucose Concentration** (mM)
Palatable diet-fed (DIO)					
vehicle	76±12	74±6	162±14	3.2±1.3	24.0±0.9
BF (100)	48±10	64±10	123±14	1.4±0.4	24.6±1.0
PIO (30)	71±17	96±19	183±38	5.5±2.0	21.9±1.6
DRF (3)	34±3**	61±7	102±8	3.3±0.9	20.6±0.4
NNC (1.5)	40±4	72±15	121±20	3.2±1.2	21.6±0.7
Chow-fed *(vehicle)*	51±10	93±20	154±20	3.5±1.1	22.9±1.4

Significance of statistical differences *vs* DIO (vehicle): $^{**}p<0.01$. Data are expressed as mean ± SEM.

observation which is consistent with previous findings in DIO Wistar rats [Pickavance *et al.,* 1999b, 2000; Widdowson *et al.,* 1997; Chapters 5-7].

That the DIO ZDF rat model does not show even moderate hyperglycaemia is in contrast with findings in the diabetic ZDF rat described in Chapter 3, which were markedly hyperglycaemic. This suggests that after only a total of 14 weeks on the HPD, the DIO ZDF rats certainly have not progressed to overt diabetes. It is possible that diabetes might develop after a prolonged period on the HPD, such as several months or a year. There was also no change in insulin secretory capacity in this model compared to chow-fed controls, which also suggests that it may only represent the very early (i.e., insulin-resistant) stages of type 2 diabetes development. However, the raised lipids in DIO rats suggest the potential for accumulation in ß-cells, but this would have to be proved, for example, by histological analysis.

Interestingly, comparing the mean absolute body weight of the DIO ZDF rats in this experiment with that of the obese ZDF rats in Chapter 3 shows that diabetes develops at a lower body weight in the obese ZDF from that which was achieved here. This suggests that the islet defect is related directly to the leptin receptor mutation, rather than to the degree of obesity. However, it should be noted that fat depots were smaller in the DIO model than in obese ZDF rats; exposure to the HPD induced a perirenal fat proportion of 0.7% (Table 4.2), for example, whereas that of the obese ZDF rats in Chapter 3 was more than twice as much (about 2%).

Although treatment with the PPAR agonists resulted in only a tendency toward improving insulin resistance, as defined by HOMA, all the compounds effectively normalised the hypertriglyceridaemia. The data obtained from this model support the hypothesis that, via the Randle cycle [Randle *et al.,* 1963], the insulin-sensitising effect of all the agonists would be closely linked to the reduced availability of FAs

(of which DIO rats have more to start with) as a fuel for skeletal muscle [Oakes *et al.,* 1994, 1997]. Coincidentally, peripheral fat mass increased significantly with the γ agonists, suggesting either enhanced FA clearance and deposition as TG in adipose tissue (both white and brown) and/or reflecting anti-lipolytic action of the drugs [Oakes *et al.,* 1994, 1997; Souza *et al.,* 1998].

Although leptin is a satiety signal in rodents [Schwartz *et al.,* 1992], its plasma concentration did not fall with any drug treatment, which means that the doses used here did not contribute via this mechanism to the observed hyperphagia and the component of weight gain which would have resulted from it (the latter having been observed only in the γ agonist-treated groups).

Lack of additional weight gain and fat accrual in the BF-treated group, combined with the plasma lipid reductions observed in this group, without a concomitant decrease in food intake, are consistent with the expected actions of a fibrate [for review, see Betteridge, 1997]. Guerre-Millo and colleagues [2000] found that fenofibrate treatment prevents high-fat diet-induced increase of body weight without influencing caloric intake in mice, suggesting that maintenance of original body weight is not driven by food intake reduction but by some other mechanism. As BF also lowered cholesterol levels, whereas the γ agonists raised them, it could be argued that, overall, an α agonist is, in fact, preferable to a γ agonist in this model. However, it did not improve insulin resistance, and its FFA-lowering effect remained less potent than that of all the γ agonists. Surprisingly, this dose of BF (100 mg/kg daily) also caused haemodilution (reduced PCV). This has not been reported before, and may be peculiar to this model, but, nonetheless, presents a potential disadvantage of this therapy. For the same reason, pioglitazone would not be the drug of choice, as its therapeutic effectiveness was no better than that of the other γ agonists, and it

caused haemodilution. This is supported by evidence presented in Chapter 7, in which pioglitazone administered at the same dose of 30 mg/kg daily in DIO female Wistar rats also caused haemodilution.

As noted in Chapter 3, the significant increase in fat pad mass in γ agonist-treated DIO ZDF rats, as compared to untreated controls, is probably a consequence of these compounds, through their selective binding to PPARγ, inducing adipogenesis by regulating expression of adipocyte-specific genes [Harris & Kletzien, 1994]. This also shows that the γ agonists DRF and NNC, which are not TZDs, have TZD-like actions.

Of the four fat pads weighed in this experiment, the interscapular brown fat pad showed the most pronounced increase in mass. This may have occurred not only because of proliferation of brown adipocytes by TZDs [Tai *et al.,* 1996], as occurs with white adipocytes [Spiegelman, 1998], but also because of infiltration by white adipocytes into the brown adipose pad [for review, see Susulic *et al.,* 1996]. This would have to be verified histologically. The fact that increased BAT depot size was observed with γ agonist, but not α agonist, treatment has been reported previously in rats [Kelly *et al.,* 1998]. These authors found this was due to increased size of lipid vacuoles and brown adipocyte size. PPARγ is more highly expressed in BAT than in WAT *in vivo* in both lean and obese Zucker rats [Gorla-Baiszczak *et al.,* 2000]. If this relationship also holds in lean ZDF rats which develop dietary obesity, it could explain the pronounced response to γ agonists in BAT here. That subcutaneous fat did not increase with treatment, whereas other fat depots did, is the reverse of the observation of Adams and colleagues [1997], in which TZDs were found to markedly enhance the differentiation of human preadipocytes from subcutaneous sites *in vitro*.

The progression of dietary obesity was reflected by plasma FFA concentrations that were raised consistently over the course of the experiment. Raised FFAs enhance insulin secretory rates by direct effects on β-cells [Chen *et al.*, 1994]. However, that DIO rats did not show this under hyperglycaemic conditions in this experiment has also been observed in humans undergoing a hyperglycaemic clamp simultaneously with an acute infused elevation in FFAs [Frias *et al.*, 2000]. It may be that there is no net effect on insulin secretion because the stimulatory effects of a high concentration of circulating FFAs are offset by the inhibitory (lipotoxic) effects once they accumulate inside the β-cells and become esterified to TG.

A decrease in circulating HDL has a well-known association with obesity, and yet plasma HDL concentrations in the DIO group were no different from those of chow-fed controls. Perhaps the level of obesity in this experiment was not excessive enough to show a difference. Also, circulating concentrations of total cholesterol are increased in obesity, yet the opposite occurred in the DIO group here, as they displayed lower total cholesterol concentration than did the chow-fed group. Further work will be required to explain this. Only BF, the α agonist, was effective in reducing cholesterol concentrations. Although increased HDL is a documented effect of fibrates due to their PPARα activation [Gervois *et al.*, 2000], in this instance, the BF action seem to have been indiscriminate, as it lowered HDL concentrations, which is a risk factor for coronary heart disease [for review, see Betteridge, 1997]. Both total and HDL cholesterol were raised by all γ agonist treatments, probably because of the enhanced fat accumulation these drugs induced. This included NNC treatment, suggesting that there is no additional *in vivo* benefit conferred by the α agonist properties of this compound in this model. This would appear to go against the findings of Murakami *et al.* (1998), who have shown that a

combined PPARα/γ activator was significantly more effective than a classical TZD in inhibiting enhanced lipogenesis and TG accumulation in the liver. Although these workers did not measure cholesterol, nor have I measured liver TG content, it is clear from this experiment that NNC is no more potent in its lipid-lowering effects than the other drugs used, and, therefore, its combined α/γ binding properties do not have the synergistic effect hoped for.

The higher pancreatic insulin content together with higher circulating concentrations of insulin and FFAs in DIO controls compared to chow-fed controls is consistent with the induction of β-cell hyperplasia by increased availability of FFAs and subsequent hyperinsulinaemia [Milburn *et al.*, 1995]. Why secretion is not different between the two groups under glucose stimulation, however, suggests that something may be interfering with insulin release under these conditions in the DIO animals.

It has been shown in both fasted rats and humans that a high circulating concentration of FFAs is essential for GSIS [Dobbins *et al.*, 1998; Stein *et al.*, 1996]. It might have been expected, therefore, that the BF-treated group would show enhanced insulin secretion compared to the γ agonist-treated groups, as BF treatment reduced FFAs to a lesser extent. A 12-h fast which increased circulating FFA concentrations (Table 4.8) was perhaps of insufficient length to bring out this difference, or, as described above, a lipotoxic effect on islets in this group may have negated any enhanced insulin secretion. The only significant change in insulin secretion using this model was the abolition of the early phase insulin response by DRF, and, therefore, may have something to do with its γ_2-preferring property. This action is undesirable, because it mimics one of the characteristic abnormalities of insulin secretion in type 2 diabetes [for review, see Polonsky *et al.*, 1996].

In summary, all the drugs used in this experiment are equipotent in terms of their effects on insulin resistance and circulating lipids, consistent with their receptor-binding assay equipotency. Generally, none of the drugs had affected pancreatic insulin content or plasma insulin concentration, and this was supported by a lack of change in insulin secretion in response to hyperglycaemia. The one exception to this was the blunted early insulin response of DRF-treated rats. On balance, and until further investigation, it would appear difficult to select with confidence a compound out of this group that is outstandingly superior in its therapeutic effects, and dose-response studies for all would be required to determine if there is an adequate separation between therapeutic and adverse effects. All γ agonist compounds, including NNC, caused weight gain, and, therefore, there was no neutralisation of weight gain by its α agonist component. There was no change in leptin concentrations, suggesting that leptin is not involved in γ agonist-induced weight gain. The reduction in FFAs, however, underscores the key message that these may play a more important role in the action of these drugs. Finally, the parameters measured here would not indicate that lean ZDF rats are more prone to developing diabetes in response to weight gain because of their genetic background than are Wistar rats.

4.5. Conclusion

The lean ZDF rat which becomes insulin-resistant on the HPD does not become hyperglycaemic or polydipsic as does the diabetic ZDF rat with the genetic mutation (Chapter 3). This experiment has shown that all the PPARγ agonists tested here improve the metabolic profile and insulin resistance in the DIO ZDF rat model equally with the α/γ mixture, and better than the α agonist alone. Weight gain

probably relates to the FFA-lowering of the γ agonists, but it does not obviously attenuate the improvement in metabolic status induced by these compounds.

CHAPTER 5

Therapeutic index for rosiglitazone in dietary obese rats: *Separation of efficacy and haemodilution, effects on body weight and plasma leptin, and assessment of insulin sensitivity at a therapeutic dose*

5.1. Introduction

As I described in the General Introduction [1.6.5 (ii)], the mechanism of action of thiazolidinediones (TZDs) is reasonably well-defined, but it is less clear what long-term side effects these agents have in man. To recap, hepatic toxicity is a rare but potentially lethal complication of troglitazone therapy [Shibuya *et al.,* 1998; Watkins & Whitcomb, 1998], but haemodilution, which occurs as a result of plasma volume expansion and has the potential outcome of cardiac hypertrophy, is a common result of TZD treatment [Cantello *et al.,* 1994; Ghazzi *et al.,* 1997; Patel *et al.,* 1998]. Perhaps the TZD side-effect which is most salient and unsettling to the patient, and which is the most consistently observed, is weight gain [Patel *et al.,* 1999; Shimizu *et al.,* 1998]. TZDs act by binding to and activating PPARγ, a nuclear receptor present in adipocytes. This then enhances the transcription of genes encoding proteins involved in lipid metabolism. It is not known how this mechanism leads to weight gain, but it may be via changes in circulating free fatty acid (FFA) and leptin concentrations and in tumour necrosis factor-alpha (TNFα) expression in fat. Although weight gain has also been observed in several animal studies of TZDs [Arakawa *et al.,* 1998; de Souza *et al.,* 1995; Hirshman *et al.,* 1995; Ikeda *et al.,* 1990; Inoue *et al.,* 1995; Yoshioka *et al.,* 1993; Zhang *et al.,* 1996], attempts to define the contributions of these various mechanisms have not been published.

It is presently unclear whether the individual TZDs differ in their liability for these effects at appropriate anti-hyperglycaemic dosages. It is true that, ultimately, long-term clinical trials will provide such information, but, in the meantime, I thought it of considerable interest to study the dose-effect relationship for the disparate actions of TZDs (e.g., insulin action-enhancing, haemodilution, cardiac hypertrophy and weight gain) in a single, appropriate animal model, namely, the DIO rat. [The appropriateness of this model for studies of type 2 diabetes and its treatment is discussed at length in the General Introduction, 1.5.1 (ii) (a) and General Methods, 2.1.2 (ii)].

The properties of TZDs, including rosiglitazone (RSG), are described in the General Introduction [1.6.5. (i)-(ii)] and their structures shown in Fig. 1.9. RSG was the TZD of choice for this experiment because, at the time, it was the most potent of the TZDs in late stage clinical development (having since been licensed for use in humans in the U.S.A. and Europe), and so was predicted to provide a clear assessment of dose-response relationships yet unexplored in animals.

5.2. Methods

5.2.1. Animals and treatment

Figure 5.1 shows the design of the dose-response experiment. Suppliers of animals, drugs and chemicals are identified in General Methods [2.1.2 (ii) and 2.1.6-7]. Thirty-six male Wistar rats (220 g) were fed the highly palatable diet (HPD) for 8 weeks to induce mild obesity, and 36 age-matched controls were fed rodent pelleted chow, the respective energy compositions of which are presented in General Methods [2.1.2 (ii) (a)]. At the end of the 8-week period, when diet-treated rats had

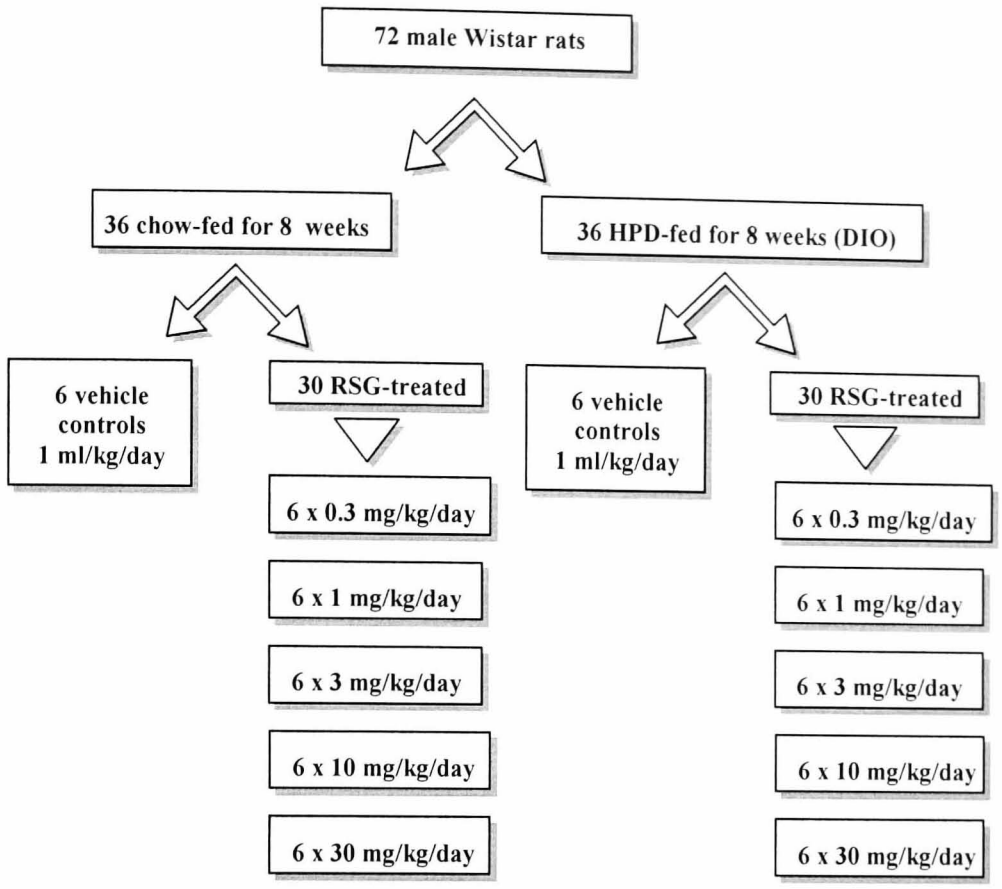

Figure 5.1. Experimental design for the study of RSG dose-response in DIO rats. Weight gain and food intake were measured daily during treatment and RSG administered for 21 days. Animals were killed in the fasted state, trunk blood collected, and plasma concentrations of glucose, insulin, TGs and FFAs measured. Plasma leptin, heart mass, PCV and epididymal fat pad mass were determined at termination in chow-fed control rats and in all DIO groups.

developed significant obesity, vehicle (1% CMC at 1 ml/kg) or RSG at five doses (0.3, 1, 3, 10 or 30 mg/kg) was given to six rats per dose group, for both DIO and chow-fed rats, by gavage daily for 21 days. Food intake and body weight were measured daily throughout the treatment period.

5.2.2. Metabolic data and tissue mass

At the end of the experiment, and after a 4-h fast, rats were killed by CO_2 inhalation. Blood was collected by cardiac puncture and plasma assayed for insulin and leptin concentrations by RIA, and for glucose, FFA and TG concentrations by diagnostic

kit [see 2.2.1 (i) (c), (ii) (a-c)]. HOMA was derived from insulin and glucose concentrations [see 2.2.3 (ii)]. In the case of all DIO rats and of chow-fed rats treated with vehicle, PCV was also measured. Hearts were excised, blotted and weighed to determine degree of cardiac hypertrophy. Body fat content was estimated by dissection and weighing of epididymal and perirenal fat pads and expressed as a percentage of total body weight.

5.2.3. Insulin sensitivity at a therapeutic dose

As a follow-up to the dose-response experiment, 20 male Wistar rats (252 g) were fed the HPD for 7 weeks to induce obesity, and 10 age-matched controls were fed chow. For 21 days, while continuing on the HPD, half of the DIO control rats were then administered vehicle, as described above, as were the chow-fed controls. The other half of the DIO group was given RSG at 3 mg/kg daily, the dose found to be therapeutic without inducing side effects in the dose-response experiment. Food intake and body weight were also measured daily throughout this treatment period. Rats were then deeply anaesthetised and their insulin sensitivity measured using the hyperinsulinaemic-euglycaemic clamp technique, as described in General Methods [2.2.3 (iii) (a)].

5.2.4. Statistical analyses

Data are expressed as mean ± SEM. Differences between DIO untreated and chow-fed controls were compared using unpaired *t*-tests. The effect of dose upon each of the parameters studied was determined by 1-way ANOVA for both the DIO and chow-fed groups, followed by Bonferroni modified *t*-tests, where critical *p* for 5

comparisons=0.01. A complete breakdown of the statistical applications used to analyse these data is presented in the General Methods section [2.4.2 (i)].

5.3. Results

5.3.1. Dietary obesity

At baseline (prior to diet treatment in the dose-response experiment), the groups destined for chow feeding or to be given the palatable diet were of similar weight (227 ± 2 *vs* 226 ± 2 g, respectively; $p>0.05$). After being fed the palatable diet for 8 weeks prior to drug treatment, rats developed mild obesity, becoming 4% heavier than chow-fed rats (540 ± 6 *vs* 520 ± 6 g; $p<0.05$). At termination, DIO (vehicle) control rats were 9% heavier (596 ± 9 g *vs* 547 ± 10 g; $p<0.01$) and had greater absolute perirenal and epididymal fat masses than chow-fed (vehicle) controls (perirenal: 11.5 ± 1.8 *vs* 7.0 ± 0.7 g; epididymal: 12.6 ± 1.4 *vs* 9.2 ± 0.6 g; both $p<0.05$). DIO control rats also tended to be more insulin resistant than chow-fed controls (45% increase in HOMA; $p=0.1$; Fig. 5.2A). Changes in lipid metabolism were also apparent in the DIO controls, with 29% higher plasma FFA ($p<0.05$), 75% higher TG and nearly three-fold higher plasma leptin concentrations than chow-fed (vehicle) controls (both $p<0.01$; Table 5.1).

5.3.2. Effects of RSG on metabolic parameters

In DIO rats, the concentration of plasma glucose was significantly reduced at 3 mg/kg of RSG (by 21%; $p<0.01$), whereas that of plasma insulin was lowered at 10 mg/kg (by 27%; $p<0.05$; Table 5.1). Neither plasma glucose nor insulin concentrations were affected by RSG treatment in chow-fed rats ($p>0.05$; Table 5.1). The HOMA model showed that RSG induced a dose-related improvement in insulin

Table 5.1. Fat pad mass and terminal plasma concentrations of hormones and metabolites in DIO and chow-fed male Wistar rats after 21-day RSG administration.

Dose (mg/kg/d)	**Insulin** (pM)	**Glucose** (mM)	**HOMA**	**FFA** (mM)	**TG** (mM)	**Leptin** (ng/ml)	**Epididymal fat mass** (%)	**Perirenal fat mass** (%)
Palatable diet-fed (DIO)								
0	143±15	5.9±0.4	6.2±0.8	0.67±0.08	3.59±0.37	29.8±7.2	2.10±0.21	1.93±0.29
0.3	142±22	5.6±0.3	5.9±1.0	0.42±0.06**	3.90±0.63	25.5±6.0	2.51±0.14*	1.98±0.20
1	122±8	5.1±0.3	4.6±0.5*	0.39±0.06**	2.81±0.38	24.2±3.8	2.66±0.10**	2.33±0.25
3	120±8	4.6±0.4**	4.0±0.2*	0.24±0.03***	2.09±0.15**	18.4±2.2**	2.12±0.14	2.01±0.18
10	104±6*	4.5±0.1**	3.5±0.2**	0.27±0.04***	1.14±0.04***	19.8±1.8**	2.61±0.12**	2.47±0.26
30	82±6**	4.7±0.5**	2.8±0.4**	0.26±0.04***	0.99±0.09***	17.5±1.4**	2.60±0.08**	2.34±0.13
Chow-fed								
0	108±12	5.4±0.4	4.3±0.7	0.52±0.08†	2.05±0.36††	10.5±1.5††	1.68±0.10	1.28±0.12
0.3	151±17	4.9±0.3	5.4±0.4	0.47±0.05	2.71±0.16	14.4±2.0	1.80±0.14	1.28±0.19
1	122±10	5.1±0.4	4.6±0.5	0.39±0.09	2.34±0.26	13.8±2.6	1.88±0.20	1.40±0.16
3	130±14	4.6±0.3	4.4±0.6	0.31±0.04**	2.21±0.32	21.9±6.0	1.81±0.18	1.47±0.22
10	112±11	4.2±0.2	3.6±0.4	0.29±0.04**	1.60±0.14	12.2±2.0	2.03±0.16	2.08±0.24**
30	105±18	4.2±0.1	3.3±0.6	0.20±0.02**	0.88±0.04**	14.2±3.3	1.95±0.15	1.93±0.14*

Statistical significance of differences *vs* corresponding controls: *$p<0.05$; **$p<0.01$; ***$p<0.0001$. Statistical significance of differences between chow-fed and DIO (vehicle) controls: $^{\dagger}p<0.05$, $^{\dagger\dagger}p<0.01$. Data are expressed as mean ± SEM.

sensitivity in DIO rats with a threshold of 1 mg/kg ($p<0.05$; Table 5.1 and Fig. 5.2A), but drug treatment did not significantly alter insulin sensitivity in chow-fed rats ($p>0.05$; Table 5.1).

FFAs were also significantly reduced by drug treatment in DIO rats, although at a lower dose (0.3 mg/kg; 37% fall; $p<0.01$) than that required for improving insulin sensitivity. Plasma TG concentrations were also reduced by RSG in DIO rats, decreasing by 42% at a threshold dose of 3 mg/kg ($p<0.01$). Both plasma FFA (by 69%) and TG (by 57%) concentrations were also reduced by RSG in chow-fed rats, but at 10-fold higher threshold doses than those required in DIO rats; i.e., 3 and 30 mg/kg, respectively (both $p<0.01$; Table 5.1).

5.3.3. Haemodynamic factors

Effects of RSG on PCV and cardiac mass in DIO rats were only apparent at doses of 10 or 30 mg/kg. At the threshold dose, there was a 3.5% fall in PCV (45.5 ± 0.5 *vs* 47.2 ± 0.3%; $p<0.05$; Fig. 5.2B) and a 13% increase in cardiac mass (2.19 ± 0.06 *vs* 1.93 ± 0.06 g; $p<0.01$; Fig. 5.2C). Thus, the therapeutic index for RSG in DIO rats (the ratio of the threshold dose for causing haemodilution/cardiac hypertrophy to that for improving insulin sensitivity) was >3 and ≤10 (also compare panels B and C with panel A in Fig. 5.2).

5.3.4. Assessment of insulin sensitivity at the therapeutic dose

Although insulin sensitivity improved at the therapeutic dose of 3 mg/kg, as measured by the HOMA index, this observation was not supported by the hyperinsulinaemic-euglycaemic clamp technique. However, the establishment of insulin resistance in this group of animals after 7 weeks of exposure to the palatable

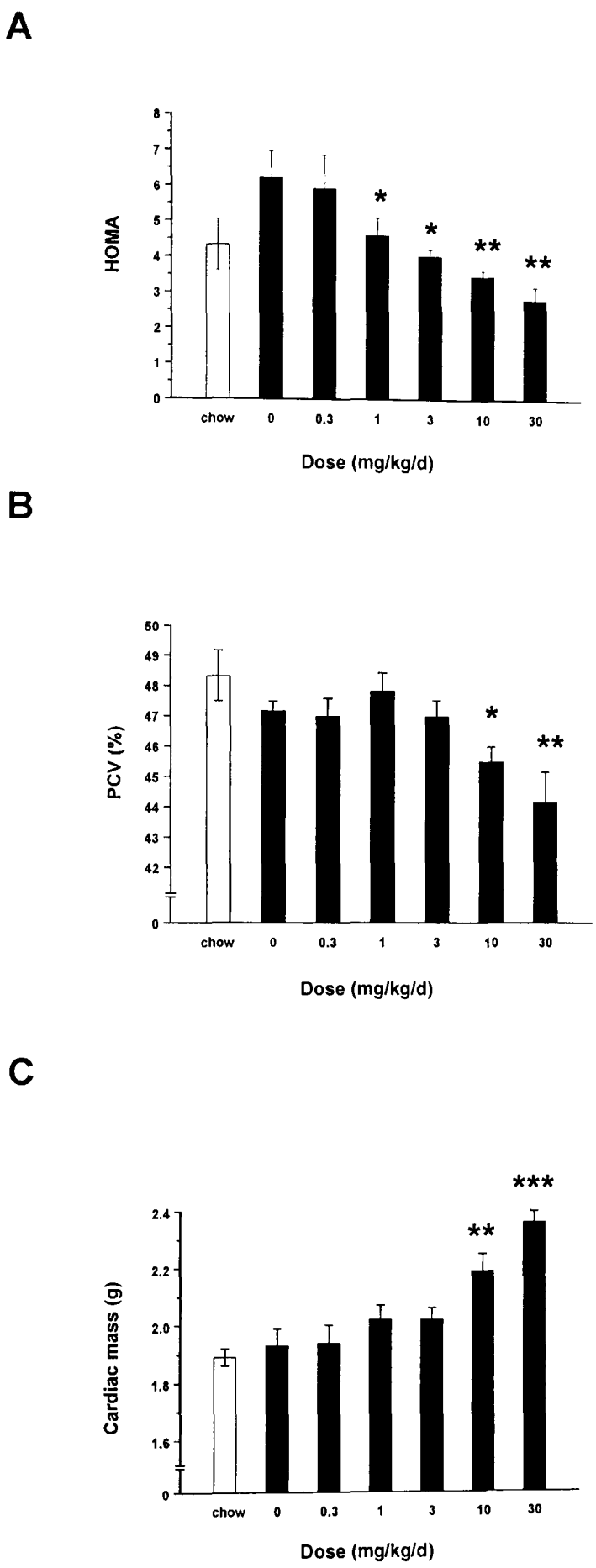

Figure 5.2. (A) Final HOMA values, (B) PCV and (C) cardiac mass in chow-fed, untreated (vehicle) controls (chow) and DIO rats treated with RSG at various doses for 3 weeks (n=6/dose group). There were no significant differences between untreated chow-fed and DIO rats. ANOVA followed by Bonferroni modified *t*-tests in the DIO group showed that insulin sensitivity (A) improved at a threshold dose of 1 mg/kg, whereas significant haemodynamic side effects (B,C) were present only at 10 mg/kg and above (*p<0.05; **p<0.01; ***p<0.0001).

diet was questionable, as plasma insulin concentrations measured prior to clamping did not differ between DIO and chow-fed rats (70.0 ± 15.4 *vs* 62.7 ± 17.0 pM; HOMA: 3.2 ± 0.8 *vs* 2.9 ± 1.0; both $p>0.05$). Although the glucose infusion rate required to maintain euglycaemia during artificially induced hyperinsulinaemia was 36% higher in DIO rats treated with 3 mg/kg/d RSG compared with untreated (vehicle) DIO rats (11.3 ± 1.9 *vs* 8.3 ± 1.4 mg/min), this did not reach statistical significance (1-way ANOVA, $p=0.2$).

5.3.5. Food intake and body weight

RSG increased food intake dose-dependently in DIO rats ($p<0.05$). In chow-fed rats, however, this effect was only seen at doses ≥3 mg/kg ($p<0.01$; Table 5.2). RSG also augmented weight gain in DIO rats (e.g., by 91.9 ± 5.3 g at 30 mg/kg *vs* 38.6 ± 4.1 g in (vehicle) controls; $p<0.0001$; Table 5.2), an effect which coincided with a 20-24% increase in gonadal fat mass ($p<0.05$; Table 5.1). Chow-fed rats did not significantly gain body weight at doses of RSG below 3 mg/kg, and their epididymal fat pad mass did not increase at any dose. However, the mass of the perirenal depot did increase significantly at 10 and 30 mg/kg ($p<0.01$; Table 5.1). Plasma FFA concentrations were significantly negatively correlated with weight gain during the three-week dosing period in both DIO ($R^2 = 0.89$; $p<0.01$) and chow-fed rats ($R^2 = 0.87$; $p<0.01$; Fig. 5.3A). Similarly, plasma FFAs were also significantly negatively correlated with calorie intake in these groups (DIO rats: $R^2 = 0.76$; $p<0.05$; chow-fed: $R^2 = 0.89$; $p<0.01$).

By contrast, whilst plasma insulin concentrations were significantly negatively correlated with both weight gain ($R^2 = 0.71$; $p<0.05$; Fig. 5.3B) and

calorie intake (R^2 = 0.72; p<0.02) in DIO rats, no such correlations were seen in chow-fed rats (p=0.43 for weight gain; Fig. 5.3B; p=0.00 for calorie intake).

Table 5.2. Cumulative energy intake and body weight gain in DIO and chow-fed male Wistar rats after 21-day administration of RSG.

Dose (mg/kg/d)	**Energy intake** (kJ)	**Body weight gain** (g)
Palatable diet-fed (DIO)		
0	10078±516	39±4
0.3	11098±319*	60±4*
1	11363±26**	68±7**
3	11428±281**	80±4***
10	12339±247**	94±4***
30	12302±325**	92±5***
Chow-fed		
0	9436±214	27±2
0.3	9744±222	29±2
1	9910±268	37±3
3	11491±1026**	60±6***
10	11119±282*	62±4***
30	11912±531**	65±6***

Statistical significance of differences *vs* corresponding controls: *p<0.05; **p<0.01; ***p<0.0001. Data are expressed as mean ± SEM. Cumulative values are those obtained after the 3-week dosing period.

5.3.6. Leptin

Plasma leptin concentrations (Table 5.1) were correlated overall with body weight across all DIO and chow-fed groups (R^2 = 0.46; p<0.01). In DIO (vehicle) control rats, the plasma leptin concentration was 65% higher than in chow-fed (vehicle)

controls ($p<0.01$). There was also a pattern of decreasing plasma leptin concentration with increasing dose of RSG in DIO rats ($p<0.01$), which was not seen in chow-fed rats ($p>0.05$; Table 5.1). Indeed, there was a significant negative correlation between plasma leptin concentrations and body weight gain ($R^2 = 0.9$; $p<0.01$; Fig. 5.3C) and calorie intake ($R^2 = 0.73$; $p<0.05$) during the three weeks of RSG administration in the DIO group, but not in the chow-fed group (for body weight: $p=0.4$; Fig. 5.3C; for calorie intake: $p=0.3$).

5.4. Discussion

These results show that RSG effectively reverses insulin resistance and lipid abnormalities in DIO rats, but does not significantly improve insulin sensitivity in chow-fed animals that are not insulin-resistant to begin with, despite their showing a similar trend in the relevant metabolic changes. These data in DIO rats support the hypothesis that, via the Randle cycle [Randle *et al.,* 1963], the insulin-sensitising effect of RSG is closely linked to the reduced availability of FAs (of which DIO rats have more) as a fuel for skeletal muscle [Oakes *et al.,* 1994, 1997]. Thus, plasma FFAs fell in DIO rats at a dose of RSG (0.3 mg/kg) that was slightly lower than that required to detect improved insulin sensitivity (1 mg/kg). Coincidentally, epididymal fat mass increased significantly at the lower dose, suggesting either enhanced FA clearance and deposition as TG in adipose tissue and/or reflecting the anti-lipolytic action of the drug [Oakes *et al.,* 1994, 1997; Souza *et al.,* 1998]. Additionally, the observation that the threshold dose for lowering concentrations of plasma TGs in DIO rats was 3 mg/kg (i.e., 10-fold higher than the lowest dose used, where FFAs were already reduced), suggests that changes in the plasma FFA concentration represent the more important trigger for improving insulin action.

Figure 5.3. Relationship between final plasma concentrations of (A) FFA, (B) insulin, (C) leptin and weight gain in chow-fed (open circles) and DIO rats (closed circles) after 3 weeks of treatment with RSG at various doses (0-30 mg/kg). There was a significant relationship between FFA concentrations and body weight gain in both groups (chow: R^2=0.87; p<0.01; DIO: R^2=0.89; p<0.01). Insulin levels were negatively correlated with weight gain in DIO rats (R^2 = 0.71; p<0.05), but not in chow-fed rats (R^2=0.1; p=0.43). Leptin concentrations were negatively correlated with body weight gain (R^2=0.9; p<0.01) in DIO rats, but not in the chow-fed group (R^2 = 0.17; p=0.4).

A

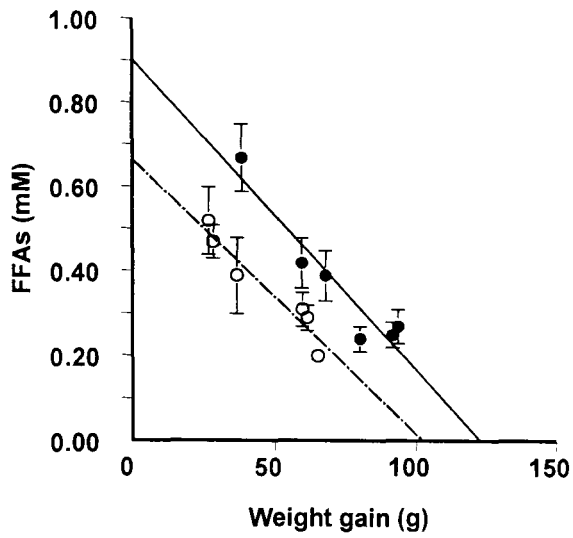
1.00
0.80
0.60
0.40
0.20
0.00
FFAs (mM)
0
50
100
150
Weight gain (g)

B

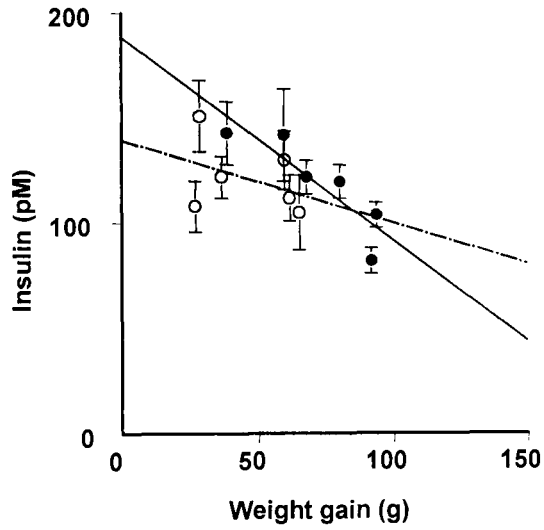
200
100
0
Insulin (pM)
0
50
100
150
Weight gain (g)

C

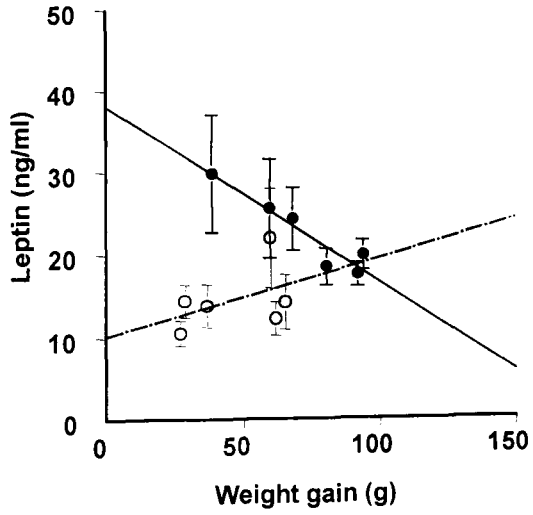
50
40
30
20
10
0
Leptin (ng/ml)
0
50
100
150
Weight gain (g)

Certainly, DIO rats chronically treated with the 3 mg/kg dose of RSG did not show a reduction in plasma insulin concentrations, and the hyperinsulinaemic-euglycaemic clamp technique only demonstrated a trend toward improved insulin sensitivity, which did not quite reach statistical significance. It would be useful to repeat this experiment with DIO rats that show elevated circulating insulin levels, indicating insulin resistance, inducible perhaps after longer exposure to the palatable diet.

Importantly, RSG was observed to enhance insulin action at a dose between 3 and 10-fold lower than that required to cause haemodilution and cardiac hypertrophy. Experience with RSG in the rat (R.E. Buckingham, unpublished data) agrees with the clinical finding that troglitazone does not influence red blood cell mass, as estimated using ^{51}Cr labelling of erythrocytes [Young *et al.,* 1997]. This suggests that plasma volume expansion is the key component of haemodilution.

Insulin and leptin are both satiety signals in rodents [Schwartz *et al.,* 1992], suggesting that the falls in both their plasma concentrations, which were evoked by RSG treatment, may have contributed to the observed side effects of hyperphagia and weight gain. The decrement in plasma leptin concentration may also have been due, at least partly, to the fall in plasma insulin, since insulin stimulates *OB* gene expression and leptin secretion from adipocytes [Hardie *et al.,* 1996; Leroy *et al.,* 1996]. Nonetheless, direct effects of TZDs on *OB* gene expression and leptin secretion have also been documented [Kallen & Lazar, 1996; Nolan *et al.,* 1996].

My data in chow-fed rats, however, suggest that changes in plasma concentrations of leptin and insulin do not entirely explain the RSG-induced hyperphagia and weight gain. Whilst RSG did not significantly influence food intake in chow-fed rats until the dose was raised to 3 mg/kg, neither plasma insulin nor leptin concentrations were reduced in these rats even at the highest dose of 30 mg/kg.

Moreover, unlike DIO rats, there was no negative correlation between plasma leptin or insulin concentration and calorie intake or weight gain in chow-fed rats. The difference in dose level for causing hyperphagia in DIO and chow-fed rats thus constitutes a conundrum and may suggest that, at least at higher dosages of RSG, an additional mechanism may be operating. Whether this mechanism is of peripheral or central identity is not certain from the present data, but it is of interest that the lowest doses that resulted in weight gain in both chow-fed and DIO animals were identical to those that reduced FFA concentrations. Furthermore, there was a highly significant negative correlation between terminal plasma FFA concentration and calorie intake or weight gain in both DIO and chow-fed rats. Thus far, however, there are no published data on whether RSG has an appetite-stimulating effect in man at anti-hyperglycaemic doses and, therefore, I cannot draw any parallels with clinical experience here.

5.5. Conclusion

This experiment has shown that RSG improves the metabolic profile and insulin resistance in the DIO rat model, and has also demonstrated clear dose separation of these beneficial effects from the adverse effects of haemodilution and cardiac hypertrophy. Weight gain, whilst seemingly closely related to the FFA-lowering and insulin-sensitising effects of RSG in DIO rats, did not conspicuously attenuate the marked improvement in metabolic status observed here.

CHAPTER 6

Insulin-sensitising actions of high and low (therapeutic) doses of rosiglitazone in combination with food restriction: *Suggested mechanisms of TZD-induced weight gain*

6.1. Assessment of the effect of a high dose of rosiglitazone on insulin sensitivity: Insulin-sensitising action of rosiglitazone is enhanced by preventing hyperphagia

6.1.1. Introduction

The data in Chapter 5 show a clear dose-dependent improvement in insulin sensitivity in dietary obese (DIO) rats treated with the thiazolidinedione (TZD), rosiglitazone (RSG). Unfortunately, weight gain and hyperphagia are also shown to be dose-dependent, occurring even at the lowest dose utilised (0.3 mg/kg). As detailed in the General Introduction [1.6.5 (v) (a)], these side effects have been commonly observed in both humans and animals treated with TZDs, but although thought to have various causes, including changes to energy intake and expenditure, their exact mechanisms remain unclear.

Interestingly, the lowest dose of RSG tested in Chapter 5 also has the beneficial effect of significantly reducing plasma concentrations of free fatty acids (FFAs) [Table 5.1; Pickavance *et al.,* 1999b]. This action improves muscle insulin sensitivity by reducing substrate competition between glucose and FFAs for uptake into skeletal muscle [Randle *et al.,* 1963] and reducing intramuscular lipid content

[Oakes *et al.,* 1994, 1997]. It was of interest, therefore, to determine if the elevated fat mass blunts the improvement in insulin sensitivity seen with this class of drugs, and whether increased food intake and/or changes to thermogenesis contribute to TZD-induced weight gain.

Hence, the hypothesis tested in this chapter was that prevention of hyperphagia and weight gain in DIO rats would enhance the insulin-sensitising efficacy of RSG. The highest dose of RSG previously tested in DIO rats (30 mg/kg) [Chapter 5; Pickavance *et al.,* 1999b] was used to induce side effects against which changes would be clearly seen.

I also did some exploratory analysis of the potential contributions to TZD-related hyperphagia, body weight gain and insulin sensitivity of other central and peripheral mediators of energy homeostasis, the functions of which are described in the General Introduction [1.3.3 (i) (a), (ii) (a) (1), (iii)]. These were hypothalamic neuropeptide Y (NPY) and skeletal muscle uncoupling protein-3 (UCP-3) gene expression, the former peptide being the most potent orexigenic signal yet known, and the latter a recently discovered regulator of thermogenesis. In addition, plasma FFA and leptin concentrations, as well as *OB* mRNA levels, were measured because of their roles in fat storage feedback systems.

6.1.2. Methods

(i) Animals and treatment

Figure 6.1.1 shows the experimental design of this study. Thirty male Wistar rats were fed the highly palatable diet (HPD) used in Chapters 4 and 5 for 10 weeks to induce dietary obesity. A further thirty age-matched rats were fed normal rodent pelleted chow, [see General Methods, 2.1.2 (ii) (a) and 2.1.5 for diet compositions

and general maintenance details]. All rats were weighed weekly throughout this period, at the end of which HPD-fed rats had developed significant obesity. A third of this group were given vehicle (1% CMC administered at 1 ml/kg body weight; n=10/30), and the remaining two-thirds were given RSG (30 mg/kg; n=20/30) by gavage daily for 14 days. In turn, half of the drug-treated DIO group (n=10/20) were pair-fed to match the food intake of the untreated (vehicle) DIO controls. Three groups of chow-fed rats (n=10/group) were treated in the same way. Food intake and body weight were measured daily throughout the treatment period. Breeders, as well as suppliers of chemicals and pharmaceuticals are identified in General Methods [2.1.2 (ii) and 2.1.6-7].

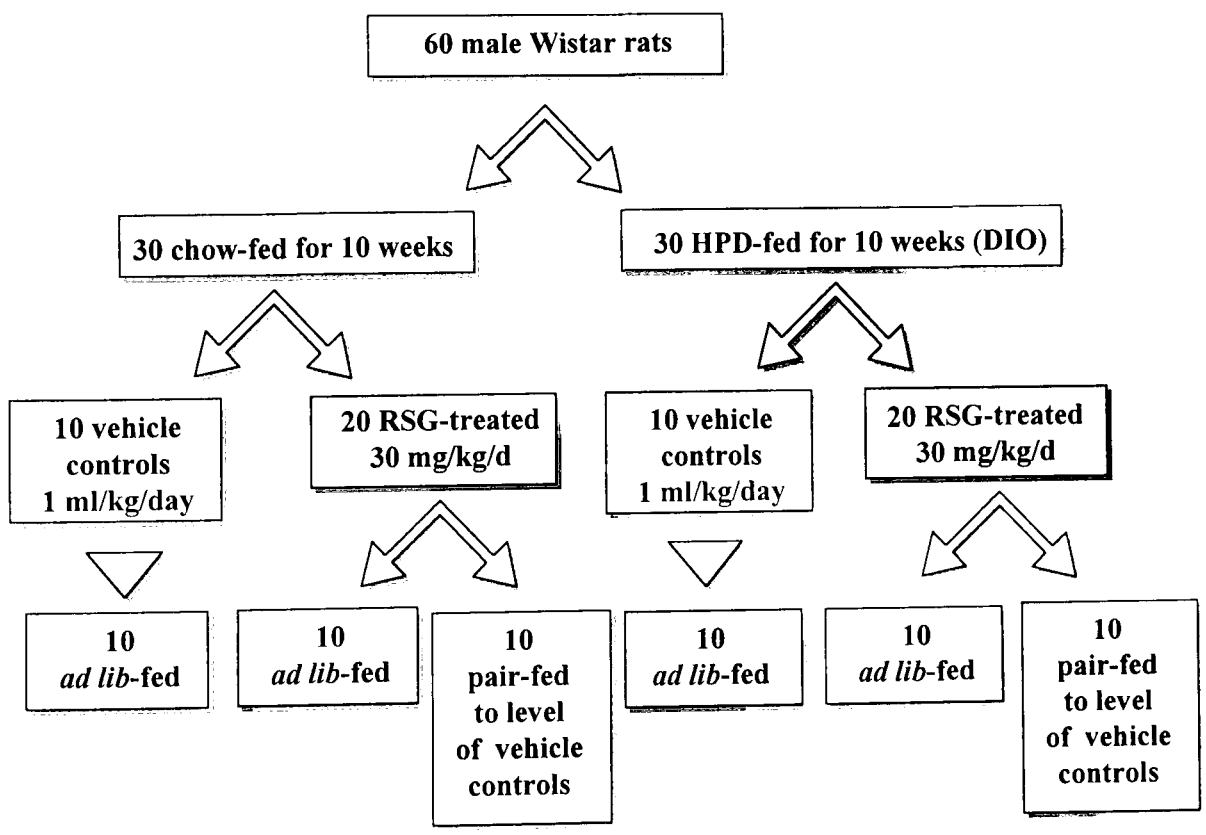

Figure 6.1.1. Experimental design for the study of high-dose RSG treatment of DIO rats. Weight gain and food intake were measured daily during treatment and RSG administered for 14 days. Animals were killed in the fasted state, trunk blood collected, and plasma concentrations of glucose, insulin, TGs, FFAs and leptin measured. Epididymal and perirenal fat pad masses were determined at termination.

(ii) Metabolic and molecular data

At the end of the 2-week treatment period, and after a 4-h fast, rats were killed by CO_2 inhalation and blood collected by cardiac puncture for later determination of plasma concentrations of glucose, FFAs, triglycerides (TGs), insulin and leptin [see General Methods, 2.2.1 (i) (c), (ii) (a-c) for commercial sources of diagnostic kits]. Insulin resistance was calculated as the HOMA index [see 2.2.3 (ii)]. Body fat content was estimated by weighing of dissected epididymal and perirenal fat pads, and these data are expressed as a percentage of terminal body weight. *OB* mRNA levels in epididymal fat were also determined. Gastrocnemius muscle was also dissected free, weighed, and snap-frozen in liquid nitrogen for later analysis of UCP-3 mRNA levels, and hypothalami were dissected from brains for measurement of NPY mRNA concentrations. All mRNA levels were measured by Northern blotting. Refer to General Methods [2.2.4] for a full description of the procedure and probes used.

(iii) Statistical analyses

Data are presented as mean ± SEM. The DIO and chow-fed (vehicle) controls were compared using unpaired *t*-tests. Results were considered statistically significant at the $p<0.05$ level. The effects of RSG treatment under both *ad lib*- and pair-fed conditions were studied separately for DIO and chow-fed rats. The significance of these effects was determined by 1-way ANOVA followed by Bonferroni *t*-tests, where critical p for 3 comparisons = 0.0167.

6.1.3. Results

(i) Dietary obesity

After 10 weeks on the palatable diet, DIO rats were 7.3% heavier than chow-fed controls (575 ± 10 *vs* 536 ± 7 g; $p<0.01$). By the end of the study, untreated (vehicle) DIO rats had greater epididymal (+65%) and perirenal (+102%) fat pad masses than untreated (vehicle) chow-fed rats (both $p<0.0001$). DIO controls also had higher plasma TG (+100%; $p<0.0001$), FFA (+78%; $p<0.05$) and leptin (+62%; $p<0.0001$) concentrations and were more insulin resistant than chow-fed controls (HOMA; $p<0.01$; Table 6.1.1).

(ii) Food intake and body weight

Ad lib-fed RSG-treated rats had higher energy intake than their respective untreated controls (chow-fed 21%; $p<0.0001$; DIO 26%; $p<0.0001$; Fig. 6.1.2A) and gained more weight. Indeed, body weight gain was greater in RSG-treated DIO rats even when food intake was matched to that of untreated DIO rats (RSG-treated, *ad lib*-fed *vs* untreated DIO rats: $p<0.0001$; RSG-treated, pair-fed *vs* untreated DIO rats: $p<0.05$; Fig. 6.1.2B). In the parallel chow-fed experiment, *ad lib*-fed, RSG-treated rats gained significant excess body weight [by 129% *vs* (vehicle) controls; $p<0.0001$], although RSG-treated, pair-fed rats did not (Fig. 6.1.2B). Fat pad mass was not altered by RSG treatment in DIO rats, but was slightly higher in RSG-treated, chow-fed rats compared to untreated controls, even when weight gain was prevented by pair-feeding (Table 6.1.1).

Table 6.1.1. Fat pad mass and terminal plasma concentrations of hormones and metabolites in DIO and chow-fed male Wistar rats after 14-day RSG administration (30 mg/kg).

Dose (mg/kg/d)	**Insulin** (pM)	**Glucose** (mM)	**HOMA**	**FFA** (mM)	**TG** (mM)	**Leptin** (ng/ml)	**Epididymal fat mass** (%)	**Perirenal fat mass** (%)
Palatable diet-fed (DIO)								
vehicle-treated, *ad lib*-fed	117±8	7.6±0.6	6.7±0.7	1.35±0.22	0.405±0.054	7.8±0.5	1.24±0.08	1.21±0.07
RSG-treated, pair-fed	59±6††	6.7±0.9	2.9±0.4†††	0.24±0.04†††	0.091±0.008†††	5.8±0.4††	1.28±0.10	1.07±0.09
RSG-treated, *ad lib*-fed	79±7††‡	7.4±0.8	4.2±0.5††‡	0.17±0.03†††	0.096±0.008†††	7.1±0.6	1.14±0.11	1.09±0.11
Chow-fed								
vehicle-treated, *ad lib*-fed	79±6**	6.8±0.4	3.9±0.3**	0.76±0.12*	0.197±0.021***	4.8±0.3**	0.75±0.04***	0.60±0.04***
RSG-treated, pair-fed	47±4††	6.2±0.5	2.2±0.2††	0.22±0.04†††	0.091±0.006†††	3.4±0.4††	0.73±0.03	0.74±0.08†
RSG-treated, *ad lib*-fed	68±6‡‡	6.4±0.6	3.2±0.3†‡	0.23±0.03†††	0.094±0.007†††	5.4±0.3‡‡	0.86±0.07	0.81±0.03††

Statistical significance of differences between chow-fed and DIO (vehicle) controls: *$p<0.05$; **$p<0.01$; ***$p<0.0001$; *vs* corresponding controls: $^{\dagger}p<0.05$, $^{\dagger\dagger}p<0.01$, $^{\dagger\dagger\dagger}p<0.0001$; between RSG-treated, pair-fed and corresponding *ad lib*-fed groups: $^{\ddagger}p<0.05$; $^{\ddagger\ddagger}p<0.01$. Data are expressed as mean ± SEM. Fat pad mass expressed as % of terminal body weight.

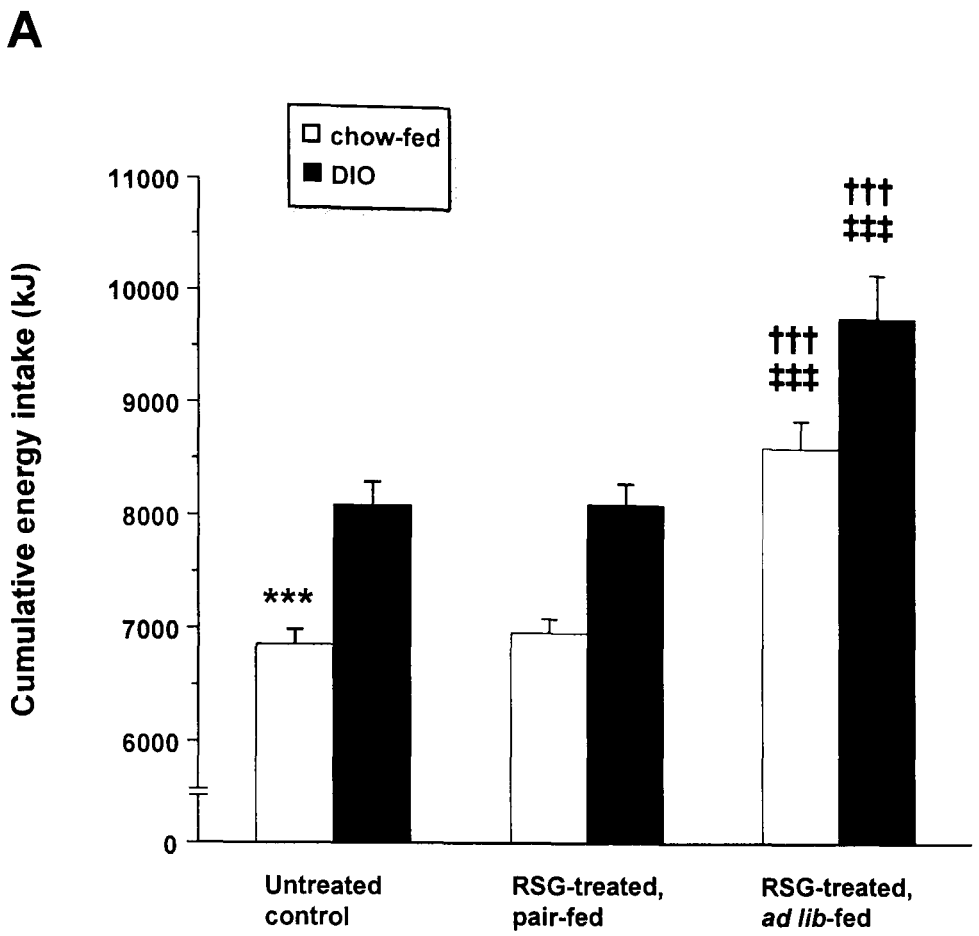

Figure 6.1.2. (A) Energy intake and (B) body weight gain in chow-fed and DIO (vehicle) control and *ad lib*- and pair-fed RSG-treated rats. Statistical significance of differences between DIO and chow-fed (vehicle) controls: $^{**}p<0.01$, $^{***}p<0.0001$; *vs* corresponding controls: $^{\dagger}p<0.05$, $^{\dagger\dagger\dagger}p<0.0001$; between RSG-treated, *ad lib*- and corresponding pair-fed: $^{\ddagger\ddagger}p<0.01$, $^{\ddagger\ddagger\ddagger}p<0.0001$.

(iii) Effects of RSG and food restriction on metabolic parameters

The mean plasma insulin concentration was significantly lower in RSG-treated DIO rats than in the DIO (vehicle) control group ($p<0.01$) and was similar to that seen in chow-fed (vehicle) controls. Pair-feeding reduced the mean plasma insulin concentration in RSG-treated DIO rats by a further 25% ($p<0.05$). Similarly, RSG treatment together with pair-feeding of chow-fed rats was also associated with lower plasma insulin than in their *ad lib*-fed, RSG-treated counterparts (Table 6.1.1). Glucose concentrations were not significantly altered by RSG administration or pair-feeding in any of the groups.

Incorporation of the glucose and insulin data into the HOMA model showed that, even without food restriction, RSG treatment improved insulin sensitivity in chow-fed rats by 18% ($p<0.05$) and was twice as effective in DIO rats, in which there was a 37% improvement ($p<0.01$; Table 6.1.1). Moreover, the enhancement of insulin sensitivity was greater still in those RSG-treated animals which were pair-fed, being 44% in chow-fed rats ($p<0.01$) and 57% in the DIO group ($p<0.0001$).

Fasting plasma FFA and TG concentrations were significantly lower in all RSG-treated rats, irrespective of the diet. Pair-feeding did not reduce TG and FFA concentrations any further in either DIO or chow-fed groups (Table 6.1.1).

(iv) Leptin and OB *mRNA levels*

In DIO (vehicle) control rats, the plasma leptin concentration was 62% higher than in chow-fed (vehicle) controls ($p<0.01$). RSG treatment alone lowered the mean plasma leptin concentration in DIO rats marginally (by 9%; $p=0.05$), an effect which was greatly enhanced by pair-feeding (26% lower; $p<0.05$; Table 6.1.1). In chow-fed rats, RSG treatment alone did not significantly influence the plasma leptin

concentration, but it was reduced by 29% in RSG-treated pair-fed rats ($p<0.01$: Table 6.1.1).

Levels of *OB* mRNA were more than twice as high in untreated (vehicle) DIO rats compared to untreated chow-fed controls ($p<0.01$). Furthermore, RSG-treated DIO rats had a 49% lower *OB* mRNA level and this was lower still in RSG pair-fed animals ($p<0.0001$). In contrast, neither RSG alone nor RSG in combination with pair-feeding significantly affected *OB* mRNA levels in chow-fed rats (Fig. 6.1.3A).

(v) NPY and UCP-3 mRNA levels

Although there was a trend towards increased NPY expression in the hypothalami of RSG-treated DIO rats, this was not statistically significant (DIO treated, *ad lib*-fed: $p=0.08$; DIO treated, pair-fed: $p=0.09$; both *vs* DIO untreated). Furthermore, there was no difference in NPY mRNA levels between DIO and chow-fed (vehicle) controls ($p>0.05$; Fig. 6.1.3B). Similarly, there were no differences in UCP-3 expression between any groups ($p>0.05$; Fig. 6.1.3C).

6.1.4. Discussion

The principal finding of this experiment is that prevention of hyperphagia by pair-feeding potentiates the insulin-sensitising effect of a high dose of RSG in DIO rats, validating the original hypothesis. However, the fact that plasma FFA concentrations were reduced no further by pair-feeding suggests that the additional improvement in insulin sensitivity produced by RSG under these circumstances is independent of circulating FFAs. This necessitates the search for other potential mechanism(s) responsible for this enhancement.

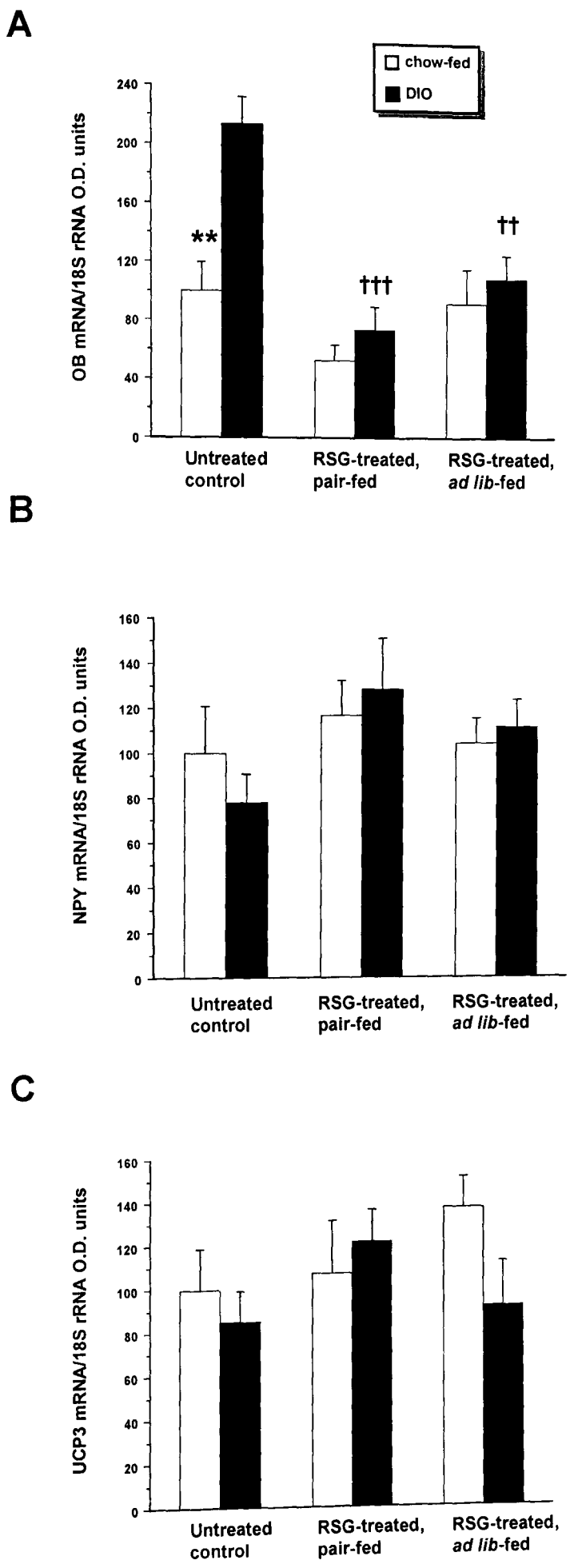

Figure 6.1.3. (A) *OB*, (B) NPY and (C) UCP-3 mRNA levels in chow-fed and DIO (vehicle) control and *ad lib*- and pair-fed RSG-treated rats. The ratio of mRNA to 18S rRNA O.D. units is expressed as a percentage of that of chow-fed controls (set to 100%). Statistical significance of differences between DIO and chow-fed (vehicle) controls: $^{**}p<0.01$; *vs* corresponding controls: $^{††}p<0.01$, $^{†††}p<0.0001$.

As observed in Chapter 5, RSG increased energy intake and body weight in both DIO and chow-fed rats [Pickavance *et al.,* 1999b]. A curious anomaly in the data here, however, and in contrast to those presented in Chapter 5, is that despite weight gain in treated DIO rats, and particularly those fed *ad lib*, epididymal and perirenal fat pad mass was not increased. This makes it difficult to answer the question posed in the introduction regarding whether or not the (expected) increase in fat mass would blunt the improved insulin sensitivity. Perhaps fat mass increased in other depots not studied here, suggesting regionalisation of fat storage in this animal model. Indeed, site-specific differentiation of pre-adipocytes by TZDs has been documented in human tissue *in vitro* [Adams *et al.,* 1997], and there is evidence of fat redistribution away from the omentum to a subcutaneous site in treated humans [Kawai *et al.,* 1999; Kelly *et al.,* 1999]. However, the fact that perirenal fat mass did increase significantly in *ad lib* chow-fed rats treated with RSG, with a similar trend in the epididymal fat pad, suggests that, at least in rats, diet itself may influence this process of regionalisation of fat storage.

A striking observation here was that although pair-feeding prevented weight gain by RSG treatment in chow-fed rats, this was only partially ameliorated in DIO rats, suggesting some impairment of energy expenditure in DIO, but not chow-fed rats. It may be that even in the absence of RSG treatment, DIO rats, because of their high caloric intake, have activated their thermogenic capacity to a maximum in order to limit their weight gain, leaving no scope to raise energy expenditure further to compensate for the adipogenic effects of RSG. By this same argument, it can be assumed that chow-fed rats possess adequate thermogenic reserve to prevent weight gain during RSG treatment, provided that food consumption is held constant. Indeed, stimulation of thermogenesis via activation of UCP-1 occurs in other forms

of dietary obesity, limiting weight gain [Rothwell & Stock, 1986]. However, in earlier studies, neither I, nor my colleagues, have found any change in brown adipose tissue (BAT) UCP-1 mRNA expression in response to RSG treatment in chow-fed rats or in dietary obesity [J. Harrold, L. Pickavance and P. Widdowson, unpublished observations]. Nonetheless, it is possible that other UCP isoforms are down-regulated directly or indirectly by RSG *in vivo* to account for the failure of pair-feeding to prevent drug-related weight gain in DIO rats. Indeed, RSG, like pioglitazone [Shimokawa *et al.,* 1998], is said to have an inhibitory action on UCP-3 expression in skeletal muscle, but, in fact, no differences in skeletal muscle UCP-3 mRNA levels were found here in response to the HPD or RSG treatment, with or without pair-feeding.

The observed fall in plasma leptin concentration in pair-fed RSG-treated DIO rats, on the other hand, points to a potential origin for reduced thermogenesis, an effect well-documented in the literature [Collins *et al.,* 1996; Hwa *et al.,* 1996; Levin *et al.,* 1996]. Hypoleptinaemia, however, was seen in both DIO rats and chow-fed rats treated with RSG in the pair-fed regimen, whilst weight gain only occurred in the DIO rats, thereby making this an unlikely mechanism. One other possible contributory mechanism to weight gain despite pair-feeding in DIO rats, is plasma volume expansion, as suggested by the observation of haemodilution in Chapter 5 [Pickavance *et al.,* 1999b].

I also investigated the mechanism by which leptin could have been controlling the hyperphagia induced by RSG. Here, RSG, with or without pair-feeding, exhibited marked inhibitory effects on adipose tissue *OB* mRNA in DIO rats, but not in chow-fed rats. This discrepancy may be related partly to the proportionally greater reduction in plasma insulin in the former, since insulin is a

potent inducer of the *OB* gene [Leroy *et al.*, 1996]. A supplementary factor, involving direct suppression of the *OB* gene by RSG [De Vos *et al.*, 1996; Kallen & Lazar, 1996] should be common to both models.

Whilst pair-feeding unmasked a marked fall in plasma leptin concentrations in both DIO and chow-fed rats treated with RSG, their *ad lib*-fed counterparts, in which hyperphagia was clearly manifest, exhibited plasma leptin levels which were not significantly reduced. Leptin influences the expression of a number of hypothalamic neurotransmitters, including NPY, an important regulator of energy intake as well as expenditure in rodents [Widdowson & Wilding, 1999]. Consistent with its lack of effect on plasma leptin in *ad lib*-fed rats, RSG did not influence hypothalamic NPY mRNA levels in either DIO or chow-fed rats. Therefore, the data presented here do not support a role for leptin in mediating the hyperphagia seen with RSG, and the lack of involvement of NPY is consistent with previous observations in lean and obese Zucker rats [Wang *et al.*, 1997]. Thus, obese Zucker rats are hyperphagic in response to RSG treatment, but their lack of an intact leptin receptor and resultant insensitivity to leptin as well as lack of dysregulation in the NPY system suggest that this side effect is independent of the leptin/NPY system. RSG must, therefore, be working via an alternative mechanism to increase appetite, which may itself be mediated by changes in circulating FFA levels. This other mechanism could, for example, involve antagonistic effects on α-MSH and, therefore, its activation of MC4-R, either directly or through stimulation of AGRP [see 1.3.3 (ii) (b) (1)].

The paradox of a markedly suppressed adipose *OB* gene expression together with a largely unchanged plasma leptin level in RSG-treated *ad lib*-fed DIO rats, can be reconciled by assuming an increase in total body fat mass in these animals, which

would be consistent with the body weight data, although not with the individual fat pad mass data.

Finally, the observation that hypothalamic NPY mRNA levels were not influenced by dietary regimen, is supported by earlier findings that a high-fat diet containing sucrose does not affect NPY mRNA either in the whole hypothalamus or specifically in the arcuate nucleus (ARC) [Kim *et al.*, 1998; Wilding *et al.*, 1992b]. Nonetheless, these workers also showed that feeding at 60% of *ad lib* intake does increase these levels, suggesting that NPY in the ARC responds to energy deficits rather than the hyperphagic stimulus related to food palatability.

6.1.5. Conclusion

Attenuation of weight gain induced by RSG administration through simultaneous prevention of excess caloric intake can improve insulin sensitivity, thereby offsetting responses potentially counterproductive to drug efficacy. This effect, however, appears to be independent of a fall in plasma FFAs. Nonetheless, when energy intake levels are matched between RSG-treated and untreated DIO rats, weight gain still occurs, although the mechanism of the implied reduction in energy expenditure which enables this remains unidentified. Although without direct evidence from the present study, it seems plausible that RSG's ability to lower both plasma FFAs and leptin, two potent thermogenic signals [Weigle *et al.*, 1998 for FFAs], impairs the ability of DIO rats to maintain constant body weight even though hyperphagia is prevented. It is possible that improved dietary control in type 2 diabetes may substantially augment the insulin-sensitising action of TZDs in humans.

6.2. *Assessment of the effect of a low dose of rosiglitazone on weight gain, insulin sensitivity and orexin expression*

6.2.1. *Introduction*

Because obesity can lead to hyperinsulinaemia [refer to General Introduction, 1.3.1 (i)-(ii), for discussion], in studying the effects of thiazolidinediones (TZDs) in dietary obesity, it is pertinent to know if TZD-related weight gain compromises the efficacy of these drugs at therapeutic doses. In Chapter 6.1, a two-week treatment of dietary obese (DIO) rats with a high dose (30 mg/kg/d) of rosiglitazone (RSG) resulted in significant weight gain, which persisted to some degree even when increased energy intake was restricted to DIO control levels. However, this dosing regime also improved insulin sensitivity, and prevention of the RSG-induced hyperphagia improved it further. Thus, the aim of the experiment described in the current chapter was to establish whether or not this effect was also relevant at a therapeutic dose at which weight gain would be less. If this were the case, then advice to maintain pre-treatment food intake would improve the efficacy of the drug in clinical use. This hypothesis could, therefore, be appropriately tested in the insulin-resistant rat model of dietary obesity used throughout most of this thesis.

The second part of this experiment involved the study of the effect of RSG treatment on orexin expression in dietary obesity. As described in the General Introduction [1.3.3 (ii) (a) (2)], orexins are recently discovered peptides expressed in hypothalamic areas involved in food intake and energy balance. It has been suggested that TZD treatment is associated with altered expression of prepro-orexin, the peptide precursor of the orexins, in the hypothalamus of the Zucker rat,

a genetic mutant model of insulin resistance [see 1.5.1 (i) (a) and 2.1.2 (i) (a) for a further description of this model]. This may be because improved insulin sensitivity with TZD treatment results in restoration of function of glucose-sensitive neurons in the lateral hypothalamic area (LHA) [Cai *et al.*, 2000], the region of orexin synthesis [for review, see Williams *et al.*, 2000]. Thus, while addressing the above question regarding the restriction of food intake during TZD treatment, the opportunity was taken to investigate prepro-orexin expression in the hypothalamus of the TZD-treated DIO (non-mutant) model of insulin resistance. Results from the pair-fed group of animals would provide some insight into the combined effect of manipulating energy intake with TZD treatment on orexin expression.

6.2.2. Methods

(i) Animals and treatment

Figure 6.2.1 shows the experimental design of this study. Exactly as described in Chapter 6.1, thirty male Wistar rats were fed the highly palatable diet (HPD) for 10 weeks to induce obesity; in this study, they were compared with ten chow-fed controls. The General Methods chapter [2.1.2 (ii) and 2.1.5] gives further detail on diet compositions, animal suppliers and animal maintenance. Rats were weighed weekly, and at the end of this period HPD-fed rats were significantly heavier than chow-fed controls. These formed the DIO group. As in the high-dose experiment (Chapter 6.1), a third of this group were given vehicle (1% CMC administered at 1 ml/kg body weight; n=10/30), and the remaining two-thirds (n=20/30) were given RSG, this time at the previously determined therapeutic dose of 3 mg/kg (see Chapter 5) by gavage daily for 14 days. In turn, half of the drug-treated DIO group

(n=10/20) were pair-fed to the food intake of the untreated (vehicle) DIO controls. Food intake and body weight were monitored daily. Chemical and pharmaceutical suppliers are identified in General Methods [2.1.6-7].

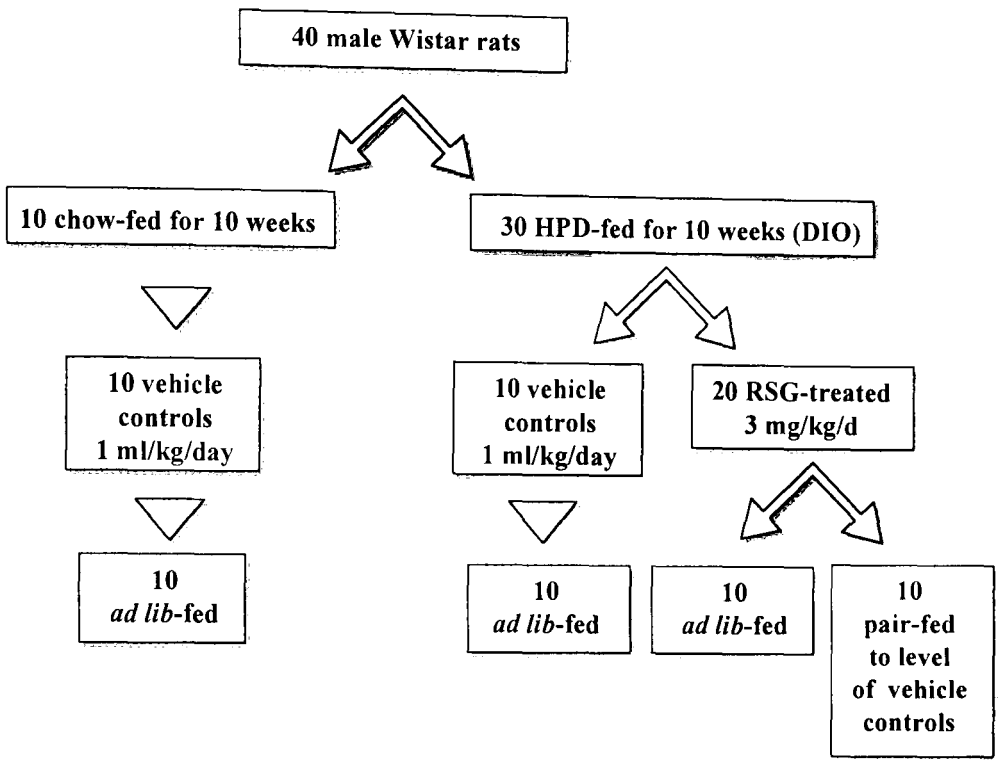

Figure 6.2.1. Experimental design for the study of low (therapeutic)-dose RSG treatment of DIO rats. Weight gain and food intake were measured daily during treatment and RSG administered for 14 days. Animals were killed in the fasted state, trunk blood collected, and plasma concentrations of glucose, insulin, TGs, FFAs and leptin measured. Epididymal and perirenal fat pad masses were determined at termination.

(ii) Metabolic and molecular data

At the end of the 2-week treatment period, and after a 4-h fast, rats were killed by CO_2 inhalation and blood collected by cardiac puncture for later determination of plasma concentrations of glucose, FFAs, triglycerides (TGs), insulin and leptin [see General Methods 2.2.1 (i) (c), (ii) (a-c) for commercial sources of diagnostic kits]. Insulin resistance was calculated as the HOMA index [see 2.2.3 (ii)]. Body fat content was estimated by weighing of dissected epididymal and perirenal fat pads and expressed as a percentage of final body weight. Orexin mRNA concentrations in

dissected hypothalami were also measured by Northern hybridisation. General Methods [2.2.4] details the procedure and probe used.

(iii) Statistical analyses

Data are presented as mean ± SEM. The DIO and chow-fed (vehicle) controls were compared using unpaired *t*-tests. Results were considered statistically significant at the $p<0.05$ level. The significance of the effects of RSG treatment under both *ad lib*- and pair-fed conditions in the DIO group were determined by 1-way ANOVA followed by Bonferroni *t*-tests, where critical *p* for 3 comparisons = 0.0167.

6.2.3. Results

(i) Dietary obesity

After 10 weeks on the HPD, DIO rats were 12% heavier than chow-fed controls (586 ± 10 *vs* 523 ± 14 g; $p<0.01$). By the end of the study, untreated (vehicle) DIO rats had greater epididymal (+42%) and perirenal (+68%) fat pad masses than untreated (vehicle) chow-fed rats ($p<0.05$ and $p<0.0001$, respectively). DIO untreated controls also had higher plasma leptin (+65%; $p<0.01$) and TG (+85%; $p<0.01$) but not FFA (+28%; $p>0.05$) concentrations. DIO controls tended to be more insulin-resistant than chow-fed controls, but this was not quite significant (+35% HOMA; $p=0.06$). They were, however, hyperinsulinaemic (+39%; $p<0.05$; Table 6.2.1).

(ii) Food intake and body weight

Ad lib-fed RSG-treated rats had higher energy intake than their untreated (vehicle) counterparts (+22%; $p<0.0001$; Fig. 6.2.2A) and gained more weight (+88%; $p<0.0001$; Fig. 6.2.2B). Body weight gain in RSG-treated, pair-fed DIO rats,

Table 6.2.1. Fat pad mass and terminal plasma concentrations of hormones and metabolites in DIO and chow-fed male Wistar rats after 14-day administration of RSG (3 mg/kg).

Dose (mg/kg/d)	**Insulin** (pM)	**Glucose** (mM)	**HOMA**	**FFA** (mM)	**TG** (mM)	**Leptin** (ng/ml)	**Epididymal fat mass** (%)	**Perirenal fat mass** (%)
Palatable diet-fed (DIO)								
vehicle-treated, *ad lib*-fed	118±11	6.7±0.2	5.8±0.5	0.87±0.06	0.48±0.04	7.1±0.3	1.38±0.11	1.31±0.06
RSG-treated, pair-fed	68±6†††	6.5±0.3	3.3±0.4†††	0.45±0.04†††	0.13±0.01†††	4.8±0.6††	1.50±0.10	1.36±0.07
RSG-treated, *ad lib*-fed	84±3††	6.6±0.1	4.1±0.2††	0.47±0.03†††	0.18±0.01†††	6.1±0.3 (p=0.06 *vs* vehicle; p=0.02 *vs* pair-fed)	1.45±0.09	1.29±0.09
Chow-fed								
vehicle-treated, *ad lib*-fed	85±2*	6.7±0.2	4.3±0.5 (p=0.056)	0.68±0.11	0.26±0.05**	4.3±0.5**	0.97±0.10*	0.78±0.08***

Statistical significance of differences between chow-fed and DIO vehicle controls: *p<0.05; **p<0.01; ***p<0.0001; *vs* corresponding controls: $^{\dagger\dagger}p$<0.01; $^{\dagger\dagger\dagger}p$<0.0001. Data are expressed as mean ± SEM. Fat pad mass expressed as % of terminal body weight.

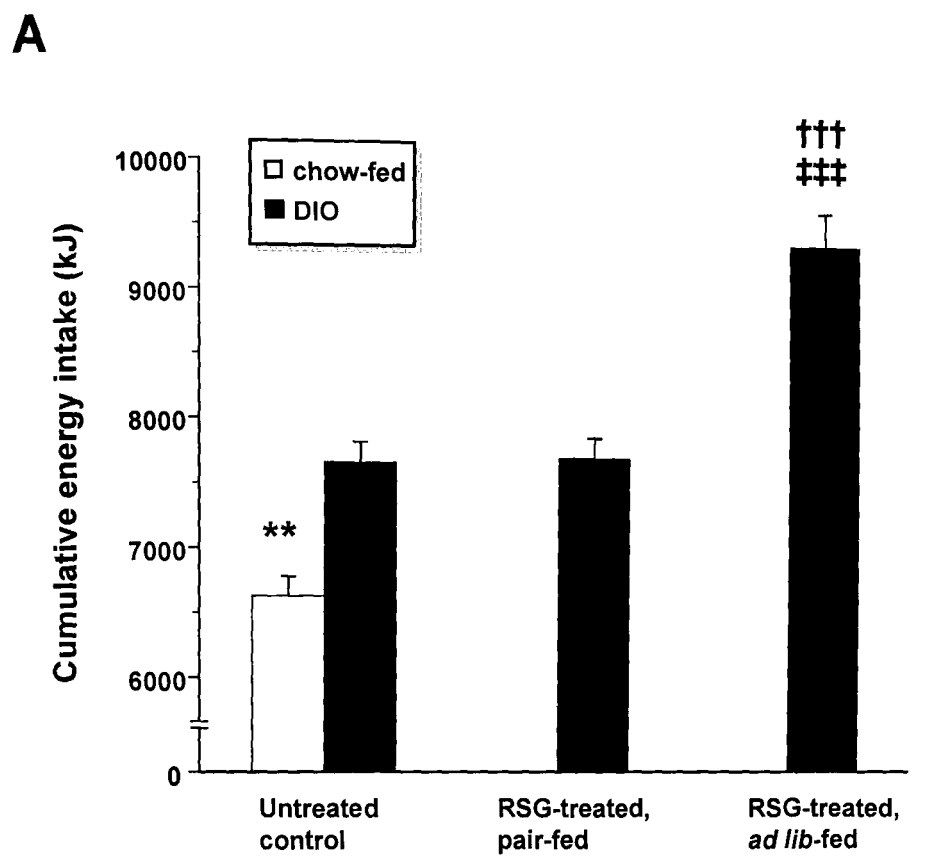

Figure 6.2.2. (A) Food intake and (B) body weight gain in chow-fed and DIO (vehicle) control and in DIO *ad lib*- and pair-fed RSG-treated rats. Statistical significance of differences between DIO and chow-fed (vehicle) controls: $^{**}p<0.01$; *vs* corresponding controls: $^{\dagger\dagger\dagger}p<0.0001$; between RSG-treated *ad lib*- and corresponding pair-fed: $^{\ddagger\ddagger\ddagger}p<0.0001$.

however, was equal with that of untreated (vehicle) counterparts (p>0.05; Fig. 6.2.2B). Fat pad mass was not altered by RSG treatment in DIO rats (p>0.05; Table 6.2.1).

(iii) Effects of RSG and food restriction on metabolic parameters

The mean plasma insulin concentration was significantly lower in RSG-treated DIO rats than in the DIO (vehicle) control group (29% fall; p<0.01) and was normalised to chow-fed control concentrations. Pair-feeding reduced the mean plasma insulin concentration in RSG-treated rats by a further 13% (p<0.05). Glucose concentrations were not significantly altered by RSG administration or pair-feeding.

Incorporation of the glucose and insulin data into the HOMA model showed that, even without food restriction, RSG treatment improved insulin sensitivity in DIO rats, in which there was a 29% improvement (p<0.01; Table 6.2.1). Moreover, the enhancement of insulin sensitivity was greater still in those RSG-treated animals which were pair-fed (+43%; p<0.0001).

Fasting plasma FFA and TG concentrations were significantly lower in RSG-treated rats (falls of 46% and 62%, respectively; both p<0.0001). Pair-feeding did not reduce TG and FFA levels any further (Table 6.2.1). RSG treatment alone lowered the mean plasma leptin concentration but not quite significantly (by 14%; p=0.06), an effect which was greatly enhanced by pair-feeding (32% lower; p<0.01; Table 6.2.1).

(iv) Orexin mRNA levels

Neither exposure to the HPD alone, nor RSG treatment with or without pair-feeding had any effect on orexin expression in the hypothalami of DIO rats ($p>0.05$; Fig. 6.2.3).

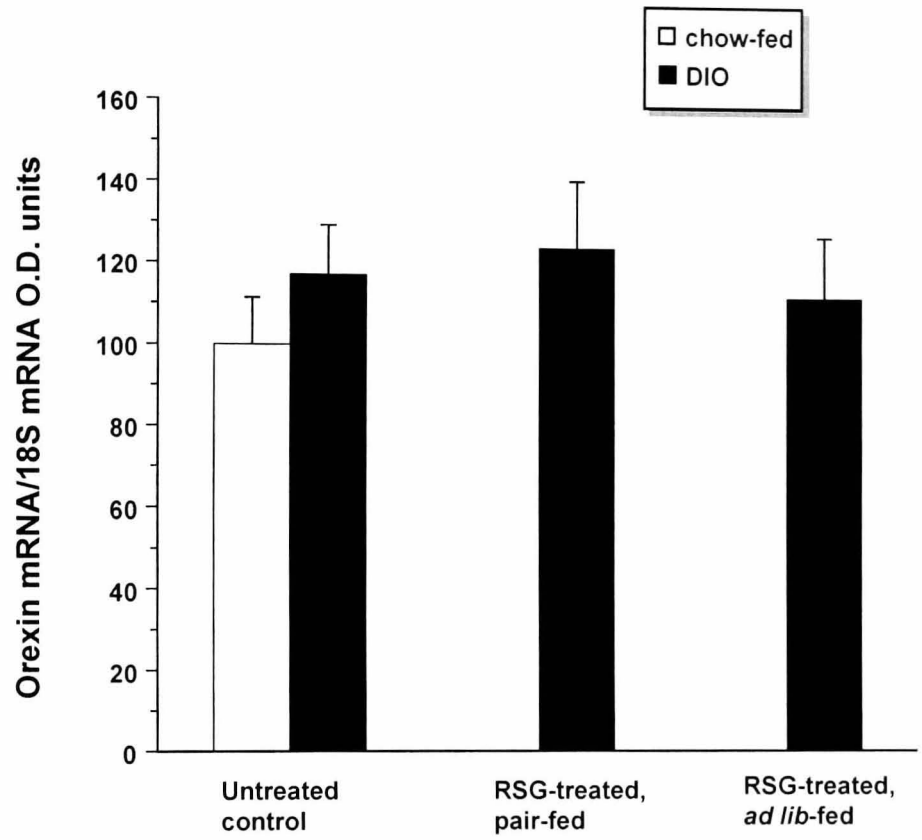

Figure 6.2.3. Orexin mRNA levels in chow-fed and DIO (vehicle) control and in DIO *ad lib*- and pair-fed RSG-treated rats. The ratio of mRNA to 18S rRNA O.D. units is expressed as a percentage of that of chow-fed controls (set to 100%). There were no statistical differences between any of the groups ($p>0.05$).

6.2.4. Discussion

The principal finding of Chapter 6.1 was that prevention of hyperphagia by pair-feeding potentiates the insulin-sensitising effect of a high dose of RSG in DIO rats. It can now be said that this is also the case with a 10-fold lower therapeutic dose of RSG. Similarly, plasma FFA concentrations reduced by this dose were reduced no

further by pair-feeding, again suggesting that the additional improvement in insulin sensitivity produced by RSG is independent of circulating FFAs.

RSG at the therapeutic dose increased energy intake and body weight in DIO rats, confirming the observations of Chapter 5 [Pickavance *et al.,* 1999b]. Despite weight gain in treated DIO rats, and particularly in those fed *ad lib*, epididymal and perirenal fat pad mass was not increased. This curious anomaly, which contrasts with data in Chapter 5, was also observed at the high dose (Chapter 6.1). The consistency of this observation underscores the difficulty in determinng whether or not the (expected) increase in fat mass caused by TZDs compromises the improvement in insulin sensitivity. As proposed previously, fat mass may have increased in other depots not looked at here [Chapter 6.1; Adams *et al.,* 1997; Kawai *et al.,* 1999; Kelly *et al.,* 1999].

The other notable observation of the high-dose study was that pair-feeding only partially prevented weight gain in RSG-treated DIO rats, suggesting impaired thermogenic capacity in this model. Clearly, this potential inadequacy is not a relevant issue at the therapeutic dose.

The data presented here confirm the high-dose data dismissing a role for leptin in mediating RSG-induced hyperphagia, as circulating leptin concentrations were unchanged in *ad lib*-fed rats, compared to those in DIO controls. This is also consistent with the lack of effect of RSG on orexin expression, suggested to reflect an animal's nutritional status [for review, see Sakurai, 1999], as does leptin [Widdowson & Wilding, 1999]. It is in contrast, however, to the findings of Cai *et al.* [2000], that orexin expression is altered by TZDs in the Zucker rat, suggesting a fundamental difference between the genetic and DIO models of insulin resistance. On the other hand, this result does agree with the lack of change in NPY mRNA

expression, also thought to regulate feeding behaviour, in response to RSG treatment in DIO [Chapter 6.1] and Zucker rats [Wang *et al.*, 1997].

6.2.5. Conclusion

These results suggest that TZD-related weight gain does not compromise the efficacy of these drugs at therapeutic doses and that in the clinical environment, patients' insulin sensitivity could be improved by their not exceeding their original level of food intake, although this may be difficult to achieve in practice. Attenuation of weight gain, even the lesser degree induced by a therapeutic dose of RSG, through simultaneous prevention of excess food intake, remains a relevant issue and worthwhile intervention, enhancing insulin sensitivity and protecting drug efficacy.

CHAPTER 7

Dose-response comparisons of three thiazolidinediones: *Rosiglitazone, pioglitazone and troglitazone treatment of insulin resistance in the diet-induced obese rat*

7.1. Introduction

As reviewed in the General Introduction [1.6.5 (i)], members of the thiazolidinedione (TZD) chemical class include rosiglitazone (RSG), pioglitazone (PIO) and troglitazone (TRO) [Henry, 1997; Kaneko, 1997; Nolan *et al.*, 1994; Saltiel & Horikoshi, 1995; Saltiel & Olefsky, 1996; Whitcomb & Saltiel, 1995]. RSG (Avandia®), the most potent of the TZDs, and PIO (ACTOS®) are currently licensed for human use in the U.S.A. and Europe. TRO (Rezulin®) has been recently withdrawn worldwide because liver failure is a rare complication of its use in humans [Shibuya *et al.*, 1998; Watkins & Whitcomb, 1998]. The properties of RSG, PIO and TRO are described in the General Introduction [1.6.5 (i)-(ii)] and their structures shown in Fig. 1.9. In brief, both RSG and TRO have been shown to attenuate overt diabetic symptoms, such as hyperglycaemia, in young ZDF rats [Smith *et al.*, 1997; Sreenan *et al.*, 1996] and both TRO and PIO lower blood pressure in *in vitro* preparations [Buchanan *et al.*, 1995; Walsh *et al.*, 1996], but a three-way comparison of the therapeutic efficacies of these three drugs in a single *in vivo* rodent model of insulin resistance, such as the dietary obese (DIO) model, has not been reported.

Firstly, a clear assessment of the dose-response relationships of these three TZDs was required. It was of particular interest to determine which of the three would have the widest separation between a therapeutic dose that improves insulin resistance and a dose which induces the side effects of haemodilution and cardiac hypertrophy. Haemodilution, which occurs as a result of plasma volume expansion and has the potential outcome of cardiac hypertrophy, is a common result of TZD treatment [Cantello *et al.*, 1994; Ghazzi *et al.*, 1997; Patel *et al.*, 1998].

The less serious side effects of weight gain and hyperphagia are also observed with TZDs in humans [Patel *et al.,* 1999] and animals [Arakawa *et al.*, 1998; de Souza *et al.*, 1995; Hirshman *et al.*, 1995; Ikeda *et al.*, 1990; Inoue *et al.*, 1995; Pickavance *et al.*, 1998a, 1999a,b, 2000; Shimizu *et al.*, 1998; Yoshioka *et al.*, 1993; Zhang *et al.*, 1996]. It was of interest to see how the drugs would differ in their liability for inducing weight gain and increased food intake at doses appropriate for improving insulin sensitivity.

7.2. Methods

7.2.1. Animals and treatment

Figure 7.1 shows the design of the three dose-response experiments. Suppliers of animals, drugs and chemicals are identified in General Methods [2.1.2 (ii), 2.1.6-7]. In the case of each of the three drugs, sixty female Wistar rats (172-178 g) were fed the highly palatable diet (HPD) for 8 weeks to induce mild obesity, and 10 age-matched controls were fed chow, the respective energy compositions of which are given in General Methods [2.1.2 (ii) (a)]. This section also outlines how female rats were used because the bioavailability of troglitazone is low in males.

At the end of the 8-week period, when HPD-treated rats had significantly increased body weight compared to controls, vehicle or drug was given daily by gavage for 21 days (10 rats/dose group). Vehicle for the RSG and PIO experiments was 1% CMC given at 1 ml/kg. Vehicle for the TRO experiment was the excipient of the drug given at 100 mg/kg. The three drugs were given in pharmacologically equipotent doses: RSG at 0.3, 1, 3, 10 or 30 mg/kg, PIO at 1, 3, 10, 30 or 100 mg/kg and TRO at 10, 30, 100, 300 or 1000 mg/kg. As TRO is better absorbed with food, it was administered just prior to the dark phase when rats consume the most. The doses of TRO required meant that it had to be administered in 10 times the volume of RSG and PIO [refer to General Methods, 2.1.7, for more details]. Food intake and body weight were measured daily throughout the treatment period.

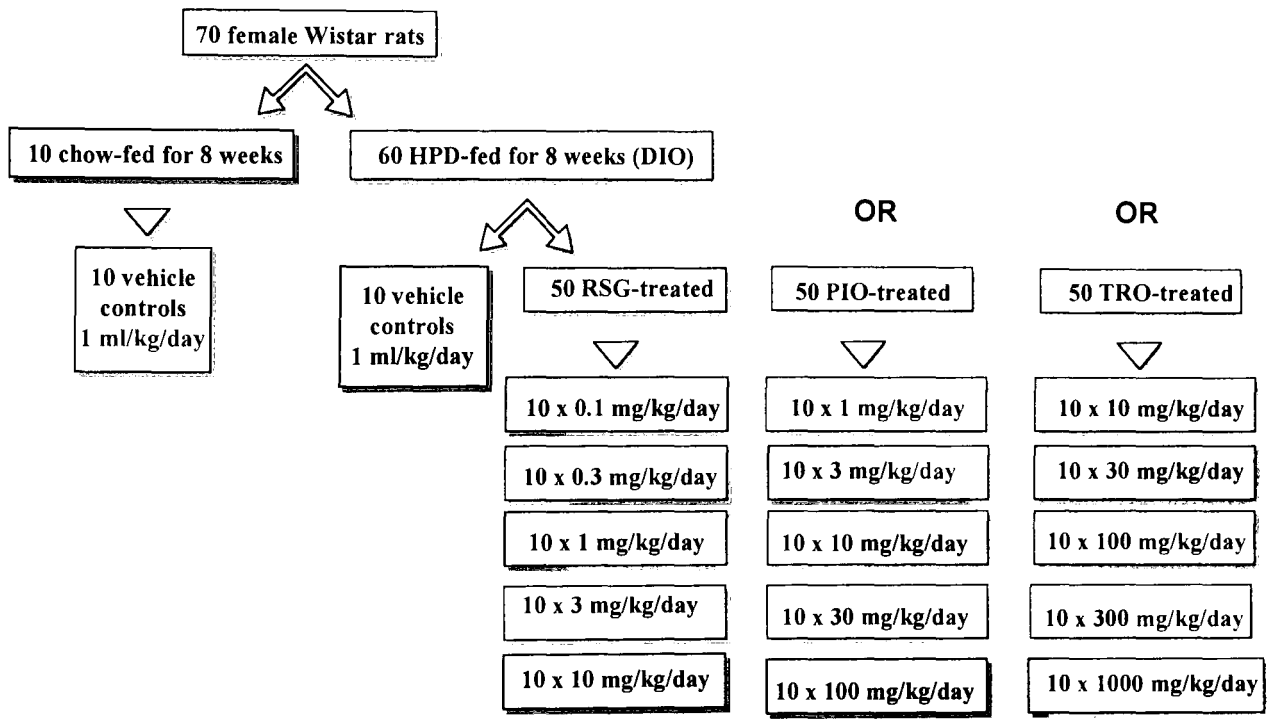

Figure 7.1. Experimental design for the study of (A) RSG, (B) PIO, and (C) TRO dose-responses in female DIO rats. Weight gain and food intake were measured daily during treatment and drugs administered for 21 days. Animals were killed in the fasted state, trunk blood collected, and plasma concentrations of glucose, insulin, TGs and FFAs and leptin measured. Heart mass, PCV, gonadal and perirenal fat pad masses were determined at termination.

7.2.2. Metabolic data and tissue mass

As described in Chapters 5 and 6, rats were killed by CO_2 inhalation after a 4-hour fast. Blood was collected by cardiac puncture and plasma assayed for insulin and leptin concentrations by RIA, and for glucose, FFA and TG concentrations by diagnostic kit [see 2.2.1 (i) (c), (ii) (a-c)]. HOMA was derived from insulin and glucose concentrations [see 2.2.3 (ii)]. PCV was also measured in all rats, and hearts were weighed to determine degree of cardiac hypertrophy. Body fat content was estimated by dissection and weighing of gonadal (parametrial) and perirenal fat pads and expressed as a percentage of total body weight.

7.2.3. Statistical analyses

Data are expressed as mean ± SEM. Differences between DIO untreated and chow-fed controls were compared using unpaired *t*-tests. The effect of dose upon each of the parameters studied was determined by 1-way ANOVA followed by Bonferroni *t*-tests, as described in Chapter 5.

7.3. Results

7.3.1. Dietary obesity

In each dose-response experiment, the groups destined to be fed HPD or chow were of similar body weight at baseline (RSG: 175 ± 1 *vs* 171 ± 1 g; PIO: 178 ± 1 *vs* 181 ± 1 g; TRO: 172 ± 1 *vs* 175 ± 2 g; all $p>0.05$). After 8 weeks of HPD consumption prior to drug treatment, rats developed mild obesity, becoming 9-15% heavier than chow-fed rats (RSG: 273 ± 3 *vs* 236 ± 4 g; PIO: 275 ± 3 *vs* 251 ± 3 g; TRO: 266 ± 2 *vs* 243 ± 3 g; all $p<0.01$).

At termination, DIO (vehicle) control rats in the RSG experiment were 18% heavier than chow-fed counterparts (290 ± 12 g *vs* 246 ± 4 g; $p<0.01$). Those in the PIO experiment were 8% heavier, which bordered on significance (285 ± 12 g *vs* 263 ± 2 g; $p=0.08$). Similarly, those in the TRO experiment were 8% heavier, also a non-significant difference (271 ± 12 g *vs* 250 ± 2 g; $p=0.1$). DIO controls in the RSG experiment correspondingly had greater absolute perirenal and gonadal fat masses than their chow-fed counterparts (perirenal: 5.03 ± 1.00 *vs* 1.40 ± 0.13 g; gonadal: 1.58 ± 0.38 *vs* 0.42 ± 0.05 g; both $p<0.01$). Those in the PIO experiment had greater absolute perirenal fat mass than chow-fed controls (4.31 ± 0.73 *vs* 2.13 ± 0.16 g; $p<0.01$), and their gonadal fat masses tended toward a significant increase (1.56 ± 0.31 *vs* 0.89 ± 0.16 g; $p=0.06$). In the TRO experiment, DIO controls showed a significant increase in both absolute fat pad masses over those of the chow-fed controls (perirenal: 3.64 ± 0.49 *vs* 1.84 ± 0.17 g; gonadal: 1.35 ± 0.19 *vs* 0.67 ± 0.06 g; both $p<0.01$).

Only in the RSG experiment did exposure to the HPD significantly increase insulin resistance [DIO (vehicle) *vs* chow-fed (vehicle) control: 51% increase in HOMA; $p<0.05$; Fig. 7.2A and Table 7.1). In both the PIO and TRO experiments, insulin resistance was increased to the same degree, about half as much as in the RSG cohort (both +24%), but not significantly ($p=0.06$ and 0.1, respectively; Figs. 7.3A, 7.4A and Tables 7.2, 7.3).

Changes in lipid metabolism were also apparent in the DIO (vehicle) controls of the RSG experiment. They showed 46% higher plasma FFA, 73% higher TG (both $p<0.01$) and nearly three-fold higher plasma leptin concentrations than chow-fed (vehicle) controls ($p<0.0001$; Table 7.1). Despite identical concentrations of

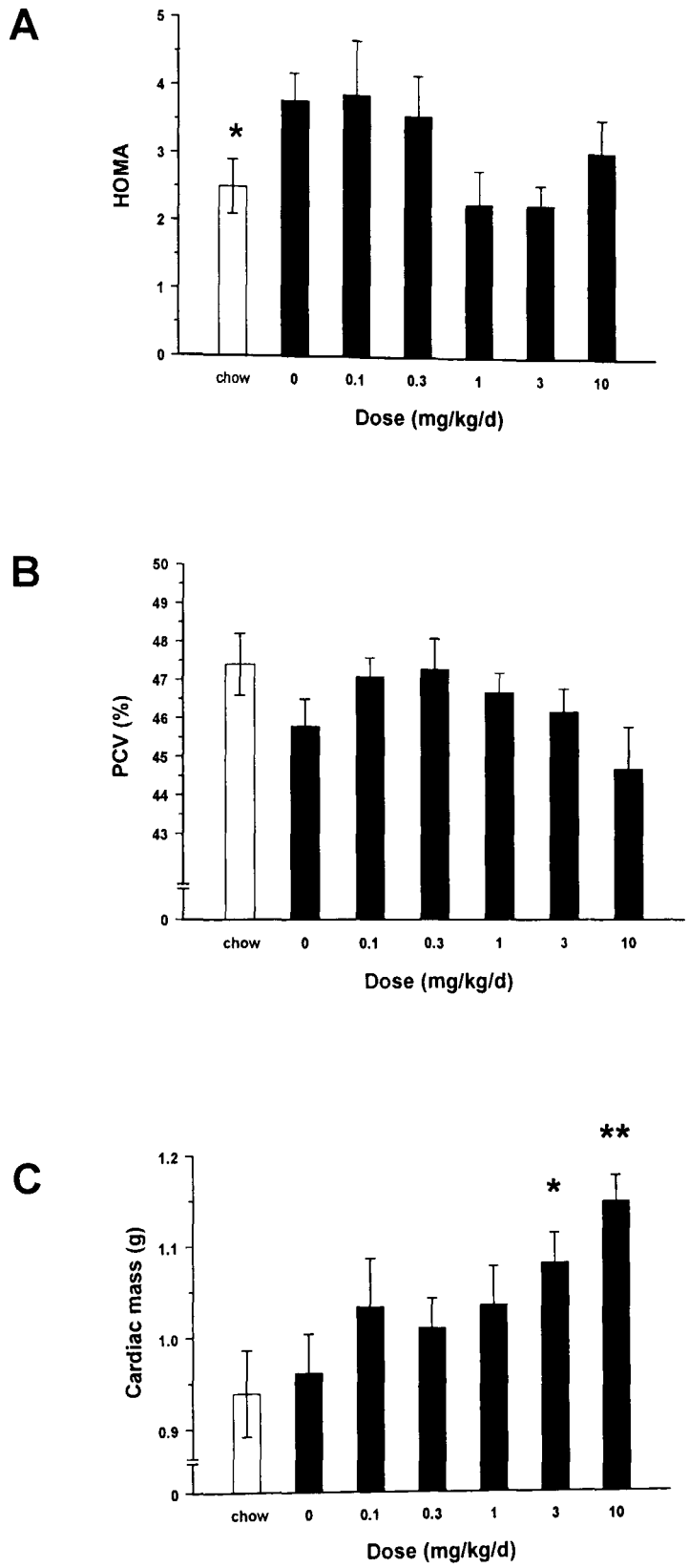

Figure 7.2. (A) Final HOMA values, (B) PCV and (C) cardiac mass in chow-fed, treated (vehicle) controls (chow) and DIO rats treated with RSG at various doses for 3 weeks (n=10/dose group). Unpaired t-tests on HOMA values showed that untreated DIO rats were more insulin-resistant than chow-fed counterparts. ANOVA followed by Bonferroni t-tests in the DIO group showed that RSG treatment increased cardiac mass at 3 mg/kg and above (panel C; *p<0.05; **p<0.01).

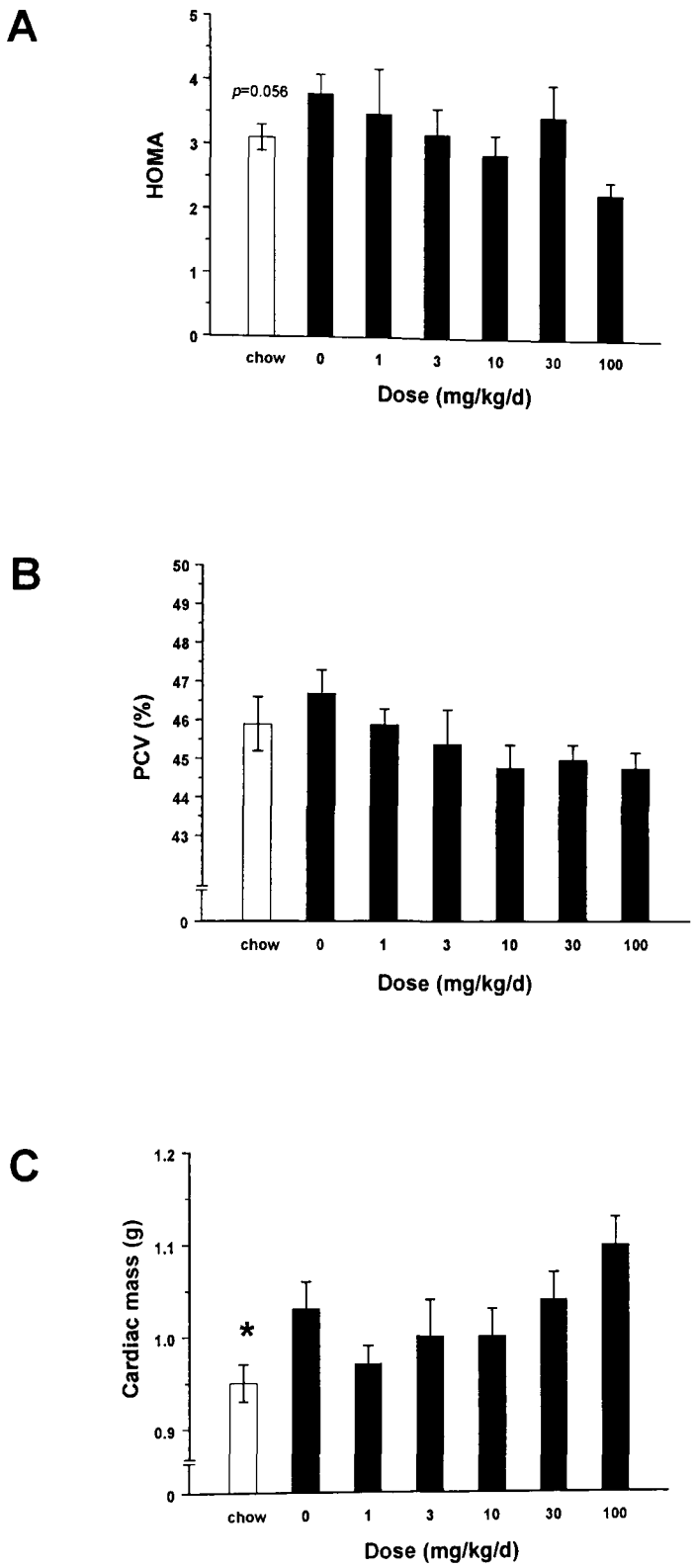

Figure 7.3. (A) Final HOMA values, (B) PCV and (C) cardiac mass in chow-fed, untreated (vehicle) controls (chow) and DIO rats treated with PIO at various doses for 3 weeks (n=10/dose group). Unpaired t-tests showed that untreated DIO rats had significantly higher heart mass than chow-fed counterparts. ANOVA followed by Bonferroni t-tests in the DIO group showed that PIO treatment induced no significant changes in insulin sensitivity as measured by HOMA and no significant haemodynamic side effects (panels B and C; *p<0.05).

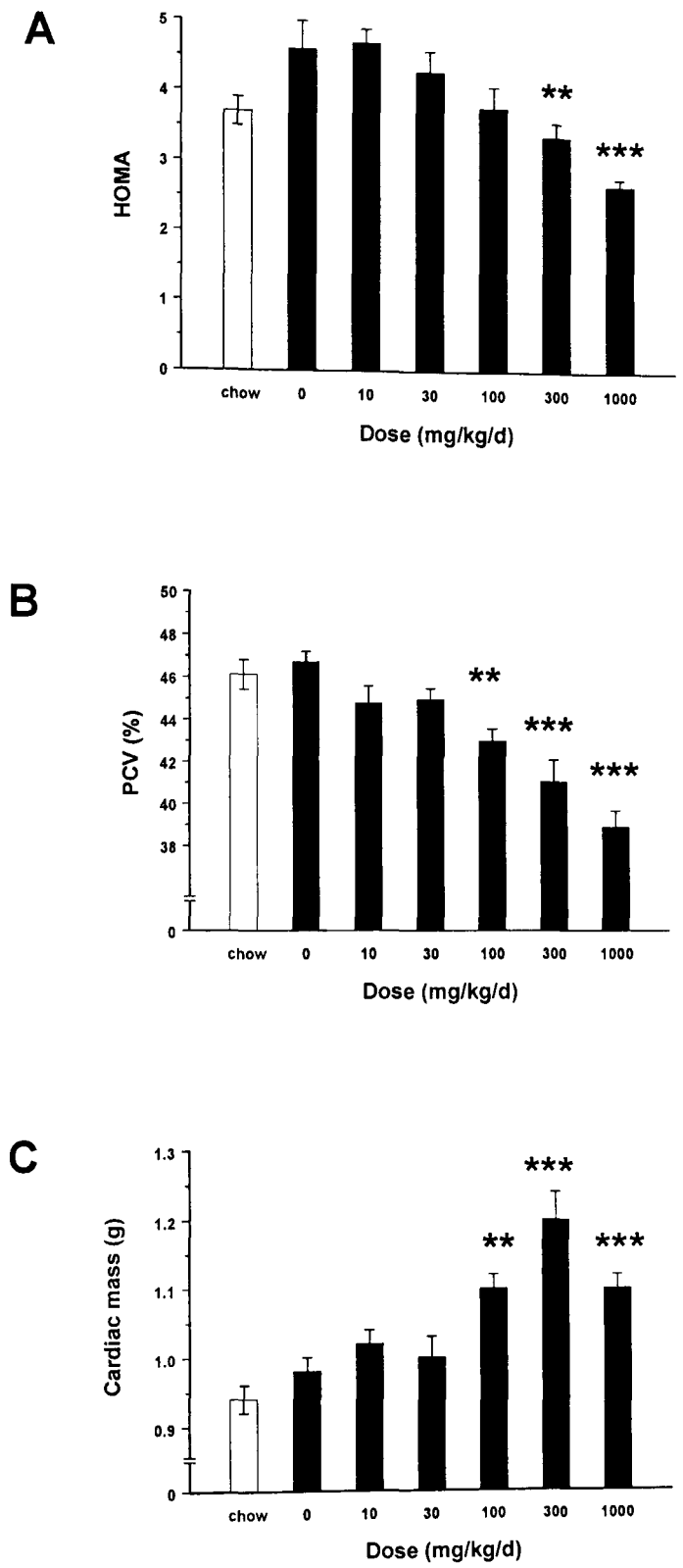

Figure 7.4. (A) Final HOMA values, (B) PCV and (C) cardiac mass in chow-fed, untreated controls (chow) and DIO rats treated with TRO at various doses for 3 weeks (n=10/dose group). There were no significant differences between untreated chow-fed and DIO rats. ANOVA followed by Bonferroni t-tests in the DIO group showed that TRO treatment induced significant haemodynamic side effects (panels B and C) at 100 mg/kg and above (**p<0.01; ***p<0.0001).

Table 7.1. Effects of 21-day administration of RSG on terminal fat pad masses and plasma concentrations of hormones and metabolites in DIO and chow-fed female Wistar rats.

Dose (mg/kg/d)	**Insulin** (pM)	**Glucose** (mM)	**HOMA**	**FFA** (mM)	**TG** (mM)	**Leptin** (ng/ml)	**Gonadal fat mass** (%)	**Perirenal fat mass** (%)
Palatable diet-fed (DIO)								
0	64±5	7.9±0.5	3.8±0.4	0.83±0.09	0.26±0.04	4.0±0.6	0.53±0.10	1.62±0.25
0.1	66±12	7.8±0.7	3.9±0.8	0.64±0.08*	0.21±0.02*	4.3±0.5	0.68±0.13	1.67±0.18
0.3	54±8	8.8±0.7	3.6±0.6	0.56±0.06**	0.18±0.02**	3.6±0.4	0.71±0.12	1.51±0.18
1	46±8	7.4±0.6	2.3±0.5	0.41±0.05***	0.14±0.01***	3.8±0.4	0.50±0.09	1.43±0.14
3	45±7	7.2±0.3	2.3±0.3	0.43±0.05***	0.15±0.01**	4.2±0.4	0.53±0.10	1.74±0.18
10	58±8	6.7±0.2	3.1±0.5	0.32±0.05***	0.13±0.01***	3.6±0.2	0.41±0.07	1.63±0.13
Chow-fed								
0	47±6*	7.1±0.2	2.5±0.4*	0.57±0.05**	0.15±0.01**	1.4±0.09***	0.17±0.02**	0.56±0.05***

Statistical significance of differences *vs* DIO (vehicle) controls: *$p<0.05$; **$p<0.01$; ***$p<0.0001$. Data are expressed as mean ± SEM. Fat pad mass expressed as % of terminal body weight.

Table 7.2. Effects of 21-day administration of PIO on terminal fat pad masses and plasma concentrations of hormones and metabolites in DIO and chow-fed female Wistar rats.

Dose (mg/kg/d)	**Insulin** (pM)	**Glucose** (mM)	**HOMA**	**FFA** (mM)	**TG** (mM)	**Leptin** (ng/ml)	**Gonadal fat mass** (%)	**Perirenal fat mass** (%)
Palatable diet-fed (DIO)								
0	80±6	6.4±0.4	3.8±0.3	0.51±0.07	0.26±0.02	5.2±0.6	0.53±0.09	1.45±0.18
1	66±8	6.9±0.5	3.5±0.7	0.63±0.06	0.20±0.01**	5.0±0.6	0.59±0.11	1.56±0.20
3	70±8	6.2±0.3	3.2±0.4	0.48±0.07	0.17±0.01***	5.6±0.6	0.47±0.07	1.56±0.14
10	62±6	6.5±0.2	2.9±0.3	0.48±0.04	0.15±0.01***	5.2±0.6	0.62±0.10	1.70±0.15
30	69±6	6.8±0.4	3.5±0.5	0.45±0.05	0.14±0.01***	4.7±0.6	0.59±0.09	1.66±0.28
100	53±3	6.0±0.3	2.3±0.2	0.41±0.02	0.11±0.004***	4.4±0.6	0.53±0.10	1.57±0.16
Chow-fed								
0	68±4	6.2±0.2	3.1±0.2 (p=0.056)	0.57±0.09	0.17±0.01**	2.3±0.2**	0.34±0.06	0.81±0.06**

Statistical significance of differences *vs* DIO (vehicle) controls: **p<0.01; ***p<0.0001. Data are expressed as mean ± SEM.

Fat pad mass expressed as % of terminal body weight.

Table 7.3. Effects of 21-day administration of TRO on terminal fat pad masses and plasma concentrations of hormones and metabolites in DIO and chow-fed female Wistar rats.

Dose (mg/kg/d)	**Insulin** (pM)	**Glucose** (mM)	**HOMA**	**FFA** (mM)	**TG** (mM)	**Leptin** (ng/ml)	**Gonadal fat mass** (%)	**Perirenal fat mass** (%)
Palatable diet-fed (DIO)								
0	80±5	7.7±0.3	4.6±0.4	0.36±0.03	0.38±0.07	8.5±0.9	0.48±0.05	1.30±0.13
10	81±3	7.8±0.3	4.7±0.2	0.27±0.04	0.28±0.03	7.8±0.5	0.50±0.05	1.46±0.10
30	76±6	7.7±0.3	4.3±0.3	0.28±0.04	0.20±0.01***	7.1±0.4	0.35±0.03	1.26±0.14
100	72±5	7.2±0.2	3.8±0.3	0.31±0.03	0.21±0.01***	5.6±0.4**	0.32±0.02**	0.96±0.06
300	61±4**	7.5±0.2	3.4±0.2**	0.18±0.03***	0.20±0.01***	5.3±0.6***	0.27±0.04**	0.31±0.03**
1000	52±2***	7.0±0.2	2.7±0.1***	0.16±0.02***	0.21±0.01**	2.5±0.5***	0.12±0.04***	0.20±0.02***
Chow-fed								
0	65±4*	7.8±0.1	3.7±0.2	0.31±0.02	0.23±0.02	4.6±0.5**	0.27±0.02**	0.37±0.02**

Statistical significance of differences *vs* DIO (vehicle) controls: *$p<0.05$; **$p<0.01$; ***$p<0.0001$. Data are expressed as mean ± SEM.

Fat pad mass expressed as % of terminal body weight.

FFAs in the chow-fed controls of both the RSG and PIO experiments (Tables 7.1, 7.2), those of the DIO (vehicle) controls in the PIO experiment were not raised significantly (p=0.6). Like the DIO controls in the RSG experiment, however, those in the PIO experiment did show raised TGs (+51%; p<0.01) and more than a two-fold increase in circulating leptin concentrations (p<0.01; Table 7.2). DIO controls in the TRO experiment showed the least changes of all, with no significant rise in FFA or TG concentrations (p=0.2 and 0.06, respectively). Leptin concentrations were raised by exposure to the HPD, however, by nearly two-fold (p<0.01; Table 7.3).

7.3.2. Effects of TZDs on metabolic parameters

Plasma insulin concentrations were raised in DIO control rats in all three experiments. These changes were significant in the RSG and TRO cohorts (+36% and 23%, respectively; both, p<0.05; Tables 7.1, 7.3) but did not quite reach significance in the PIO experiment (+19%; p=0.07; Table 7.2). Accordingly, these concentrations fell dose-dependently with both RSG and TRO treatment, but only significantly dropping below DIO control concentrations with the highest doses of TRO (300 and 1000 mg/kg; Table 7.3). In all three cohorts, the concentration of plasma glucose was unchanged by the HPD or by drug treatment (all p>0.05). In general, the HOMA model showed that all three drugs induced dose-related improvements in insulin sensitivity, but only significantly in the TRO cohort at a threshold of 300 mg/kg (p<0.01; Table 7.3 and Fig. 7.4).

RSG treatment produced a marked dose-dependent reduction in both fasting plasma FFA and TG concentrations, at a threshold of the lowest dose used (0.1 mg/kg; 23% and 19% falls, respectively; both p<0.05; Table 7.1). In contrast, PIO caused a similar reduction in TGs (threshold 1 mg/kg; 21% fall; p<0.05), but did not

reduce FFA concentrations significantly at any dose (Table 7.2). Like RSG, TRO treatment was effective in reducing both FFA and TG concentrations, but only at higher doses (threshold for FFAs: 300 mg/kg; 52% fall; threshold for TGs: 30 mg/kg; 47% fall). Thus, the dose required to reduce FFA and insulin concentrations in this cohort was the same, 300 mg/kg (Table 7.3).

7.3.3. Haemodynamic factors

RSG treatment had no significant effect on PCV, but increased cardiac mass in DIO rats by 12.5% at a threshold dose of 3 mg/kg (0.96 ± 0.04 *vs* 0.94 ± 0.05 g; $p<0.05$; Fig. 7.2C). PIO treatment had no significant side effects at all, with no marked changes in PCV or cardiac mass at any dose (all $p>0.05$; Figs. 7.3B, C). In contrast to both RSG and PIO, TRO treatment both reduced PCV and increased cardiac mass at the threshold dose of 100 mg/kg: There was an 8% fall in PCV (46.7 ± 0.5 *vs* 43.0 ± 0.6%; $p<0.01$; Fig. 7.4B) and a 15% increase in cardiac mass (0.98 ± 0.02 *vs* 1.13 ± 0.02 g; $p<0.01$; Fig. 7.4C). As described above [7.3.2], using HOMA as the measure of insulin sensitivity, there were no significant improvements in this parameter with RSG or PIO treatments. Thus, a therapeutic index (the ratio of the threshold dose for causing haemodilution/cardiac hypertrophy to that for improving insulin sensitivity) cannot be calculated on this basis for these two drugs. However, falls in FFA and TG concentrations are also indices of improved insulin sensitivity (see Chapter 5), and, on this basis, RSG has a therapeutic index of 30. For PIO, a therapeutic index remains impossible to calculate despite the ability of this drug to induce a fall in TGs at a threshold of 1 mg/kg because a toxic threshold dose has not been identified within the range of doses used here. Presumably, this threshold is greater than 100, the maximum dose tried, suggesting a very high therapeutic index.

Using the threshold doses for reductions in HOMA, FFAs and TGs, the therapeutic index for TRO can be calculated as >0.3 and ≤3.3 (compare panels B and C with panel A in Fig. 7.4; see also Table 7.3), a relatively narrow margin of safety reflecting the drug's toxicity. However, the limitations of using therapeutic index as a measure of drug safety must be borne in mind; namely, that it is based on animal toxicity data which may not reflect forms of toxicity that are clinically important, and it takes no account of idiosyncratic toxic reactions [Rang *et al.*, 2000].

7.3.4. Food intake and body weight

Energy intake in the RSG-treated animals was increased dose-dependently (all $p<0.05$; Table 7.4), as it was in PIO-treated animals, although not significantly ($p=0.3$; Table 7.5). In sharp contrast, intake in TRO-treated rats was reduced dose-dependently, albeit only significantly at the highest dose of 1000 mg/kg ($p<0.0001$; Table 7.6) Even the DIO controls in this experiment showed reduced calorie intake compared to those in the RSG and PIO cohorts (compare Table 7.6 with 7.4 and 7.5).

The absolute body weights of the rats destined for each dose group were similar before treatment at comparable doses in each of the RSG, PIO and TRO experiments (compare Tables 7.4, 7.5 and 7.6). Despite these equivalent starting weights, and equipotent doses, only the DIO rats in the RSG experiment gained weight dose-dependently (all $p<0.05$; Table 7.4). This effect, however, did not coincide with increases in either gonadal or perirenal fat pad mass ($p>0.05$; compare Table 7.4 with 7.1). Both PIO and TRO DIO cohorts gained less than the RSG one, whether treated or untreated (compare Tables 7.4, 7.5 and 7.6). PIO-treated DIO rats showed a trend toward an increase in weight gain compared to that of their untreated

DIO counterparts, but this did not quite reach signficance (p=0.08). Like RSG-treated DIO rats, they showed no change in either fat pad mass (p>0.05; Table 7.2).

Table 7.4. Effects of 21-day administration of RSG on cumulative energy intake and body weight gain in DIO and chow-fed female Wistar rats.

Dose (mg/kg/d)	**Energy intake** (kJ)	**Body weight prior to treatment** (g)	**Body weight gain** (g)
Palatable diet-fed (DIO)			
0	11512±436	271±10	19±3
0.1	12472±371*	279±8	27±4*
0.3	12652±364*	271±6	24±5
1	12420±386*	269±5	29±3*
3	13192±460**	275±4	37±3***
10	13050±372**	272±5	37±2***
Chow-fed			
0	5816±107***	236±4*	11±1*

Statistical significance of differences *vs* DIO (vehicle) controls: *p<0.05; **p<0.01; ***p<0.0001. Data are expressed as mean ± SEM.

In contrast, but consistent with their reduced food intake, the TRO-treated animals lost weight and showed significant reductions in both fat pad masses at the higher doses (all p<0.01; Tables 7.3 and 7.6). The expected decline in plasma leptin concentrations with increasing dose (see Chapter 5) was observed with TRO treatment at a threshold of 100 mg/kg (p<0.01; compare Tables 7.1, 7.2 and 7.3).

Table 7.5. Effects of 21-day administration of PIO on cumulative energy intake and body weight gain in DIO and chow-fed female Wistar rats.

Dose (mg/kg/d)	**Energy intake** (kJ)	**Body weight prior to treatment** (g)	**Body weight gain** (g)
Palatable diet-fed (DIO)			
0	9495±304	275±11	12±2
1	9612±325	273±6	15±3
3	9665±445	274±9	19±3
10	9958±231	276±7	18±2
30	10296±256	277±7	23±2
100	10128±195	276±6	20±4
Chow-fed			
0	6422±135***	252±3 (p=0.052)	11±2

Statistical significance of differences *vs* DIO (vehicle) controls:

***p<0.0001. Data are expressed as mean ± SEM.

7.4. Discussion

Overall, the female DIO rat model does not appear to be as robust as the male version described in Chapter 5. Body weight gain was not as great in females as in males exposed to the HPD, despite similar energy intake (compare Table 5.2 and 7.2), suggesting sexual differentiation in thermogenic mechanisms that cope with excess fat. The results of the RSG experiment were generally as expected, in that the female DIO rats gained weight and increased food intake in a dose-dependent manner and were more insulin-resistant than their chow-fed counterparts, showing falls, albeit short of statistical significance, in circulating insulin concentrations and HOMA values. Whereas male DIO rats showed significant RSG dose-dependent

Table 7.6. Effects of 21-day administration of TRO on cumulative energy intake and body weight gain in DIO and chow-fed female Wistar rats.

Dose (mg/kg/d)	**Energy intake** (kJ)	**Body weight prior to treatment** (g)	**Body weight gain** (g)
Palatable diet-fed (DIO)			
0	6218±233	266±9	4±5
10	6642±158	266±6	9±3
30	6665±210	264±5	13±3
100	6430±189	265±2	13±3
300	5776±209	268±6	-3±6
1000	4764±232***	266±4	-13±4**
Chow-fed			
0	6075±184	243±3	7±1

Statistical significance of differences *vs* DIO (vehicle) controls: $^{**}p<0.01$; $^{***}p<0.0001$. Data are expressed as mean ± SEM.

reductions in insulin, glucose and lipid concentrations (Table 5.1), the female model is sufficient to bring out significant reductions in circulating lipids only (Table 7.1). Thus, this failure to develop very marked insulin resistance meant that the TZDs used could not bring about obvious improvements in insulin sensitivity.

The effects of the three TZDs were variable. PIO treatment at doses equipotent with RSG doses did not have much effect on any of the parameters studied except TG concentrations. Insulin concentrations were higher in PIO- than RSG-treated animals, reflecting the relative lack of potency of this drug in reducing insulin resistance. Body weights across the two experiments were similar, with the PIO-treated rats gaining less than those given RSG. The TRO results are especially difficult to interpret. Energy intake in the rats treated with this drug was greatly reduced perhaps because these animals had full stomachs after being administered

ten times the volume of drug suspension that rats in the other two experiments were administered. This effect was seen even in the TRO DIO (vehicle) controls, demonstrating a non-specific effect of the therapy. The stress of being administered such a large volume may also have had a part to play in discouraging rats from consuming their usual amount. At high doses, TRO had the opposite effect to that of the other two TZDs by causing weight loss rather than gain, demonstrating a toxic effect of the drug at high doses. Perhaps a preferable way to study the effects of TRO in this model would be to administer the drug in food, as other researchers have done, at a concentration of only 0.2% [Miles *et al.,* 1997]. Of course, determining whether or not the differences observed between the three drugs are significant would require direct comparison by running all treatment groups in one single study, a design which could only be managed with extensive technical assistance.

Had insulin resistance been robustly shown in this model, it could have been suggested that these data, as those in Chapter 5, support the hypothesis that, via the Randle cycle [Randle *et al.,* 1963], the insulin-sensitising effects of these three TZDs are linked to the reduced availability of fatty acids (FAs), as a fuel for skeletal muscle [Oakes *et al.,* 1994, 1997], as all three had marked effects on circulating lipids. TRO was the only TZD, however, which showed a combined improvement in insulin resistance and reduction in circulating lipids, but this was neutralised by the induction of haemodilution and cardiac hypertrophy at the same high doses. Thus, TRO appears to be an inadequate therapy in this model due to its toxicity.

All three TZDs had a dose-dependent TG-lowering effect in common, consistent with that observed in humans. Specifically, low or normal TG concentrations remain unchanged by TZD therapy, but elevated TGs are reduced at low TZD doses, consistent with findings in obese, insulin-resistant rat and primate

models [see Chapter 5 and Table 5.1; Hallakou *et al.,* 1997; Ikeda *et al.,* 1990; Kemnitz *et al.,* 1994]. There was a difference between RSG and PIO therapy, in that RSG had an effect on both FFAs and TGs, whereas PIO had an effect only on TGs. Overall, PIO treatment of the DIO rodent model appeared to have little therapeutic effect, which is consistent with the findings in humans, in whom there have been minimal, if any, changes in HDL and total cholesterol concentrations observed. Still, PIO produces a better than neutral lipid profile and is, therefore, clinically effective [Wasada *et al.,* 1996]. PIO appears to lack relative potency in the DIO rodent model, however, as it fails to reduce both insulin and FFA concentrations. Overall, therefore, RSG appears to be the most effective of the three TZDs in this model. It reduced both FFA and TG concentrations at a threshold of 0.1 mg/kg, a dose 30 times below that which induced cardiac hypertrophy. However, it is important to remember that reduction in FFA and TG concentrations is a surrogate index of insulin sensitivity, and the therapeutic efficacy of these TZDs must be proven by a glucose- and insulin-lowering effect, which were not evident here.

In Chapter 5, an increase in gonadal (epididymal) fat mass with RSG treatment was observed to coincide with the dose required to reduce circulating FFAs, suggesting either enhanced FA clearance and deposition as TG in adipose tissue and/or reflecting the anti-lipolytic action of the drug [Oakes *et al.,* 1994, 1997; Souza *et al.,* 1998]. This was not the case with the female DIO model. Indeed, no significant increase was seen in either of the two fat pad masses measured. This does not necessarily mean that the potential mechanisms described above do not operate in this model, but that changes may take place in a different fat depot not examined here, such as the subcutaneous [Adams *et al.*, 1997].

An interesting observation was that of the relative circulating TG and FFA concentrations in male and female DIO rats. In Chapter 5, concentrations of TGs in males are up to ten times higher than those of FFAs (Table 5.1), whereas the reverse appears to be true of females in this study: Although FFA concentrations are about the same in females as in males, their TG concentrations are roughly one-tenth those of males. This has been noted in other studies (E. Naderali, unpublished observations).

Perhaps the most outstanding finding was that the female DIO rat, just like the male DIO rat, is highly sensitive to the decrease in FFAs induced by RSG treatment, and this decrease occurs along with an increase in food intake. As discussed in Chapter 5, this relationship may be explained by a reduction in hepatic FA oxidation resulting in reduced hepatic energy production in turn causing increased food intake [Friedman *et al.*, 1999]. On the other hand, PIO disproportionately influences TG concentrations, and the effects of TRO produce results lying in between. Of course, the interpretation of these results is complicated by the considerable differences between control group lipid concentrations in each cohort, and by the toxic effects of TRO therapy at high doses (300 and 1000 mg/kg).

It is well-known that circulating leptin concentrations are a reflection of fat mass [Widdowson & Wilding, 1999]. Paradoxically, however, the increasing fat mass usually seen with increasing TZD doses coincides with progressively reduced leptin concentrations [see Chapter 5.3.6], due to repression of *OB* gene expression by these drugs [de Vos *et al.*, 1996]. It is important to note, therefore, that the decline in leptin concentration observed with TRO treatment will not have been due to this molecular mechanism but to the toxicity at high doses causing fat loss as a result of reduced energy intake.

Insulin and leptin are both satiety signals in rodents [Schwartz *et al.*, 1992], and it was suggested in Chapter 5 that the falls in both their plasma concentrations in the male DIO rat, which were evoked by RSG treatment, may have contributed to the observed side effects of hyperphagia and weight gain. These side effects were also observed in the female DIO rat, but they cannot be explained by the same mechanism with as much certainty because no leptin reduction was observed. The failure of leptin to be suppressed by TZD treatment, together with the observation that female leptin concentrations were about 2-fold lower than those of males, may be due to a sex difference. It may be possible that the falls in insulin, although not signficant, contributed to weight gain and increased food intake. The marked RSG-induced fall in FFAs and increase in weight are also likely to be closely related, but it must noted that there may be other, as yet unidentified direct or indirect signals to the brain which encourage hyperphagia and, hence, weight gain.

7.5. Conclusion

Because insulin resistance, as measured by the HOMA model, was not consistently established in the female DIO model, it is difficult to make a firm comparison between the drugs as to which effectively reverses this condition. This experiment has shown that of the three TZDs tested, RSG comes the closest to improving the metabolic profile in the DIO rat model and has also demonstrated clear dose separation of these beneficial (lipid-lowering) effects from the adverse effect of cardiac hypertrophy.

Perhaps the most notable finding, consistent with that described in male rats in Chapter 5, remains the exquisite sensitivity of DIO rats to the decrease in FFAs produced by RSG and its coupling to increased food intake.

It is particularly the problems inherent in administering TRO that caution us when interpreting these comparative data. The most that can be stated with confidence is that there is a differentiating effect on lipids between TZDs.

CHAPTER 8

General Discussion

Treatment of both genetic (ZDF) and DIO models of insulin resistance and type 2 diabetes with TZDs has shown that, in general, these compounds improve insulin sensitivity. MCC-555-treatment of ZDF rats also suggests that TZDs maintain ß-cell function. The results of treating DIO rats with RSG suggest that this drug is effective; furthermore, its therapeutic efficacy and adverse effects occurred at distinctly separate doses in dose-response analyses. It also improved insulin sensitivity and lipid metabolism when weight gain was prevented, suggesting that avoidance of weight gain in conjunction with drug therapy may be the key to enhancing the metabolic action of all TZDs. As TZD-induced weight gain is associated with reduced circulating levels of FFAs, it is the direct lipogenic properties, as well as those secondary to improved insulin action, and anti-lipolytic properties which appear to be the cornerstone of the therapeutic effects of this class of drugs.

Through their ability to improve insulin sensitivity in the insulin-resistant state, TZDs are becoming established as treatment for type 2 diabetes and may have a preventive role. These compounds appear to operate through alteration of fuel selection by body tissues and of insulin signalling. As with most drugs, however, their effectiveness is tempered by side effects, including hyperphagia and weight gain, possibly occurring via changes in circulating FFA and leptin concentrations, and, at high doses, fluid retention and cardiac hypertrophy, the mechanisms of which remain uncertain, but are discussed in greater detail below.

The therapeutic effects of TZDs are to improve insulin resistance and maintain islet function. Much of the work presented here provided support for the insulin-sensitising property of TZDs. Chronic MCC-555 treatment of young, pre-diabetic ZDF rats increased fat pad mass, suggesting increased glucose entry into adipose tissue and conversion to fat, aside from the direct lipogenic and anti-lipolytic properties of the drug. Hyperinsulinaemic-euglycaemic clamping of these animals corroborated these data, showing suppression of HGP, consistent with improved insulin sensitivity. These results extend previous findings on this drug's improvement of insulin resistance in Zucker rats and mature ZDF rats with established diabetes [Upton *et al.,* 1998].

Increased fat mass also resulted from RSG and PIO treatment of the DIO model (male) and was suggested by dose-dependent weight gain in RSG-treated female DIO rats, and might, in future, be confirmed by increased mass (not measured here) of fat deposits other than gonadal and perirenal. Improved insulin sensitivity was also indicated by dose-dependent reductions in HOMA values in RSG-treated male DIO rats.

TZD-induced insulin sensitisation in skeletal muscle occurs by reducing substrate competition with glucose [Randle *et al.,* 1963] and by lowering the intramuscular TG and DAG content [Oakes *et al.,* 1994, 1997]. However, the downstream skeletal muscle TG/DAG content, which is likely to be regulated by lipid supply via the circulation, was not measured here. Reduced concentrations of plasma FFAs and TGs, a further index of improved insulin sensitivity, and consistent with the increases in fat mass, were always induced dose-dependently with RSG treatment, whereas results with PIO and TRO were inconsistent. However, many of these data showed trends toward statistical significance, suggesting that the studies

may have lacked statistical power. Clearly, technical difficulties and cost implications limited the number of animals that could be used. Nevertheless, the data generated in this thesis provide useful information to perform power calculations prior to undertaking any studies in the future.

Plasma concentrations of TGs and FFAs were also significantly reduced by all the drugs tested in the DIO ZDF model, although it did not appear that this ability was greater with the combined PPARα/γ agonist, NNC 61-0029. However, α/γ pharmacological binding data would be required to prove the selectivity of this drug. Data from *in vitro* binding studies have shown it to be so [K. Wassermann, personal communication], suggesting, therefore, that its *in vivo* effects are different.

Prevention of hyperphagia and weight gain during RSG treatment of the DIO model also showed a further improvement in insulin sensitivity, but without a further fall in plasma FFA concentration. This suggests that some mechanism other than, or in addition to, FFA flux changes may be responsible for this improvement. The additional mechanism(s) operating could involve other actions of TZDs which have been shown to improve intracellular insulin signal transduction in skeletal muscle and which must be independent of the effects of plasma FFAs. These actions may include reduced tissue TNFα protein levels [Murase *et al.*, 1998], although TaqMan® analysis of gastrocnemius muscle from RSG-treated rats in Chapter 6.2 has shown that TNFα gene transcripts were unchanged from control levels [SmithKline Beecham (SKB) Pharmaceuticals, unpublished observations]. Other possibilities are inhibition of PKC translocation to the cell membrane [Schmitz-Peiffer *et al.*, 1997], increased insulin-stimulated autophosphorylation of insulin receptors [Iwanishi *et al.*, 1993; Kobayashi *et al.*, 1992], and increased PI-3K activity [Loviscach *et al.*, 1999; Zhang *et al.*, 1994]. In adipose tissue, improved insulin sensitivity might also be due

to reduced expression of TNFα [Hofmann *et al.,* 1994], and, in fact, TNFα mRNA levels were reduced in the WAT of RSG-treated animals from the same experiment (6.2) [SKB, as above]. Therefore, it could be that when the TZD-induced reduction in TNFα expression in fat causes a reduction in circulating and local concentrations of TNFα, thereby altering FFA and leptin secretion from adipose tissue [Sethi & Hotamisligil, 1999], this, in turn, might improve insulin action in skeletal muscle [Hotamisligil & Spiegelman, 1994] and in this way indirectly improve muscle insulin sensitivity. Improved insulin sensitivity could also be due to reduced leptin and resistin levels [Qian *et al.,* 1998; Steppan *et al.,* 2001]. Indeed, RSG-treated animals in this study have been shown to have reduced leptin mRNA levels in WAT, and, similarly, reduction in resistin expression has been shown in the treated animals [SKB, as above]. This is encouraging, but still leaves open to speculation the degree to which RSG itself is involved in this suppression at this dose, and how much is simply due to the reduction in fat mass resulting from food restriction and, therefore, to a proportional fall in adipose-specific protein transcription.

Finally, the SNS would seem to be a logical candidate for TZD actions through its major role in maintenance of homeostasis, exerting its effects on food intake, energy expenditure, vascular resistance and cardiac output, all of which have shown TZD-mediated changes [Day, 1999; for review, see *The Sympathetic Nervous System*, 1998]

Treatment with MCC-555 also prevented signs of β-cell damage in the ZDF model, including reduction of pancreatic insulin content, suggesting that TZD intervention may rescue some of the remaining β-cell function in older ZDF rats. Further work might be needed, however, to confirm that the apoptotic cells in the pancreas, which were less numerous in treated animals, were, in fact, β-cells; e.g.,

double-immunolabelling for insulin. The literature supports the notion that it is likely that apoptotic islet cells are β-cells, but only indirectly, through demonstration of raised expression of iNOS or overproduction of ceramide together with reduced insulin output from cultured ZDF islets [Shimabukuro *et al.*, 1997b; 1998a].

In contrast, islet concentrations of insulin in the pancreata of the DIO ZDF (control) model (Chapter 4) were raised above normal and were raised further by TZD treatment or treatment with TZD-like compounds. However, this was consistent with the fact that insulin resistance, as measured by HOMA, was not significantly altered by the drugs used in this experiment. Thus, lean ZDF rats do not become diabetic, nor does it appear that they become significantly insulin-resistant, when they develop obesity equivalent to that of obese, diabetic (*fa/fa*) ZDF rats. This suggests that insulin resistance and β-cell dysfunction in diabetic ZDF rats occur as a result of the leptin receptor mutation itself affecting islet function in some way, rather than simply occurring secondary to fat accumulation. This is a potentially important observation which has not yet been published. Despite a similar degree of obesity to that in ZDF rats, the heterozygous DIO ZDF rat does not develop the same degree of hyperleptinaemia (only 2-fold *vs* 5-6-fold, compared to controls), presumably because the leptin receptor is intact. It may be, therefore, that the DIO ZDF rat accumulates lipid in the β-cell to a much lesser degree than in the adipocyte. This unique resistance to the lipopenic actions of leptin has been highlighted previously in the diabetic ZDF rat in contrast to another obese, hyperphagic model, the VMH-lesioned rat. When these animals are made hyperleptinaemic, in contrast to ZDF rats, their islet fat level remains normal and they show a reduction in fat mass (50%) intermediate between that of normal rats and obese ZDF rats [Koyama *et al.*, 1998].

Weight gain was observed with MCC-555 treatment of diabetic ZDF rats and with RSG treatment of the DIO model. Similarly, all PPARγ agonists in Chapter 4 caused weight gain in the DIO ZDF rat. This coincided with increases in food intake in the DIO model, but not in the diabetic ZDF rat treated with MCC-555. This may be due to the fact that the drug sometimes acts only as a partial PPARγ agonist [Reginato *et al.,* 1998], and that it has a different structure and, therefore, different metabolism to that of the full agonists. As discussed in Chapter 3, the weight gain effect of MCC-555 in the ZDF diabetic rats may be the combined effect of the drug's agonist activity and the arresting of the catabolic processes of diabetes through the preservation of β-cell function.

Generally, the side effects of weight gain and hyperphagia may occur through suppression of systemic supplies of FFAs and leptin, respectively, as these were both reduced with most of the drugs tested. As discussed above, there was evidence for the involvement of FFA changes in most DIO studies. Although these were not studied in the genetic model, there is ample evidence in the literature that this is also the case in the ZDF rat [Sreenan *et al.,* 1996; Zhang *et al.,* 1996].

RSG caused hyperphagia and weight gain in the DIO rat in a dose-dependent manner, supporting long-established findings with other TZDs in both animals and man [De Vos *et al.,* 1996; Shimizu *et al.,* 1998; Wang *et al.,* 1997; Zhang *et al.,* 1996]. The literature has also shown that RSG does not clear FFAs (^{3}H-palmitate) from the circulation of high-fat-fed rats, implicating the anti-lipolytic action (reduction in the release of FA into the circulation), rather than enhanced clearance efficiency, as being the crucial factor in the weight gain side effects of the drug, whereas the hyperphagia side effect probably results from the PPARγ-induced downregulation of leptin [Oakes *et al.,* 1997]. The refractoriness of the plasma TG

concentration in the presence of lower FFA levels may also signal reduced lipolysis, resulting in reduced supply of FFAs against a background of increased food consumption and the generation of additional circulating TG-rich lipoproteins. Generally, the literature on dyslipidaemia supports FFAs as being the more important trigger to insulin sensitivity improvement than TGs, but it is inconsistent on the effects of TZDs on TG clearance from the circulation. In one *ex vivo* study [Lefebvre *et al.,* 1997], epididymal fat LPL mRNA and activity were increased by RSG, but in a study using rat adipocytes in culture, both troglitazone (TRO) and RSG inhibited LPL activity [Ranganathan & Kern, 1998]. However, it is important to note that the association between a fall in circulating FFAs and improved insulin sensitivity and weight gain is just that—that such a reduction actually causes these changes is merely implied.

Persistent weight gain in pair-fed DIO rats suggested that hyperphagia is not the only component responsible for TZD-induced weight gain; indeed, the implication is that TZDs also induce a fall in energy expenditure. This might occur through a reduction in UCP activity, although this did not appear to be the case, at least with UCP-3 expression. There is no literature evidence to suggest that TZDs down-regulate expression of UCP-2 (not measured here) in various strategic tissues, and the evidence is inconsistent with regard to UCP-1. On the other hand, the effects of leptin on energy expenditure in rodents are well known [Collins *et al.,* 1996; Hwa *et al.,* 1996; Levin *et al.,* 1996] and, moreover, leptin's thermogenic properties are mediated via stimulation of BAT UCP-1 [Scarpace *et al.,* 1997] and skeletal muscle UCP-3 expressions [Cusin *et al.,* 1998]. The failure of RSG to significantly reduce circulating leptin without concomitant pair-feeding is, therefore, certainly consistent

with unchanged UCP expression. It is therefore difficult to implicate down-regulation of UCPs in weight gain with RSG at the present time.

The relationships between the (expected) raised circulating leptin concentrations in DIO rats and central neurotransmitters involved in the regulation of food intake also could have provided the answer to this question. However, whilst reduced plasma leptin concentrations in the pair-fed groups would have been expected to lead to increased NPY expression in the hypothalamus [Schwartz *et al.*, 1996] and, in turn, to hyperphagia and decreased sympathetic firing rates to BAT [Egawa *et al.*, 1991], there was no evidence that this mechanism was operative here. That neither NPY nor orexin appear to have been prime hypothalamic candidate peptides for tranducing the hyperphagic signal is perhaps an unexpected result, but this has also been demonstrated in Zucker fatty rats [NPY: Wang *et al.*, 1997] and DIO Wistars [orexin: Cai *et al.*, 2000] given insulin-sensitising doses of RSG. However, RSG-induced weight gain was also negatively correlated with circulating concentrations of leptin and insulin, the former being supported by other studies of TZD treatment of type 2 diabetes in humans [Walsh *et al.*, 1996] and animals [McCormack *et al.*, 1989; Zhang *et al.*, 1996].

As mentioned above, TZDs can also cause haemodilution secondary to fluid retention, leading to cardiac hypertrophy. This was not examined in the ZDF diabetic rat treated with MCC-555, but this drug has previously been found to be free of haematological and cardiac side effects [Ishii *et al.*, 1996]. Although the non-TZD PPAR agonists DRF 2593 and NNC 61-0029 used in the DIO ZDF model appeared no more therapeutically effective than the TZD, PIO, they had no significant effect on PCV or cardiac mass, whereas PIO reduced PCV significantly. Given the known problems with TZDs and oedema, due to increased plasma volume [Cantello *et al.*,

1994; Ghazzi *et al.,* 1997; Patel *et al.,* 1998], this could be an important finding as regards further development of these two novel drugs. This difference could be due to structural differences between these drugs and TZDs, which separate therapeutic and adverse effects. Possible confirmation of this could be obtained through a dose-response study such as that presented in Chapter 5 on RSG.

RSG was the only therapeutically effective TZD in the DIO model to also cause these adverse effects, but at clearly separate (supratherapeutic) doses. These effects can be partly explained by a known inhibitory effect of TZDs on vascular smooth muscle cell Ca^{2+} flux (independent of their effect on PPARγ and alleviation of other diabetes-related complications which themselves are associated with hypertension, such as hyperlipidaemia and insulin resistance [Ren *et al.,* 1996; Zhang *et al.,* 1994]) and, therefore, peripheral vascular resistance [Buchanan *et al.,* 1995; Fujiwara *et al.,* 1995; Nakamura *et al.,* 1998; Song *et al.,* 1997; Verma *et al.,* 1998; Walker *et al.,* 1998; Walsh *et al.,* 1996; Zhang *et al.,* 1994]. Other ingredients of a haemodynamic action, including reduced diastolic blood pressure and increased cardiac index and stroke volume index, have been reported during the clinical use of TRO [Ghazzi *et al.,* 1997]. By extrapolation, it is possible that haemodilution in both rat and man, and cardiac hypertrophy in rat, though not seemingly in man [Driscoll *et al.,* 1997; Ghazzi *et al.,* 1997], can be traced back, at least partly, to this inhibitory effect on vascular smooth muscle cell Ca^{2+} flux.

A thorough examination of all potential causes of increased plasma volume is beyond the scope of this thesis, but brief speculation leads to the following possibilities: TZDs may effect various long-term regulators of water balance and, hence, adjustment of blood volume to vascular capacity; for example, vasopressin secretion stimulates water resorption by the kidney, and, indeed, TZDs have been

shown to exert their hypotensive effects by inhibiting vasopressin agonist-induced Ca^{2+} entry into vascular smooth muscle [Asano *et al.*, 1999; Buchanan *et al.*, 1995]. TZDs could be implicated in inhibiting the release of atrial natriuretic peptide from the heart, thereby decreasing renal excretion of salt and water, but there is no published evidence of this yet [for review, see Rang *et al.*, 2000]. In addition, the discovery that a prostaglandin is the natural ligand of PPARγ [Forman *et al.*, 1995] suggests a role for prostaglandins in PPARγ-mediated nuclear signalling. Indeed, PPARγ is expressed in the medullary collecting duct of the kidney in the rat, rabbit and human, implicating TZD involvement with the prostaglandin-mediated changes in renal medullary cell growth [Braissant *et al.*, 1996; Guan *et al.*, 1997; Yang *et al.*, 1999]. These results imply that sodium retention occurs possibly through a direct effect of TZDs on the renal tubules. On the other hand, the effects of TZDs may be indirect, resulting from their improved insulin action; i.e., a relationship between insulin resistance and increased Na^+/Li^+ countertransport activity of erythrocytes has been established in hypertensive diabetic subjects, although not mediated by compensatory hyperinsulinaemia [Giordano *et al.*, 1997; Pinkney *et al.*, 1995]. The improvement in insulin resistance and hypertension brought about by TZDs therefore implicates these drugs in decreasing this countertransport activity, but, to date, there have been no published data on this subject.

Whilst my study suggests that RSG exhibits dose-differentiation for its effects on haemodilution in the DIO rat, the situation is unresolved for TRO and PIO. Again, using larger groups of animals and thereby increasing statistical power could potentially clarify these results. TRO is a more potent Ca^{2+} channel blocker than PIO [Nakamura *et al.*, 1998], and an earlier study indicated that TRO, but not RSG, relaxes human subcutaneous arterial resistance vessels, albeit apparently by a

prostaglandin-related mechanism [Walker *et al.*, 1998]. Nonetheless, a recent report that RSG also causes haemodilution in man at anti-hyperglycemic doses [Patel *et al.*, 1998], suggests that the situation may be more complex than the picture presented here for DIO rats. Clearly this is an issue which requires additional evaluation.

Although the haemodilution action of TZDs has not been fully explained in the literature and was not quantified here, it remains another possible explanation for weight gain in RSG-treated animals by changing the level of body water. Why this component would play a greater role in DIO rats than in chow-fed rats treated with RSG, possibly explaining the apparent differential sensitivity to RSG between the two groups, remains mysterious, unless it is closely related to the insulin-sensitising mechanism. However, one must bear in mind that it is fat accrual which is the major contributor to weight gain in TZD treatment, with water retention likely forming only a very small component of this side effect.

In summary, the work presented in this thesis was unique in that these drugs have not been tested in this way before. It was important to study the DIO rodent model of insulin resistance, as the effects of TZD treatment have previously been demonstrated primarily in mutant models of type 2 diabetes, and as such were not yet directly applicable to human diabetes. Demonstrating insulin-sensitising effects in a non-genetic model would have provided a strong rationale for testing such agents early in the course of type 2 diabetes in humans. It is difficult to say yet if the observations in the ZDF model with inherited leptin resistance are generally applicable to the DIO model. This is partly because of the variablility inherent in establishing insulin resistance in the latter. In addition, although leptin resistance appears to be consistently acquired in the DIO model, as reflected in its hyperleptinaemia, it is usually more modest than that in ZDF rats and does not

respond significantly to TZD treatment unless at a comparable (supranormal) level to that in ZDF rats.

Thus, this body of work has provided pre-clinical evaluation data in relevant animal models of insulin resistance and type 2 diabetes that flesh out existing knowledge of TZD action, and, importantly, provide a basis for clinical trials. These experiments have confirmed that TZD therapy is a significant advance for the treatment of these conditions, but problems still remain. RSG treatment, although therapeutically effective, nontheless produces increased food intake and undesirable weight gain. Three-way TZD comparison showed that whilst this study confirmed the findings that RSG improves insulin action in the DIO rat dose-dependently, the situation is unresolved for TRO because of toxicity and difficulties inherent in drug administration. Overall, PIO was less potent than RSG and appeared slightly less efficacious in the model studied, but clinical evidence in humans would suggest a similar therapeutic effect with both drugs. Indeed, there is evidence to show that both RSG and PIO significantly reduce fasting plasma glucose in humans [Patel *et al.,* 1999; Wasada *et al.,* 1996]. As MCC-555 was effective in attenuating full diabetic symptoms in the ZDF model, did not cause hyperphagia and is free of haematological side effects [Ishii *et al.,* 1996], it would be interesting to do a dose-response assessment of its properties in the DIO model to ascertain how well it compares with the full PPARγ agonists. Justification for exploiting this drug's potential further comes from the work of Reginato and colleagues [1998], who have found MCC-555 to have a greater hypoglycaemic potency, despite a binding affinity of less than 1/10 that of RSG. Further development of compounds with TZD-like properties, such as DRF 2593 and NNC 61-0029, would be helpful. The insulin-

sensitising properties of these two drugs was suggested in part by ubiquitous increases in fat mass and reduced circulating FFA and TG concentrations.

Future directions might involve testing leptin replacement therapy as a means of counteracting the TZD-induced suppression of OB expression, and, hence, increased food intake and weight gain. In addition, it would be interesting to further investigate the role of FFAs and the effects of the HPD and TZDs at the cellular level; i.e., at the level of changes to the pancreatic islets in the DIO model. Shafrir [2000] reviews the work on spiny mice maintained on a high-fat diet. These animals develop obesity and often diabetes, as well as pancreatic hyperplasia and hypertrophy. Interestingly, they have a low insulin secretion response, despite ample pancreatic insulin content, suggesting that high pancreatic insulin content observed in the DIO ZDF model of Chapter 4 may be associated with islet cell disruption. Future studies could therefore include an examination of whether or not the pancreatic changes of overt diabetes are established in the DIO model used here, in addition to the metabolic changes observed, and whether or not TZD treatment is effective in treating this aspect of the disease also.

The more serious side effects of fluid retention and increased cardiac mass were also highlighted in all TZD dose-response studies. Increased understanding of these actions may lead to a refinement of TZD synthesis and/or development of a new generation of agents with novel mechanisms of action.

In summary, TZDs are effective in rat models of diabetes and insulin resistance. Early intervention with these agents in the course of diabetes may improve insulin sensitivity and maintain ß-cell function. RSG, in particular, can be used with a wide safety margin. Metabolic improvements brought about by TZD treatment in DIO rats are greater if weight gain is prevented, suggesting that these

drugs would be even more effective clinically if weight gain were avoided. Weight gain appears closely linked with a reduction in circulating levels of FFAs which itself appears to underpin the therapeutic benefits of this class of drugs.

References

Adams M, Montague CT, Prins JB, Holder JC, Smith SA, Sanders L, Digby JE, Sewter CP, Lazar MA, Chatterjee KK, O'Rahilly S (1997) Activators of peroxisome proliferator-activated receptor γ have depot-specific effects on human preadipocyte differentiation. *J Clin Invest* **100**: 3149-3153

Amri EZ, Bonino F, Aihaud G, Abumrad NA, Grimaldi PA (1995) Cloning of a protein that mediates transcriptional effects of fatty acids in preadipocytes. Homology to peroxisome proliferator-activated receptors. *J Biol Chem* **270**: 2367-2371

Anai M, Funaki M, Ogihara T, Kanda A, Onishi Y, Sakoda H, Inukai K, Nawano M, Fukushima Y, Yazaki Y, Kikuchi M, Oka Y, Asano T (1999) Enhanced insulin-stimulated activation of phosphatidylinositol 3-kinase in the liver of high-fat fed rats. *Diabetes* **48**: 158-169

Andres R, Swerdloff R, Posefsky T, Coleman D (1966) Manual feedback technique for the control of blood glucose concentration. In: Skeegs LT, Jr (ed) *Automation in analytical chemistry*. Mediad, New York, pp 486-491

Animal Scientific Procedures Act (1986) Home Office, London

Anti-Digoxigenin-AP, Fab fragments package insert (1999) Boehringer Mannheim, Germany

Arakawa K, Ishihara T, Aoto M, Inamasu M, Saito A, Ikezawa K (1998) Actions of novel antidiabetic thiazolidinedione, T-174, in animal models of non-insulin-dependent diabetes mellitus (NIDDM) and in cultured muscle cells. *Br J Pharmacol* **125**: 429-436

Arch J (2000) Orexins, feeding and the big picture. *Br J Nutr* **84**: 1-4

Asano M, Nakajima T, Iwasawa K, Morita T, Nakamura F, Imuta H, Chisaki K, Yamada N, Omata M, Okuda Y (1999) Troglitazone and pioglitazone attenuate agonist-dependent Ca^{2+} mobilization and cell proliferation in vascular smooth muscle cells. *Br J Pharmacol* **128**: 673-683

Auwerx J (1999) PPARγ, the ultimate thrifty gene. *Diabetologia* **42**: 1033-1049

Bailey CJ, Flatt PR (1997) Animal syndromes of non-insulin-dependent diabetes mellitus. In: Pickup J, Williams G (eds) *Textbook of diabetes*. Blackwell Science Ltd, Oxford, pp 23.1-23.25

Bailey CJ, Williams G, Pickup JC (1997) New drugs in the management of diabetes mellitus and its complications. In: Pickup J, Williams G (eds) *Textbook of diabetes*. Blackwell Science Ltd, Oxford, pp 84.1-84.30

Barman Balfour JA, Plosker GL (1999) Rosiglitazone. *Drugs* **57**: 921-930

Barroso I, Gurnell M, Crowley VEF, Agostini M, Schwabe JW, Soos MA, Maslen GL, Williams TDM, Lewis H, Schafer AJ, Chatterjee VKK, O'Rahilly S (1999) Dominant negative mutations in human PPARγ associated with severe insulin resistance, diabetes mellitus and hypertension. *Nature* **402**: 880-883

Beck B, Stricker-Krongrad A, Burlet A, Max J-P, Musse N, Nicolas J-P, Burlet C (1994) Macronutrient type independently of energy intake modulates hypothalamic neuropeptide Y in Long-Evans rats. *Brain Res Bull* **34**: 85-91

Beck-Nielsen H & Groop LC (1994) Metabolic and genetic characterization of pre-diabetic states. Sequence of events leading to non-insulin-dependent diabetes mellitus. *J Clin Invest* **94**: 1714-1721

Berger J, Bailey P, Biswas C, Cullinan CA, Doebber TW, Hayes NS, Saperstein R, Smith RG, Leibowitz MD (1996) Thiazolidinediones produce a conformational change in peroxisomal proliferator-activated receptor-γ: binding and activation correlate with antidiabetic actions in db/db mice. *Endocrinology* **137**: 4189-4195

Bertin E, Nguyen P, Guenounou M, Durlach V, Potron G, Leutenegger M (2000) Plasma levels of tumor necrosis factor-alpha (TNF-α) are essentially dependent on visceral fat amount in type 2 diabetic patients. *Diabetes Metab* **26**: 178-182

Bethge H, Haring HU (1998) The thiazolidinediones—a new therapeutic agent for type 2 diabetes. *Arzneimittelforschung* **48**: 97-119

Betteridge J (1997) Lipid disorders in diabetes mellitus. In: Pickup J, Williams G (eds) *Textbook of diabetes*. Blackwell Science Ltd, Oxford, pp 55.1-55.31

Bishop AE, Polak JM (1997) The anatomy, organization and ultrastructure of the islets of Langerhans. In: Pickup J, Williams G (eds) *Textbook of diabetes*. Blackwell Science Ltd, Oxford, pp 6.1-6.16

Bloom SR, Long RG (1982) *Radioimmunoassay of gut regulatory peptides.* WB Saunders Company Ltd, London

Boado RJ, Golden PL, Levin N, Pardridge WM (1998) Up-regulation of blood-brain barrier short-form leptin receptor gene products in rats fed a high fat diet. *J Neurochem* **71**: 1761-1764

Boehringer Mannheim catalogue (1997) Boehringer Mannheim (Diagnostics & Biochemicals) Ltd., Sussex, U.K.

Bone AJ, Gwilliam DJ (1997) Animal models of insulin-dependent diabetes mellitus. In: Pickup J, Williams G (eds) *Textbook of diabetes*. Blackwell Science Ltd, Oxford, pp 16.1-16.16

Bonilla S, Redonnet A, Noël-Suberville C, Pallet V, Garcin H, Hiqeuret P (2000) High-fat diets affect the expression of nuclear retinoic acid receptor in rat liver. *Br J Nutr* **83**: 665-671

Bonora E, Targher G, Alberiche M, Bonadonna RC, Saggiani F, Zenere MB, Monauini T, Muggeo M (2000) Homeostasis model assessment closely mirrors the glucose clamp technique in the assessment of insulin sensitivity: studies in subjects with various degrees of glucose tolerance and insulin sensitivity. *Diabetes Care* **23**: 57-63

Boss O, Muzzin P, Giacobino J-P (1998) The uncoupling proteins: a review. *Eur J Endocrinol* **139**: 1-9

Bowen Jones D, Gill GV (1997a) Insulin-dependent diabetes mellitus. In: Pickup J, Williams G (eds) *Textbook of diabetes*. Blackwell Science Ltd, Oxford, pp 12.1-12.13

Bowen Jones D, Gill GV (1997b) Non-insulin-dependent diabetes mellitus: an overview. In: Pickup J, Williams G (eds) *Textbook of diabetes*. Blackwell Science Ltd, Oxford, pp 17.1-17.13

Braissant O, Foufelle F, Scotto C, Dauca M, Wahli W (1996) Differential expression of peroxisome proliferator-activated receptors (PPARs): tissue distribution of PPAR-alpha, -beta, and -gamma in the adult rat. *Endocrinology* **137**: 354-366

Bredt DS, Snyder SH (1989) Nitric oxide mediates glutamate-linked enhancement of cGMP levels in the cerebellum. *Proc Natl Acad Sci USA* **86**: 9030-9033

British National Formulary (1994) British Medical Association, London.

Buchanan TA, Meehan WP, Jeng YY, Yang D, Chan TM, Nadler JL, Scott S, Rude RK, Hsueh WA (1995) Blood pressure lowering by pioglitazone. Evidence for a direct vascular effect. *J Clin Invest* **96**: 354-360

Burant CF, Sreenan S, Hirano K-I, Tai T-AC, Lohmiller J, Lukens J, Davidson NO, Ross S, Graves RA (1997) Troglitazone action is independent of adipose tissue. *J Clin Invest* **100**: 2900-2908

Busquets S, Sanchis D, Alvarez B, Ricquier D, López-Soriano FJ, Argilés JM (1998) In the rat, tumor necrosis factor alpha administration results in an increase in both UCP2 and UCP3 mRNAs in skeletal muscle: a possible mechanism for cytokine-induced thermogenesis? *FEBS Lett* **440**: 348-350

Cabanac M, Richard D (1996) The nature of the Ponderostat: Hervey's hypothesis revived. *Appetite* **26:** 45-54

Cabrero A, Llaverias G, Roglans N, Alegret M, Sanchez R, Adzet T, Laguna JC, Vazquez M (1999) Uncoupling protein-3 mRNA levels are increased in white adipose tissue and skeletal muscle of bezafibrate-treated rats. *Biochem Biophys Res Comm* **260**: 547-556

Cai XJ, Lister CA, Buckingham RE, Pickavance L, Wilding J, Arch JRS, Wilson S, Williams G (2000) Down-regulation of orexin gene expression by severe obesity in

the rats: studies in Zucker fatty and Zucker diabetic fatty rats and effects of rosiglitazone. *Mol Brain Res* **77**: 131-137

Cantello BCC, Cawthorne MA, Cottam GP, Duff PT, Haigh D, Hindley RM Lister CA, Smith SA, Thurlby PL (1994) [[ω-(heterocyclylamino)alkoxy]benzyl]-2,4-thiazolidinediones as potent antihyperglycemic agents. *J Med Chem* **37**: 3977-3985

Carey VJ, Walters EE, Colditz GA, Solomon CG, Willett WC, Rosner BA, Speizer FE, Manson JE (1997) Body fat distribution and risk of non-insulin-dependent diabetes mellitus in women. The Nurses' Health Study. *Am J Epidemiol* **145**: 614-619

Chang S, Graham B, Yakubu F, Lin D, Peters JC, Hill JO (1990) Metabolic differences between obesity-prone and obesity-resistant rats. *Am J Physiol* **259**: R1103-1110

Chen S, Ogawa A, Ohneda M, Unger RH, Foster DW, McGarry JD (1994) More direct evidence for a malonyl-CoA-carnitine palmitoyltransferase I interaction as a key event in pancreatic beta-cell signaling. *Diabetes* **43**: 878-883

Chomczynski P, Sacchi N (1987) Single-step method of RNA isolation by acid guanidium thiocyanate-phenol-chloroform extraction. *Anal Biochem* 162: 156-159

Chua SC Jr, Chung WK, Wu-Peng S *et al.* (1996) Phenotypes of mouse diabetes and rat fatty due to mutations in the OB (leptin) receptor. *Science* **271**: 994-996

Ciaraldi TP, Carter L, Mudaliar S, Kern PA, Henry RR (1998) Effects of tumor necrosis factor-alpha on glucose metabolism in cultured human muscle cells from nondiabetic and type 2 diabetic subjects. *Endocrinology* **139**: 4793-4800

Ciaraldi TP, Huber-Knudsen K, Hickman M, Olefsky JM (1995) Regulation of glucose transport in cultured muscle cells by novel hypoglycaemic agents. *Metabolism* **44**: 976-981

Clapham JC, Arch JRS, Chapman H, Haynes A, Lister C, Moore GBT, Piercy V, Carter SA, Lehner I, Smith SA, Beeley LJ, Godden RJ, Herrity N, Skehel M, Changani KK, Hockings PD, Reid DG, Squires SM, Hatcher J, Trail B, Latcham J, Rastan S, Harper AJ, Cadenas S, Buckingham JA, Brand MD, Abuin A (2000) Mice overexpressing human uncoupling protein-3 in skeletal muscle are hyperphagic and lean. *Nature* **406**: 415-418

Clark A, de Koning EJ, Hattersley AT, Hansen BC, Yajnik CS, Poulton J (1995) Pancreatic pathology in non-insulin dependent diabetes (NIDDM). *Diabetes Res Clin Pract* **Suppl**: S39-47

Clark JB, Palmer CJ (1982) The diabetic Zucker rat—a new model for non-insulin-dependent diabetes. *Diabetes* **30**: 126A

Clark JB, Palmer CJ (1983) The diabetic Zucker rat. *Proc Soc Exp Biol Med* **173**: 68-75

Clément K (1999) *Obesity matters* **2**: 6-7

Collins S, Kuhn CM, Petro AE, Swick AG, Chrunyk BA, Surwit RS (1996) Role of leptin in fat regulation. *Nature* **380**: 677

Corbett JA, Sweetland MA, Wang JL, Lancaster JR Jr, McDaniel ML (1993) Nitric oxide mediates cytokine-induced inhibition of insulin secretion by human islets of Langerhans. *Proc Natl Acad Sci USA* **90**: 1731-1735

Cullingford TE, Bhakoo K, Peuchen S, Dolphin CT, Patel R, Clark JB (1998) Distribution of mRNAs encoding the peroxisome proliferator-activated α, β, and γ and the retinoid X receptor α, β, and γ in the rat central nervous system. *J Neurochem* **70**: 1366-1375

Cusin I, Zakrzewska KE, Boss O Muzzin P, Giacobino JP, Ricquier D, Jeanrenaud B, Rohner-Jeanrenaud F (1998) Chronic central leptin infusion enhances insulin-stimulated glucose metabolism and favors the expression of uncoupling proteins. *Diabetes* **47**: 1014-1019

D-glucose package insert (2000) Roche Diagnostics, Milton Keynes, UK

Darnell J, Lodish H, Baltimore D (1990) *Molecular cell biology.* W.H. Freeman & Company, New York

Dawson VL, Dawson TM, London ED, Bredt DS, Snyder SH (1991) Nitric oxide mediates glutamate neurotoxicity in primary cortical cultures. *Proc Natl Acad Sci USA* **88**: 6368-6371

Day C (1999) Thiazolidinediones: a new class of antidiabetic drugs. *Diabet Med* **16**: 179-192

DeFronzo R (1988) The triumvirate: beta cell, muscle, liver. A collusion responsible for NIDDM. *Diabetes* **37**: 667-685

DeFronzo RA, Tobin JD, Andres R (1979) Glucose clamp technique: a method for quantifying insulin secretion and resistance. *Am J Physiol* **237:** E214-E233

de Souza CJ, Yu JH, Robinson DD, Ulrich RG, Meglasson MD (1995) Insulin secretory defect in Zucker fa/fa rats is improved by ameliorating insulin resistance. *Diabetes* **44**: 984-991

De Vos P, Lefebvre A-M, Miller SG, Guerre-Millo M, Wong K, Saladin R, Hamann LG, Staels B, Briggs MR, Auwerx J (1996) Thiazolidinediones repress *ob* gene expression in rodents via activation of peroxisome proliferator-activated receptor γ. *J Clin Invest* **98**: 1004-1009

DIG system's user's guide for filter hybridization (1995) Boehringer Mannheim GmbH, Biochemica, Germany.

Digby JE, Montague CT, Sewter CP, Sanders L, Wilkison WO, O'Rahilly S, Prins JB (1998) Thiazolidinedione exposure increases the expression of uncoupling protein 1 in cultured human preadipocytes. *Diabetes* **47**: 138-141

Dinulescu DM, Fan W, Boston BA, McCall K, Lamoreux ML, Moore KJ, Montagno J, Cone RD (1998) *Mahogany (mg)* stimulates feeding and increases basal metabolic rate independent of its suppression of *agouti*. *Proc Natl Acad Sci USA* **95**: 12707-12712

Djouadi F, Weinheimer CJ, Saffitz JE, Pitchford C, Bastin J, Gonzalez FJ, Kelly DP (1998) A gender-related defect in lipid metabolism and glucose homeostasis in peroxisome proliferator-activated receptor-α-deficient mice. *J Clin Invest* **102**: 1083-1091

Dobbins RL, Chester MW, Daniels MB, McGarry JD, Stein DT (1998) Circulating fatty acids are essential for efficient glucose-stimulated insulin secretion after prolonged fasting in humans. *Diabetes* **47**: 1613-1618

Dogterom P, Jonkman JHG, Vallance SE (1999) Rosiglitazone: no effects on erythropoiesis or premature red cell destruction. *Diabetes* **48**: 98A

Driscoll J, Ghazzi M, Perez J, Huang S, Whitcomb R (1997) A 96-week follow-up on cardiac safety in patients with Type II diabetes treated with troglitazone. *Diabetes* **46** Suppl 1: 149A

Dubois M, Pattou F, Kerr-Conte J, Gmyr V, Vandewalle B, Desreumaux P, Auwerx J, Schoonjans K, Lefebvre J (2000) Expression of peroxisome proliferator-activated receptor γ (PPARγ) in normal human pancreatic islet cells. *Diabetologia* **43**: 1165-1169

Dyslipidaemia (1997) In: Vince M (ed) *Obesity*. Colwood House Medical Publications (UK) Ltd, Berkshire

Egawa M, Yoshimatsu H, Bray GA (1991) Neuropeptide Y suppresses sympathetic activity to interscapular brown adipose tissue in rats. *Am J Physiol* **260**: R328-334

Elahi, D (1996) In praise of the hyperglycemic clamp. A method for assessment of β-cell sensitivity and insulin resistance. *Diabetes Care* **19:** 279-286.

Elbrecht A, Chen Y, Cullinan CA, Hayes N, Leibowitz MD, Moller DE, Berger J (1996) Molecular cloning, expression and characterization of human peroxisome proliferator activated receptors gamma1 and gamma2. *Biochem Biophys Res Comm* **224**: 431-437

Emilsson V, O'Dowd J, Wang S, Heyman R, Cawthorne MA (1999) Effects of rexinoids and thiazolidinedione on levels of UCP isoforms and PGC-1 in the obese Zucker rat. *Diabetologia* **42**: 206A

Emoto M, Nishizawa Y, Maekawa K, Hiura Y, Kanda H, Kawagishi T, Shoji T, Okuno Y, Morii H (1999) Homeostasis model assessment as a clinical index of

insulin resistance in type 2 diabetic patients treated with sulphonylureas. *Diabetes Care* **22**: 818-822

Enari M, Sakahira H, Yokoyama H, Okawa K, Iwamatsu A, Nagata S (1998) A caspase-activated Dnase that degrades DNA during apoptosis, and its inhibitor ICAD. *Nature* **391**: 43-50

Flecknell PA (1986) *Laboratory Animal Anaesthesia.* Academic Press Ltd., London

Flier JS (2000) The missing link with obesity? *Nature* **409**: 292-293

Forman BM, Chen J, Evans RM (1997) Hypolipidemic drugs, polyunsaturated fatty acids, and eicosanoids are ligands for peroxisome proliferator-activated receptors α and δ. *Proc Natl Acad Sci USA* **94**: 4312-4317

Forman BM, Tontonoz *P*, Chen J, Brun, RP, Spiegelman, BM, Evans RM (1995) 15-deoxy-Δ12, 14 prostoglandin J2 is a ligand for the adipocyte determination factor PPARγ. *Cell* **83**: 803-812

Free fatty acids, half-micro test package insert (2000) Roche Diagnostics, Milton Keynes, UK

Friedman JE, De Vente JE, Peterson RG, Dohm LD (1991) Altered expression of muscle glucose transporter GLUT4 in diabetic fatty Zucker rats (ZDF/Drt-*fa*). *Am J Physiol* **261**: E782-E788

Freidman MI, Harris RB, Ji H, Ramirez I, Tordoff MG (1999) Fatty acid oxidation affects food intake by altering hepatic energy status. *Am J Physiol* **276**: R1046-1053

Frias JP, Basabe L, Macaraeg G, Kruszynska YT (2000) Lack of effect of a physiological elevation of plasma non-esterified fatty acid levels on insulin secretion. *Diabetes Metab* **26**: 133-139

Fujiwara T, Ohsawa T, Miyamoto M, Ushiyama S, Matsuda K, Horikoshi H (1995) Troglitazone (CS-045) acutely increases skin blood flow in dexamethasone-induced diabetic obese Zucker rats and normal rats. *Diabetes* **44** Suppl 1: 72A

Fürnsinn C, Neschen S, Noe C, Bisschop M, Roden M, Vogl C, Schneider B, Waldhäusl W (1997) Acute non-insulin-like stimulation of rat muscle glucose metabolism by troglitazone in vitro. *Br J Pharmacol* **122**: 1367-1374

Gavin J, Golay A, Rissanen A (1998) *Obesity and type 2 diabetes.* Synergy Medical Education, Surrey

Gavrieli Y, Sherman Y, Ben-Sasson SA (1992) Identification of programmed cell death in situ via specific labeling of nuclear DNA fragmentation. *J Cell Biol* **119**: 493-501

Gervois P, Torra IP, Fruchart JC, Staels B (2000) Regulation of lipid and lipoprotein metabolism by PPAR activators. *Clin Chem Lab Med* **38**: 3-11

Ghazzi MN, Perez JE, Antonucci TK, Driscoll JH, Huang SM, Faja BW, Whitcomb RW (1997) The Troglitazone Study Group: Cardiac and glycemic benefits of troglitazone treatment in NIDDM. *Diabetes* **46**: 433-439

Giaccari A, Morviducci L, Zorretta D, Sbraccia P, Leonetti F, Caiola S, Buongiorno A, Bonadonna RC, Tamburrano G (1995) In vivo effects of glucosamine on insulin secretion and insulin sensitivity in the rat: Possible relevance to the maladaptive responses to chronic hyperglycaemia. *Diabetologia* **38:** 518-524

Gimble JM, Robinson CE, Wu X, Kelly KA, Rodriguez BR, Kliewer SA, Lehmann JM, Morris DC (1996) Peroxisome proliferator-activated receptor-γ activation by thiazolidinediones induces adipogenesis in bone marrow stromal cells. *Molec Pharmacol* **50**: 1087-1094

Giordano M, Castellino P, Solini A, Canessa ML, DeFronzo RA (1997) Na^+/Li^+ countertransport activity in hypertensive non-insulin-dependent diabetic patients: role of insulin resistance and anti-hypertensive treatment. *Metabolism* **46**: 1316-1323

Giraudo SQ, Kotz CM, Grace MK, Levine AS, Billington CJ (1994) Rat hypothalamic NPY mRNA and brown fat uncoupling protein mRNA after high-carbohydrate or high-fat diets. *Am J Physiol* **266**: R1578-R1583

Glorian M, Franckhauser-Vogel S, Robin D, Robin P, Forest C (1998) Glucocorticoids repress induction by thiazolidinediones, fibrates, and fatty acids of phosphoenolpyruvate carboxykinase gene expression in adipocytes. *J Cell Biochem* **68**: 298-308

Goa KL, Barradell LB, Plosker GL (1996) Bezafibrate. An update of its pharmacology and use in the management of dyslipidaemia. *Drugs* **52**: 725-753

Gorla-Baiszczak A, Siegrist-Kaiser C, Boss O, Burger AG, Meier CA (2000) Expression of peroxisome proliferator-activated receptors in lean and obese Zucker rats. *Eur J Endocrinol* **142**: 71-78

Gorson DM (1999) Significant weight gain with rezulin therapy. *Arch Intern Med* **159**: 99

Gottlicher M, Widmark E, Li Q, Gustafsson JA (1992) Fatty acids activate a chimera of the clofibric acid-activated receptor and the glucocorticoid receptor. *Proc Natl Acad Sci USA* **89**: 4653-4657

Green LC, Wagner DA, Glogowski J, Skipper PL, Wishnok JS, Tannenbaum SR (1982) Analysis of nitrate, nitrite, and [15N]nitrate in biological fluids. *Anal Biochem* **126**: 13-138

Greene ME, Blumberg B, McBride OW, Yi YF, Kronquist K, Kwan K, Hsieh L, Greene G, Nimer SD (1995) Isolation of the human peroxisome proliferator activated receptor gamma cDNA: expression in hematopoietic cells and chromosomal mapping. *Gene Expr* **4**: 281-289

Guan Y, Zhang Y, Davis L, Breyer MD (1997) Expression of peroxisome proliferator-activated receptors in urinary tract of rabbits and humans. *Am J Physiol* **273**: F1013-F1022

Guerre-Millo M, Gervois P, Raspe E, Madsen L, Poulain P, Derudas B, Herbert J-M, Winegar DA, Willson TM, Fruchart J-C, Berge RK, Staels B (2000) Peroxisome proliferator-activated receptor α activators improve insulin sensitivity and reduce adiposity. *J Biol Chem* **275**: 16638-16642

Haendeler J, Zeiher AM, Dimmeler S (1999) Nitric oxide and apoptosis. *Vit Horm* **57**: 49-77

Halaas JL, Boozer C, Blair-West J, Fidahusein N, Denton DA, Friedman JM (1997) Physiological response to long-term peripheral and central leptin infusion in lean and obese mice. *Proc Natl Acad Sci USA* **94**: 8878-8883

Hallakou S, Doaré L, Foufelle F, Kergoat M, Guerre-Millo M, Berthault M-F, Dugail I, Morin J, Auwerx J, Ferré P (1997) Pioglitazone induces in vivo adipocyte differentiation in the obese Zucker *fa/fa* rat. *Diabetes* **46**: 1393-1399

Halle M, Berg A, Northoff H, Keul J (1998) Importance of TNF-α and leptin in obesity and insulin resistance: a hypothesis on the impact of physical exercise. *Exerc Immunol Rev* **4**: 77-94

Hardie LJ, Guilhot N, Trayhurn *P* (1996) Regulation of leptin production in cultured mature white adipocytes. *Horm Metab Res* **28**: 685-689

Harmon JS, Gleason CE, Stephan POT, *et al.* (2000) Bezafibrate, a lipid-lowering drug, improves insulin gene expression in the lean Zucker rat but not in the hyperglycemic Zucker diabetic fatty rat. *J Invest Med* **48** Suppl: 20A

Harris MI (1996) Impaired glucose tolerance—prevalence and conversion to NIDDM. *Diabetes Med* **13**: S9-S11

Harris PK, Kletzien RF (1994) Localization of a pioglitazone response element in the adipocyte fatty acid-binding protein gene. *Mol Pharmacol* **45**: 439-445

Harrold JA, Widdowson PS, Clapham JC, Williams G (2000a) Individual severity of dietary obesity in unselected Wistar rats: relationship with hyperphagia. *Am J Physiol* **279**: E340-E347

Harrold JA, Widdowson PS, Williams G (1999a) Altered energy balance causes selective changes in melanocortin-4 (MC4-R), but not melanocortin-3 (MC3-R), receptors in specific hypothalamic regions. Further evidence that activation of MC4-R is a physiological inhibitor of feeding. *Diabetes* **48**: 267-271

Harrold JA, Williams G, Widdowson PS (1999b) Changes in hypothalamic agouti-related protein (AGRP), but not α-MSH or pro-opiomelanocortin concentrations in dietary-obese and food-restricted rats. *Biochem Biophys Res Commun* **258**: 574-577

Harrold JA, Williams G, Widdowson PS (2000b) Early leptin response to a palatable diet predicts dietary obesity in rats: key role of melanocortin-4 receptors in the ventromedial hypothalamic nucleus. *J Neurochem* **74**: 1224-1228

Haubenwallner S, Essenburg AD, Barnett BC, Pape ME, DeMattos RB, Krause BR, Minton LL, Auerbach BJ, Newton RS, Leff T, Bisgaier CL (1995) Hypolipidemic activity of select fibrates correlates to changes in hepatic lipolipoprotein C-III expression: A potential physiologic basis for their mode of action. *J Lipid Res* **36**: 2541-2551

Heitmeier MR, Scarim AL, Corbett JA (1999) Double-stranded RNA inhibits β-cell function and induces islet damage by stimulating β-cell production of nitric oxide. *J Biol Chem* **274**: 12531-12536

Henry RR (1997) Thiazolidinediones. *Endocrinol Metab Clin North Am* **26**: 553-573

Hervey GR (1969) Regulation of energy balance. *Nature* **222**: 629-631

Hirshman MF, Fagnant PM, Horton ED, King PA, Horton ES (1995) Pioglitazone treatment for 7 days failed to correct the defect in glucose transport and glucose transporter translocation in obese Zucker rat (fa/fa) skeletal muscle plasma membranes. *Biochem Biophys Res Comm* **208**: 835-845

Hissin PJ, Karnieli E, Simpson IA, Salans LB, Cushman SW (1982) A possible mechanism of insulin resistance in the rat adipose cell with high-fat/low carbohydrate feeding. Depletion of intracellular glucose transport systems. *Diabetes* **31**: 589-592

Hofmann C, Lorenz K, Braithwaite SS Colca JR, Palazuk BJ, Hotamisligil GS, Spiegelman BM (1994) Altered gene expression for tumor necrosis factor-α and its receptors during drug and dietary modulation of insulin resistance. *Endocrinology* **134**: 264-270

Hopkins SJ (1985) Principal drugs. An alphabetical guide to modern therapeutic agents. Faber and Faber, London.

Hotamisligil GS, Arner P, Caro JF, Alkinson RL, Spiegelman BM (1995) Increased adipose tissue expression of tumor necrosis factor-alpha in human obesity and insulin resistance. *J Clin Invest* **95**: 2409-2415

Hotamisligil GS, Shargill NS, Spiegelman BM (1993) Adipose expression of tumor necrosis factor-α: a direct role in obesity-linked insulin resistance. *Science* **259**: 87-91

Hotamisligil GS, Spiegelman BM (1994) TNF-α: a key component of obesity-diabetes link. *Diabetes* **43**: 1271-1278

Hwa JJ, Ghibaudi L, Compton D, Fawzi AB, Strader CD (1996) Intracerebroventricular injection of leptin increases thermogenesis and mobilizes fat metabolism in *ob/ob* mice. *Horm Metab Res* **28**: 659-663

Ibrahimi A, Teboul L, Gaillard D, Amri E-Z, Ailhaud G, Young P, Cawthorne MA, Grimaldi PA (1994) Evidence for a common mechanism of action for fatty acids and thiazolidinedione antidiabetic agents on gene expression in preadipose cells. *Molec Pharmacol* **46**: 1070-1076

Ikeda H, Taketomi S, Sugiyama Y, Shimura Y, Sohda T, Meguro K, Fujita T (1990) Effects of pioglitazone on glucose and lipid metabolism in normal and insulin resistant animals. *Arzneim-Forsch/Drug Res* **40**: 156-162

Infinity™ Cholesterol Reagent package insert (2000) Sigma Diagnostics®, Inc., St. Louis, MO

Infinity™ Triglycerides Reagent package insert (2000) Sigma Diagnostics®, Inc., St. Louis, MO

Inoue I, Takahashi K, Katayama S, Harada Y, Negishi K, Itabashi A, Ishii J (1995) Effect of troglitazone (CS-045) and bezafibrate on glucose tolerance, liver glycogen synthase activity, and β-oxidation in fructose-fed rats. *Metabolism* **44**: 1626-1630

Ishii S, Wasaki M, Ohne T, Ueno H, Tanaka H (1996) MCC-555: A highly potent thiazolidinedione lacking hematological and cardiac side-effects. *Diabetes* **45** Suppl 2: 141A

Isseman I, Green S (1990) Activation of a member of the steroid hormone receptor superfamily by peroxisome proliferators. *Nature* **347**: 645-650

Iwanishi M, Kobayashi M (1993) Effect of pioglitazone on insulin receptors of skeletal muscle from high-fat-fed rats. *Metabolism* **42**: 1017-1021

Jebb, S (1999a) The weight of the nation. Obesity in the UK. Report commissioned by the Bread for Life Campaign, The Flour Advisory Bureau Ltd, London

Jebb, S (1999b) *Obesity matters* **2**: 6

Jeck T, Riesen WF, Keller U (1997) Comparison of bezafibrate and simvastatin in the treatment of dyslipidaemia in patients with NIDDM. *Diabet Med* **14**: 564-570

Jensen DR, Schlaepfer IR, Morin CL, Pennington DS, Marcell T, Ammon SM, Gutierrez-Hartmann A, Eckel RH (1997) Prevention of diet-induced obesity in transgenic mice overexpressing skeletal muscle lipoprotein lipase. *Am J Physiol* **273**: R683-R689

Johnson MD, Campbell LK, Campbell RK (1998) Troglitazone: review and assessment of its role in the treatment of patients with impaired glucose tolerance and diabetes mellitus. *Ann Pharmacother* **32**: 337-348

Jung RT (1997) Obesity and nutritional factors in the pathogenesis of non-insulin-dependent diabetes mellitus. In: Pickup J, Williams G (eds) *Textbook of diabetes*. Blackwell Science Ltd, Oxford, pp 19.1-19.23

Kahn CR, Chen L, Cohen SE (2000) Unraveling the mechanism of action of thiazolidinediones. *J Clin Invest* **106**: 1305-1307

Kahn SE, Andrikopoulos S, Verchere CB (1999) Islet amyloid: a long recognized but underappreciated pathological feature of type 2 diabetes. *Diabetes* **48**: 241-253

Kallen CB, Lazar MA (1996) Antidiabetic thiazolidinediones inhibit leptin (*ob*) gene expression in 3T3-L1 adipocytes. *Proc Natl Acad Sci USA* **93**: 5793-5796

Kaneko T (1997) Troglitazone (CS-045): a new antidiabetic agent. *Horm Metab Res* **29**: 203-213

Kaplan NM (1989) The deadly quartet. Upper-body obesity, glucose intolerance, hypertriglyceridemia, and hypertension. *Arch Intern Med* **149**: 1514-1520

Kastner P, Mark M, Chambon P (1995) Nonsteroid nuclear receptors: what are genetic studies telling us about their role in real life? *Cell* **83**: 859-869

Kawaguchi M, Koshimura K, Murakami Y, Tsumori M, Gonda T, Kato Y (1999) Antihypertensive effect of insulin via nitric oxide production in the Zucker diabetic fatty rat, an animal model for non-insulin-dependent diabetes mellitus. *Eur J Endocrinol* **140**: 341-349

Kawai K, Kawasaki-Tokui Y, Odaka T, Tsuruta F, Kazui M, Iwabuchi h, Nakamura T, Kinoshita T, Ikeda T, Yoshioka T, Komai T, Nakamura K-i (1997) Disposition and metabolism of the new oral antidiabetic drug troglitazone in rats, mice and dogs. *Drug Res* **47**: 356-368

Kawai T, Takei I, Oguma Y Ohashi N, Tokui M, Oguchi S, Katsukawa F, Hirose H, Shimada A, Watanabe K, Saruta T (1999) Effects of troglitazone on fat distribution in the treatment of male type 2 diabetes. *Metabolism* **48**: 1102-1107

Kawamori R, Kinoshita J, Ikeda M, Kubota M, Wada M, Kanda T, Ikebuchi M, Todo R, Yamasaki Y (1997a) Pioglitazone (AD-4833) enhances hepatic glucose uptake in NIDDM, an assessment by the euglycemic hyperinsulinemic clamp combined with oral glucose load. *Diabetes* **46** Suppl 1: 242A

Kawamori R, Kinoshita J, Ikeda M, Kubota M, Wada M, Kanda T, Ikebuchi M, Todo R, Yamasaki Y (1997b) Pioglitazone ameliorates insulin resistance in NIDDM. *Diabetologia* **40** Suppl 1: A306

Kazumi T, Yoshino G, Iwai M, Matsuba K, Matsushita M, Iwatani I, Kasama T, Yoshida M, Baba S (1990) Long-term effects of bezafibrate on in vivo VLDL-triglyceride production in the rat. *Diabetes Res Clin Pract* **9**: 163-168

Keen H, Barnes DJ (1997) The diagnosis and classification of diabetes mellitus and impaired glucose tolerance. In: Pickup J, Williams G (eds) *Textbook of diabetes*. Blackwell Science Ltd, Oxford, pp 2.1-2.10

Kelly IE, Han TS, Walsh K, Lean ME (1999) Effects of a thiazolidinedione compound on body fat and fat distribution of patients with type 2 diabetes. *Diabetes Care* **2**: 288-293

Kelly LJ, Vicario PP, Thompson GM, Candelore MR, Doebber TW, Ventre J, Wu MS, Meurer R, Forrest MJ, Conner MW, Cascieri MA, Moller DE (1998) Peroxisome proliferator-activated receptors gamma and alpha mediate in vivo regulation of uncoupling protein (UCP-1, UCP-2, UCP-3) gene expression. *Endocrinology* **139**: 4920-4927

Kemnitz JW, Elson DF, Roecker EB, Baum ST, Bergman RN, Meglasson MD (1994) Pioglitazone increases insulin sensitivity, reduces blood glucose, insulin, and lipid levels, and lowers blood pressure, in obese, insulin-resistant rhesus monkeys. *Diabetes* **43**: 204-211

Kieffer TJ, Heller RS, Leech CA, Holz GG, Habener JF (1997) Leptin suppression of insulin secretion by the activation of ATP-sensitive K+ channels in pancreatic beta-cells. *Diabetes* **46**: 1087-1093

Kim EM, Welch CC, Grace MK, Billington CJ, Levine AS (1998) Effects of palatibility-induced hyperphagia and food restriction on mRNA levels of neuropeptide-Y in the arcuate nucleus. *Brain Res* **806**: 117-121

Kliewer SA, Forman BM, Blumberg B, Ong ES, Borgmeyer U, Mangelsdorf DJ, Umesono K, Evans RM (1994) Differential expression and activation of a family of murine peroxisome proliferator-activated receptors. *Proc Natl Acad Sci USA* **91**: 7355-7359

Kliewer SA, Lenhard JM, Willson TM, Patel I, Morris DC, Lehmann JM (1995) A prostaglandin J_2 metabolite binds peroxisome proliferator-activated receptor γ and promotes adipocyte differentiation. *Cell* **83**: 813-819

Kobayashi M, Iwanishi M, Egawa K, Shigeta Y (1992) Pioglitazone increases insulin sensitivity by activating insulin receptor kinase. *Diabetes* **41**: 476-483

Kopelman PG (2000) Obesity as a medical problem. *Nature* **404**: 635-643

Koyama K, Shimabukuro M, Chen G, Wang M-Y, Lee Y, Kalra PS, Dube MG, Kalra SP, Newgard CB, Unger RH (1998) Resistance to adenovirally induced hyperleptinaemia in rat. Comparison of ventromedial hypothalamic lesions and mutated leptin receptor. *J Clin Invest* **102**: 728-733

Kraegen EW, Clark PW, Jenkins AB, Daley EA, Chisolm DJ, Storlien LH (1991) Development of muscle insulin resistance after liver insulin resistance in high-fat-fed rats. *Diabetes* **40**: 1397-1403

Kraegen EW, James DE, Storlien LH, Burleigh KM, Chisolm DJ (1986) In vivo insulin resistance in individual peripheral tissues of the high fat fed rat: assessment by euglycaemic clamp plus deoxyglucose administration. *Diabetologia* **29**: 192-198

Kruszynska YT (1997) Metabolic disturbances in diabetes mellitus. In: Pickup J, Williams G (eds) *Textbook of diabetes*. Blackwell Science Ltd, Oxford. pp 29.1-29.25

Lambe KG, Tugwood JD (1996) A human peroxisome-proliferator-activated receptor γ is activated by inducers of adipogenesis, including thiazolidinedione drugs. *Eur J Biochem* **239**: 1-7

Lee Y, Hirose H, Ohneda M, Johnson JH, McGarry JD, Unger RH (1994) Beta-cell lipotoxicity in the pathogenesis of non-insulin-dependent diabetes mellitus of obese rats: impairment in adipocyte-beta-cell relationships. *Proc Natl Acad Sci USA* **91**: 10878-10882

Lee Y, Hirose H, Zhou YT, Esser V, McGarry JD, Unger RH (1997) Increased lipogenic capacity of the islets of obese rats. A role in the pathogenesis of NIDDM. *Diabetes* **46**: 408-413

Lee Y-H, Sauer B, Gonzalez FJ (1998) Laron dwarfism and non-insulin-dependent diabetes mellitus in the Hnf-1α knockout mouse. *Mol Cell Biol* **18**: 3059-3068

Lefebvre A-M, Peinado-Onsurbe J, Leitersdorf I, Briggs MR, Paterniti JR, Fruchart J-C, Fievet C, Auwerx J, Staels B (1997) Regulation of lipoprotein metabolism by thiazolidinediones occurs through a distinct but complementary mechanism relative to fibrates. *Arterioscler Thromb Vasc Biol* **17**: 1756-1764

Lehmann JM, Moore LB, Smith-Oliver TA, Wilkison WO, Willson TM, Kliewer SA (1995) An antidiabetic thiazolidinedione is a high affinity ligand for peroxisome proliferator-activated receptor γ. *J Biol Chem* **270**: 12953-12956

Leroy P, Dessolin S, Villageois P, Chun Moon B, Friedman JM, Ailhaud G, Dani C (1996) Expression of *ob* gene in adipose cells. *J Biol Chem* **271**: 2365-2368

Levin BE (1999) Arcuate NPY neurons and energy homeostasis in diet-induced obese and resistant rats. *Am J Physiol* **276**: R382-R387

Levin BE, Dunn-Meynell AA (1997) Dysregulation of arcuate nucleus preproneuropeptide Y mRNA in diet-induced obese rats. *Am J Physiol* **272**: R1365-R1370

Levin BE, Dunn-Meynell AA, Balkan B, Keesey RE (1997) Selective breeding for diet-induced obesity and resistance in Sprague-Dawley rats. *Am J Physiol* **273**: R725-R730

Levin BE, Keesey RE (1998) Defense of differing body weight set points in diet-induced obese and resistant rats. *Am J Physiol* **274**: R412-R419

Levin BE, Triscari J, Hogan S, Sullivan AC (1987) Resistance to diet-induced obesity: food intake, pancreatic sympathetic tone, and insulin. *Am J Physiol* **252**: R471-R478

Levin BE, Triscari J, Sullivan AC (1983) Relationship between sympathetic activity and diet-induced obesity in two rat strains. *Am J Physiol* **245**: R367-R371

Levin N, Nelson C, Gurney A, Vandlen R, De Sauvage F (1996) Decreased food intake does not completely account for adiposity reduction after *ob* protein infusion. *Proc Natl Acad Sci USA* **93**: 1726-1730

Lin L, York DA, Bray GA (1996) Comparison of Osborne-Mendel and S5B/PL strains of rat: central effects of galanin, NPY, β-casomorphin and CRH on intake of high-fat and low-fat diets. *Obes Res* **4**: 117-124

Lin X, Braymer HD, Bray GA, York DA (1998) Differential expression of insulin receptor tyrosine kinase inhibitor (fetuin) gene in a model of diet-induced obesity. *Life Sci* **63**: 145-153

Linco mouse leptin RIA kit package insert (1997) Linco Research, Inc., St. Louis, MO

Loviscach M, Nikoulina S, Carter L, Rehman N, Ciaraldi TP, Henry RR (1999) The acute action of troglitazone involves signaling pathways different from insulin. *Diabetes* **48**: 335A

Lowell BB, Spiegelman BM (2000) Towards a molecular understanding of adaptive thermogenesis. *Nature* **404**: 652-660

Lowenstein CJ, Dinerman JL, Snyder SH (1994) Nitric oxide: a physiological messenger. *Ann Intern Med* **120**: 227-237

Lowry OH, Rosebrough NJ, Farr AL, Randall RJ (1951) Protein measurements with the Folin phenol reagent. *J Biol Chem* **193**: 265-275

Maegawa H, Tachikawa-Ide R, Ugi S, Iwanishi M, Egawa K, Kikkawa R, Shigeta Y, Kashiwagi A (1993) Pioglitazone ameliorates high glucose induced desensitization of insulin receptor kinase in Rat 1 fibroblasts in culture. *Biochem Biophys Res Commun* **197**: 1078-1082

Martin G, Schoonjans K, Lefebvre A-M, Staels B, Auwerx J (1997) Co-ordinate regulation of the expression of the fatty acid transport protein and acyl-CoA synthetase genes by PPARα and PPARγ activators. *J Biol Chem* **272**: 28210-28217

Matsuda J, Hosoda K, Itoh H, Son C, Doi K, Hanaoka I, Inoue G, Nishimura H, Yoshimasa Y, Yamori Y, Odaka H, Nakao, K (1998) Increased adipose expression of the uncoupling protein-3 gene by thiazolidinediones in Wistar fatty rats and in cultured adipocytes. *Diabetes* **47**: 1809-1814

Matsuda J, Hosoda K, Itoh H, Son C, Doi K, Tanaka T, Fukunaga Y, Inoue G, Nishimura H, Yoshimasa Y, Yamori Y, Nakao K (1997) Cloning of rat uncoupling protein-3 and uncoupling protein-2 cDNAs: their gene expression in rats fed high-fat diet. *FEBS Lett* **418**: 200-204

Matsui H, Okumura K, Kawakami K, Hibino M, Toki Y, Ito T (1997) Improved insulin sensitivity by bezafibrate in rats: relationship to fatty acid composition of skeletal-muscle triglycerides. *Diabetes* **46**: 348-353

Matthews DR, Clark A (1997) B-cell defects and pancreatic abnormalities in non-insulin-dependent diabetes mellitus. In: Pickup J, Williams G (eds) *Textbook of diabetes*. Blackwell Science Ltd, Oxford, pp 21.1-21.16

Matthews DR, Hosker JP, Rudenski AS, Naylor BA, Treacher DF, Turner RC (1985) Homeostasis model assessment: insulin resistance and β-cell function from fasting plasma glucose and insulin concentration in man. *Diabetologia* **28**: 412-419

McCormack JG, Dean HG, Jennings GJ, Blundell JE (1989) Effects of chronic low doses of *d*-Fenfluramine on weight gain and calorie intake, brown adipose tissue thermogenic parameters and brain neurotransmitter content in rats fed chow or palatable diets. *Int J Obes* **13**: 635-633

McDaniel ML, Kodon G, Hill JR, Marshall JA, Corbett JA (1996) Cytokines and nitric oxide in islet inflammation and diabetes. *Proc Soc Exp Biol Med* **211**: 24-32

Milburn JL, Hirose H, Lee YH, Nagasawa Y, Ogawa A, Ohneda M, BeltrandelRio H, Newgard CB, Johnson JH, Unger RH (1995) Pancreatic β-cells in obesity: evidence for induction of functional, morphologic, and metabolic abnormalities by increased long chain fatty acids. *J Biol Chem* **270**: 1295-1299

Miles PD, Romeo OM, Higo K, Cohen A, Rafaat K, Olefsky JM (1997) TNF-alpha-induced insulin resistance in vivo and its prevention by troglitazone. *Diabetes* **46**: 1678-1683

Mukherjee R, Jow L, Croston GE, Paterniti JR (1997) Identification, characterization, and tissue distribution of human peroxisome proliferator-activated receptor (PPAR) isoforms PPAR gamma2 versus PPAR gamma1 and activation with retinoid X receptor agonists and antagonists. *J Biol Chem* **272**: 8071-8076

Mukherjee R, Jow L, Noonan D, McDonnel DP (1994) Human and rat peroxisome proliferator activated receptors (PPARs) demonstrate similar tissue distribution but different responsiveness to PPAR activators. *J Steroid Biochem Mol Biol* **51**: 157-166

Murakami K, Tobe K, Ide T, Mochizuki T, Ohashi M, Akanuma Y, Yazaki Y, Kadowski T (1998) A novel insulin sensitizer acts as a coligand for peroxisome proliferator-activated receptor-alpha (PPAR-alpha) and PPAR-gamma: effect of PPAR-alpha activation on abnormal lipid metabolism in liver of Zucker fatty rats. *Diabetes* **47**: 1841-1847

Murase K, Odaka H, Suzuki M, Tayuki N, Ikeda H (1998) Pioglitazone time-dependently reduces tumour necrosis factor-α level in muscle and improves metabolic abnormalities in Wistar fatty rats. *Diabetologia* **41**: 257-264

Murphy GJ & Holder JC (2000) PPAR-γ agonists: therapeutic role in diabetes, inflammation and cancer. *TiPS* **21**: 469-474

Nagle DL, McGrail SH, Vitale J, Woolf EA, Dussault Jr BJ, DiRocco L, Holmgren L, Montagno J, Bork P, Huszar D, Fairchild-Huntress V, Ge P, Keilty J, Ebeling C, Baldini L, Gilchrist J, Burn P, Carlson GA, Moore KJ (1999) The mahogany protein is a receptor involved in suppression of obesity. *Nature* **398**: 148-152

Nakamura Y, Ohya Y, Onaka U, Fujii K, Abe I, Fujishima M (1998) Inhibitory action of insulin-sensitizing agents on calcium channels in smooth muscle cells from resistance arteries of guinea-pig. *Br J Pharmacol* **123**: 675-682

Nishimura Y, Inoue Y, Takeuchi H, Oka Y (1997) Acute effects of pioglitazone on glucose metabolism in perfused rat liver. *Acta Diabetol* **34**: 206-210

Nisoli E, Carruba MO (2000) Apoptosis of adipocytes. *Obesity matters* **3**: 11-14

Nolan JJ, Ludvik B, Beerdsen *P*, Joyce M, Olefsky J (1994) Improvement in glucose tolerance and insulin resistance in obese subjects treated with troglitazone. *N Engl J Med* **331**: 1188-1193

Nolan JJ, Olefsky JM, Nyce MR, Considine RV, Caro JF (1996) Effect of troglitazone on leptin production. Studies in vitro and in human subjects. *Diabetes* **45**: 1276-1278

Nolte LA, Hansen PA, Chen MM, Schluter JM, Galve EA, Holliszy JO (1998) Short-term exposure to tumor necrosis factor-alpha does not affect insulin-stimulated glucose uptake in skeletal muscle. *Diabetes* **47**: 721-726

Oakes ND, Camilleri S, Furler SM, Chisholm DJ, Kraegen EW (1997) The insulin sensitizer, BRL 49653, reduces systemic fatty acid supply and utilization and tissue lipid availability in the rat. *Metabolism* **46**: 935-942

Oakes ND, Kennedy CJ, Jenkins AB, Laybutt DR, Chisholm DJ, Kraegen EW (1994) A new antidiabetic agent, BRL 49653, reduces lipid availability and improves insulin action and glucoregulation in the rat. *Diabetes* **43**: 1203-1210

O'Brien M, Okragly A, Warner T, Kalil R, Wolswijk G (1998) DeadEnd™ colorimetric apoptosis detection system: applications in pathology. *Promega Notes* **69**: 2-9

Ogawa S, Takeuchi K, Sugimura K, Fukuda M, Lee R, Ito S, Sato T (2000) Bezafibrate reduces blood glucose in type 2 diabetes mellitus. Metabolism **49**: 331-334

Ohlson LO, Larsson B, Svärdsudd K, Welin H, Eriksson H, Wilhemsen L, Björnstorp P, Tibblin G (1985) The influence of body fat distribution on the incidence of diabetes mellitus: 13.5 years of follow-up of the participants in the study of men born in 1913. *Diabetes* **34**: 1055-1058

Ohneda M, Inman LR, Unger RH (1995) Caloric restriction in obese prediabetic rats prevents ß-cell depletion, loss of ß-cell GLUT2 and glucose incompetence. *Diabetologia* **38**: 173-179

Ohneda M, Johnson JH, Lee YH, Nagasawa Y, Unger RH (1994) Post-GLUT-2 defects in beta-cells of non-insulin-dependent diabetic obese rats. *Am J Physiol* **267**: E968-E974

Okuno A, Ikeda K, Shiota M, Fujiwara T, Yoshioka S, Sugano T. Horikoshi H (1997) Acute effects of troglitazone on glucose metabolism in the absence or presence of insulin in perfused rat hindlimb. *Metabolism* **46**: 716-721

Ookuma K, Barton C, York DA, Bray GA (1998) Differential response to kappa-opioidergic agents in dietary fat selection between Osborne-Mendel and S5B/P1 rats. *Peptides* **19**: 141-147

Orci L, Ravazzola M, Baetens D, Inman L, Amherdt M, Peterson R, Newgard CB, Johnson JH, Unger RH (1990) Evidence that down-regulation of β-cell glucose transporter in non-insulin-dependent diabetes may be the cause of diabetic hyperglycaemia. *Proc Natl Acad Sci USA* **87**: 9953-9957

Oshida Y, Kako M, Nakai N, Shimomura Y, Li L, Sato J, Ohsawa I, Sato Y (1999) Troglitazone improves insulin-stimulated glucose utilization associated with an increased muscle glycogen content in obese Zucker rats. *Endocr J* **46**: 723-730

Ozel B, Youngren JF, Kim JK, Goldfine ID, Sung CK, Youn JH (1996) The development of insulin resistance with high fat feeding in rats does not involve either decreased insulin receptor tyrosine kinase activity or membrane glycoprotein PC-1. *Biochem Mol Med* **59**: 174-181

Pagliassotti MJ, Knobel SM, Shahrokhi KA, Manzo AM, Hill JO (1994) Time course of adaptation to a high-fat diet in obesity-resistant and obesity-prone rats. *Am J Physiol* **267**: R659-R664

Panz VR, Wing JR, Raal FJ, Kedda MA, Joffe BI (1997) Improved glucose tolerance after effective lipid-lowering therapy with bezafibrate in a patient with lipoatrophic diabetes mellitus: a putative role for Randle's cycle in its pathogenesis. *Clin Endocrinol* **46**: 365-368

Patel J, Anderson RJ, Rappaport EB (1999) Rosiglitazone monotherapy improves glycaemic control in patients with type 2 diabetes: a twelve-week, randomized, placebo-controlled study. *Diabetes Obes Metab* **1**: 165-172

Patel J, Miller E, Hu J, Granett J (1997) BRL 49653 (a thiazolidinedione) improves glycemic control in NIDDM patients. *Diabetes* **46** Suppl 1: 150A

Patel J, Miller E, Patwardhan R (1998) The Rosiglitazone 011 Study Group: Rosiglitazone (BRL 49653) monotherapy has significant glucose lowering effect in type 2 diabetic patients. *Diabetes* **47** Suppl 1: 17A

Paulik MA, Lenhard JM (1997) Thiazolidinediones inhibit alkaline phosphatase activity while increasing expression of uncoupling protein, deiodinase, and increasing mitochondrial mass in C3H10T1/2 cells. *Cell Tissue Res* **290**: 79-87

Pearson SL, Cawthorne MA, Clapham JC, Dunmore SJ, Holmes SD, Moore GBT, Smith SA, Tadayyon M (1996) The thiazolidinedione insulin sensitiser, BRL 49653, increases the expression of PPAR-γ and aP_2 in adipose tissue of high-fat-fed rats. *Biochem Biophys Res Comm* **229**: 752-757

Peterson RG (1994) The Zucker diabetic fatty (ZDF) rat. In: Shafrir E (ed) *Lessons from animal diabetes*. Smith-Gordon, London, pp 225-230

Pharmacia Insulin RIA 100 package insert (1998) Pharmacia & Upjohn Diagnostics AB, Uppsala, Sweden

Pick A, Clark J, Kubstrup C, Levisetti M, Pugh W, Bonner-Weir S, Polonsky KS (1998) Role of apoptosis in failure of β-cell mass compensation for insulin resistance and β-cell defects in the male Zucker Diabetic Fatty rat. *Diabetes* **47**: 358-364

Pickavance L, Buckingham R, Wilding J (1999a) Insulin-sensitising action of rosiglitazone is enhanced by food restriction. *Diabetologia* **42** Suppl 1: A181

Pickavance L, Buckingham R, Wilding J (2001) Insulin-sensitising action of rosiglitazone is enhanced by preventing hyperphagia. *Diabetes Obes Metab* **3**: 171-80

Pickavance L, Tadayyon M, Widdowson P, Buckingham R, Wilding J (1998a) Therapeutic index for rosiglitazone in dietary obese rats and effects on body weight and plasma leptin. *British Diabetic Association Meeting, Harrogate*

Pickavance L, Tadayyon M, Widdowson PS, Buckingham RE, Wilding JPH (1999b) Therapeutic index for rosiglitazone in dietary obese rats: separation of efficacy and haemodilution. *Br J Pharmacol* **128**: 1550-1576

Pickavance L, Widdowson PS, Foster JR, Ishii S, Tanaka H, Williams G (1999c) The thiazolidinedione, MCC-555, prevents nitric oxide synthase induction in the pancreas of the ZDF rat. *Br J Pharmacol* **128**: 116P

Pickavance L, Widdowson PS, King P, Ishii S, Tanaka H, Williams G (1998b) The development of overt diabetes in young Zucker Diabetic Fatty (ZDF) rats and the effects of chronic MCC-555 treatment. *Br J Pharmacol* **125**: 767-770

Pickavance LC, Widdowson PS, Vernon RG, Williams G (1999d) Neuropeptide Y receptor alterations in the hypothalamus of lactating rats. *Peptides* **20**: 1055-1060

Pinkney JH, Denver AE, Foyle WJ, Foster C, Yudkin JS (1995) Insulin resistance and not hyperinsulinaemia determines erythrocyte Na^+/Li^+ countertransport in non-insulin-dependent diabetes mellitus. *J Hum Hypertens* **9**: 685-686

Polonsky KS, Sturgis J, Bell GI (1996) Non-insulin-dependent diabetes mellitus—a

genetically programmed failure of the beta cell to compensate for insulin resistance. *New Engl J Med* **334**: 777-783

Prentice A (1998) Obesity—the inevitable penalty of civilization? *Obesity matters* **1**: 17-20

Qian H, Hansman GJ, Compton MM, Azain MJ, Hartzell DL, Baile CA (1998) Leptin regulation of peroxisome proliferator-activated receptor-gamma, tumor necrosis factor factor, and uncoupling protein-2 expression in adipose tissues. *Biochem Biophys Res Commun* **246**: 660-667

Raman P, Foster SE, Stokes MC, Strenge JK, Judd RL (1998) Effect of troglitazone (Rezulin) on fructose 2,6-biphosphate concentration and glucose metabolism in isolated rat hepatocytes. *Life Sci* **62**: PL89-94

Randle PJ, Hales CN, Garland PB, Newsholme EA (1963) The glucose fatty-acid cycle. Its role in insulin sensitivity and the metabolic disturbances of diabetes mellitus. *Lancet* April **13**: 7285-7290

Rang HP, Dale MM, Ritter JM (2000) *Pharmacology*. 4th ed. Harcourt Publishers, Edinburgh

Ranganathan S, Kern PA (1998) Thiazolidinediones inhibit lipoprotein lipase activity in adipocytes. *J Biol Chem* **273**: 26117-26122

Reaven GM (1988) Role of insulin resistance in human disease. *Diabetes* **37**: 1595-1607

Reginato MJ, Bailey ST, Krakow SL, Minami C, Ishii S, Tanaka H, Lazar MA (1998) A potent antidiabetic thiazolidinedione with unique peroxisome proliferator-activated receptor γ-activating properties. *J Biol Chem* **273**: 32679-32684

Ren J, Dominguez LJ, Sowers JR, Davidoff AJ (1996) Troglitazone attenuates high-glucose-induced abnormalities in relaxation and intracellular calcium in rat ventricular myocytes. *Diabetes* **45**: 1822-1825

Ribon V, Johnson JH, Camp HS, Saltiel AR (1998) Thiazolidinediones and insulin resistance: peroxisome proliferatoractivated receptor gamma activation stimulates expression of the CAP gene. *Proc Natl Acad Sci USA* **95**: 14751-14756

Ricquier D (1998) Candidate genes for obesity: where are we now? *Obesity matters* **1**: 15-16

Rieusset J, Auwerx J, Vidal H (1999) Regulation of gene expression by activation of the peroxisome proliferator-activated receptor γ with rosiglitazone (BRL 49653) in human adipocytes. *Biochem Biophys Res Comm* **265**: 265-271

Rothwell NJ, Stock MJ (1986) Brown adipose tissue and diet-induced thermogenesis. In: Trayhurn P, Nicholls DG (eds) *Brown adipose tissue*. Edward Arnold, London, pp 269-298

Rothwell NJ, Stock MJ (1988) The cafeteria diet as a tool for studies of thermogenesis. *J Nutr* **118**: 925-928

Sagatal package insert (1994) Rhône Mérieux, Harlow, Essex, U.K.

Saltiel AR, Horikoshi H (1995) Thiazolidinediones are novel insulin-sensitizing agents. *Curr Opin Endocrinol Diabetes* **2**: 341-347

Saltiel AR, Olefsky, JM (1996) Thiazolidinediones in the treatment of insulin resistance and type II diabetes. *Diabetes* **45**: 1661-1669

Sambrook J, Fritsch EF, Maniatis T (1989) Extraction, purification, and analysis of messenger RNA from eukaryotic cells. In: Nolan C (ed) *Molecular cloning. A laboratory manual.* Cold Spring Harbor Laboratory Press, New York, pp 7.3-7.84

Sandouk T, Reda D, Hofmann C (1993) The antidiabetic agent pioglitazone increases expressionof glucose transporters in 3T3-F442A cells by increasing messenger ribonucleic acid transcript stability. *Endocrinology* **133**: 352-359

Scarpace PJ, Matheny M, Pollock BH, Tumer N (1997) Leptin increases uncoupling protein expression and energy expenditure. *Am J Physiol* **273**: E226-E230

Schmidt A, Endo N, Rutledge SJ, Vogel R, Shinar D, Rodan GA (1992) Identification of a new member of the steroid hormone receptor superfamily that is activated by a peroxisome proliferator and fatty acids. *Mol Endocrinol* **6**: 1634-1641

Schmitz-Peiffer C, Oakes ND, Browne CL, Kraegen EW, Biden TJ (1997) Reversal of chronic alterations of skeletal muscle protein kinase C from fat-fed rats by BRL-49653. *Am J Physiol* **273**: E915-E921

Schoonjans K, Staels B, Auwerx J (1996) The peroxisome proliferator activated receptors (PPARs) and their effects on lipid metabolism and adipocyte differentiation. *Biochim Biophys Acta* **1302**: 93-109

Schwartz MW, Baskin DG, Bukowski TR, Kuijper JL, Foster D, Lasser G, Prunkard DE, Porte Jr D, Woods SC, Seeley RJ, Weigle DS (1996) Specificity of leptin action on elevated blood glucose and hypothalamic neuropeptide Y gene expression in *ob/ob* mice. *Diabetes* **45**: 531-535

Schwartz MW, Figlewicz DP, Baskin DG, Woods SC, Porte D (1992) Insulin in the brain: a hormonal regulator of energy balance. *Endocrine Rev.* **13**: 387-413

Schwartz MW, Woods SC, Porte Jr D, Seeley RJ, Baskin DG (2000) Central nervous system control of food intake. *Nature* **404**: 661-671

Sethi JK, Hotamisligil GS (1999) The role of TNFα in adipocyte metabolism. *Cell Dev Biol* **10**: 19-29

Shafrir E (2000) Overnutrition in spiny mice (*Acomys cahirinus*): beta-cell expansion leading to rupture and overt diabetes on fat-rich diet and protective

energy-wasting elevation in thyroid hormone on sucrose-rich diet. *Diabetes Metab Res Rev* **16**: 94-105

Shao D, Rangwala SM, Bailey ST, Krakow SL, Reginato MJ, Lazar MA (1998) Interdomain communication regulating ligand binding by PPAR-γ. *Nature* **396**: 377-380

Shibata T, Matsui K, Nagao K, Shinkai H, Yonemori F, Wakitani K (1999) Pharmacological profiles of a novel oral antidiabetic agent, JTT-501, an isoxazolidinedione derivative. *Eur J Pharmacol* **364**: 211-219

Shibata T, Matsui K, Yonemori F, Wakitani K (1998) JTT-501, a novel oral antidiabetic agent, improves insulin resistance in genetic and non-genetic insulin-resistant models. *Br J Pharmacol* **125**: 1744-1750

Shibuya A, Watanabe M, Fujita Y, Saigenji K, Kuwao S, Takahashi H, Takeuchi H (1998) An autopsy case of troglitazone-induced fulminant hepatitis. *Diabetes Care* **21**: 2140-2143

Shimabukuro M, Higa M, Zhou Y-T, Wang M-Y, Newgard CB, Unger RH (1998a) Lipoapoptosis in β-cells of obese pre-diabetic *fa/fa* rats. *J Biol Chem* **273**: 32487-32490

Shimabukuro M, Koyama K, Lee Y, Unger RH (1997a) Leptin- or troglitazone-induced lipopenia protects islets from interleukin 1ß cytotoxicity. *J Clin Invest* **100**: 1750-1754

Shimabukuro M, Ohneda M, Lee YH, Unger RH (1997b) Role of nitric oxide in obesity-induced ß-cell disease. *J Clin Invest* **100**: 290-295

Shimabukuro M, Zhou Y-T, Lee Y, Unger RH (1998b) Troglitazone lowers islet fat and restores beta cell function of Zucker Diabetic Fatty rats. *J Biol Chem* **273**: 3547-3550

Shimabukuro M, Zhou Y-T, Levi M, Unger RH (1998c) Fatty acid-induced β cell apoptosis: A link between obesity and diabetes. *Proc Natl Acad Sci USA* **95**: 2498-2502

Shimizu H, Tsuchiya T, Sato N, Shimomura Y, Kobayashi I, Mori M (1998) Troglitazone reduces plasma leptin concentration but increases hunger in NIDDM patients. *Diabetes Care* **21**: 1470-1474

Shimokawa T, Kato M, Watanabe Y, Hirayama R, Kurosaki E, Shikama H, Hashimoto S (1998) In vivo effects of pioglitazone on uncoupling protein-2 and –3 mRNA levels in skeletal muscle of hyperglycemic KK mice. *Biochem Biophys Res Comm* **251**: 374-378

Sidlo J, Zaviacic M, Kvasnicka P (1995) Night and day differences in the food-intake of laboratory rats Wistar and Koletsky strains. *Bratisl Lek Listy* **96**: 655-657

Smith SA, Lister CA, Hughes MG, Buckingham RE (1997) The PPAR γ agonist, BRL 49653, prevents progression to diabetes in Zucker diabetic fatty rats. *Diabetologia* **4** Suppl 1: A46

Solomon SS, Mishra SK, Cwik C, Rajanna B, Postlethwaite AE (1997) Pioglitazone and metaformin reverse insulin resistance induced by tumor necrosis factor-alpha in liver cells. *Horm Metab Res* **29**: 379-82

Song J, Walsh MF, Igwe R, Ram JL, Barazi M, Dominguez LJ, Sowers JR (1997) Troglitazone reduces contraction by inhibition of vascular smooth muscle cell Ca^{2+} currents and not endothelial nitric oxide production. *Diabetes* **46**: 659-664

Souza SC, Yamamoto MT, Franciosa MD, Lien *P*, Greenberg AS (1998) BRL 49653 blocks the lipolytic actions of tumor necrosis factor-α. A potential new insulin-sensitizing mechanism for thiazolidinediones. *Diabetes* **47**: 691-695

Spiegelman BM (1998) PPAR-gamma: adipogenic regulator and thiazolidinedione receptor. *Diabetes* **47**: 507-514

Sreenan S, Keck S, Fuller T, Cockburn B, Burant CF (1999) Effects of troglitazone on substrate storage and utilization in insulin-resistant rats. *Am J Physiol* **276**: E1119-E1129

Sreenan S, Sturgis J, Pugh W, Burant CF, Polonsky KS (1996) Prevention of hyperglycemia in the Zucker diabetic fatty rat by treatment with metformin or troglitazone. *Am J Physiol* **271**: E742-E747

Staels B, Schoonjans K, Fruchart JC, Auwerx J (1997) The effects of fibrates and thiazolidinediones on plasma triglyceride metabolism are mediated by distinct peroxisome proliferator activated receptors (PPARs). *Biochimie* **79**: 95-99

Steele R (1959) Fluences of glucose loading and of injected insulin on hepatic glucose output. *Ann NY Acad Sci* **82**: 420-430

Stein DT, Esser V, Stevenson BE, Lane KE, Whiteside JH, Daniels MB, Chen S, McGarry JD (1996) Essentiality of circulating fatty acids for glucose-stimulated insulin secretion in the fasted rat. *J Clin Invest* **97**: 2728-2735

Steppan CM, Bailey ST, Bhat S, Brown EJ, Banerjee RR, Wright CM, Patel HR, Ahima RS, Lazar MA (2001) The hormone resistin links obesity to diabetes. *Nature* **409**: 307-312

Stock M (1999) *Obesity matters* **2**: 5

Storlien LH, James DE, Burleigh KM, Chisolm DJ, Kraegen EW (1986) Fat feeding causes widespread *in vivo* insulin resistance, decreased energy expenditure, and obesity in rats. *Am J Physiol* **251**: E576-E583

Surwit RS, Petro AE, Parekh P, Collins S (1997) Low plasma leptin in response to dietary fat in diabetes- and obesity-prone mice. *Diabetes* **46**: 1516-1520

Susulic VS, Lowell BB (1996) Brown adipose tissue and the regulation of body fat stores. *Curr Opin Endo Diabetes* **3**: 44-50

Sympathetic nervous system, The (1998) In: Abbot C (ed) *Obesity*. Colwood House Medical Publications (UK) Ltd, Berkshire

Tachi N, Tomogane H, Yokoyama A (1981) Diurnal patterns of food intake and plasma corticosterone levels in lactating rats. *Physiol Behav* **27**: 481-486

Tai T-AC, Jennermann C, Brown KK, Oliver BB, MacGinnitie MA, Wilkison WO, Brown HR, Lehmann JM, Kliewer SA, Morris DC, Graves RA (1996) Activation of the nuclear receptor peroxisome proliferator-activated receptor γ promotes brown adipocyte differentiation. *J Biol Chem* **271**: 29909-29914

Tang Y, Osawa H, Onuma H, Nishimiya T, Ochi M, Makino H (1999) Improvement in insulin resistance and the restoration of reduced phosphodiesterase 3B gene expression by pioglitazone in adipose tissue of obese diabetic KKAy mice. *Diabetes* **48**: 1830-1835

Tang-Christensen M, Larsen PJ, Thulesen J, Rømer J, Vrang N (2000) The proglucagon-derived peptide, glucagon-like peptide-2, is a neurotransmitter involved in the regulation of food intake. *Nature Med* **6**: 802-807

Terrettaz J, Jeanrenaud B (1983) In vivo hepatic and peripheral insulin resistance in genetically obese (*fa/fa*) rats. *Endocrinology* **112**: 1346-1351

Teruel T, Clapham JC, Smith SA (1999) PPARα activation by Wy 14643 induces transactivation of the rat UCP-1 promoter without increasing UCP-1 mRNA levels and attenuates PPARγ-mediated increases in UCP-1 mRNA levels induced by rosiglitazone in fetal rat brown adipocytes. *Biochem Biophys Res Comm* **264**: 311-315

Teruel T, Smith S, Clapham JC (1999) Rosiglitazone and Wy 14643 act synergistically to enhance UCP-3 expression in brown adipocytes. *Diabetes* **48**: 266A

Trayhurn P, Duncan JS (1994) Rapid chemiluminescent detection of the mRNA for uncoupling protein in brown adipose tissue by Northern hybridization with a 32-mer oligonucleotide end-labelled with digoxigenin. *Int J Obesity* **18**: 449-452

Trayhurn P, Duncan JS, Rayner DV (1995) Acute cold-induced suppression of *ob* (obese) gene expression in white adipose tissue of mice: mediation by the sympathetic system. *Biochem J* **311**: 729-733

Tremblay A, Imbeault P, Chevrier J, Richard D (1999) Obesity as a response to environmental stress and pollution. *Obesity matters* **2**: 14-16

Tri Reagent™ technical bulletin (1998) Sigma, St Louis, MO

Tsuboyama-Kasaoka N, Tsunoda N, Maruyama K, Takahashi M, Kim H, Ikemoto S, Ezaki O (1998) Up-regulation of uncoupling protein 3 (UCP3) mRNA by exercise training and down-regulation of UCP3 by denervation in skeletal muscles. *Biochem Biophys Res Comm* **247**: 498-503

Turner NC, Clapham JC (1998) Insulin resistance, impaired glucose tolerance and non-insulin-dependent diabetes, pathologic mechanisms and treatment: current status and therapeutic possibilities. *Prog Drug Res* **51**: 33-94

Type II diabetes (1996) In: Weitkamp E (ed) *Obesity*. Colwood House Medical Publications (UK) Ltd, Berkshire

UK Prospective Diabetes Study Group (1998) Intensive blood-glucose control with sulphonylureas or insulin compared with conventional treatment and risk of complications in patients with type 2 diabetes (UKPDS 33). UK Prospective Diabetes Study (UKPDS) Group. *Br Med J* **317**: 703-713

Unger RH (1991) Diabetic hyperglycaemia: Link to impaired glucose transport in pancreatic β-cells. *Science* **251**: 1200-1205

Unger RH (1995) Lipotoxicity in the pathogenesis of obesity-dependent NIDDM: Genetic and clinical implications. *Diabetes* **44**: 863-870

Unger RH (1997) How obesity causes diabetes in Zucker Diabetic Fatty rats. *Trends Endocrinol Metab* **7**: 276-282

University's accreditation scheme training group. Home Office licensees induction training notes (1995) Module 4, University of Liverpool, pp. 3-5

Upton R, Widdowson PS, Ishii S, Tanaka H, Williams (1998) Improved metabolic status and insulin sensitivity in obese fatty (*fa/fa*) Zucker rats and Zucker Diabetic Fatty (ZDF) rats treated with the thiazolidinedione, MCC-555. *Br J Pharmacol* **125**: 1708-1714

Upton R, Widdowson PS, Kadowaki S, Williams G (1997) Improved insulin sensitivity in Zucker and ZDF rats following chronic treatment with the novel thiazolidinedione, MCC-555. *Br J Pharmacol* **122**: 149P

Uysal KT, Wiesbrock SM, Marino MW, Hotamisligil GS (1997) Protection from obesity-induced insulin resistance in mice lacking TNF-alpha function. *Nature* **389**: 610-614

Van Heek M, Compton DS, France CF, Tedesco RP, Fawzi AB, Graziano MP, Sybertz EJ, Strader CD, Davis Jr HR (1997) Diet-induced obese mice develop peripheral, but not central, resistance to leptin. *J Clin Invest* **99**: 385-390

Vander AJ, Sherman JH, Luciano, DS (1985) *Human physiology. The mechanisms of body function.* McGraw-Hill, Toronto

Vaisse C (1999) Melanocortin-4 receptor: from molecule to man. *Obesity matters* **2**: 23-26

Vaisse C, Halaas JL, Horvath CM Darnell Jr JE, Stoffel M, Friedman JM (1996) Leptin activation of Stat3 in the hypothalamus of wild-type and *ob/ob* mice but not *db/db* mice. *Nature Genet* **14**: 95-97

Verma S, Bhanot S, Arikawa E, Yao L, McNeill JH (1998) Direct vasodepressor effects of pioglitazone in spontaneously hypertensive rats. *Pharmacology* **56**: 7-16

Vettor R, Pagano C, Granzotto M, Englaro P, Angeli P, Blum WF, Federspil G, Rohner-Jeanrenaud F, Jeanrenaud B (1998) Effects of intravenous neuropeptide Y on insulin secretion and insulin sensitivity in skeletal muscle in normal rats. *Diabetologia* **41:** 1361-1367

Vidal-Puig AJ, Considine RV, Jimenez-Liñan M, Werman A, Pories WJ, Caro JF, Flier JS (1997) Peroxisome proliferator-activated receptor gene expression in human tissues. Effects of obesity, weight loss, and regulation by insulin and glucocorticoids. *J Clin Invest* **99**: 2416-2422

Viguerie-Bascands N, Saulnier-Blache J-S, Dandine M, Dauzats M, Daviaud D, Langin D (1999) Increase in uncoupling protein-2 mRNA expression by BRL49653 and bromopalmitate in human adipocytes. *Biochem Biophys Res Comm* **256**: 138-141

Walker AB, Naderali EK, Chattington PD, Buckingham RE, Williams G (1998) Differential vasoactive effects of the insulin sensitizers rosiglitazone (BRL 49653) and troglitazone on human small arteries in vitro. *Diabetes* **47**: 810-814

Walsh MF, Barazi M, Syed A, Igwe R, Zhang F, Sowers JR (1996) Troglitazone induces both immediate and delayed relaxation in rat tail arteries. *Int Congress of Endocrinology* (San Francisco): P3-858

Wang J, Akabayashi A, Dourmashkin J,Yu HJ, Alexander JT, Chae HJ, Leibowitz SF (1998) Neuropeptide Y in relation to carbohydrate intake, corticosterone and dietary obesity. *Brain Res* **802**: 75-88

Wang M-Y, Shimabukuro M, Lee Y, Trinh KY, Chen J-L, Newgard CB, Unger RH (1999) Adenovirus-mediated overexpression of uncoupling protein-2 in panreatic islets of Zucker Diabetic rats increases oxidative activity and improves β-cell function. *Diabetes* **48**: 1020-1025

Wang Q, Dryden S, Frankish HM, Bing C, Pickavance L, Hopkins D, Buckingham R, Williams G (1997) Increased feeding in fatty Zucker rats by the thiazolidinedione BRL 49653 (rosiglitazone) and the possible involvement of leptin and hypothalamic neuropeptide Y. *Br J Pharmacol* **122**: 1405-1410

Wasada T, Omori Y, Sasaki H, Kawamori R, Yamasaki Y, Baba S, Shichiri M, Kaneko T (1996) Effect of pioglitazone (AD-4833) on insulin-stimulated glucose disposal in NIDDM, an assessment by the euglycemic hyperinsulinemic clamp method. *Diabetes* **45** Suppl 2: 73A

Watkins PB, Whitcomb RW (1998) Hepatic dysfunction associated with troglitazone. *New Eng J Med* **338**: 916-917

Weigle DS, Selfridge LE, Schwartz MW, Seeley RJ, Cummings DE, Havel PJ, Kuijper JL, BeltrandelRio H (1998) Elevated free fatty acids induce uncoupling protein 3 expression in muscle. *Diabetes* **47**: 298-302

Whitcomb RW, Saltiel AR (1995) Oncologic, endocrine and metabolic: thiazolidinediones. *Exp Opin Invest Drugs* **4**: 1299-1309

Widdowson PS, Farnworth M, Dunn D, Wyatt I (1996) Evidence that L-2-chloropropionic acid-induced neurotoxicity involves a constitutive nitric oxide synthase. *Br J Pharmacol* **119**: 374-378

Widdowson PS, Henderson L, Pickavance L, Buckingham R, Tadayyon M, Arch JR, Williams G (1999) Hypothalamic NPY status during positive energy balance and the effects of the NPY antagonist, BW 1229U91, on the consumption of highly palatable energy-rich diet. *Peptides* **20**: 367-372

Widdowson PS, Upton R, Buckingham R, Arch J, Williams G (1997) Inhibition of food response to intracerebroventricular injection of leptin is attenuated in rats with diet-induced obesity. *Diabetes* **46**: 1782-1785

Widdowson PS, Upton R, Henderson L, Buckingham R, Wilson S, Williams G (1997) Reciprocal regional changes in brain NPY receptor density during dietary restriction and dietary-induced obesity in the rat. *Brain Res* **774**: 1-10

Widdowson PS, Wilding JPH (1999) Hypothalamic neuropeptide Y and its neuroendocrine regulation by leptin. In: Ur E (ed) *The neuroendocrinology of leptin. Front Horm Res*, vol **26**, Karger, Basel, pp 71-85

Wilding J, Widdowson P, Williams G (1997) Neurobiology. *Br Med Bull* **53**: 286-306

Wilding J, Williams G (1997) Diabetes mellitus and disorders of lipid and intermediary metabolism. In: Souhami R, Moxham J (eds) *Textbook of medicine*. Harcourt and Brace, Edinburgh, pp 796-839

Wilding JP, Gilbey SG, Jones PM, Mannan MM, Ghatei MA, Bloom SR (1992a) Dexfenfluramine treatment and hypothalamic neuropeptides in diet-induced obesity in rats. *Peptides* **13**: 557-563

Wilding JPH, Gilbey SG, Mannan M, Aslam N, Ghatei MA, Bloom SR (1992b) Increased neuropeptide Y content in individual hypothalamic nuclei, but not neuropeptide Y mRNA, in diet-induced obesity in rats. *J Endocrinol* **132**: 299-304

Wilding JPH, Kruszynska YT, Lambert PD, Bloom SR (1995) Acute effects of central neuropeptide Y injection on glucose metabolism in fasted rats. *Clin Sci* **89**: 543-548

Williams G (1994) Management of non-insulin-dependent diabetes mellitus. *Lancet* **343**: 95-100

Williams G, Harrold JA, Cutler DJ (2000) The hypothalamus and the regulation of energy homeostasis: lifting the lid on a black box. *Proc. Nutr. Soc.* **59**: 385-396

Williams G, Steel JH, Cardoso H, Ghatei MA, Lee YC, Gill JS, Burrin JM, Polak JM, Bloom SR (1988) Increased hypothalamic neuropeptide Y concentrations in diabetic rat. *Diabetes* 37: 763-772

Williams G, Wilding J (1997) The central nervous system and diabetes mellitus. In: Pickup J, Williams G (eds) *Textbook of diabetes.* Blackwell Science Ltd, Oxford, pp 65.1-65.30

Wilson TM, Cobb JE, Cowan DJ, Wiethe RW, Correa ID, Prakash SR, Beck KD, Moore LB, Kliewer SA, Lehmann JM (1996) The structure-activity relationship between peroxisome proliferator-activated receptor gamma agonism and the antidiabetic activity of thiazolidinediones. *J Med Chem* **39**: 665-668

Wollheim CB (2000) Beta-cell mitochondria in the regulation of insulin secretion: a new culprit in type II diabetes. *Diabetologia* **43**: 265-277

Xing G, Zhnag L, Heynen T, Yoshikawa T, Smith S, Weiss S, Detara-Wadleigh S (1995) Rat PPAR delta contains a CGG triplet repeat and is prominently expressed in the thalamic nuclei. *Biochem Biophys Res Comm* **217**: 1015-1025

Yang T, Michele DE, Park J, Smart J, Smart AM, Lin Z, Brosius III FC, Schnermann JB, Briggs JP (1999) Expression of peroxisome proliferator-activated receptors and retinoid X receptors in the kidney. *Am J Physiol* **277**: F966-F973

Yki-Järvinen H, Williams G (1997) Insulin resistance in non-insulin-dependent diabetes mellitus. In: Pickup J, Williams G (eds) *Textbook of diabetes.* Blackwell Science Ltd, Oxford, pp 20.1-20.13

Yoon JW, Sherwin RS, Kwon H, Jun HS (2000) Has GAD a central role in type 1 diabetes? *J Autoimmun* **15**: 273-278

Yoshioka S, Nishino H, Shiraki T, Ikeda K, Koike H, Okuno A, Wada M, Fujiwara T, Horikoshi H (1993) Antihypertensive effects of CS-045 treatment in obese Zucker rats. *Metabolism* **42**: 75-80

Young MMR, Squassante L, Werner J (1997) Troglitazone has no effect on the red cell mass or other erythropoietic parameters. *Diabetologia* **40** Suppl 1: A311

Young PW, Buckle DR, Cantello BCC, Chapman H, Clapham JC, Coyle PJ, Haigh D, Hindley RM, Holder JC, Kallender H, Latter AJ, Lawrie KWM, Mossakowska D, Murphy GJ, Roxbee-Cox L, Smith SA (1998) Identification of high-affinity binding sites for the insulin sensitizer rosiglitazone (BRL-49653) in rodent and human adipocytes using a radioiodinated ligand for peroxisomal proliferator-activated receptor γ. *J Pharmacol Exp Ther* **284**: 751-759

Zhang B, Graziano MP, Doebber TW, Leibowitz MD, White-Carrington S, Szalkowski DM, Hey PJ, Wu M, Cullinan CA, Bailey P, Lollman B, Frederich R, Flier JS, Strader CD, Smith RG (1996) Down-regulation of the expression of the obese gene by an antidiabetic thiazolidinedione in Zucker Diabetic Fatty rats and *db/db* mice. *J Biol Chem* **271**: 9455-9459

Zhang B, Szalkowski D, Diaz E, Hayes N, Smith R, Berger J (1994) Potentiation of insulin stimulation of phosphatidylinositol 3-kinase by thiazolidinedione-derived antidiabetic agents in Chinese hamster ovary cells expressing human insulin receptors and L6 myotubes. *J Biol Chem* **269**: 25735-25741

Zhang F, Sowers JR, Ram JL, Standley PR, Peuler JD (1994) Effects of pioglitazone on calcium channels in vascular smooth muscle. *Hypertension* **24**: 170-175

Zhang HY, Reddy SR, Kotchen TA (1994) Antihypertensive effect of pioglitazone is not invariably associated with increased insulin sensitivity. *Hypertension* **24**: 106-110

Zhang Y, Proenca R, Maffei M, Barone M, Leopold L, Friedman JM (1994) Positional cloning of the mouse obese gene and its human homologue. *Nature* **372**: 425-432

Zhou YT, Shimabukuro M, Wang MY, Lee Y, Higa M, Milburn JL, Newgard CB, Unger RH (1998) Role of peroxisome proliferator-activated receptor α in disease of pancreatic β cells *Proc Natl Acad Sci USA* **95**: 8898-8903

Zhu YJ, Alvares K, Huang Q, Rao MS, Reddy JK (1993) Cloning of a new member of the peroxisome proliferator-activated receptor gene family from mouse liver. *J Biol Chem* **268**: 26817-26820

Zucker LM, Zucker TF (1961) Fatty, a new mutation in the rat. *J Hered* **52**: 275-278

Zucker TF, Zucker LM (1962) Hereditary obesity in the rat associated with high serum fat and cholesterol. *Proc Soc Exp Biol Med* **110**: 165-171